Final Report Version 1.1

Returning to Saturn
Design Synthesis Exercise

Group 6

Technische Universiteit Delft

TU Delft Delft University of Technology

Challenge the future

Final Report Version 1.1

Design Synthesis Exercise

by

Group 6

Francesca Argenziano	4543130
Niels Bakx	4559975
Andreas Bironti	4530802
Thomas Britting	4554116
Danny Gasman	4537351
Giulia Gatti	4437438
Carmen Nerea Immerzeel	4581415
Gydo Kempenaar	4238338
Nora Sulaikha	4532600
Bas Tindemans	4466225

Version	Date	Description
v1	25-06-19	Draft version
v1.1	01-07-19	Feedback comments

July 2019

Tutor: D. Dirkx
Coaches: S.M. Cazaux
R. Hedayati

The image on the front page was made internally.

TU Delft Delft University of Technology

[This page is intentionally left blank]

Executive Overview

The intent of this report is to present the final design phase of the Exploration of Plumes and Oceans of the Saturnian System (EPOSS) mission, as a part of the deliverables of the AE3200 Design Synthesis Exercise of Spring 2019. Following the design presented in [9] and [10], it details and elaborates on the concept selected in [10].

EPOSS Mission

The objective of the EPOSS mission is as follows:

> To gain a deeper understanding of the origins of our Solar System and the conditions for life by studying the workings and composition of the Saturnian System. [10]

To fulfil said objective, a trade-off was performed to consider feasible options. The design of a single spacecraft was selected to execute the mission. A general overview of the design choices made for its subsystems is presented in Table 1.

Table 1: Overview of EPOSS design.

Subsystem	**Description**		**Mass [kg]**	**Nominal Power [W]**
Payload	*Instruments*	JANUS (Imaging) VIMS (Spectrometer) REASON (Radar) BELA (Altimeter) MERMAG (Magnetometer) MORE (Radio Science) ENIJA (Particle Characterization) INMS (Particle Characterization)	137.2	< 105.3
ADCS	*Sensors*	3 Star Trackers, 2 IMUs, 3 Sun Sensor	52.2	77
	Actuators	4 Momentum wheels 16 Monopropellant thrusters		
Propulsion	*Dual Mode System*	Hydrazine Fuel Tank Nitrogen Tetroxide Oxidiser Tank Helium Pressurant Tank Feedlines and Valves	345.8	0
TT&C	*1 HGA (Ka-band)* *2 LGA (X-band)*	BPSK modulation, turbo coding ΔDOR regenerative pseudo-noise 99% tolerance	144.3	73.3
C&DH	On Board Computer (Airbus OSCAR) Solid State Recorder (NEMO) Harness (cable and wiring)		36.1	32.3
Power	9 Americium based RTGs 2 Lithium-ion batteries		289.6	46.6
Thermal	*External*	Louvres, radiators, MLI, coating	37.1	4.2
	Internal	RTGs, Capillary Pumped Loop		
Structures	*Main structure*	Cylindrical structure AL 7075-T6 and CFRP Skirt, stiffeners, stringers and supports	187.6	13
	Mechanisms	Radar deployment mechanism Magnetometer boom deployment Antenna pointing device		
Total		**Total Dry**	1229.9	351.7
		Total Wet	4288.2	

EPOSS in the Space Market

For the mission to be socially and economically sustainable, it has to be supported by numerous stakeholders, some of them being key for the mission's success. The scientific community is identified as the main target of the mission. Besides it, governments and space agencies (namely ESA, NASA, and SpaceX) are relevant stakeholders.
The expected scientific output of the mission is declared to be a favourable in terms of market, under consideration of the present interest in Enceladus and the Saturnian System.

Subsystems

A discussion on all vehicle's subsystems is done as follows.

Trajectory and Orbit

Trajectory starts with an interplanetary phase transfer costing a ΔV of 769.5 m/s. After launch in 2028, the spacecraft is brought to orbit by the Falcon Heavy, and reaches the Saturnian System in 2038 after gravity assists (Earth-Venus-Earth-Earth-Saturn) and Deep Space Manoeuvres (DSM).
After the trajectory shown in Figure 1, Saturn orbit injection (SOI) takes place between the F and G rings, subsequently encountering Enceladus as shown in Figure 2.

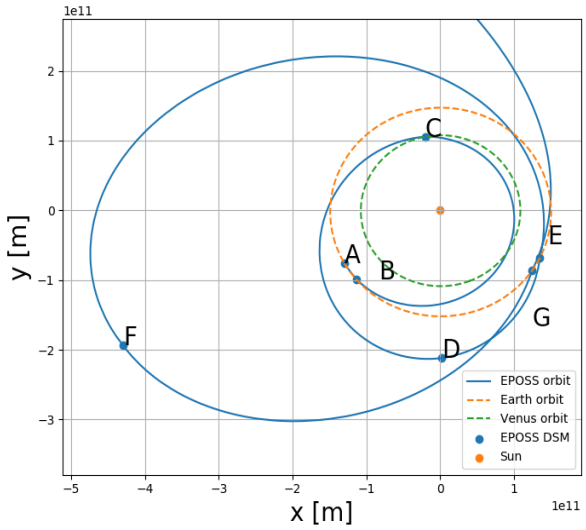

Figure 1: Zoomed-in interplanetary trajectory.

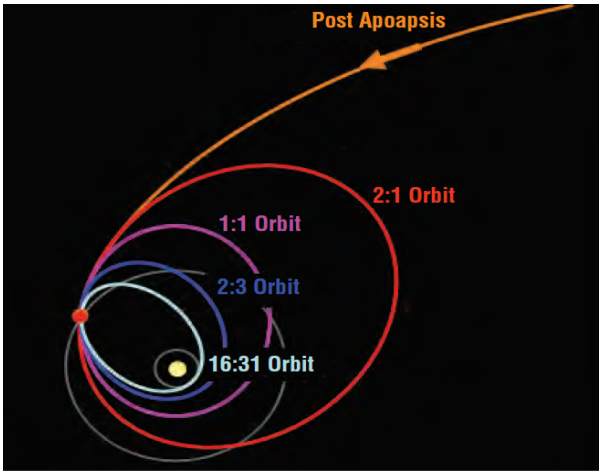

Figure 2: Illustration of Enceladus encounter through resonance hopping [90, figure 3.1.1-4].

Four Enceladus flybys are included in the in-system orbit design for science at the poles. Four Daphnis flybys are designed with two dedicated to the leading edge and north pole, and two dedicated to trailing edge and south pole. After a moon tour, EPOSS enters Enceladus' orbit, where it performs the majority of the mission's science throughout 457 Enceladean days. Crashing into Tethys is selected as the end-of-life strategy.

Payload

Payload consists of eight instruments, as indicated in Table 1, which are necessary for the compliance of the science requirements and objectives.
All primary science is performed in 457 Enceladus days of EPOSS orbiting Enceladus, four Enceladus flybys and four Daphnis flybys. Said science consists of primarily surface imaging, spectrometry, magnetic field measurements, gravity measurements, bulk composition, and particle characterisation.

Table 2: Daphnis traceability matrix.

Instruments			**JANUS**	**VIMS**	**REASON**	**MERMAG**	**BELA**	**MORE**	**ENIJA**	**INMS**
Operational time			28 minutes in flyby	28 minutes in flyby	5.5 minutes in flyby	\	5.5 minutes in flyby	\	110 minutes in flyby	\
Daphnis	Science objectives	Requirement								
	Plumes and Particles	PLD-08.06								
		PLD-08.07								
		PLD-08.08								
		PLD-08.09								
		PLD-08.10								
		PLD-08.11								
	Geophysical	PLD-08.01.01								
		PLD-08.02.01								
	Remote sensing	PLD-08.03								
		PLD-08.04								
		PLD-08.05								

Table 3: Enceladus traceability matrix.

Instruments			**JANUS**	**VIMS**	**REASON**	**MERMAG**	**BELA**	**MORE**	**ENIJA**	**INMS**
Operational time			141 days in orbit with i = 60 deg and 0.3 days in orbit with i = 90 deg	2.1 days in orbit with i = 60 deg	2 days in orbit with i = 60 deg	1 day in orbit with i = 45 deg and 229 days in orbit with i = 60 deg	21 days in orbit with i = 60 deg and 1.6 days in orbit with i = 90 deg	1.5 days in orbit with i = 45 deg, 320 days in orbit with i = 60 deg and 2.1 days in orbit with i = 90 deg	42 days in orbit with i = 60 deg and 0.3 days in orbit with i = 90 deg	42 days in orbit with i = 60 deg and 0.3 days in orbit with i = 90 deg
Enceladus	Science objectives	Requirement								
	Plumes and Particles	PLD-02.02								
		PLD-02.03								
		PLD-02.05								
	Geophysical	PLD-01								
	Remote sensing	PLD-04								
		PLD-05								
		PLD-05.01								
		PLD-06								
	In-Situ	PLD-03								
		PLD-07								

Measurements are performed by numerous instruments at a time, acting as main (in green) and supporting (in yellow) for the measurement, as shown in the traceability matrices (Table 3, Table 2). This distribution calls for time at the end of orbiting to send data back. Since said time is available during end of life trajectory, no reduction of payload use is necessary. An analysis of the instruments characteristics, use in mission, and spacecraft capabilities shows that the current design meets all requirements stipulated for payload. Secondary science is also addressed.

Attitude Determination and Control System

Attitude Determination and Control System (ADCS) is divided into sensors and actuators, as given in Table 1. Three-axis stabilisation is provided, using BELA altimeter as driving for the pointing accuracy requirement of 50 μrad. Furthermore, it complies with the pointing accuracy to Earth of 87 μrad and engine pointing requirements of 5 deg.

Propulsion

A pressure fed, dual mode system, relying on bipropellant main engine and monopropellant reaction control system (RCS) has been selected. The propellant is hydrazine as fuel and nitrogen tetroxide as oxidiser. The main engine will use this combination as bipropellant whereas the RCS thrusters will use hydrazine as monopropellant with a catalyst for decomposition.

Telemetry, Tracking, and Command

One high gain antenna (HGA) using Ka-band and two low gain antennas (LGA) using X-band have been selected (Table 1). The latter cannot be used for science data transmission, but can be used for receiving commands. For the data downlink of the HGA, the average is 150 kbit/s is used.

Command and Data Handling

An on-board computer (OBC), a solid state recorder and a harness compose the command and data handling (C&DH) subsystem.
As OBC, EPOSS will implement the Airbus OSCAR, highly reliable and capable of complying with housekeeping and data requirements.
The chosen solid state recorder (SSR) is the Airbus NEMO 1200, having a 0.5 TB user capacity and a fully redundant unit. Said SSR will collect all excess data to be sent at the end of the orbiting phase.

Power

The power subsystem has to provide 351.7 W nominal power and a peak power of 467.7 W. This is achieved through nine Americium-based Radioisotope Thermoelectric Generators (RTGs) for nominal operations. Two Lithium-ion rechargeable batteries contribute towards peak power requirement.
Using Americium-241 instead of the scarce Plutonium alternative implies heavier, more costly RTGs with a better performance across time. Thorough assessment of risks and sustainability concerns introduced by RTGs is performed to defend this choice.

Thermal Control

Internal thermal control ensures temperature stays within predetermined ranges through use of RTGs and heat pipes. External thermal control regulates heat absorption and dissipation through sun shielding, louvres, radiators, Multi-Layer Insulation (MLI) and coating.
This selection and further design detailing is performed under consideration of the conditions

throughout the whole mission so as to ensure proper functioning in most critical temperatures. The proper functioning is defined as the operating temperature range which is driven by the batteries.

Structures

An aluminium alloy 7075-T6 semi-monocoque strengthened cylindrical structure is chosen. Support for the HGA is made out of CFRP. Structure and mechanisms components are given in Table 1, which are based on the most critical load case, being longitudinal vibrations.

Final Design

Integration of the aforementioned subsystems is done under consideration of their interaction. Integration is done during the subsystems design phase to ensure concurrent development, and after to provide the necessary hardware interfaces with launcher and ground station. With regards to layout, requirements coming from the placement of instruments and structures yield the distribution shown in Figure 3 and Figure 4.

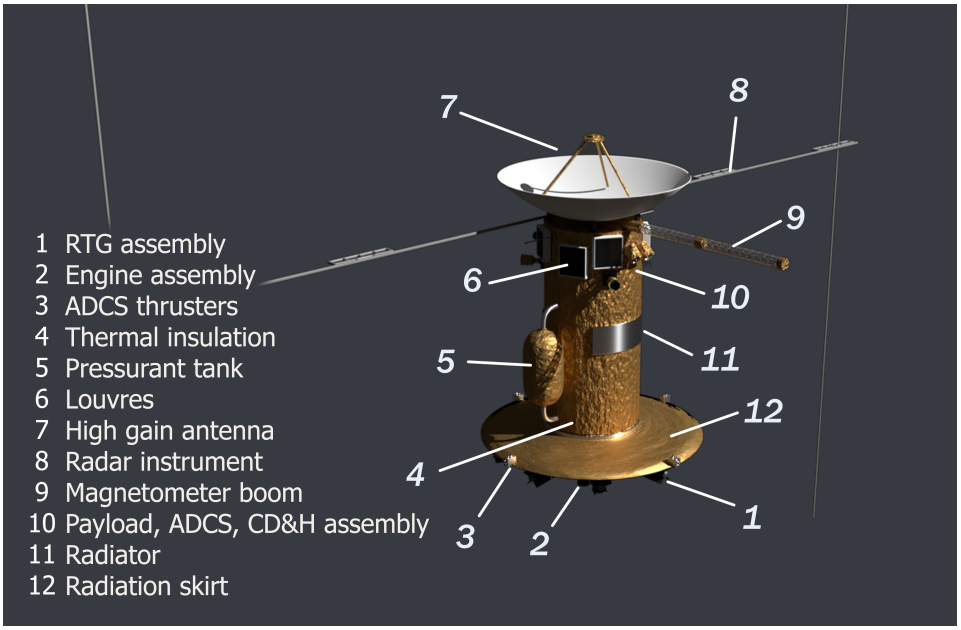

Figure 3: External view of the EPOSS vehicle.

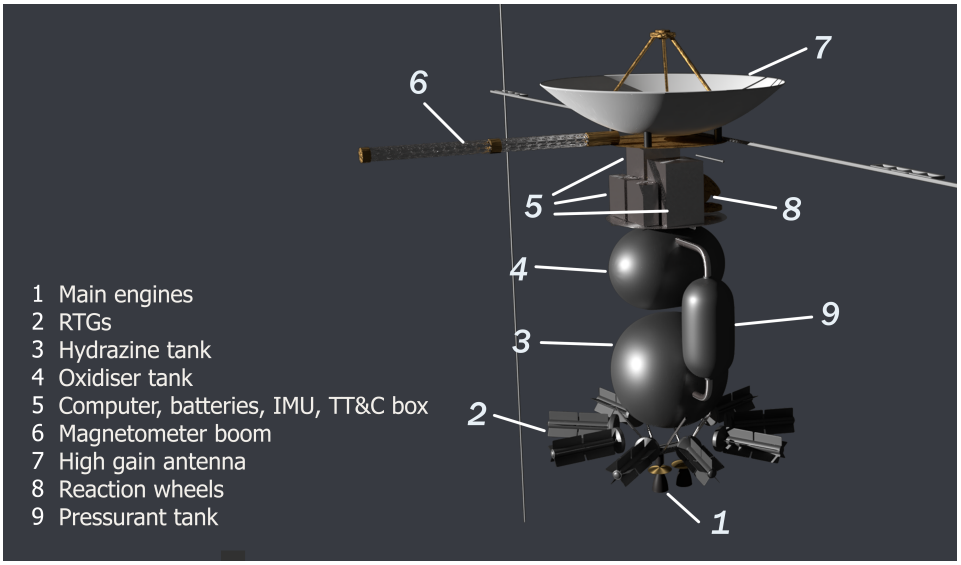

Figure 4: Internal view of the EPOSS vehicle

The system's risk is assessed through a technical risk map and a fault tree diagram. Mitigation of the integrated spacecraft assesses: launcher adaptor failure, power regulator failure, impact of bodies on the system and short circuit of electrical interface. Valve and engine failure score highest in the technical risk map, mitigation is discussed in the respective subsystems. Despite a final reliability of 61.7% being found from statistical data, this value is not deemed representative for the mission, and a higher final system reliability is expected due to the number of missions that have flown similar mission with no significant failures and due to the extensive testing that is performed in pre-launch. Through a sensitivity analysis, the system is deemed satisfactorily flexible and adaptable to modifications.

Spacecraft Budgets

The mission is required to be under a budget of 1.5 B € (MIS-14). The current design costs 1.43 B €, as shown in Table 4. EPOSS has a total dry mass of 1229.9 kg and a nominal and peak power budget of 351.7 W (Table 1).

Operations and Logistics

Pre-launch activities span design, development and production of the spacecraft.
Launch will take place the 19-04-2028 in the Vandenberg Air Force Base (VAFB), with the SpaceX fully reusable Falcon Heavy. The NASA Deep Space Network (DSN) is used for communication. The LGAs are used for transmission during Venus flybys; after the second Earth gravity assist, the HGA is mainly used.
Logistics discusses the development of a more detailed design, subsystem and integration testing, flight hardware production and launch preparation concerns. This is further discussed with regards to development and manufacturing, assembly and integration.

Mission Considerations

Availability of the spacecraft at launch date is proven through description and planning of design, manufacturing, and testing of the system. Furthermore, the spacecraft can perform all measurements and send back the data within the stipulated mission duration.
Maintainability will only be possible for the ground station and on-board software. Related to

Table 4: Cost budget of the EPOSS mission.

EPOSS	
Element	**Cost [M € in FY2019]**
Payload	270
Operations	
Software cost	19.9
Ground system	60.1
Launch vehicle	79.9
Production	160.9
Program level	54.9
Spacecraft bus	
Power	573.5
Thermal	4.8
ADCS	17.5
TT&C	29.2
C&DH	5.4
Propulsion	1.7
Structures	14.8
Total dry mass cost	**646.9**
Total cost	**1022.8**
Total cost with 40% margin	**1431.9**

this, safety is discussed with regards to workers and operations.

Sustainability is considered consistently throughout the design by application and assessment of compliance with the EPOSS Sustainability and Planetary Protection Policy (ESPPP), which refers to methods and requirements on economical, social, and environmental sustainability. Selected parameters are considered in more detail, these result in the observation that the use of hydrazine, Americium RTGs, the end of life strategy, the launch site, and the launcher, do not compromise EPOSS' sustanability targets.

Conclusions and Recommendations

The EPOSS objectives are deemed to be of highly relevant for the scientific community. By considering all requirements in depth and providing measures for verification and validation, as well as thorough risk and sensitivity studies, the team is confident all requirements can be met. Furthermore, the design proves to be sustainable so far. In other words, progress is satisfactory.
After evaluation of the design, recommendations are provided for future work, the general ones being:

- The team suggests to conduct further research so as to decrease the number of unknowns and thereby increasing EPOSS' inherent reliability and to adress all uncertainties.
- As the interaction of different space agencies is required for this mission to succeed, it is recommended to study the political ramifications of an international collaboration
- Considering the amount of time and the complexity of the project, a further improvement is to implement more models to validate the results drawn in these ten weeks.

Contents

Nomenclature

Abbreviations

Δ DOR	Delta Differential One-way Ranging
η	Degradation
EOM	End Of Mission
ADCS	Attitude Determination and Control System
Am	Americium
BELA	BepiColombo Laser Altimeter
BER	Bit Error Rate
BOL	Beginning of Life
BPSK	Binary Phase-Shift Keying
BWG	Beam Waveguide
C&DH	Command & Data Handling
CA	Closest Approach
CDU	Command Detector Unit
CFRP	Carbon Fiber Reinforced Plastics
COSPAR	Committee on Space Research
CPL	Capillary Pumped Loop
DOD	Depth of Discharge
DSE	Design Synthesis Exercise
DSM	Deep Space Manoeuvre
DSN	Deep Space Network
DST	Deep Space Transponder
E	Earth Gravity Assist
E2T	Enceladus to Titan
EEPROM	Elecrically Erasable Programmable Read-Only Memory
EFM	Enceladus Flagship Mission
EIRP	Effective Isotropic Radiated Power
EM	Engineering Model
ENIJA	Enceladus Icy Jet Analyser
EOI	Enceladus Orbit Insertion
EOL	End of Life
EOM	End of Mission
ESA	European Space Agency
ESPPP	EPOSS Sustainability and Planetary Protection Policy
FAA	Federal Administration of Aviation
FBD	Functional Breakdown Diagram
FEA	Finite Element Analysis
FFD	Functional Flow Diagram
FM	Flight Model
GA	Gravity Assist
GALA	Ganymede Laser Altimeter
HEF	High Efficiency
HGA	High Gain Antenna
IMU	Inertial Measurement Unit
INMS	Ion and Neutral Mass Spectrometer
INSRP	Interagency Nuclear Safety Review Panel
IPS	Instruction per Second
JANUS	Jovis, Amorum ac Natorum Undique Scrutator
JET	Journey to Enceladus and Titan
JPL	Jet Propulsion Laboratory
JUICE	JUpiter ICy Moons Explorer
Ka-T	Ka-Transponder
LGA	Low Gain Antenna
LIFE	Life Investigation for Enceladus
MERMAG	Magnetic Field Investigation
MLI	Multi-Layer Insulation
MOI	Moment of Inertia
MORE	Mercury Orbiter RadioScience Experiment
NASA	National Aeronautics and Space Administration
NEPA	National Environmental Policy Act
NNL	National Nuclear Laboratory
OBC	On-Board Computer
PID	Partial-Integral-Differential
PM	Project Management
PN	Pseudo-Noise
Pu	Plutonium
QM	Qualification Model
QPSK	Quadratic Phase-Shift Keying
RAM	Random-Access Memory
REASON	Radar for Europa Assessment and Sounding: Ocean to near-Surface
RTG	Radioisotope Thermoelectric Generator
SE	System Engineering
SLOC	Single Lines of Code
SOI	Saturn Orbit Insertion
SSR	Solid State Recorder

STM	Structural and Thermal Model
T2B	Weighted-voting Balanced Tausworthe, voting ν=2
T4B	Weighted-voting Balanced Tausworthe, voting ν=4
T&O	Trajectory and Orbit
TandEM	Titan and Enceladus Mission
TCU	Telemetry Control Unit
TIGER	Titan Imaging and Geology, Enceladus Reconnaissance
TSSM	Titan Saturn System Mission
TT&C	Telemetry, Tracking & Command
TUDAT	TU Delft Astrodynamics Toolbox
TWTA	Travelling-Wave Tube Amplifier
V	Venus Gravity Assist
VAFB	Vandenberg Air Force Base
VIMS	Visual And Infrared Mapping Spectrometer

Constants

σ	Stefan-Boltzmann constant	$5.668 \cdot 10^{-8}$ [W/m^2 · K^4]
g	Standard Earth gravity at sea level	9.80665 [m/s^2]
K	Boltzmann constant	$1.3806 \cdot 10^{-23}$ [J/K]

Symbols

α	Absorptivity	[-]
Δ Q	Difference in received heat	[W]
ΔV	Velocity change	[m/s]
ϵ	Emissivity	[-]
λ	Field strength function	[−]
μ	Standard gravitational parameter	[m^{3}s^{-2}]
ρ	Plume's density	[kg/ m^3]
σ_{cr}	Critical buckling stress	[MPa]
σ_{tot}	Total stress	[MPa]
θ	Maximum spacecraft rotation	[rad]
D	Spacecraft's residual dipole moment	[A· m^2]
H	Spacecraft's angular momentum	[Nms]
P	Orbital Period	[s]
T_m	Magnetic disturbance torque	[N· m]
V_∞	Hyperbolic velocity at infinity	[m/s]
A	Area	[m^2]
a	Semi-major axis	[m]
A_r	Spacecraft's cross-sectional area	[m^2]
C	Heat capacity	[J/kg· K]
C_d	Spacecraft's coefficient	[-]
c_m	Centre of mass	[m]
cp_a	Aerodynamic centre of pressure	[m]
E	Young's modulus	[GPa]
e	Eccentricity	[-]
E_b/N_0	Normalised signal-to-noise ratio	[dB]
f_{lat}	Lateral vibrations	[Hz]
f_{long}	Longitudinal vibrations	[Hz]
g_x	G forces in longitudinal direction	[-]
g_y	G forces in lateral direction	[-]
I	Moment of Inertia	[m^4]
i	Inclination	[deg]
I_y	Moment of inertia in Y-axis	[kg· m^2]
I_z	Moment of inertia in Z-axis	[kg· m^2]
I_{sp}	Specific impulse	[s]
L	Length	[m]
L_p	Path loss	[dB]
m	Magnetic moment of Saturn	[N· m^2]
m	Mass	[kg]
R	Data rate	[bit/s]
R	Radial distance from centre of body to spacecraft	[m]
R	Radius	[m]
T	Temperature	[K]
t	Time	[s]
t	thickness	[m]
T_a	Aerodynamic disturbance torque	[N· m]
T_d	Driving disturbance torque	[N· m]
T_g	Gravity disturbance torque	[N·m]
V	Spacecraft's velocity	[m/s]
W_e	Electrical power	[W]
W_t	Thermal power	[W]

1 Introduction

Since the discovery of other planets and their arrangement in the universe, mankind has wondered whether life exists outside Earth and if so, where and how. Many theories and studies have been done on this matter and on how the planets in our system exist and interact. Since the end of the Cassini-Huygens mission in 2017 and its discovery of plumes, cryovolcanic eruptions of ionized water vapor on Enceladus, the scientific community has been eager to determine the possibility of life on the moon. This has led to the development of the mission EPOSS: the Exploration of Plumes and Oceans of the Saturnian System. This mission comes with the project objective *to design a spacecraft that successfully performs the indicated measurements and contributes to the characterisation of Enceladus and Daphnis within ten weeks with ten students.* Therefore, EPOSS will contribute towards answering quests on extra-terrestrial life and the process of planetary formation, within the time and workforce resources appointed by the Design Synthesis Exercise (DSE).

In this report, a preliminary design of the mission and the spacecraft to be built is detailed. In chapter 2, an overview of the mission is given. Chapter 3 expands on the necessity of the mission as well as how EPOSS will compete in the space market with an analysis of interested stakeholders. From chapter 4 on, the subsystems are analysed. The chapter covers the necessary trajectory to reach Saturn along with the optimal in-System trajectory in order to meet primary science goals. Chapter 5 describes the instruments used in EPOSS which characterise the entire science phase of the mission. The attitude determination and control system is defined in chapter 6, followed by the description of the propulsion system in chapter 7. Chapter 8 and chapter 9 defines the telemetry and tracking subsystem used to communicate to the ground station on Earth and the command and data handling system of EPOSS. The design of the power, thermal, and spacecraft structure are elaborated in chapters 10, 11, and 12. The final design, including the integration methods and final layout is presented in chapter 13, followed by chapter 14 which outlines the total mass, cost, and power budgets of EPOSS. Each subsystem and final design chapters include their own sensitivity and risk analyses. An overview of the operations and logistics involved with mission EPOSS and a post DSE planning is presented in chapter 15. Chapter 16 delves into the availability, maintainability and safety of the whole mission as well as the sustainability considerations taken in to account during the design of EPOSS. Finally, chapter 17 summarises the report and design so far and presents a list of recommendations for future consideration.

2 Mission Overview

The icy moon Enceladus is an interesting object to explore particularly due to the presence of a subsurface ocean in the south pole, and therefore the potential for the development of life[71]. Moreover, the rings of Saturn and the interaction with the shepherd moons are an attractive phenomenon to study in order to bring answers on the origin of our Solar System and planet formation [68]. From this, the mission need statement is derived which stipulates that the aim of the EPOSS mission is

> To gain a deeper understanding of the origins of our Solar System and the conditions for life by studying the workings and composition of the Saturnian System. [10]

To pursue the information necessary to answer such questions, the EPOSS mission is developed. Principal characteristics of the spacecraft which will begin its journey to Saturn on the 19^{th} of April 2028 are presented in Table 2.1. In section 2.1 a brief overview of the concept trade-off is given. Following the functional flow diagram mentioned in section 2.2. After this the functional breakdown diagrams are provided in section 2.3 and the chapter is ended with the requirement analysis of the overall mission requirements in section 2.4. These two tools are used as reference to define what functions the EPOSS mission has to satisfy (FFD) and to provide drivers to how well they must be done (requirement analysis).

2.1. Concept Trade-off

An extensive trade-off was done in order to choose the best of the final three concepts, which resulted from a selection based on feasibility. The concepts entering the trade off were: Single spacecraft, double spacecraft and swarm spacecraft. The main differentiation between them was the separation of payload and science objectives per vehicle [10].
Mass, power, and cost budgets were obtained for each option and were used to assess six criteria; which are here listed in order of decreasing weight: scientific yield, operational cost, power, launch cost, sustainability and risk. The result of the trade off and as such, the final concept to be detailed further in this report, is a single spacecraft configuration. The other two options, double spacecraft or swarm configuration, are left behind due to having less promising budgets, although they would allow for diversified and dedicated mission objectives. The single spacecraft will carry out the mission by itself, thus carrying all necessary payload.
Next to that, the options within subsystems of the spacecraft were explored and traded-off as well, in order to have subsystems which meet their criteria the best. These criteria were different from the aforementioned ones, as these subsystems all have their specific points of interest to look at. These chosen systems are worked out in further detail in this report, as well as an overall design of the spacecraft as a whole.

2.2. Functional Flow Diagrams

The functional flow diagrams (FFDs), shown in Figure 2.1-2.2 present the functions of the spacecraft during the mission. It describes different phases of the mission, and what must be done during these phases. There are three levels, for which level one shows the general functions performed during the mission, as well as the general phases. The second level details these general functions and phases, and level three expands on some functions shown in level

two. Furthermore, a numbering system is present. The first digit represents the general level, the second digit the second level, and the third digit the third level functions.
The flow diagram can be read as follows. Functions that are expanded upon contain a letter below or next to them. In the next level, dotted lines separate different sub-functions from each other. As such, by linking the letter to the letter shown above the box, the correct section can be found. Furthermore, the flow between sub-functions is shown per level, to further illustrate the interactions between functions.
The functional flow is an important tool during the design as it shows the interactions between different mission functions, thus illustrating how the subsystems must work together. This is used during the design of the different subsystems in order to size the subsystems accordingly. Further design integration tools include the N2-chart, which will be presented in section 13.1.

Table 2.1: Overview of the EPOSS design.

Subsystem	**Description**		**Mass [kg]**	**Nominal Power [W]**
Payload	*Instruments*	JANUS (Imaging) VIMS (Spectrometer) REASON (Radar) BELA (Altimeter) MERMAG (Magnetometer) MORE (Radio Science) ENIJA (Particle Characterisation) INMS (Particle Characterisation)	137.2	<105.3
ADCS	*Sensors*	3 Star Trackers, 2 IMUs, 3 Sun Sensor	52.2	77
	Actuators	4 Momentum wheels 16 Monopropellant thrusters		
Propulsion	*Dual Mode System*	Hydrazine Fuel Tank Nitrogen Tetroxide Oxidiser Tank Helium Pressurant Tank Feedlines and Valves	345.8	0
TT&C	*1 HGA (Ka-band)* *2 LGA (X-band)*	BPSK modulation, turbo coding two-way regenerative pseudo-noise 99% tolerance	144.3	73.3
C&DH	On Board Computer (Airbus OSCAR) Solid State Recorder (NEMO) Harness (Cable and Wiring)		36.1	32.3
Power	9 Americium based RTGs, 2 Lithium-ion batteries		289.6	46.6
Thermal	*External control*	Louvres, radiators, MLI, coating	37.1	4.2
	Internal control	RTGs, Capillary Pumped Loop		
Structures	*Main structure*	Cylindrical structure AL 7075-T6 and CFRP Skirt, stiffeners, stringers and supports	187.6	13
	Mechanisms	Radar deployment mechanism Magnetometer boom deployment Antenna pointing device		
Total		**Total Dry**	1229.9	351.7
		Total Wet	4288.2	

2.3. Functional Breakdown Diagrams

The functional breakdown diagram (FBD) (see Figure 2.3) is based on the FFD presented in section 2.2, but instead of the flow and direct relationships between functions, it shows the hierarchical structure of the functions. Furthermore, it expands certain functions into another level of detail when applicable. The numbering system is the same as the one described in section 2.2, and it serves a similar purpose in the design process.

2.4. Requirement Analysis

In this section, the compliance of the mission profile with the requirements is checked. The mission requirements, given in Table 2.2, are general requirements extrapolated by the stakeholders specific science requirements [35] since those apply mainly to the payload subsystems and others. The mission requirements refer to what the mission should accomplish in the general sense. The quantitative subsystem-specific requirements are presented and discussed in the subsystem's specific chapter. The overall space segment requirements are given in Table 2.3; these requirements apply to the final design of the spacecraft as a whole. Lastly, the launcher requirements are shown subsection 15.1.2. The verification method and the sections where compliance can be found are presented in the third and fifth column respectively. Table 2.2 and 2.3 present verification methods to be applied. These methods are defined as follows [43]:

- **Analysis:** Show compliance with the requirement by means of mathematical analysis.
- **Test:** Show compliance using testing under representative conditions.
- **Demonstration:** Compliance with a requirement is established by operation of the component.
- **Inspection:** Inspection of the documentation or product to show compliance with the requirement, often related to measurements and weights.

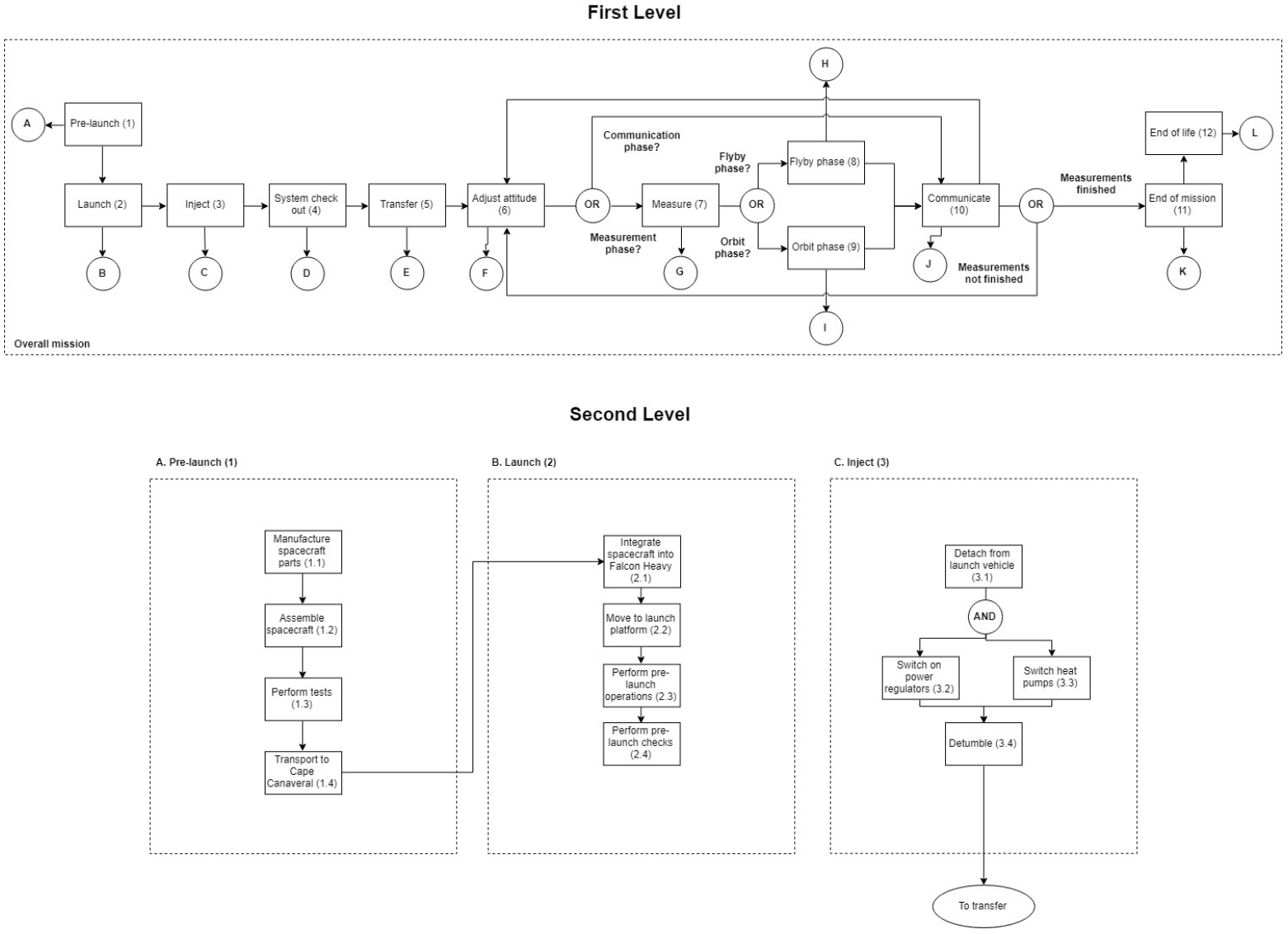

Figure 2.1: Part one of the FFD.

Second Level (Continued)

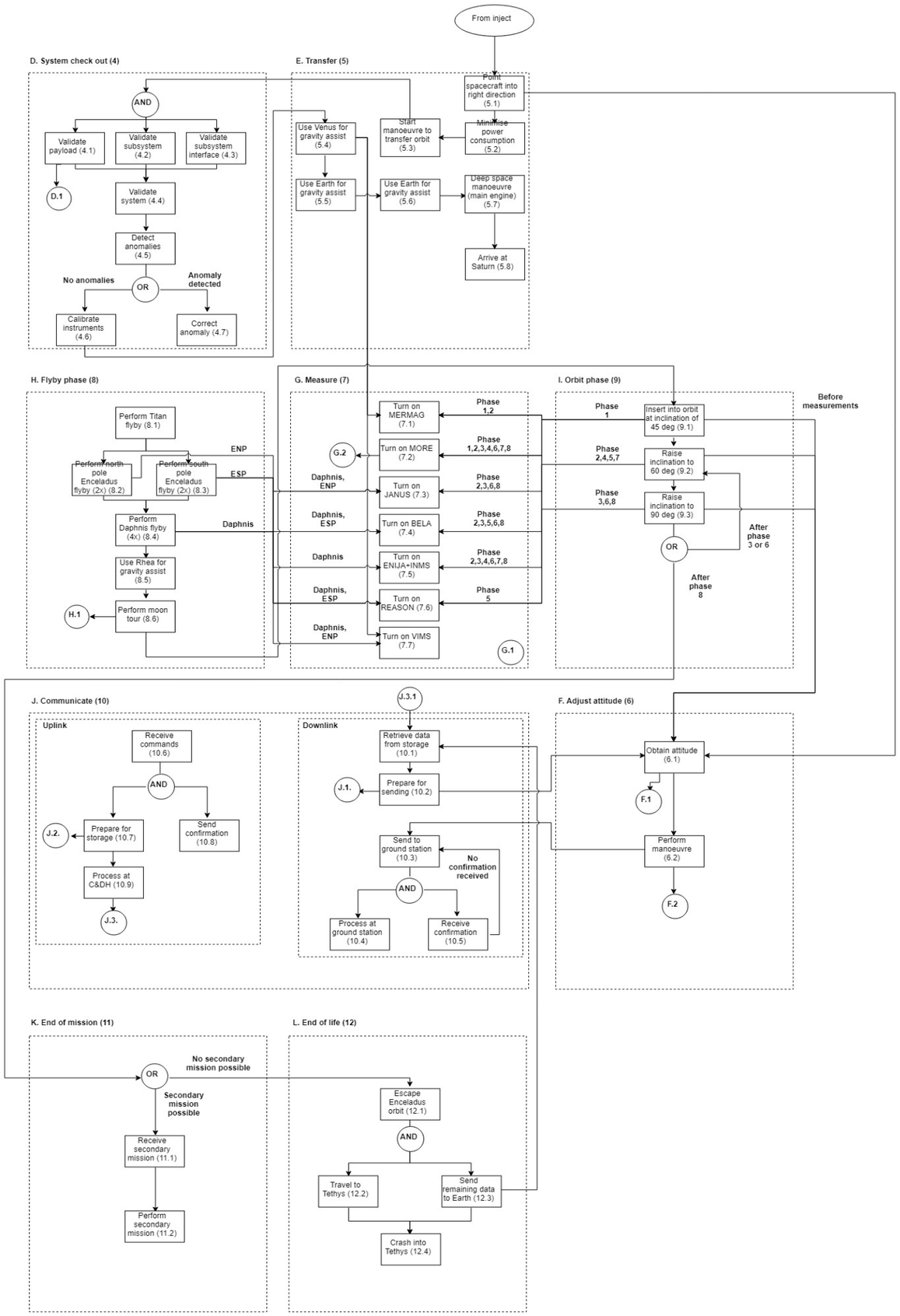

Third Level

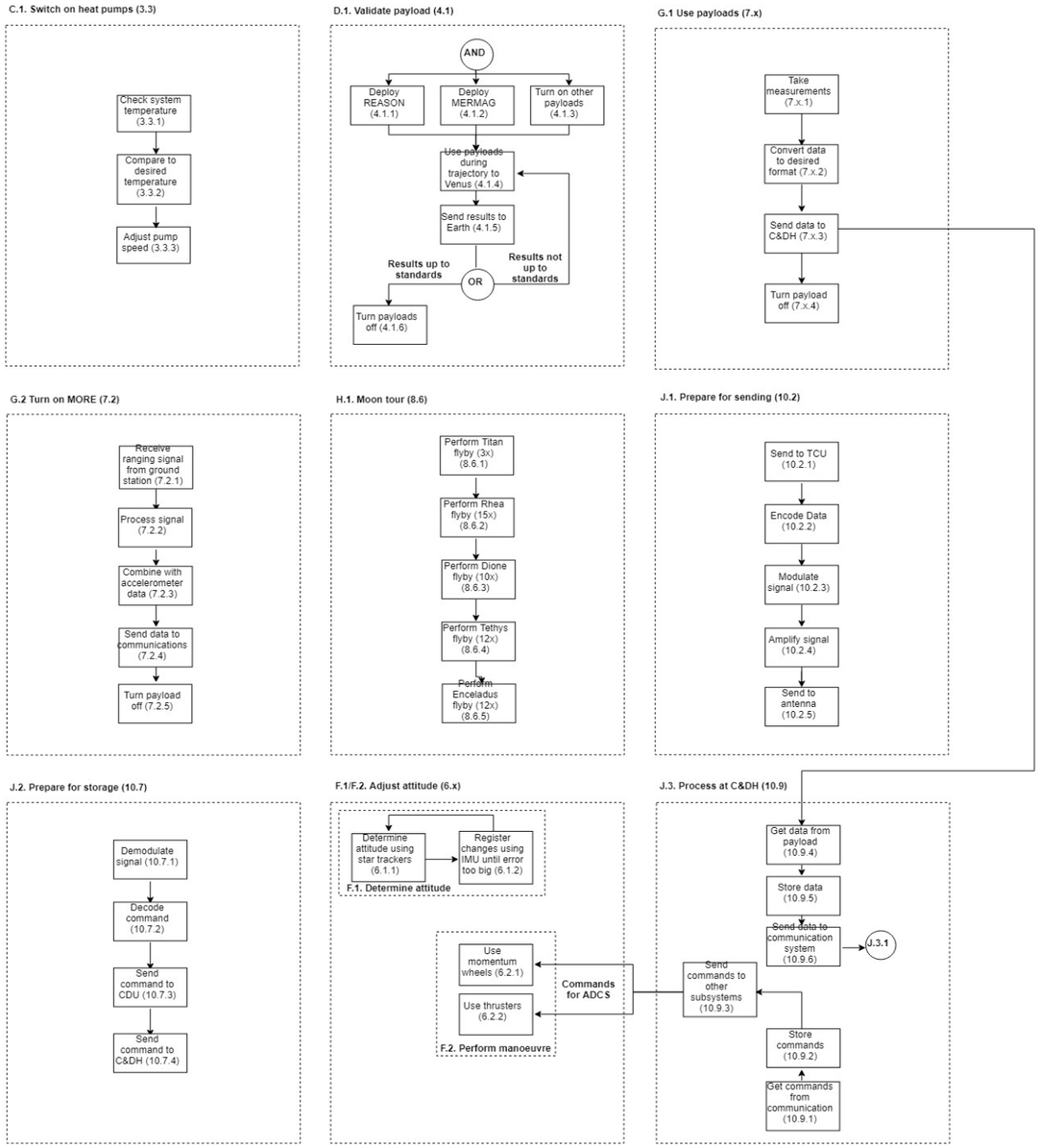

Figure 2.2: Part two of the FFD.

- Mission EPOSS
  - Pre-launch (1)
    - Manufacture spacecraft parts (1.1)
    - Assemble spacecraft (1.2)
    - Perform tests (1.3)
    - Transport to Vandenberg Air Force Base (1.4)
  - Launch (2)
    - Integrate spacecraft into Falcon Heavy (2.1)
    - Move to launch platform (2.2)
    - Perform pre-launch operations (2.3)
    - Perform pre-launch checks (2.4)
  - Inject (3)
    - Detach from launch vehicle (3.1)
    - Switch on power regulators (3.2)
    - Switch on heat pumps (3.3)
      - Check system temperature (3.3.1)
      - Compare to desired temperature (3.3.2)
      - Adjust pump speed (3.3.3)
    - Detumble (3.4)
  - System check out (4)
    - Validate payload (4.1)
      - Deploy REASON (4.1.1)
      - Deploy MERMAG (4.1.2)
      - Turn on other payloads (4.1.3)
      - Use payloads during trajectory to Venus (4.1.4)
      - Send results to Earth (4.1.5)
      - Turn payloads off (4.1.6)
    - Validate subsystem (4.2)
    - Validate subsystem interface (4.3)
    - Validate system (4.4)
    - Detect anomalies (4.5)
    - Calibrate instruments (4.6)
    - Correct anomaly (4.7)
  - Transfer (5)
    - Point spacecraft into right direction (5.1)
    - Minimise power consumption (5.2)
    - Start manoeuvre to transfer orbit (5.3)
    - Use Venus for gravity assist (5.4)
    - Use Earth for gravity assist (5.5)
    - Use Earth for gravity assist (5.6)
    - Deep space manoeuvre (main engine) (5.7)
    - Arrive at Saturn (5.8)
  - Adjust attitude (6)
    - Obtain attitude (6.1)
      - Determine attitude using star trackers (6.1.1)
        - Find pattern of brightest stars (6.1.1.1)
        - Compare to reference (6.1.1.2)
      - Register changes using IMU until error too big (6.1.2)
        - Measure acceleration of rotation (6.1.2.1)
        - Deduct change from original reference (6.1.2.2)
    - Perform manoeuvre (6.2)
      - Use momentum wheels (6.2.1)
      - Use thrusters (6.2.2)
        - Manoeuvre using thrusters (8.2.2.1)
        - Use thrusters for momentum dumping (8.2.2.1)
  - Measure (7)
    - Turn on MERMAG (7.1)
    - Turn on MORE (7.2)
    - Turn on JANUS (7.3)
    - Turn on BELA (7.4)
    - Turn on ENIJA+INMS (7.5)
    - Turn on REASON (7.6)
    - Turn on VIMS (7.7)
    - Take measurements (7.x.1)
    - Convert data to desired format (7.x.2)
    - Send data to C&DH (7.x.3)
    - Turn payload off (7.x.4)
    - Receive ranging signal from ground station (7.2.1)
    - Process signal (7.2.2)
    - Combine with accelerometer data (7.2.3)
    - Send data to communications (7.2.4)
    - Turn payload off (7.2.5)
  - Flyby phase (8)
    - Perform Titan flyby (8.1)
    - Perform north pole Enceladus flyby (2x) (8.2)
    - Perform south pole Enceladus flyby (2x) (8.3)
    - Perform Daphnis flyby (4x) (8.4)
    - Use Rhea for gravity assist (8.5)
    - Perform moon tour (8.6)
      - Perform Titan flyby (3x) (8.6.1)
        - Raise periapse (8.6.1.1)
        - Capture Rhea's orbit (8.6.1.2)
      - Perform Rhea flyby (15x) (8.6.2)
      - Perform Dione flyby (10x) (8.6.3)
      - Perform Tethys flyby (12x) (8.6.4)
      - Perform Enceladus flyby (12x) (8.6.5)
  - Orbit phase (9)
    - Insert into orbit at inclination of 45 deg (9.1)
    - Raise inclination to 60 deg (9.2)
    - Raise inclination to 90 deg (9.3)
  - Communicate (10)
    - Retrieve data from storage (10.1)
    - Prepare for sending (10.2)
      - Send to TCU (10.2.1)
      - Encode Data (10.2.2)
      - Modulate signal (10.2.3)
      - Amplify signal (10.2.4)
      - Send to antenna (10.2.5)
    - Send to ground station (10.3)
    - Process at ground station (10.4)
    - Receive confirmation (10.5)
    - Receive commands (10.6)
    - Prepare for storage (10.7)
      - Demodulate signal (10.7.1)
      - Decode command (10.7.2)
      - Send command to CDU (10.7.3)
      - Send command to C&DH (10.7.4)
    - Send confirmation (10.8)
    - Process at C&DH (10.9)
      - Get commands from communication (10.9.1)
      - Store commands (10.9.2)
      - Send commands to other subsystems (10.9.3)
      - Get data from payload (10.9.4)
      - Store data (10.9.5)
      - Send data to communication system (10.9.6)
  - End of mission (11)
    - Receive secondary mission (11.1)
    - Perform secondary mission (11.2)
  - End of life (12)
    - Escape Enceladus orbit (12.1)
    - Travel to Tethys (12.2)
    - Send remaining data to Earth (12.3)
    - Crash into Tethys (12.4)

Figure 2.3: FBD of the EPOSS mission.

Table 2.2: Overall mission requirements compliance matrix.

Code	Requirement	Verification Method	Compliance	Section
MIS-01.01	The mission shall characterise the thickness of the crust of Enceladus.	Analysis	✓	5.4.1
MIS-02.01	The mission shall characterise the plume of Saturn's Icy Moon Enceladus.	Analysis	✓	5.4.1
MIS-03.01	The mission shall determine the gravity field of Enceladus.	Analysis	✓	5.4.1
MIS-04.01	The mission shall characterise the surface of Saturn's Icy Moon Enceladus.	Analysis	✓	5.4.1
MIS-07.01	The mission shall characterise the magnetic field of Enceladus.	Analysis	✓	5.4.1
MIS-08	The mission shall visit at least one Saturn shepherd moon, to be selected from Prometheus, Daphnis, Pan, Atlas, Janus and Epimetheus.	Analysis	✓	5.4.2
MIS-08.01	The mission shall characterise the surface morphology of the shepherd moon.	Analysis	✓	5.4.2
MIS-08.02	The mission shall characterise the surface composition of the shepherd moon.	Analysis	✓	5.4.2
MIS-08.03	The mission shall make observations of the leading edge of the shepherd moon.	Analysis	✓	4.1.2
MIS-08.04	The mission shall make observations of the trailing edge of the shepherd moon.	Analysis	✓	4.1.2
MIS-08.05	The mission shall determine the bulk composition of the shepherd moon within 5% of its total mass.	Analysis	✓	5.4.2
MIS-08.06	The mission shall determine the composition of the ring particles in the vicinity of the selected shepherd moon.	Inspection	✓	5.4.2
MIS-08.07	The mission shall determine the size distribution of the ring particles in the vicinity of the selected shepherd moon.	Analysis	✓	5.4.2
MIS-08.08	The mission shall determine the dynamics of the ring particles in the vicinity of the selected shepherd moon.	Analysis	✓	5.4.2
MIS-08.09	The mission shall determine the composition of the particles in the gap of the selected shepherd moon.	Analysis	✓	5.4.2
MIS-08.10	The mission shall determine the size distribution of the particles in the gap of the selected shepherd moon.	Analysis	✓	5.4.2
MIS-08.11	The mission shall determine the dynamics of the particles in the gap of the selected shepherd moon.	Analysis	✓	5.4.2
MIS-09:	The mission duration in Saturnian system shall be greater than 4 years.	Analysis	✓	4.1.2
MIS-10	The mission shall have a reliability higher than 0.9, excluding launch failure.	Analysis	✓	13.5
MIS-11	A clear end-of-life strategy shall be included in the mission design.	Analysis	✓	4.3.7, 16.4
MIS-12	The mission shall have full compliance with Planetary Protection, as set out by the COSPAR.	Inspection	✓	16.4
MIS-14	The full mission cost without payload cost shall be less than 1.5 B € in FY2019.	Inspection	✓	14.3
MIS-15	The mission shall launch by 2030.	Analysis	✓	15, 4.1
MIS-16	The mission shall reach the Saturnian system by 2038.	Analysis	✓	15, 4.1
MIS-00.01	The mission shall comply with EPOSS Sustainability Policy [11].	Inspection	✓	16.4
MIS-00.02	The mission's probability of Earth impact upon injection shall not exceed 1 in a million .	Analysis	✓	16.3, 16.4.2

Table 2.3: Overall system requirement compliance matrix

Code	Requirement	Verification Method	Compliance	Section
SSR-11	A clear end-of-life strategy shall be included in the mission design.	Analysis	✓	4.3.7,16.4
SSR-00.05	The system shall satisfy all in-mission checks.	Test	✓	2.2
SSR-00.06	The system shall include in-mission validation process for the overall system.	Demonstration	✓	15.2.2
SSR-00.07	The system shall have a maximum dry mass of 2600 kg.	Inspection	✓	14.1
SSR-00.08	The system shall consume a nominal power of maximum 750 W.	Demonstration	✓	10.3.2
SSR-00.09	The system shall consume a maximum peak power of 1000 W.	Demonstration	✓	14.2
SSR-00.10	The system shall consume a safe-mode power consumption of maximally 400 W.	Demonstration	✓	10.3.1
SSR-00.11	The system's mass shall account for 10 % safety margin.	Analysis	✓	14.1
SSR-00.12	The system shall allow for mission modifications after launch.	Analysis	✓	8.1
SSR-00.13	The system shall be designed to comply with all risks listed in the risk register.	Inspection	✓	13.5
SSR-00.14	The system shall be able to operate in vacuum with a minimum pressure of $1.33 \cdot 10^{-11}$ Pa [12].	Analysis	✓	7.3.2
SSR-00.15	The system shall be able to operate in the range of radiative environments of the mission between 0 and 7000 W.	Analysis	✓	11.3
SSR-00.16	The system shall be designed to comply with the sustainability document named ESPPP.	Inspection	✓	16.4

3 EPOSS in the Space Market

In order to assess the appeal of EPOSS from a business perspective, it is important to underline the added value that the mission would provide. In section 3.1, the opportunities for the mission are discussed. Following, section 3.2 analyses the possible stakeholders which would be interested in supporting the mission. Finally in section 3.3, the possible market for the mission are described.

3.1. Opportunities for the Mission

Since the end of life of Cassini in 2017, no spacecraft has approached the Saturnian system.[1] Regardless of the years passing, the scientific community is continuously looking for new opportunities to further explore Saturn and its moons, as shown by the many proposals (see section 3.3). The EPOSS mission aims to fill the gap in scientific knowledge regarding the discovery of life and other impending questions. To do so, it is crucial to define the market opportunities for the EPOSS mission.

Primary Payload

The EPOSS mission is characterised by a strong scientific yield which can be seen by the requirements in Table 2.2, as the mission specifically targets the scientific community. By orbiting Enceladus, EPOSS answers questions that arose after the flybys performed by Cassini, regarding the composition of the moon. By flying through the plumes located on the south pole of the moon, EPOSS aims to collect and identify larger molecules, hopefully leading to the discovery of molecules linked to life, such as biomarkers, in the subcrustal ocean. Other findings will be related to the overall geophysical composition of the moon and its role in the formation of Saturn's rings. By performing Daphnis flybys, the team will also characterise the geophysical composition of the shepherd moon, but will especially collect solid particles while moving through Saturn's rings. This will bring to light the relationship between the shepherd moon and composition of the rings, and how Daphnis is responsible for the 'ripples' recorded by Cassini. This information combined with the comparability of the Saturnian System to the Solar System allows for a better explanation of the workings of the latter. These topics are important for the scientific community, as the data collected by EPOSS is of extraordinary value to fill the gaps in knowledge in astrophysics and other sciences.

Secondary Payload

Considering the no-profit nature of the European Space Agency (ESA), the EPOSS mission itself will not provide any profit to the organisation, other than the one related to scientific knowledge. However, at the current state of the design, a value of 230 kg, plus 504.7 kg of necessary propellant to account for the extra mass, can be allocated to miscellaneous components without the spacecraft exceeding the maximum dry mass as from requirement SSR-00.07 in Table 2.3. This mass can be open to external stakeholders to purchase and place instruments which can be used for secondary science. By imposing that the extra instruments do not interfere with and operate at the same time as the primary payload on board of EPOSS, around 134.5 W can be allocated to these instruments. Different opportunities during the

[1] Retrieved from `https://solarsystem.nasa.gov/planets/saturn/exploration` last opened on July 2, 2019

mission may be of interest for secondary payload. The moon tour performed by the spacecraft in order to reach the bodies of interest, will give a unique opportunity to perform extra scientific measurements, for example by characterising the particles around the moon Rhea. The Venus flyby will also give an opportunity to use the secondary payload.

3.2. Stakeholders Analysis

In order for the EPOSS mission to succeed, it is necessary to introduce figures to support the project. For this reason, an analysis of stakeholders which may be introduced to the organisation of the EPOSS will be performed below.

Scientific Community

Considering the EPOSS is characterised by the scientific yield of the mission, it comes to no surprise that the scientific community represents the main stakeholder for this programme. Academia would mainly be interested in data collected during the mission about the Saturnian system and its workings. Since the observations of the moon Enceladus by Cassini, many questions regarding the moon's composition and the possibility to find life on it have been raised by many experts in the field. The EPOSS mission aims to fill the scientific gap and provide answers to questions about the conditions for life in Enceladus and find molecules which could be linked to said life. Additionally, by observing the shepherd moon Daphnis, the EPOSS team aims to address the questions about the workings of the Solar System with a focus on particle distribution and dynamics. Academia can be involved in the project by helping designing the scientific segment of the mission such as the instruments, by processing the data acquired, and by drawing conclusions that can answer the questions which arose prior of the beginning of the mission.

Government

EPOSS can be attractive to governments of different countries as being involved in such a project shows great initiative in innovative scientific projects. This can greatly help the public image of a country, as space exploration generally is seen as progressive and revolutionary. By endorsing scientific undertakings, governments can improve and stimulate the national academia by providing unique data collected during the mission lifetime. This stakeholder can contribute to the EPOSS mission by providing funding, which is usually retrieved from taxpayers, and by providing the necessary facilities for the mission to take place and succeed. It is important to highlight that the government, as a stakeholder, is able to stop or slow down the project, by perhaps revoking the funding and the accessibility to the facilities necessary to fulfil the mission. The prevent this, the stakeholder should be fully engaged in the project with perhaps yearly meetings so to have an overview on the progress.

Space Agencies

Different space agencies from around the world will be part of the mission, due to the funding and facilities that they may supply. Space agencies are important stakeholders as they aim to conduct missions on behalf of government institutions (or privates) within a certain budget and time frame. EPOSS may be an interesting opportunity to visit Saturn and its moons again after the end of life mission of Cassini in 2017. Different space agencies will be involved in this mission. The main agency which can be considered is ESA, as this project falls under their jurisdiction and the main funding will be provided by them. The National Aeronautics and Space Administration (NASA) also plays an important role, as the mission requires the use of the Deep Space Network and the launch site, the Vandenberg Air Force Base, which are operated by NASA. SpaceX will also be involved, as the EPOSS team plans to use the Falcon

Heavy, a launcher operated by the aforementioned company. In providing the instruments, other space agencies will play a role. These stakeholders may hold the project by refusing to collaborate due to political reason, or by refusing to provide facilities and help in developing the project. It is thus crucial to have the agencies involved in the planning and design of the EPOSS to keep engagement, and perhaps allow access to the data recorded during the mission.

3.3. Market Analysis

The progress in the determination of the basic requirements for habitability has never flourished so much until the Cassini mission, which went from discovering the first extraterrestrial hydro-thermal system to setting the foundation for the research of life outside Earth [101]. When discovering the phenomenon of the plumes and their interaction with the formation of Saturn's rings, many scientists hinted the fact that the Saturnian System may be a scaled version of the Solar System. With EPOSS' direct access to the ocean via the plumes, the astrobiological study of Enceladus and its aqueous environment results into being the easiest of all planets to investigate, which can definitely be attractive to stakeholders [19].

According to [19], a Berkeley meeting attended by different experts and members of the Cassini mission underlined the necessity for a new space mission in order to fully understand the data collected by the spacecraft launched in 1997. Since 2007, a number of missions for the observation of moons such as Enceladus and Titan have been proposed. In 2008, the Titan Saturn System Mission (TSSM) was proposed as a combined mission of NASA and ESA. This concept was the result of merging the Titan and Enceladus Mission (TandEM) from ESA and the Titan Explorer from NASA with the objective of finding life on these moons [91]. However, the TSSM was discarded in order to focus more on missions to Jupiter such as the JUpiter ICy Moons Explorer (JUICE) and Europa Clipper mission [101]. In 2011, the Jet Propulsion Laboratory (JPL) proposed the Journey to Enceladus and Titan (JET) mission with the aim of mapping the gravity field of these two bodies. Due to the uncertainty of certain subsystems used in the design, the mission was not selected for further development [106]. Another concept involving collecting samples from the plumes is the Life Investigation for Enceladus (LIFE) which was not further developed due to issues related to returning the samples safely [117]. Finally, the last proposal is the Explorer of Enceladus and Titan (E^2T), an ESA mission for the assessment of habitability and evolution of these Saturnian moons [74].

The continuous effort from different space agencies to propose missions with the aim of assessing the conditions for life and studying the workings of the Solar System, shows the relentless effort of the scientific community for further exploration of the Saturnian system. With the current development of the EPOSS mission, the further evolution of this mission could fill a gap in the scientific community and be the first space mission to dive in the niche field of moons and their workings.

4 Trajectory and Orbit

This chapter introduces EPOSS' interplanetary transfer and in-system orbit design. A design overview is presented in section 4.1. An overview of the requirements and their verification is presented in section 4.2. Various methods employed to support the design and verify the trajectory requirements are introduced in section 4.3. Verification and validation, a sensitivity analysis, and risk analysis, are discussed in section 4.4, section 4.5, and section 4.6 respectively.

4.1. Design Overview

An overview of the Trajectory and Orbit (T&O) design is presented in this section, detailing a total of 34 separate orbit design elements, separated into eight phases and a contingency budget. A table describing orbit parameters and a ΔV budget per orbit design elements is included for each phase. A complete overview of the ΔV budget is presented in subsection 4.1.3. Methods and sources used to derive these values are presented in section 4.3. All distances are with respect to the central body's core.

4.1.1. Interplanetary Transfer

Phase one: After launch in April 2028, the Falcon Heavy brings EPOSS into an orbit with a V_∞ of 3.5 km/s. After that it does a number of gravity assists, E-V-E-E-S, and Deep Space Manoeuvres (DSM) to reach the Saturnian system 9.8 years after launch, in February 2038, with a total interplanetary ΔV of 769.46 m/s.

A gravity assist flyby uses the angular momentum of other celestial bodies to provide a (free) change in direction and magnitude of the velocity vector, which makes it possible to save mission time and/or fuel mass. This allows the spacecraft to have a higher payload capability. Also, due to the movement of those bodies a DSM is needed to properly align the spacecraft with the celestial body. This is characterised by an impulse at a certain point along the leg between two bodies. [122]

The interplanetary transfer in heliocentric frame can be seen in Figure 4.1, details of point A-G are highlighted in Figure 4.2. The steps are described in Table 4.1. The Venus flyby radius is equal to 2.36 times the radius of Venus. This Venus flyby is taken as the hottest environment in the mission for thermal design, which is further elaborated upon in subsection 11.3.1. After the Venus flyby, EPOSS does two Earth flybys with a flyby radius of 1.08 and 1.10 times the radius of Earth, respectively, where the relative velocity is even more increased. This increase in energy is also the reason why the apoapse in the second leg is bigger. This sequence allows it to transfer from Earth to Saturn (ID-I) in a leg time of 2006.6 d, or 5.5 y.

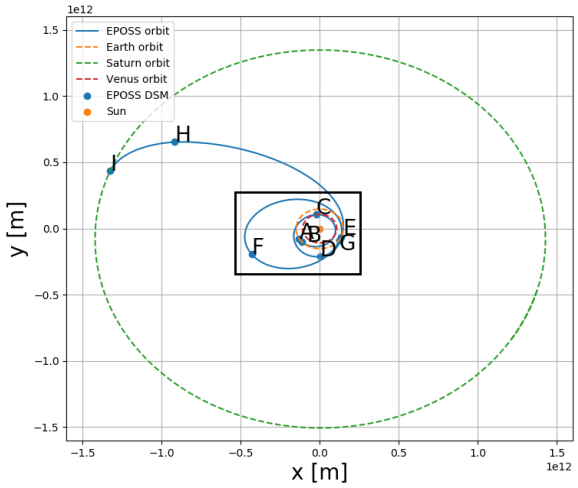

Figure 4.1: Interplanetary trajectory E-V-E-E-S.

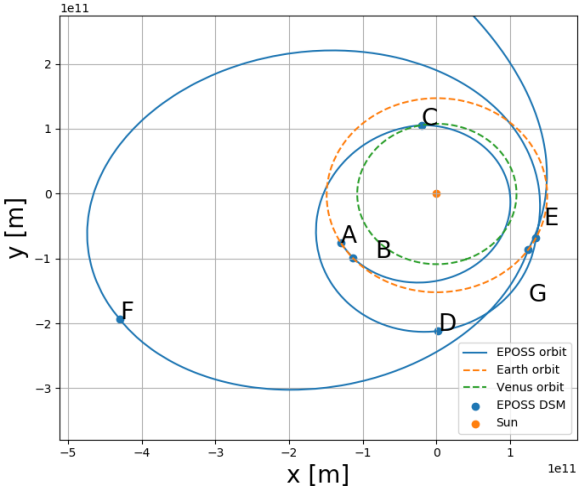

Figure 4.2: Zoomed-in interplanetary trajectory.

Table 4.1: Interplanetary transfer details.

ID	Type	Where	Leg time [d]	Delta V [m/s]
A	Launch	Earth	10336.9 [mjd2000]	V_∞ = 3500.0 m/s
B	DSM	Earth-Venus	After 9.9	24.7
C	GA	Venus	173.7	0.0
D	DSM	Venus-Earth	After 219.1	5.6
E	GA	Earth	319.4	0.0
F	DSM	Earth-Earth	After 667.7	197.9
G	GA	Earth	1087.4	0.0
H	DSM	Earth-Saturn	After 985.6	541.2
I	Arrival	Saturn	2006.6	V_∞ = 5237.3 m/s

4.1.2. In System Orbit

Phase two: Saturn Orbit Insertion (SOI) occurs between Saturn's F and G rings at a distance of 160,000 km (Closest Approach (CA)) via an injection burn (SOI-1). Orbit at arrival is tangent to where orbit injection occurs. EPOSS' capture orbit has a geometry of $160 \cdot 10^3$ $\times 11,879 \cdot 10^3$ km. An apoapse burn (SOI-2) will increase the orbit to $1,300 \cdot 10^3$ $\times 11,879 \cdot 10^3$ km. EPOSS' Saturn capture orbit is illustrated in Figure 4.3 and its parameters are described in Table 4.2.

Phase three: EPOSS' orbit geometry is reduced in size from $1,300 \cdot 10^3$ $\times 11,879 \cdot 10^3$ km to $257 \cdot 10^3$ $\times 1,300 \cdot 10^3$ km. Four dedicated Titan flybys (Titan FB-1 through Titan FB-4) are included in the design to facilitate this change. Each consecutive orbit is designed to be resonant with Titan's orbital period. Results are summarised in Table 4.2 and an illustration is provided in Figure 4.4.

Table 4.2: Orbit details for the capture orbit and subsequent resonance hopping sequence [90, p. 3-4].

Orbit design element	SOI-1	SOI-2	Titan FB-1	Titan FB-2	Titan FB-3	Titan FB-4
Periapse [km]	160,000	1,310,000	1,310,000	1,139,191	561,451	257,000
Apoapse [km]	11,879,328	11,879,328	2,580,087	1,310,000	1,310,000	1,310,000
Inclination [deg]	26.8	26.8	26.8	21.4	15.9	10.45
Resonance [Titan-EPOSS]	[-]	[-]	02:01	01:01	02:03	16:31
orbital period [day]	87.2	99.9	31.9	15.9	10.6	8.2
ΔV [m/s]	561	350	6	6	6	10

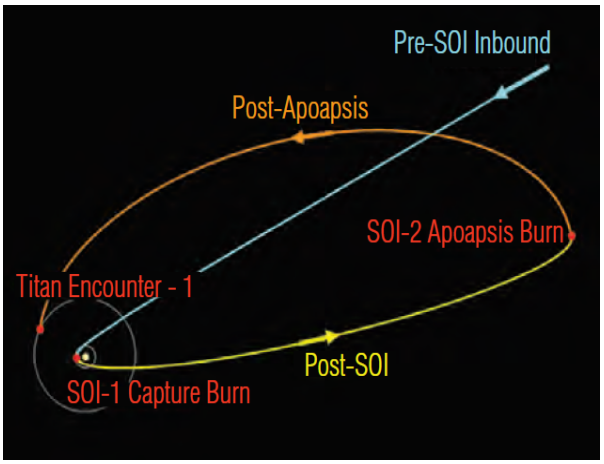

Figure 4.3: Description of the capture orbit including burns and Titan encounter [90, figure 3.1.1-3].

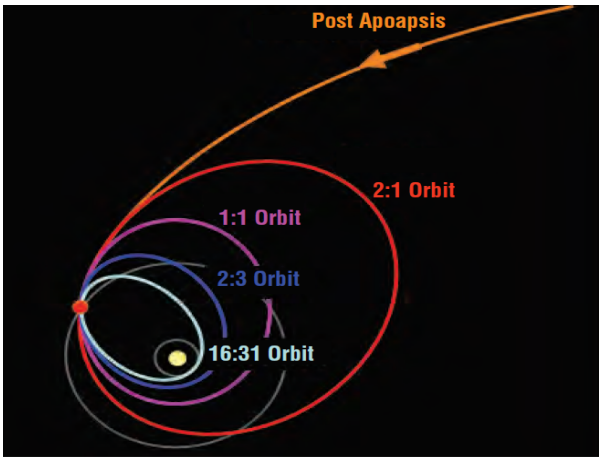

Figure 4.4: Illustration of resonance orbit designs for Enceladus encounter [90, figure 3.1.1-4].

Phase four: Four Enceladus flybys (Enceladus FB-1 through Enceladus FB-4) are included in the design. One flyby (red) is dedicated to imaging the northern pole with a closest approach at 1500 km. Three flybys are dedicated to the south pole where two flybys (gold, green) are dedicated to radar science with closest approaches at 200 km and one (blue) to imaging with a closest approach at 1500 km. Flyby geometries are described in Table 4.3, EPOSS' projection on Enceladus' surface within imaging range (for flybys one and two) and radar range (flybys three and four) is illustrated in Figure 4.5. This projection is equivalent to the ground track in the plane containing the north pole and the line tangent to the moon's orbit. EPOSS' distance to the moon per flyby is presented in Figure 4.6.

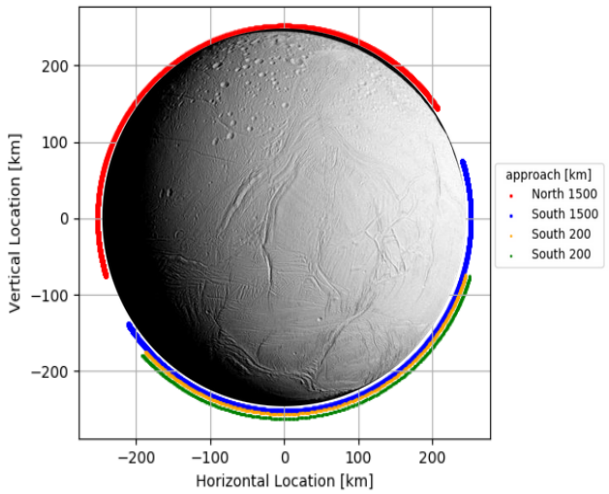

Figure 4.5: Illustration of EPOSS' projected surface position within imaging/radar distance for each flyby.

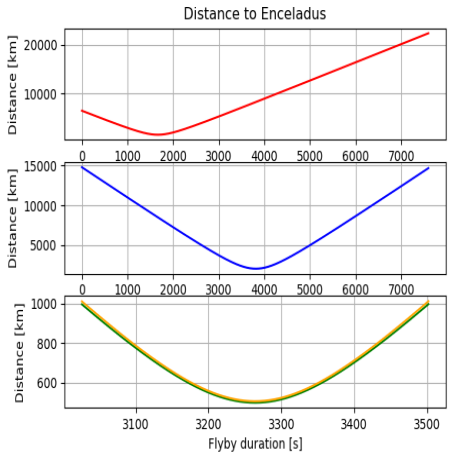

Figure 4.6: Illustration of EPOSS' variation of distance to Enceladus with time per flyby (see subsection 4.3.4).

Phase five: A fifth Titan flyby reduces orbit size further. Four Daphnis flybys (Daphnis FB-1 to Daphnis FB-4) are designed to observe Daphnis' leading edge (2x: red, blue) and to observe its trailing edge (2x: orange, green). Results are described in Table 4.3. Surface projection during imaging and radar observations are presented in Figure 4.7 and Figure 4.8 respectively

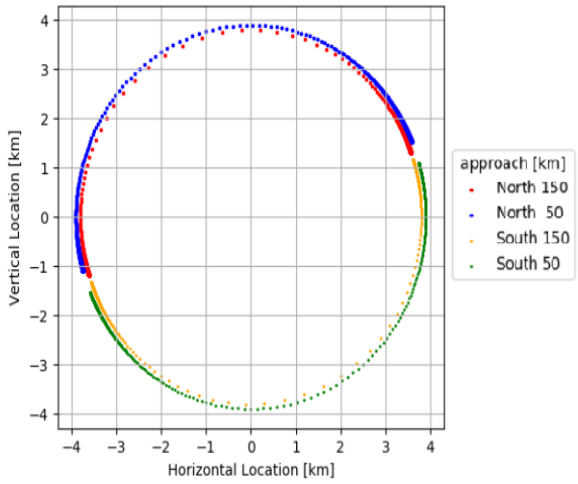

Figure 4.7: Illustration of EPOSS' projected surface position within imaging distance per Daphnis flyby.

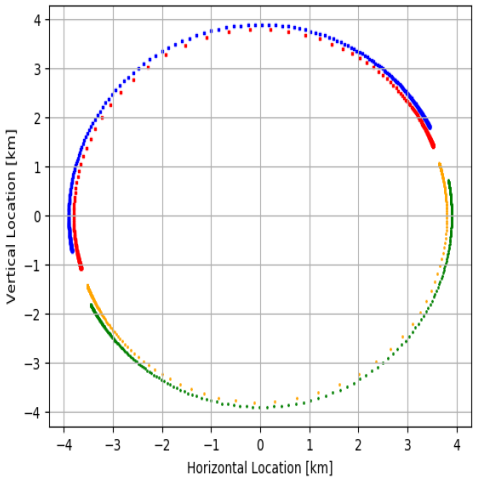

Figure 4.8: Illustration of EPOSS' projected surface position within radar distance per Daphnis flyby.

Table 4.3: Orbit details for the Enceladus, Titan-5, and Daphnis flybys.

Orbit Design Element	Enceladus FB-1	Enceladus FB-2	Enceladus FB-3	Enceladus FB-4	Titan FB-5	Daphnis FB-1	Daphnis FB-2	Daphnis FB-3	Daphnis FB-4
Distance at periapse [km]	4,100	4,800	2,200	2,200	[-]	450	150	150	450
Periapse [km]	257,000				136,505				
Apoapse [km]	1,310,000								
Inclination [deg]	5	6	3	3	5	5	5	5	5
Close approach [deg]	111.5	17.3	282.6	282.6	[-]	111.8	113.6	281.3	287.6
$T_{Imaging}$ [min]	190.7	186.5	198.3	198.3	[-]	61.8	62.6	63.4	64.2
T_{Radar} [min]	0	0	54.9	54.9	[-]	5.5	5.6	5.6	5.5
orbital period [day]	8.2	8.2	8.2	8.2	7.75	14.6	14.6	14.6	14.6
ΔV [m/s]	6	6	6	6	10	12.3	6	6	6

Phase six: A moon tour including a series of non-tangent V_∞ leveraging manoeuvres (see [28]) is included in the design to reduce the required Enceladus orbit insertion (EOI) velocity change. Periapse is raised to 527.11 km to initiate the tour via three Titan flybys (Titan FB-6*8). Tour design includes fifteen Rhea flybys (Rhea Tour), ten Dione flybys (Dione Tour), twelve Tethys flybys (Tethys Tour), twelve Enceladus flybys (Enceladus Tour-1), and Enceladus Orbit Insertion (EOI-1). Secondary science for this phase is described in subsection 5.4.3. Parameters for this moon tour may be found in Table 4.4.

Table 4.4: Orbit details for the moon tour [28, p. 184].

Orbit design element	Titan FB-6*8	Rhea Tour	Dione Tour	Tethys Tour	Enceladus Tour-1	EOI-1
Final periapse [km]	527,108	377,400	294,6000	257,000	257,000	[-]
Number of Flybys [-]	3	15	10	12	12	[-]
period [day]	26.4	363	190	158	233	1
ΔV [m/s]	18	146	26	12	102	129

Phase seven: EPOSS enters Enceladus orbit at a 45 deg inclination and 200 km altitude (Prep-1). After two Enceladus days inclination is raised to 60 deg and altitude is lowered to 150 km for the nominal phase (Nom-1). When orbiting Enceladus EPOSS' orbit design includes three Nominal orbit phases (Nom-1 through Nom-3) alternated by polar phases (Pol-1 through Pol-3). The final polar phase is followed by a return to its preparation orbit (Prep-2). The orbiting phase is summarised in Table 4.5. Note that days are presented in Enceladean days for consistency with the description presented for the in-orbit science requirements subsection 5.4.1

Ground track for the nominal and polar orbits are illustrated in Figure 4.9 and Figure 4.10 respectively. Altitude variations, inclination variations, and the three-dimensional orbit can be seen in Figure 4.11 and Figure 4.12.

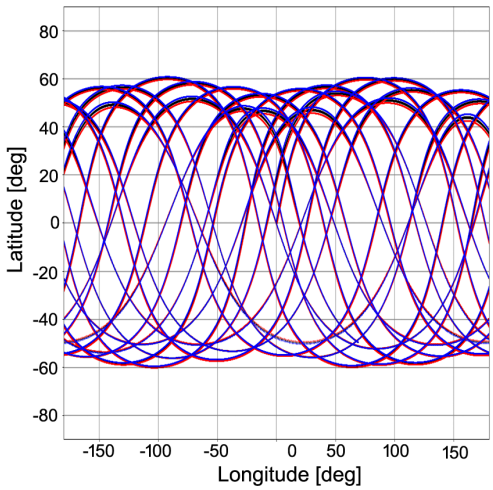

Figure 4.9: Five day nominal orbit ground track (black lines). VIMS coverage (blue and red lines).

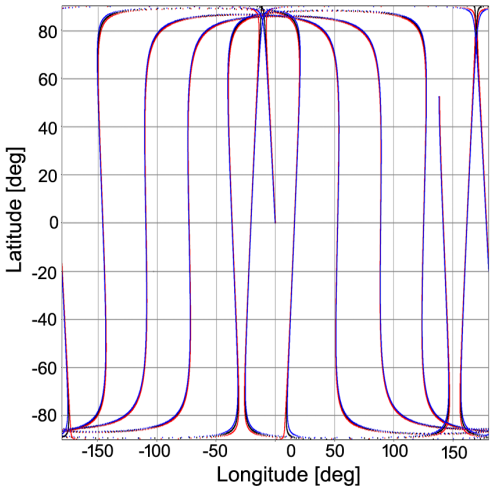

Figure 4.10: Polar orbit ground track (black lines). VIMS coverage (blue and red lines).

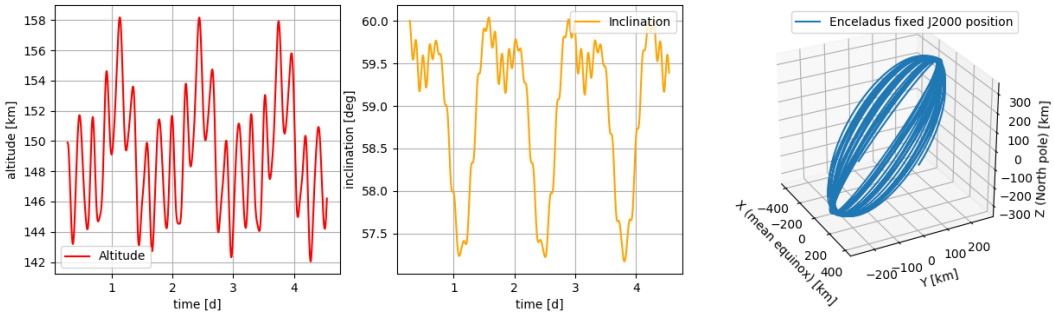

Figure 4.11: Altitude and inclination variations for the nominal orbit (5 days).

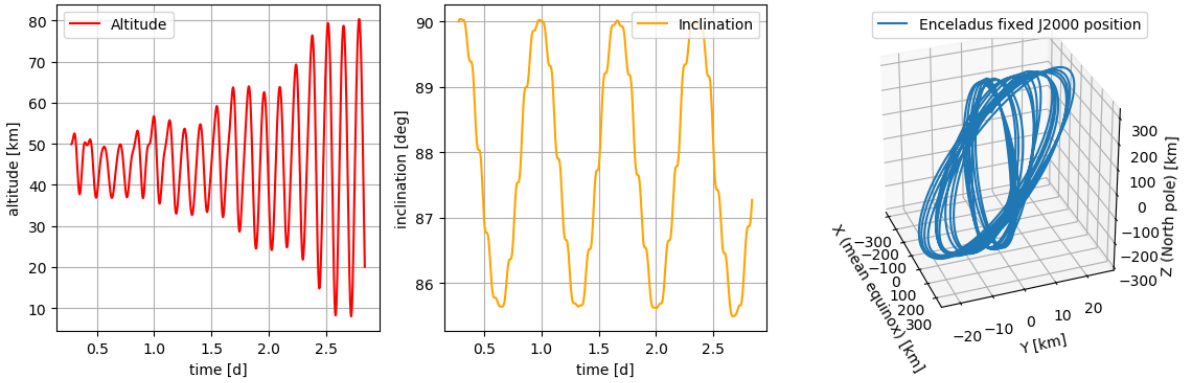

Figure 4.12: Altitude and inclination variations for the polar orbit (3 days).

Table 4.5: Description of orbiting phase characteristics.

Orbit design element	Preparation	Nom-1	Pol-1	Nom-2	Pol-2	Nom-3	Pol-3	EOM preparation
Altitude [km]	200	150	50	150	50	150	50	200
Inclination [deg]	45	60	90	60	90	60	90	45
Duration [Enceladus day]	2	204	1	144	1	104	1	2
ΔV Maintenance [m/s]	0.14	38.2	10	19.5	10	19.5	10	0.14
ΔV Inclination [m/s]	34.9	77.9	77.9	77.9	77.9	77.9	110.6	[-]

Phase eight: End of mission is designed to allow for extended mission designs. Orbit design accounts for Enceladus orbit ejection via an inverted insertion manoeuvre (Eject-1). Twelve Enceladus flybys (Enceladus Tour-2) raise apoapse to Tethys, inverting initial Enceladus approach (Enceladus Tour-1)[28, p. 184]. End of life occurs through a prospected Tethys impact (EOL-1). End of mission duration is 235 days and requires a velocity change of 231 m/s. Future iterations of the in-system orbit design may account for alternative EOL designs.

Contingency: EPOSS' contingency budget accounts for overall trajectory. To account for uncertainties in orbit determination around Enceladus (subsection 4.3.8), a 307 m/s contingency budget is included for the orbiting phase. To account for uncertainties in both manoeuvre specifications and orbit design, an additional 309.9 m/s is budgeted. Thus, total contingency budget is equal to 616.9 m/s. A complete overview of the budget and the percentages taken to determine them is presented in Table 4.6.

4.1.3. ΔV budget

The current projected velocity change, including contingencies, is 3696 m/s. Mission duration for both interplanetary transfer and in-system amount to 15.76 years. In system ΔV is equal to 2366 m/s. In system mission duration is 5.97 years. Results, decomposed per mission phase, are summarised in Table 4.6 and described in section 4.1.

Table 4.6: Current mission design ΔV budget.

Phase	Description	ΔV [m/s]	Duration
1	Interplanetary Transfer	1330	9.8 y
2	Orbit Capture	350.5	187.1 d
3	Resonance Tour	28	66.6 d
4	Enceladus flybys	24	28.7 d
5	Daphnis flybys	40.3	66.2 d
6	Moon Tour	433	970.4 d
7	Enceladus orbiting	642.3	624.5 d
8	End of mission	231	235 d
–	Contingency	616.9	[-]
–	Total	3696	15.76 y

4.2. Requirement Analysis

In this section the compliance of the trajectory subsystem is laid out via a compliance matrix (Table 4.7) as well as the verification methods employed to verify the trajectory and orbit subsystem.

As can be seen, the majority of the requirements are verified by analysis. This is due to the subsystem comprising mostly of software. This is also the reason why there is no mass and volume requirement. The C&DH subsystem will cope with this and thus the power budget for trajectory is a part of the C&DH budget. However, the specific number or fraction of this is beyond the scope of this project.

Table 4.7: Compliance matrix for the trajectory and orbit subsystem.

Code	Requirement	Verification Method	Compliance	Section
T&O-00.82	Trajectory shall be modifiable in-mission.	Analysis	✓	4.3.8, 4.3.8
T&O-02.04.01	The T&O subsystem shall allow for a fly-through through the plume with a temporal resolution of 2 months.	Analysis	✓	4.3.6
T&O-02.04.02	The T&O subsystem shall include at least one flyby through the plumes when Enceladus is on its furthest point form Saturn.	Analysis	✓	5.4.1, 4.3.6
T&O-02.04.03	The T&O subsystem shall include at least one flyby through the plumes when Enceladus is on its closest point form Saturn.	Analysis	✓	5.4.1, 4.3.6
T&O-03.02	The trajectory and orbit shall allow for the collection of data necessary to determine the gravity field to deg ≥ 8.	Analysis	✓	5.4.1, 4.3.6
T&O-08.01.02	The trajectory and orbit shall allow for surface observation over at least 50% of the surface of Enceladus.	Analysis	✓	4.1.2
T&O-08.01.02.01	The trajectory shall allow for minimally 50% of observation to include the surface between -20 and 20 deg latitude.	Analysis	✓	4.1.2
T&O-08.01	The trajectory and orbit subsystem shall include a visit of at least one Saturn shepherd moon, to be selected from Prometheus, Daphnis, Pan, Atlas, Janus, and Epimetheus.	Analysis	✓	4.1.2
T&O-08.03	The trajectory shall allow the observations of the leading edge of the shepherd moon.	Analysis	✓	5.4.2, 4.1.2
T&O-08.04	The trajectory shall allow the observations of the trailing edge of the shepherd moon.	Analysis	✓	5.4.2, 4.1.2
T&O-00.16.01	The orbit around Enceladus shall be in the altitude range of [30 - 160] km.	Analysis	✓	4.1.2
T&O-11.01	The trajectory and orbit subsystem shall include an end-of-life disposal trajectory.	Analysis	✓	4.3.7
T&O-00.83	The trajectory and orbit subsystem shall include calibration of transfer trajectory at initiation of transfer.	Test	✓	6.3.1
T&O-00.84	The trajectory and orbit shall allow for enough time and orbits for the required collection of data.	Analysis	✓	5.4.1
T&O-00.85	The trajectory and orbit shall be modifiable upon detection of impacting bodies.	Test	✓	6.3.3
T&O-00.86	The trajectory and orbit subsystem shall have a maximum mass of <->kg	Inspection	✓	-
T&O-00.87	The trajectory and orbit subsystem shall have a maximum volume of <->m^3.	Inspection	✓	-
T&O-00.88	The trajectory and orbit subsystem shall need a nominal power of maximally <->W.	Demonstration	✓	-
T&O-00.89	The trajectory and orbit subsystem shall need a peak power of maximally <->W.	Demonstration	✓	-
T&O-00.90	The trajectory and orbit subsystem shall include an in-mission validation process.	Analysis	✓	6.3.1
T&O-00.91	A safety margin of 5% shall be applied when using off-the-shelf components.	Analysis	✓	4.3.8
T&O-00.92	A safety margin of 10% shall be applied when using existing technology with minor modifications.	Analysis	✓	4.3.8
T&O-00.93	A safety margin of 15% shall be applied when using existing technology with major modifications.	Analysis	✓	4.3.8
T&O-00.94	A safety margin of 20% shall be applied when using completely new components.	Analysis	✓	4.3.8
T&O-00.95	The uplink data transferred for trajectory and orbit subsystem purposes shall take part of maximally 8% of the total.	Analysis	✓	9.3
T&O-00.96	The downlink data transferred for trajectory and orbit subsystem purposes shall take part of maximally 8% of the total.	Analysis	✓	9.3
T&O-00.97	The T&O subsystem shall have a cost of maximum 18.620 M €.	Inspection	✓	14.3
T&O-00.98	The T&O subsystem shall have a minimum reliability of 96.3 %.	Analysis	✓	13.5
T&O-00.99	The T&O subsystem shall have a data rate of maximally 0.0022 kb/s.	Demonstration	✓	9.2

4.3. Design Approach

This section details the design approach used to define orbit design elements discussed heretofore. Methods to evaluate potential design solutions and their implementation are elucidated. These methods include rigorous and critical studies of comparable missions, including actual and concept mission designs for scientific missions to Jupiter and Saturn, and through first order analysis of proposed orbits.

4.3.1. General

These methods are used extensively for analysing in-system orbit designs:
Extensive use of Titan gravity assists is used for the in-system orbit design. This allows for both reduction of ΔV requirements and maximum orbit design flexibility during the mission as each Titan flyby may impart ΔV_{Titan} = 800 m/s on EPOSS [26, p. 4]. Additionally, Cassini demonstrated through Titan flybys that orbit inclination may be changed in excess of 14 deg (Δi_{Titan}) [8, Table 1]. This value is used to define the number of Titan flybys required for Enceladus approach (4x), Daphnis approach (1x), and Rhea approach (3x). Furthermore, incorporating Titan gravity assists allow for maximum flexibility of the in-system mission design (see Table 4.7, T&O-00.82).

Moon flybys may require pre-flyby targeting and post-flyby clean-up manoeuvres. The flyby ΔV is derived from comparable missions and studies. Europa Clipper accounts for a velocity change of 2.78 m/s per flyby [24]. Cassini's orbit has demonstrated as little as a ΔV of

0.358 m/s per flyby [113]. Concept designs such as Enceladus Flagship Mission (EFM) and the analysis by Stefano Campagnole suggest flyby ΔV requirements of 10 and 6 m/s respectively [28]. To be conservative, whilst not over-designing ΔV requirements, a value of 6 m/s is chosen per flyby and 10 m/s per flyby including encounter manoeuvres [90, Table 3.3.3-4]. Encounter manoeuvres entail two additional orbit changing manoeuvres to change the orbital period causing the relative phase (moon-EPOSS) to shift, thereby requiring more ΔV. The flyby ΔV is used for sizing Titan flybys (1-4, 6-8), Enceladus flybys (2-4), Daphnis flybys (2-4), and EOL (1). The encounter ΔV for Titan flybys 4 and 5.

First order estimates for orbital periods were derived from Kepler's third law [65, p. 130]. With Saturn as central body (gravitational parameter: $\mu = 3.793 \cdot 10^{16}\ m^3/s^2$),[1] and orbit geometry as given in the tables in the previous section, the periods were found for SOI (1, 2), Titan flybys (5-8), Enceladus flybys (1-4), and the Daphnis flybys (1-4).

The vis-viva equation [65, eq. (6-4)] (see below) is used to find first order estimates of required manoeuvre ΔV. By considering the velocity at apoapse (V_a) and periapse (V_p) for subsequent orbit designs (semi-major axis (a), distance at apoapse (r_a [m]), distance at periapse (r_p [m]), and eccentricity (e)), an estimate of the required ΔV is found. Combined with ΔV_{Titan} the number of Titan flybys was determined (see above).

$$V_p = \sqrt{\frac{1+e}{1-e}\frac{\mu}{a}} \qquad V_a = \sqrt{\frac{1-e}{1+e}\frac{\mu}{a}} \qquad e = \frac{r_a - r_p}{r_a + r_p} \tag{4.1}$$

4.3.2. Interplanetary Transfer

The interplanetary transfer result is retrieved from [84, table 7.2], which uses the MGA-1DSM PyGMO optimization problem.[2] The input for this optimisation is the sequence of gravity assists (GA), launch interval, a range of leg times and a range of launch V_∞ values. The model also assumes that at least and only one DSM is done per leg. The output is the launch date, leg times, cartesian position per time interval, ΔV of the DSM, time of DSM and flyby radius. The total interplanetary ΔV with Saturn Orbit Insertion (SOI) of 1.330 km/s is not the most optimal velocity change that this optimisation problem found. However, other results have a launch date between 2022 and 2024 which is not feasible for this mission due to design, production and development time. One example is the development of the power subsystem, which is described in section 10.6 [84, p. 71]. It should be noted that there might be a more optimal result which is especially specified for EPOSS, but designing the optimisation problem with DSM is considered to be out of the scope of this study. However, the data retrieved from [84] is imported in a model to get the preferred output such as the cartesian position at a certain time. This can be seen in Figure 4.1.

The Venus Earth gravity assist is commonly used as a method to manipulate the orbit to achieve a large relative velocity with respect to Earth. This is especially useful for visiting outer planets and hence this is also used on EPOSS [50].

The result can be compared to a Hohmann transfer with a leg time of 6.089 y and a ΔV of 17.627 km/s or an optimal high thrust transfer with a leg time of 8.638 y and a ΔV 6.910

[1] Retrieved from `https://nssdc.gsfc.nasa.gov/planetary/factsheet/saturnfact.html` last opened on June 18, 2019

[2] Retrieved from `http://esa.github.io/pygmo/documentation/problems.html#PyGMO.problem.mga_1dsm_tof` last opened on June 17, 2019

km/s, where no use of a gravity assist is made. It can be seen that even though the transfer time of 9.8 y is longer, the savings on ΔV is major. [83] [42] [59, table 1.4.8.]

4.3.3. Saturn Capture Orbit

The main criteria for orbit insertion design are sufficient reliability (see Table 4.7, T&O-00.98), and sufficiently low ΔV to reduce cost (see Table 2.2, MIS-14). Multiple SOI geometries are studied. Insertions employing Titan aerogravity assists (one) are discarded due to an unacceptable risk of EPOSS burning up , resulting from inexperience with such manoeuvres [5, p. 14] and insufficient orbit determination accuracy at insertion [8, p. 2]. Initial estimates indicate that insertion near Titan (r = 1,300,000 km), accounting for the Titan gravity assist, requires a ΔV of 2127 m/s-Δ V_{Titan} = 1327 m/s. Insertion between Saturn's F and G rings (i.e. r = 160,000 km[3]) requires a ΔV of 835 m/s. Thus, further studies considered approach geometries near Saturn discussed hereafter.

Cassini demonstrated that insertion through the gap between the F and G rings is feasible.[4] Additionally, many contemporary Saturn moon orbiter concept designs include similar insertion geometries through the F-G gap [64] [90, p. 3-3]. Insertion through gaps closer to Saturn results in unacceptable risk of EPOSS impacting with Saturn's rings due to gap sizes[1] in conjunction with orbit determination accuracy at insertion, and due to insufficient knowledge on the composition of these regions[64, p. 5].

An initial estimate of insertion ΔV used in this section is computed using the vis-viva equation [65, eq. (6-4)] rewritten to:

$$\Delta V_{Insertion} = \sqrt{V_{\infty}^2 + \frac{\mu_{Saturn}}{r_{Saturn}}} - \sqrt{\frac{\mu_{Saturn}}{r_{Saturn}}} \tag{4.2}$$

V_{∞} describes hyperbolic excess velocity ms^{-1} and r the distance to the central body m. Values used are V_{∞} = 5247 m/s (subsection 4.1.1) and r values as described above. The actual ΔV is derived from the interplanetary transfer study discussed in subsection 4.3.2.

Capture orbit geometry (following SOI-1) is designed similar to Cassini's[5] and the Enceladus flagship mission concept (similar design and mission) [90]. Capture orbit geometry will be $11,879 \cdot 10^3 \times 160 \cdot 10^3$ km.

At apoapse the periapse will be raised to intersect with Titan's orbit (r = 1,300,000 km) for future in-system gravity assists [90, p. 3-4]. For future orbit design EPOSS' will be assumed to always encounter Titan at this distance. ΔV for the periapse raise (SOI-2) is taken from the same source as the geometry of the capture orbit [90, p. 3-4].

4.3.4. Flyby Geometry

Titan flyby geometry is designed to quickly reduce orbit size (semi-major axis (a), r_p, and r_a) and inclination. Orbit inclination depends on the intended target. At insertion EPOSS' orbit

[3]Retrieved from 17/06/2019https://caps.gsfc.nasa.gov/simpson/kingswood/rings/ last opened on June 17, 2019

[4]Retrieved from http://sci.esa.int/cassini-huygens/34955-approach-and-arrival/ last opened on June 17, 2019

[5]Retrieved from https://www.esa.int/esapub/bulletin/bullet92/b92kohlh.htm last opened on June 19, 2019

is inclined by 26.74° with respect to Titan's orbital plane.[6] To observe Enceladus Titan flybys (1-4) reduce inclination with 5.5 deg per flyby (max is 14). To observe Daphnis inclination is increased to five deg (Titan Fb-5) In order to create sufficient distance between EPOSS and Saturn's rings during the transition through its rings. To initiate the moon tour (subsection 4.3.5) inclination is reduced to zero (Titan FB-6).

Titan flyby orbit geometries follow from the Intended target. To encounter Enceladus a resonance hopping orbit design (Titan FB 1-4) is proposed based on research put forward for EFM [90, p. 3-4] and by Stefano Campagnola [28]. Such a design reduces orbit size quickly by minimising periods between flybys through resonance between EPOSS' orbital period and Titan's orbital period [96]. Geometries for the remaining Titan flybys depend on the target moons where periapse for Enceladus flybys is r_p=257,000 km (Titan FB-4) [90], at Daphnis is 136,505 km,[7] (Titan FB-5) and at Rhea is 527,108 km (Titan FB-8)

During Enceladus flybys (1-4) EPOSS will be resonant with both Titan and Enceladus [90, p. 3-4]. For Daphnis flybys EPOSS will be made resonant with Daphnis' orbital period after the first encounter by lowering apoapse to 1,295,000 km at the expense of 12.3 m/s (Equation 4.1) resulting in an encounter every two EPOSS orbits.

To design the Daphnis and Enceladus flyby geometries (i.e. EPOSS' angle of closest approach, semi-major axis, and orbital inclination) two simplifying assumptions are made. A small angle approximation of $\pm$ four deg around periapse is assumed. Where the small angle approximation is applicable the problem is reduced to a two dimensional problem (i.e. relative variation in radial distance to Saturn is negligible for the region of interest). The second assumption is that the velocity computed for periapse (Equation 4.1) is considered constant. EPOSS' orbit periapse will be designed to coincide with the target moon's orbit. To define the aforementioned flyby geometry software is developed by the authors to iterate over a large range of distance at periapse and inclination combinations. For each combination the bodies are propagated with constant velocities from starting-positions defined by the required closest approach (see section 5.4). Additional constraints for flyby geometry (i.e. EPOSS' orbit determination during flybys) include: limited inclination variation per flyby to reduce ΔV requirements, the ability to observe both body's northern and southern poles, the ability to observe Daphnis' leading- and trailing edge, and maximising the period for imaging and radar science.
Outputs of this process meet the aforementioned requirements and are given in terms of angle of closest approach, available time for radar science, and available time for imaging. The resultant flyby geometries meeting the scientific requirements stipulated in subsection 5.4.1 are presented in Table 4.3.

For Daphnis flybys Saturn's rings impose an additional safety concern. The Keeler gap width is 30 kilometres. [8] Orbit determination for interplanetary spacecraft may be up to 5 metres accurate [119]. EPOSS' orbit is designed to transition through the centre of the Keeler gap (i.e. 15 km from the edge). An offset of 5 metres in orbit determination is thus inconsequential to the spacecraft's safety. Additionally, using the equation for distance to a focus for an ellipse[9]

[6] Retrieved from `https://nssdc.gsfc.nasa.gov/planetary/factsheet/saturnfact.html` last opened on June 22, 2019
[7] Retrieved from `https://solarsystem.nasa.gov/moons/saturn-moons/daphnis/in-depth/` last opened on June 19, 2019
[8] Retrieved from `https://caps.gsfc.nasa.gov/simpson/kingswood/rings/` last opened on June 17, 2019
[9] Retrieved from `https://en.wikipedia.org/wiki/Ellipse` last opened on June 19, 2019

to determine the distance to Saturn it is found that at 3000 kilometres from periapse the radial distance differs with 15 kilometres (i.e. it crosses over the rings). For the designed orbit geometry (see Table 4.3, inclination of fie degrees) this results in an altitude of 264.5 kilometres above the plane containing Saturn's rings. The rings are approximately 99 meters wide[10], consequentially, EPOSS is not at risk of impacting Saturn's rings.

4.3.5. Moon Tour

EPOSS will feature a moon tour, selected based on duration and ΔV reduction, proposed and detailed by Ryan P. Russel and Stefano Campagnola [28] to reduce the required Enceladus orbit insertion ΔV. Details are summarised in Table 4.4. To initiate the moon tour periapse is raised to Rhea's orbit as described in subsection 4.3.1.

4.3.6. Orbiting Enceladus

Enceladus orbit insertion manoeuvres were derived from two sources. The first source indicates that a 200 km and 45 deg inclination orbit after insertion is feasible [90, p. 3-18]. The second source provides a velocity change associated with such a manoeuvre, equivalent to 129 m/s [28], following on the previously discussed moon tour. Enceladus orbit insertion design for EPOSS' is designed to insert at a 45 deg inclination, 200 km altitude initial orbit (Prep-1).

To meet the scientific requirements (see Table 4.7, T&O-02.04.01 through 02.04.03) when in orbit around Enceladus, as stipulated in Table 5.4.1, the orbit is designed such that it includes nominal orbit phases and polar orbit campaigns. Periods between the various in-orbit phases and their geometries are described in detail in subsection 5.4.1. The nominal orbit is designed to be at an inclination of 60 deg at an altitude of 150 km. The polar orbit campaign is designed to be at an inclination of 90 deg, at an altitude of 50 km.

To study the feasibility of these orbit designs both literature and orbit propagation software (TU Delft Astrodynamics Toolbox (TUDAT)[11]) have been used. Literature indicates that orbits up to ± 64 deg may be stable and that orbits exceeding this angle will become ballistic within short periods of times ranging from days to weeks [109]. These instabilities result from strong perturbations induced by Saturn's close proximity and Enceladus' comparative small mass, through Enceladus' non-spherical gravity field and via the difference in radii between Enceladus' poles [109]. Consequentially, these orbits are to be avoided at all costs when designing the nominal Enceladus orbiting phase. For the short period polar campaigns orbit designs with angles in excess of 85 deg have been studied.

TUDAT[9] software was used for propagating potential nominal orbits. Gravity fields for the Sun, Jupiter, Saturn, Enceladus, and Saturn's more massive moons were included. Additionally, up to second degree and second order harmonics for Saturn's and Enceladus' gravity fields were included in the study of feasible orbits (i.e. J2, C21, C22, S21 and S22). Solar radiation pressure was also included (coefficient 1.2, area 4.0). The orbit geometries studied for the nominal phase have inclinations ranging from 45 to 66 deg, where for each inclination varies altitudes were studied ([50, 100, 150, 200)]. This analysis used a Runge-Kutta4 method with a fixed step size of 5.0 seconds. Results were post-processed using Python software to obtain variations in altitude, inclination, longitude and latitude (i.e. coverage), and ascending nodes,

[10]Retrieved from `https://caps.gsfc.nasa.gov/simpson/kingswood/rings/` Last opened on June 23, 2019

[11]Retrieved from: `http://tudat.tudelft.nl/` last opened on June 20, 2019

amongst others. To meet the scientific requirements, as described in section 5.3, and based on the requirements associated with the selected instruments (see section 5.4), a preferred nominal and polar orbit are defined. From the range of feasible nominal orbits the orbit design with an inclination of 60 deg and altitude of 150 km was chosen.

Polar campaigns around Enceladus are inherently not stable [109] [90, p. 3-18]. Propagation of orbits with inclinations [84, 90] and altitudes [50, 100] confirm this behaviour, resulting in ballistic orbits after two to three days. To meet requirements three polar campaigns are included with inclinations of 90 deg and altitudes of 50 km. To avoid critical failure these polar campaigns will last at most a single Enceladus day.

ΔV requirements for combined velocity and inclination changes (see Table 4.5, transitioning between subsequent orbit geometries) were studied using the law of cosines and the method described in [65, p. 149]. Velocity for different altitude orbits around Enceladus were defined using Equation 4.1. Results for transitioning between different geometries and inclinations are summarised in Table 4.5. Periods for various orbits are discussed in subsection 5.4.1 and included in the same table (in Enceladus days).

Orbit maintenace strategies are taken from comparable mission designs such as the Titan Saturn System Mission (TSSM) [64], the decadal survey by NASA of a potential Enceladus orbiter [109], and EFM [90]. Orbit maintenance for a single day of the polar campaign will be equivalent to 10 m/s (Pol-1 through 3), Orbit maintenance for the sixty deg inclination phase is 50 m/s per year (Nom-1 through 3).

The resulting ground tracks, altitude variations, inclination variations and a three dimensional render of the orbit are presented in subsection 4.1.2.

4.3.7. End of Mission

End of mission design will avoid impacting moons with potential subsurface oceans, in accordance with the EPOSS Sustainability and Planetary Protection Policy (ESPPP). End of Mission designs including Saturn are discarded as no sufficient ΔV can be acquired to pass over the rings (Equation 4.1). End of Mission at Mimas (2) and Tethys (3) are also considered. Less ΔV is required to raise periapse to Tethys than to reduce orbit to Mimas ([28], Equation 4.1). Additionally, Tethys is both larger and more massive than Mimas. Thus, the chance of successful end of life increases. An inverted moon tour to the one described in subsection 4.3.5 is designed to take EPOSS from Enceladus to Tethys (Enceladus Tour-2).

4.3.8. Contingency

To account for uncertainties in orbit design a contingency value applied to all manoeuvres has been included. This value accounts for an additional thirteen percent ΔV to accommodate any future changes. This value reflects the state of the current detail design. A contingency of 13% is taken as primarily minor and major modifications to existing orbit designs are used to design EPOSS' orbit (see Table 4.7, T&O 00,93 and T&O 00.92).
To account for uncertainties in the stability of the orbit design a large orbit phase contingency is included. Results are summarised in subsection 4.3.6. This contingency value accounts for an additional 200 percent ΔV dedicated to orbit maintenance and a 77 m/s ΔV associated with an additional inclination change. This budget is inspired by EFM [90, p. 3-1] but is lower as increased knowledge about orbits around Enceladus is available. This contingency allows for additional flexibility for in-system orbit design (T&O-00.82).

4.4. Verification & Validation

Several V&V methods are employed. The requirement verification methods are described in Table 4.7. It can be seen that for the main design properties of this subsystem analysis is used as the verification method. This is because trajectory and orbit is done with software and propagation measures; it is not a physical object. However, the mass, power, and cost as well as the safety margins can be verified upon inspection.

Four models are validated as part of T&O verification and validation. The software developed for TUDAT for identifying and detailing the interplanetary transfer orbit and the orbits in the Enceladus orbit phase (subsection 4.3.6). Further software was developed by the authors for analysis of the obtained coverage during the Enceladus orbit phase (section 4.1) and for the analysis and selection of (feasible) flyby geometries (subsection 4.3.4).

The models used to detail orbits around Enceladus and the results produced through TUDAT when using these models are validated by comparison with research on Enceladus orbiters and their orbit designs, and through an analysis of expected results for basic orbit propagation. Basic orbit propagation of unperturbed two body problems and perturbed (including higher degree gravitational fields) two body problems result in the expected circular orbit and right ascension of the ascending node respectively. When expanding the model to describe Saturn's system, including J2 values for Saturn and Enceladus (subsection 4.3.6), the results indicate stable orbits at 45 deg, with increasingly larger oscillations in altitude, eccentricity, and amplitude for increasingly larger inclinations. These results coincide with research indicating that orbits with inclinations at ninety deg will become ballistic after 2-3 days (Figure 4.12) and that orbits in excess of 50 deg become increasingly less stable [109] [97] [90]. Thus, the results produced for the Enceladus orbit phase, presented in the overview, are validated through this study. Additionally, the orbits propagated here have been used to validate the model detailing in-orbit coverage. The unperturbed orbit resulted in expected constant distance between two measurements and swath width. The perturbed Enceladus orbit resulted in variations in swath width and pacing corresponding to variations in altitude and velocity profiles. This indicates that these results are valid.

TUDAT was also used to validate results presented for the interplanetary transfer [84]. The ΔV budget is influenced a lot by the addition of the interplanetary transfer. Since this budget is retrieved from a single source, it should be made sure that this result is feasible. The inputs from the paper (launch V_{inf}, leg times, DSM burns and times and rotation angles of GA) have been imported into TUDAT,[1] which showed the same result as the paper.

The flyby geometries designed to meet the scientific requirements at Daphnis and Enceladus, stipulated in section 5.4, were validated through a study of the accuracy of the obtained results (see Table 4.3 for EPOSS' orbit geometry, see subsection 4.3.4 for the method). The flyby geometry is approximated to be co-circular (two dimensional problem) for a region of $\pm$ four degrees around EPOSS' periapse at both Daphnis and Enceladus. The accuracy of the solution is studied by comparing the obtained results for distance and ground track to the actual three dimensional results for two critical cases. This entails a study of the distance at $\pm$ four degrees from EPOSS' periapse at first Enceladus and second Daphnis. The resultant deviation, using the equation for radial distance introduced in subsection 4.3.4, is found to be less than 0.11 percent. Consequentially it is found that the results are sufficiently accurate

and that the obtained geometries shall satisfy the requirements stipulated in section 5.4.

4.5. Sensitivity Analysis

In the design phase some parameters are more influencing than others. The change in value of those parameters are discussed in this section. Firstly, the number of flyby of Enceladus/-Daphnis can change. This can be due to a more strict payload requirement which leads to more observations, or if the flyby scientific yield is decreased per fly by, for instance due to a change in altitude. If the number of flybys are increased, the amount of manoeuvres is increased and thus the ΔV and mission time is increased. Therefore, the flyby number should be kept to a minimum when designing the trajectory design. This also holds for the Enceladus orbit. Secondly, if the launch window is changed, the trajectory is changed because of the ephemerides of the planets. This change can lead to a reduction/increase in ΔV. As already mentioned before in subsection 4.3.2, if the mission was to be launched in 2024 there would be a reduction of interplanetary ΔV of 517.7 m/s [84, table 7.2]. Finally, if the requirement of plume observations change by a means of observation accuracy, the 60 deg orbit would no longer be sufficient and more polar/higher inclination campaigns need to be done in order to fulfil the requirement. This adds extra ΔV to the budget. Now, it needs a ΔV of 87 m/s per polar campaign for inclination raise and maintenance. If the number of polar campaigns is doubled this would imply an extra ΔV of 261 m/s to the budget.

4.6. Risk Analysis

The failures in trajectory can be caused by several instances, which are further elaborated upon in this section. After the highest risks are identified, a fault tree diagram is given in Figure 4.13 as well as a mitigation of the risks.

1. **TRR-0.1 Polar orbit transition & maintenance failure:** during the orbit phase at Enceladus, there will be a number of transitions from an inclination of 60 deg to 90 deg. As it is known that a 90 deg inclination orbit is unstable and that the exact gravity field of Enceladus is not known yet, it imposes a risk on the trajectory and the propagation of it. To mitigate this risk a contingency budget is taken into account which can be seen in subsection 4.1.2.
2. **TRR-0.2 Impact with other body:** the propagation of the trajectory, interplanetary as well as in-system, did not consider other bodies except for the ones that are relevant to the mission. For instance, EPOSS could impact with an asteroid and cause potential mission failure. The mitigation measures are introduced in the structural design (section 6.6), an on-board navigation camera which identifies bodies along the way and a requirement for the propulsion subsystem to perform manoeuvres to avoid this risk.
3. **TRR-0.3 Incorrect ΔV budget:** The possibility of underestimating the required number of flybys and time in orbit around Enceladus, may lead to an underestimation of the required ΔV. By including a ΔV budget and incorporating Titan flybys and a modifiable end of mission the ramifications of this deficiency and the risk it poses to the primary requirements of EPOSS are mitigated.

These risks are laid out in a fault tree which can be seen in Figure 4.13.

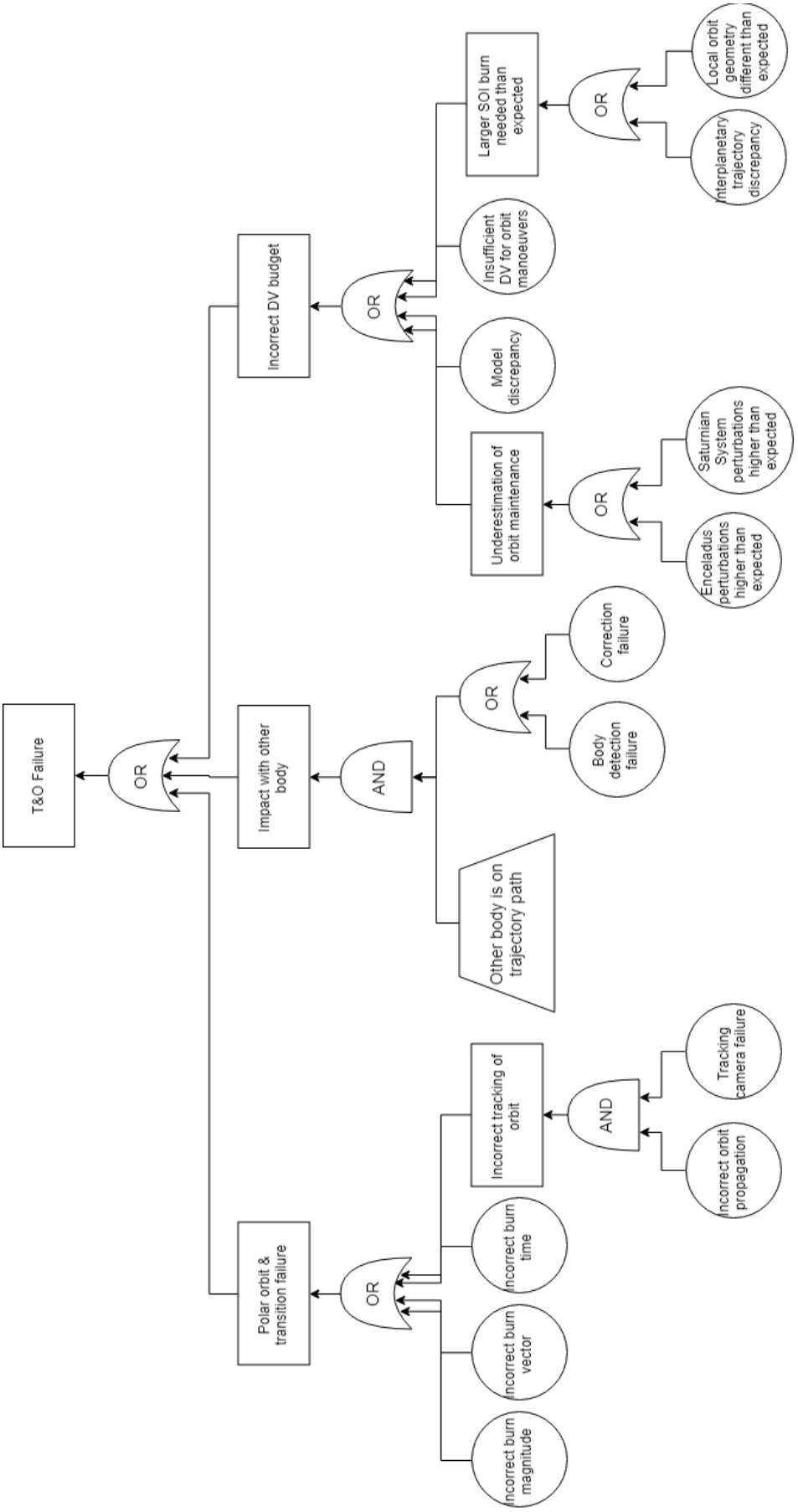

Figure 4.13: Fault tree of the trajectory and orbit subsystem.

5 Payload

This chapter discusses the selected payload, giving an overview of the instruments in section 5.1. A traceability matrix is shown and discussed in section 5.2, followed by a requirement analysis in section 5.3. The approach and compliance with requirements is then justified in section 5.4, where secondary science is also discussed. Verification and validation, sensitivity analysis, and risk analysis are discussed in section 5.5, section 5.6, and section 5.7 respectively.

5.1. Design Overview

A total of eight instruments have been selected for the EPOSS mission. Said selection is the outcome of a thorough trade-off that considered both the EPOSS requirements and the capabilities of existing instruments, as presented in [10]. As of now, the instruments comprising the payload are as presented in Table 5.1, where corresponding mass, power and data rates are also given. To the masses presented, a 10% contingency is added to account for modifications which can be seen in Table 14.3. Table 5.6 shows that the EPOSS mission has met the following requirements: PLD-00.18, PLD-00.19, PLD-00.24, PLD-00.25, PLD-00.30, PLD-00.31 (Table 5.4), PLD-00.44, PLD-00.45, PLD-00.49, PLD-00.50, PLD-00.55, PLD-00.56 (Table 5.5) and PLD-00.67 (Table 5.6).
Only one major change has been made since the payload list presented in the previous report [10], namely the use of the *Jovis, Amorum ac Natorum Undique Scrutator* (JANUS) (from the JUpiter ICy Moons Explorer (JUICE)) instead of the Titan Imaging and Geology, Enceladus Reconnaissance (TIGER) (from Enceladus to Titan (E2T)). Said modification was necessary because TIGER does not fulfil all imaging requirements (PLD-05.01, Table 5.5), namely, it does not image in the visible spectra. JANUS, conversely, can image in both the visible and near infrared spectra.
The T&O and payload subsystems optimised the trajectory for satisfying the requirements and came up with the allocation of the instruments during the trajectory. This allocation can be found in Table 5.7, Table 5.8, and Table 5.9.

Table 5.1: Overview of payload instruments, with corresponding mass, power and data rates.

	Imaging	Spectrometer	Radar	Altimeter	Magnetometer	Radio science	Particle characterisation	
Instrument	**JANUS** [51][69]	**VIMS** [1]	**REASON** [2]	**BELA** [58]	**MERMAG** [103]	**MORE** [103]	**ENIJA** [74]	**INMS** [74]
Mission	JUICE	Cassini	Europa Clipper	BepiColombo	BepiColombo	BepiColombo	E2T	E2T
Mass [kg]	27.5	37.1	32.3	12.1	2.5	3.5	3.5	6.2
Nominal power [W]	42.0	27.2	55.0	43.2	4.7	15.0	14.2	34.0
Nominal data rate [kb/s]	7.3	182.8	25000.0	1.1	2.3	0	0.5	0.5

5.2. Traceability Matrix

The relation between instruments and their primary scientific goals is illustrated using a traceability matrix. All mission goals are complied with (see Table 5.4, Table 5.5, and Table 5.6). As the table indicates, some instruments can also be used towards fulfilment of a particular requirement even when not being dedicated to it. Per science category (row), green boxes implicate that its respective instrument(s) are the primary data sources, yellow boxes imply that data from these instruments (secondary) can augment or replace the data from primary sources. Due to restrictions in data downlink not all secondary science instruments are used per science category.

Table 5.2: Daphnis traceability matrix.

Instruments			**JANUS**	**VIMS**	**REASON**	**MERMAG**	**BELA**	**MORE**	**ENIJA**	**INMS**
Minimum operational time			28 minutes in flyby	28 minutes in flyby	5.5 minutes in flyby	\	5.5 minutes in flyby	\	110 minutes in flyby	\
Daphnis	Science objectives	Requirement								
	Plumes and Particles	PLD-08.06								
		PLD-08.07								
		PLD-08.08								
		PLD-08.09								
		PLD-08.10								
		PLD-08.11								
	Geophysical	PLD-08.01.01								
		PLD-08.02.01								
	Remote sensing	PLD-08.03								
		PLD-08.04								
		PLD-08.05								

Table 5.3: Enceladus traceability matrix.

Instruments			**JANUS**	**VIMS**	**REASON**	**MERMAG**	**BELA**	**MORE**	**ENIJA**	**INMS**
Minimum operational time			141 days in orbit with i = 60 deg and 0.3 days in orbit with i = 90 deg Two flybys	2.1 days in orbit with i = 60 deg Two flybys	2 days in orbit with i = 60 deg Two flybys	1 day in orbit with i = 45 deg and 229 days in orbit with i = 60 deg Two flybys	21 days in orbit with i = 60 deg and 1.6 days in orbit with i = 90 deg	1.5 days in orbit with i = 45 deg, 320 days in orbit with i = 60 deg and 2.1 days in orbit with i = 90 deg Four flybys	42 days in orbit with i = 60 deg and 0.3 days in orbit with i = 90 deg	42 days in orbit with i = 60 deg and 0.3 days in orbit with i = 90 deg
Enceladus	Science objectives	Requirement								
	Plumes and Particles	PLD-02.02								
		PLD-02.03								
		PLD-02.05								
	Geophysical	PLD-01								
	Remote sensing	PLD-04								
		PLD-05								
		PLD-05.01								
		PLD-06								
	In-Situ	PLD-03								
		PLD-07								

Primary instruments provide sufficient (accurate) data to meet science requirements. Time indicated in days refers to Enceladean days (32.8 h). From Table 5.2 and Table 5.3 it is seen that the following requirements about the operating time are met: PLD-00.21, PLD-00.27, PLD-00.33, PLD-00.40, PLD-00.47, PLD-00.52, PLD-00.58 (Table 5.4, Table 5.5).
As seen in the matrix, not all requirements are fulfilled by more than one instrument. For particle characterisation at Daphnis, for example, only ENIJA operates. In said cases, failure of instrument is more detrimental to the mission. There where numerous supporting instruments are available (for example JANUS, REASON, ENIJA and INMS supporting PLD-06, Table 5.5), failure of the main instrument (VIMS) would not compromise aquisition of data.

5.3. Requirement Analysis

A compliance is filled in to expand on the traceability matrix to include a description of requirements related to accuracy and instrument specifications. The payload complies with all requirements following on a series of iterations, explained in detail in section 5.4.

Table 5.4: Compliance matrix for the payload requirements [1/3].

Code	Requirement	Verification Method	Compliance	Section
PLD-01	The payload shall characterise the thickness of the crust of Enceladus up to 2 km.	Analysis	✓	5.4.1
PLD-08.01.01	The payload shall characterise the surface morphology of the shepherd moon with spatial resolution better than 50 m.	Analysis	✓	5.4.2
PLD-08.02.01	The payload shall characterise the surface composition of the shepherd moon with spatial resolution better than 50 m.	Analysis	✓	5.4.2
PLD-00.17	The Radar shall operate in the altitude range of 10-1000 km for required observations.	Analysis	✓	4.1.2
PLD-00.18	The Radar's operating maximum data rate shall be below 84000 kb/s.	Demonstration	✓	5.1
PLD-00.19	The Radar's nominal power consumption shall be below 58 W.	Demonstration	✓	5.1
PLD-00.20	The Radar's minimum storage memory required is 1700000 Mb.	Analysis	✓	9.3.2
PLD-00.21	The Radar's total operating time from launch to end-of-life shall have a minimum of 50 h.	Analysis	✓	5.2
PLD-00.22	The Radar's operating temperature range is 233 to 328 K.	Test	✓	11.3.2
PLD-00.23	The Altimeter shall operate in the altitude range of 10 to 10000 km for required observations.	Analysis	✓	4.1.2
PLD-00.24	The Altimeter's operating maximum data rate shall be below 1.5 kb/s.	Demonstration	✓	5.1
PLD-00.25	The Altimeter's nominal power consumption shall be below 46 W.	Demonstration	✓	5.1
PLD-00.26	The Altimeter's minimum storage memory required is 900 Mb.	Analysis	✓	9.3.2
PLD-00.27	The Altimeter's total operating time from launch to end-of-life shall have a minimum of 90 h.	Analysis	✓	5.2
PLD-00.28	The Altimeter's operating temperature range is 233 to 328 K.	Test	✓	11.3.2
PLD-02.02	The payload shall be able to characterise the particles in Enceladus' plume of mass larger than 500 amu.	Analysis	✓	5.4.1
PLD-02.03	The payload shall be able to characterise the particles in Enceladus' plume up to size of 2000 amu.	Analysis	✓	5.4.1
PLD-02.05	The Particle Analyzer shall measure the particles in Enceldaus' plume at least 24 times with a temporal resolution of 2 months.	Analysis	✓	5.4.1
PLD-08.06	The payload shall determine the compostion of the ring particles in the vicinity of the selected shepherd moon.	Analysis	✓	5.4.2
PLD-08.07	The payload shall determine the size distribution of the ring particles in the vicinity of the selected shepherd moon.	Analysis	✓	5.4.2
PLD-08.08	The payload shall determine the dynamics of the ring particles in the vicinity of the selected shepherd moon.	Analysis	✓	5.4.2
PLD-08.09	The payload shall determine the compostion of the particles in the gap of the selected shepherd moon.	Analysis	✓	5.4.2
PLD-08.10	The payload shall determine the size distribution of the particles in the gap of the selected shepherd moon.	Analysis	✓	5.4.2
PLD-08.11	The payload shall determine the dynamics of the particles in the gap of the selected shepherd moon.	Analysis	✓	5.4.2
PLD-00.29	The Particle Analyzer shall operate in the altitude range of 0 to 200 km when observing the plumes.	Analysis	✓	5.4.1
PLD-00.30	The Particle Analyzer's operating maximum data rate shall be below 0.55 kb/s.	Demonstration	✓	5.1
PLD-00.31	The Particle Analyzer's nominal power consumption shall be below 36 W.	Demonstration	✓	5.1
PLD-00.32	The Particle Analyser's minimum storage memory required is 1800 Mb.	Analysis	✓	9.3.2
PLD-00.33	The Particle Analyser's total operating time from launch to end-of-life shall have a minimum of 1018 h.	Analysis	✓	5.2
PLD-00.34	The Particle Analyser's operating temperature range is 233 to 328 K.	Test	✓	11.3.2

Table 5.5: Compliance matrix for the payload requirements [2/3].

Code	Requirement	Verification Method	Compliance	Section
PLD-08.03	The payload shall make observations of the leading edge of the shepherd moon.	Analysis	✓	5.4.2
PLD-08.04	The payload shall make observations of the trailing edge of the shepherd moon.	Analysis	✓	5.4.2
PLD-04	The payload shall produce global surface imaging in visible and near infrared of Enceladus with a spatial resolution better than 2 km.	Analysis	✓	5.4.1
PLD-05	The payload shall be able to image selected areas of Enceladus in the visible and near infrared spectra with spatial resolution of better than 50 m.	Analysis	✓	5.4.1
PLD-05.01	The payload shall be able to image selected areas of Enceladus in the visible and near infrared spectra in wavelength range between 350 nm to 5100 nm.	Analysis	✓	5.4.1
PLD-00.35	The Imaging Subsystem's field of view shall be maximum of 1.72 x 1.29 deg^2.	Demonstration	✓	5.4.1
PLD-00.36	The Imaging System shall operate in the altitude range of 10 to 10000 km.	Analysis	✓	4.1.2
PLD-00.37	The Imaging System's operating maximum data rate shall be below 8 kb/s.	Demonstration	✓	5.1
PLD-00.38	The Imaging System's nominal power consumption shall be below 45 W.	Demonstration	✓	5.1
PLD-00.39	The Imaging System's minimum storage memory required is 36000 Mb.	Analysis	✓	9.3.2
PLD-00.40	The Imaging System's total operating time from launch to end-of-life shall have a minimum of 3500 h.	Analysis	✓	5.2
PLD-00.41	The Imaging System's operating temperature range is 233 to 328 K.	Test	✓	11.3.2
PLD-08.05	The payload shall determine the bulk compostion of the shepherd moon within 5% of its total mass.	Analysis	✓	5.4.2
PLD-06	The payload shall be able to determine the global and surface composition of Enceladus with a spatial resolution better than 10 km	Analysis	✓	5.4.1
PLD-08.02.01	The payload shall characterise the surface composition of the shepherd moon with spatial resolution better than 50 m.	Analysis	✓	5.4.2
PLD-00.42	The Spectrometer's instantaneous field of view shall be maximum of 0.0005 x 0.0005 rad^2.	Demonstration	✓	5.4.1
PLD-00.43	The Spectrometer shall operate in the altitude range of 10 to 10000 km.	Analysis	✓	4.1.2
PLD-00.44	The Spectrometer's operating maximum data rate shall be below 185 kb/s.	Demonstration	✓	5.1
PLD-00.45	The Spectrometer's nominal power consumption shall be below 30 W.	Demonstration	✓	5.1
PLD-00.46	The Spectrometer's minimum storage memory required is 14000 Mb.	Analysis	✓	9.3.2
PLD-00.47	The Spectrometer's total operating time from launch to end-of-life shall have a minimum of 50 h.	Analysis	✓	5.2
PLD-00.48	The Spectrometer's operating temperature range is 233 to 328 K.	Test	✓	11.3.2
PLD-07	The payload shall characterise the magnetic field of Enceladus with accuracy better than 0.5 nT.	Analysis	✓	5.4.1
PLD-00.49	The Magnetometer's operating maximum data rate shall be below 3 kb/s.	Demonstration	✓	5.1
PLD-00.50	The Magnetometer's nominal power consumption shall be below 5 W.	Demonstration	✓	5.1
PLD-00.51	The Magnetometer's minimum storage memory required is 7000 Mb.	Analysis	✓	9.3.2
PLD-00.52	The Magnetometer's total operating time from launch to end-of-life shall have a minimum of 5500 h.	Analysis	✓	5.2
PLD-00.53	The Magnetometer's operating temperature range is 233 to 328 K.	Test	✓	11.3.2
PLD-03	The payload shall be able to determine the global gravity field of Enceladus up to degree and order >= 8.	Analysis	✓	5.4.1
PLD-00.54	The Radio science shall operate in the altitude range of 0 to 200 km.	Analysis	✓	5.4.1
PLD-00.55	The Radio science's operating maximum data rate shall be below 0 kb/s.	Demonstration	✓	5.1
PLD-00.56	The Radio science's nominal power consumption shall be below 16 W.	Demonstration	✓	5.1
PLD-00.57	The Radio science's minimum storage memory required is 0 Mb.	Analysis	✓	9.3.2
PLD-00.58	The Radio science's total operating time from launch to end-of-life shall have a minimum of 7700 h.	Analysis	✓	5.2
PLD-00.59	The Radio science's operating temperature range is 283 to 303 K.	Test	✓	11.3.3
PLD-00.60	The payload shall operate at an overall altitude range of 0 to 10000 km.	Analysis	✓	4.1.2

Table 5.6: Compliance matrix for the payload requirements [3/3].

Code	Requirement	Verification Method	Compliance	Section
PLD-00.61	The payload shall allow for maximum lateral accelerations of 2g for stability during operation.	Test	✓	12.3.2
PLD-00.62	The payload shall allow for maximum angular accelerations of 6g mrad/s^2 for stability during operation.	Test	✓	12.3.2
PLD-00.63	The payload shall have a nominal power consumption of maximally 280 W on Enceladus.	Analysis	✓	10.3.2
PLD-00.64	The payload shall have a nominal power consumption of maximally 200 W on the shepherd moon.	Analysis	✓	10.3.2
PLD-00.65	The payload shall have a peak power consumption of maximally 135 W on Enceladus.	Analysis	✓	10.3.2
PLD-00.66	The payload shall have a peak power consumption of maximally 135 W on the shepherd moon.	Analysis	✓	10.3.2
PLD-00.67	The payload shall have a maximum mass of 200 kg.	Inspection	✓	5.1
PLD-00.68	The payload shall have a maximum volume of 1 m^3.	Inspection	✓	13.2
PLD-00.69	The system shall include in-mission validation system of payload.	Inspection	✓	2.2
PLD-00.70	The failure of one scientific instruments shall not compromise separate payload data acquisition.	Test	✓	5.2
PLD-00.71	Payload shall be able to identify bodies within a 20000 km range.	Analysis	✓	6.3.3
PLD-00.73	A safety margin of 5% shall be applied when using off-the-shelf components.	Analysis	✓	5.1
PLD-00.74	A safety margin of 10% shall be applied when using existing technology with minor modifications.[3]	Analysis	✓	5.1
PLD-00.75	A safety margin of 15% shall be applied when using existing technology with major modifications. [4]	Analysis	✓	5.1
PLD-00.76	A safety margin of 20% shall be applied when using completely new components.	Analysis	✓	5.1
PLD-00.77	The payload shall have a reliability of minimum 90.1%.	Analysis	✓	5.7
PLD-00.78	The payload shall have a minimum data rate of 0 kb/s.	Demonstration	✓	5.1
PLD-00.79	The payload shall have a maximum folded height of 3.5 m	Inspection	✓	12.3.1
PLD-00.80	The payload shall have a maximum folded width of 0.75 m	Inspection	✓	12.3.1
PLD-00.81	The payload shall be functional at the start of end of life	Analysis	✓	5.7

5.4. Design Approach

This section gives an overview of data recording distribution, and justifies requirement compliance for Enceladus (subsection 5.4.1) and Daphnis (subsection 5.4.2). Secondary science is considered in subsection 5.4.3.

5.4.1. Enceladus

Payload use

Enceladus payload requirements are met trough a combination of four flybys and an orbiting phase lasting 457 Enceladean days, and having a maximum nominal power of 105.3 W (Table 10.4). Twelve additional Enceladus flybys are performed before orbit insertion. These are not used for the main science as the spacecraft's ground-track will be above the equator, already covered during orbiting (subsection 4.1.2). The orbiting phase mainly consists of a 60 deg inclination orbit which allows for near global coverage from a height of 150 km, indicated as phase 2,4,5 and 7 in Table 5.7. As the camera, spectrometer, altimeter, and radar are shielded when the spacecraft crosses the plumes at this altitude (section 13.2), coverage at the poles is not achieved during the orbiting phase. Coverage will be achieved through dedicated flybys at the poles, flying at a higher altitude where the spacecraft does not interact with plumes (subsection 4.1.2). Particles of the plumes are characterised through the inclusion of three polar phases (3, 6 and 8 in Table 5.7, with 90 deg inclination and 50 km altitude) dedicated to said plumes. The 60 deg inclination orbit observes 15% of the plumes ensuring sufficient temporal coverage, complying with requirements as described in Table 5.4.1.

Table 5.7: Payload use summary per orbiting phase around Enceladus.

Orbiting phases	i [deg]	T [d=32.8 h]	JANUS	VIMS	REASON	BELA	MERMAG	MORE	ENIJA	INMS
phase 1	45	2					✓	✓		
phase 2	60	204	✓	✓			✓	✓	✓	✓
phase 3	90	1	✓			✓	✓	✓	✓	✓
phase 4	60	104					✓	✓	✓	✓
phase 5	60	40			✓	✓				
phase 6	90	1				✓	✓	✓	✓	✓
phase 7	60	104						✓	✓	✓
phase 8	90	1				✓	✓	✓	✓	✓

The four Enceladus flybys included with the in-system orbit design ensure global coverage through high altitude flybys, thereby spanning both poles. They complete the measurements taken during the orbiting phases (Table 5.8). Considering the high data volumes created mainly by imaging and the Radar for Europa Assessment and Sounding: Ocean to near-Surface (REASON) (Table 5.1), the flybys are split up: two for imaging and spectrometer use and two for radar and altimeter use.

Table 5.8: Payload use summary per Enceladus flyby.

Enceladus flyby	Time [d]	Closest approach [km]	Location	JANUS	VIMS	REASON	BELA	MERMAG	MORE	ENIJA	INMS
1	8.22	1500	North pole	✓	✓				✓		
2	8.22	1500	South pole	✓	✓				✓		
3	8.22	200	South pole			✓	✓		✓		
4	8.22	200	South pole			✓	✓		✓		

Note that in Table 5.7 and Table 5.8, check-marks do not indicate continuous operation of the corresponding instrument. Instead, operation time is distributed across the orbiting and flyby phases, considering constraints such as lighting conditions, pointing requirements, and communication time. When data is being sent to Earth during orbiting, seventy percent of the daytime, only radio science takes place. The remaining thirty percent is used for other science. This division allowed the necessary coverage for data recording under light conditions, whilst still providing sufficient time to send back data. At the end of orbiting, 0.23 TB of data will remain to be sent, a amount that can be stored and sent before end of life (subsection 8.3.1, subsection 9.3.2). Further description of the instruments operating times is given below.

Requirement compliance

Imaging: JANUS spans a spectral range of 350 – 1050 nm meeting requirement PLD-00.05.01 (Table 5.5) [51], allowing for visible and near infrared requirement for imaging (PLD-04, PLD-05, Table 5.5). The field of view is $1.72 \cdot 1.29$ deg^2 and the pixel scale 15 μrad/pix [51]. By imaging during the four Enceladus flybys, the spatial resolution of 2 km is achieved (PLD-04), and poles are covered (Figure 4.5, see subsection 4.1.2). Selected imaging with 2.25 m accuracy (meeting the 50.0 m required by PLD-05, Table 5.5) is done during the orbiting phases, where the camera is on during illuminated periods for a total of 141 Enceladean days spread across 205 days of 60 and 90 deg inclination orbits. Said duration is selected under consideration of the swath width at low altitudes. Arriving at spring, full coverage under illumination conditions is possible. Images will provide insight on the what the surface is like, beneficial for investigations of tectonics or landing areas.

Surface Composition: Having an instantaneous field of view of $0.5 \cdot 0.5$ mrad^2 and a total field of view of 60·60 pixels, the Visual And Infrared Mapping Spectrometer (VIMS) IR is used during two Enceladus flybys giving a resolution better than 10 km [23] (Figure 4.5). Remaining

areas are mapped at higher resolution (75.0 m accuracy) during orbiting (Figure 4.9). Global coverage is ensured by allocating 20 minutes per orbit in the nominal orbit phase (i.e. 60 deg inclination) to surface composition measurements.

Radar: REASON is operating 16 minutes per flyby during 40 Europa flybys for Europa Clipper [102]. For EPOSS, it operates the same amount of time across 40 orbits of Enceladus around Saturn at a 60 deg inclination. Furthermore, it operates 16 minutes during two flybys when crossing over the south pole (the ground coverage is shown in Figure 4.5), creating crossing ground-tracks. BELA, the laser altimeter, is always operating when the radar is, allowing for higher accuracy in geophysical analysis [112].
The radar reaches 4.5 km at 10 m vertical resolution with its very high frequency (VHF) antenna. On top of that, it reaches 30 km depth with 100 m vertical resolution with a high frequency (HF) antenna [102] [112]. With these, both the Saturnian and anti-Saturnian hemispheres are covered, and PLD-01 (Table 5.4), requiring crust thickness characterisation up to 2 km, is met.

Altimetry: As mentioned above, the BepiColombo Laser Altimeter (BELA)[5], works whenever subsurface sounding is operating, for accurate characterisation of subsurface layers [112]. Its use is, despite this, not restricted to radar operating time. It works a total of 22.6 days distributed across the 60 and 90 deg orbits and 16 minutes during two flybys over the south pole (32 minutes total), further described in subsection 4.1.2. This strategy allows for global coverage, interesting for tectonics of landing site determination.

Magnetic field: The magnetometer for JUICE is used for induced magnetic field as evidence for subsurface ocean on Ganymede, Europa and Callisto. It is used as an indication on required operation time for the EPOSS magnetometer. For JUICE, it reaches 0.1 nT in 36 days for Europa [69]. The Magnetic Field Investigation instrument (MERMAG) is operating 229 Enceladean days across a 310 day period, resulting in in-depth characterisation of the magnetic field with a 0.5 nT accuracy [103] (PLD-07, Table 5.5).

Radio Science: Polar orbit for one year gives fairly accurate results for up to degree 20 by tracking 8 h per day in a one-year nominal mission with the Mercury Orbiter Radio-Science Experiment (MORE) [41]. For EPOSS, the inclusion of polar orbits during the orbiting phase is limited (see subsection 4.3.6), so degree eight accuracy is reached through more extensive tracking.
According to [108], order 12 can be achieved at Enceladus with 65 degree inclination (200 km altitude) over 267 days of orbiting. For EPOSS, MORE is used during connection time with Earth, operating a total of 323.6 Enceladean days distributed across the 420 days Enceladus orbiting phase, and during the four Enceladus flybys, thus meeting PLD-03 (Table 5.5). Degree eight or higher implies gravity anomalies will be identified accurately, providing information on body structure.

Plumes: Orbiting around Enceladus at 60 deg inclination and 150 km altitude gets 15% of plume content (from density at ground level) every four orbits of Enceladus around Saturn [99]. This is supplemented by three polar orbits at 50 km to get measurements of plumes where particle density is higher which satisfies requirement PLD-00.29 (Table 5.4) (Figure 4.9,

[5]Note BELA was chosen over the Ganymede Laser Altimeter (GALA) because, despite the latter having better performance, it is heavier and requires more power [51] [58]. After a trade-off, and under consideration that using BELA is still sufficient for EPOSS' scientific goals, reduced power and mass are deemed more important than better performance.

Figure 4.10). Continuous characterisation at tiger stripes in these scenarios means it meets the two month temporal requirement (PLD-02.05, Table 5.4). Furthermore, flying at different heights provides insight in change in composition and density as a function of location. The Enceladus Icy Jet Analyser (ENIJA) and the Ion and Neutral Mass Spectrometer (INMS) characterise particles in a range of 1-2000 amu, complying with PLD-02.02 and PLD-02.03 (Table 5.4) [74].

5.4.2. Daphnis

Payload use

Daphnis science takes place across four flybys that are almost equivalent with regards to payload use. This is possible since the body is small and data storage does not reach unfeasible values.

Table 5.9: Payload use summary per Daphnis flyby.

Daphnis flyby	T [d]	Closest approach [km]	Location	JANUS	VIMS	REASON	BELA	MERMAG	MORE	ENIJA	INMS
1	14.6	150	North pole	✓	✓	✓	✓			✓	
2	14.6	150	South pole	✓	✓	✓	✓			✓	
3	14.6	50	North pole	✓	✓	✓	✓			✓	
4	14.6	50	South pole	✓	✓	✓	✓			✓	

Again, checkmarks indicate instrument use but not that it is operating continuously. Details on time distribution are given below.

Requirement compliance

Imaging: Imaging at Daphnis takes place during all four flybys of the shepherd moon (with coverage shown in Figure 4.7). The camera is allocated a total of 28 minutes per flyby. Measurements will take place in bursts under adequate illumination conditions, ranging from a global resolution of 1.00 km/pixel to 2.25 m/pixel in selected areas. As shown in Figure 4.7 and Figure 4.8, both leading and trailing edge will be spanned, meeting PLD-08.03 and PLD-08.04 (Table 5.5).

Radar: REASON is to operate when under 1000 km altitudes, resulting in 5.5 operative minutes (section 4.1) during each of the four flybys, reaching up to 25 m accuracy [25][102]. Despite this implying a reduced amount of measurements, Daphnis size is small enough to be completely characterised within the allocated time (see Figure 4.8). Use of radar sounding on such a small body has been done in the past [92] [100]. This is therefore expected to be possible, maybe requiring modifications of the instrument.

Altimetry: Again, BELA operates with the radar, 5.5 minutes per flyby. Achieving pole-to-pole ground track is done through operation over an altitude range of 50–1050 km [48]. With both radar and altimeter use, global surface morphology is obtained, meeting PLD-08.01.01 (Table 5.4).

Spectrometer: VIMS-IR operates at CA±14 minutes (Figure 4.7). This allows for surface composition analysis, complemented by the radar measurements, with an accuracy of 37.5 m, meeting the 50 m required by PLD-08.02.01 (Table 5.4) [23].

Bulk composition: Imaging and spectrometer measurements allow for accurate volume determination. From radar data, core distribution is available. Mass can be derived from said

data as surface composition is known from VIMS. This is preferred to doing so from radio science, under consideration that limited flybys of such a small body would be insufficient for accurate determination of its gravity field, thus not meeting the bulk composition accuracy required (5%). Therefore, from radar, camera and spectrometer, bulk composition is determined (accuracy is expected to be satisfactory, but remains to be precisely defined) meeting PLD-08.05 (Table 5.5).

Ring particles: CA takes place at 50 and 150 km for both north and south pole flybys, providing information on the particle variation over space. Furthermore, spacecraft crosses ring plane during flybys, covering regions of interest. ENIJA operates at CA ±55 minutes, identifying composition, size distribution and dynamics of particles in a 1-2000 amu range, meaning PLD-08.08, PLD-08.09, PLD-08.10 and PLD-08.11 (Table 5.4) are met [74]. Note use of this instrument during the moon tour will give further information on ring distribution across the Saturnian System.

5.4.3. Secondary Science

During the mission, several opportunities for secondary science arise. A brief overview of possible payload use is given below.

Firstly, the Venus flyby is addressed. At a CA altitude of 8230.4 km, radar (REASON) and altimeter (BELA) can not be used. Equally, particle characterisation is not of interest. MORE cannot be used for it uses Ka-band, only possible with the high gain antenna which is working as Sun shield during the flyby. Lastly, JANUS can not be operated since solar torque is too high and stability can not be achieved. That leaves MERMAG (interesting for solar wind and characterisation of flux ropes) and VIMS (for examination of cloud processes and composition distribution) as only payload to be used.

During the moon tour, MERMAG and MORE can be used continuously at numerous stages for definition of solar wind and Saturn's magnetic field and gravity field, respectively. In a similar manner, JANUS can be used throughout the tour, working in short periods to image the moons. VIMS can provide 10 km resolution when at 20000 km of a body [23].

Some points of interest, like Rhea's composition or the particles surrounding Rhea, Dione, and Tethys can be addressed by use of BELA, REASON, ENIJA and INMS as spacecraft gets closer to the body.[6] Morphology and core characterization of the moons and ring particles distribution and dynamics across the system are some of the secondary scientific outputs. Although not necessary, science can be expanded at end of mission, further explained in subsection 4.3.7

Furthermore, bodies other than Venus and the moons can be examined. A more in-depth secondary science analysis study is out of the scope of this report.

5.5. Verification & Validation

Since instruments used are taken from other missions, verification and validation has already been performed or will be performed to some extent [34][116].

Special attention needs to be payed to instruments that are not fully developed yet or have not been used in space. Equally, adapting some of the instruments to the EPOSS mission and environment will imply changes in each instrument, raising a need for additional verification and validation. Therefore, two parameters need special attention: technology readiness level and similarity between EPOSS and the instrument's intended target.

For verification, an extensive analysis through mathematical models simulating the environment, operation conditions and instrument specifications can be performed to see whether

[6] Retrieved from `https://solarsystem.nasa.gov/moons/saturn-moons/` last opened on June 18, 2019

the payload would meet the science objectives stated by the requirements [34]. Some parameters, such as power consumption or data rate, can be verified through tests. On the other hand, sizes and weights can be checked through inspection. Earth flybys can be used for calibration of instruments and further verification.
As for validation, more issues arise. The instruments are expected to collect data in an environment for which either no or limited data is available. Because of this, hypothesised results based on theory can be used for comparison on ground in combination with data from other missions with similar target or using the same payload.

5.6. Sensitivity Analysis

During this phase, multiple factors affected the design of the payload differently. Here, the viability of the EPOSS payload design will be analysed when said factors change.

Data rate to Earth: Being one of the main parameters affecting payload use, data rate is to be assessed for sensitivity. If it is reduced, sending the same amount of data back to Earth takes longer. Whereas there is plenty time to send data after flybys, this is not the case for the orbiting phase with the current trajectory profile, although it is flexible (subsection 4.3.7). With the current distribution, 0.23 TB are stored by end of orbiting, needing to be sent back before EOL. Reducing data rate by 20% and 40% would call for and 48% and 96% increase in data storage by end of orbiting, respectively. Needed data storage is thus highly sensitive to data rate variations. Equally, this implies more time is needed between orbiting and EOL for sending data back. Rearranging payload use across mission, reducing instrument operation time or modifying the trajectory would be possible if the aforementioned changes took place. Therefore, a limited reduction of data rate change is not considered mission critical. An increase has the opposite effect, and is beneficial for the mission.

Number of flybys: Both Enceladus and Daphnis flybys have been designed to cover requirements. An increase in flybys would be beneficial in both cases, although not necessary, allowing for more measurements. A decrease, on the other hand, would not be critical for Enceladus but call for a bigger scientific output during the orbiting phase. For Daphnis, on the other hand, it would imply limitations in measurements. Global coverage might become problematic in this case, and only possible through use of other instruments or increased spacecraft manoeuvres.

Orbiting phase duration: Increase in orbiting phase duration would be beneficial for sending data. Scientific output wouldn't significantly increase under consideration that orbiting phase is already quite long. A decrease would not be critical but call for more instruments being used simultaneously, with the corresponding increase in data storage. As seen in Table 5.7, plume, radio science and magnetic field measurements could be compromised.

Altitudes: Payload can only operate within certain ranges. Increasing altitudes in orbiting phase would compromise plume study, as density decreases with height. Equally, flying above 1000 km it would be problematic for altimetry and subsurface sounding [102][48]. Optimal heights have been chosen, so an increase would not necessarily imply not meeting the requirements, but hinder scientific output. For the flybys, both for Enceladus and Daphnis, REASON and BELA set maximum heights, as explained for orbiting. Above 1000 km altimetry and subsurface sounding would be hindered. Different instruments could be selected if this happened.

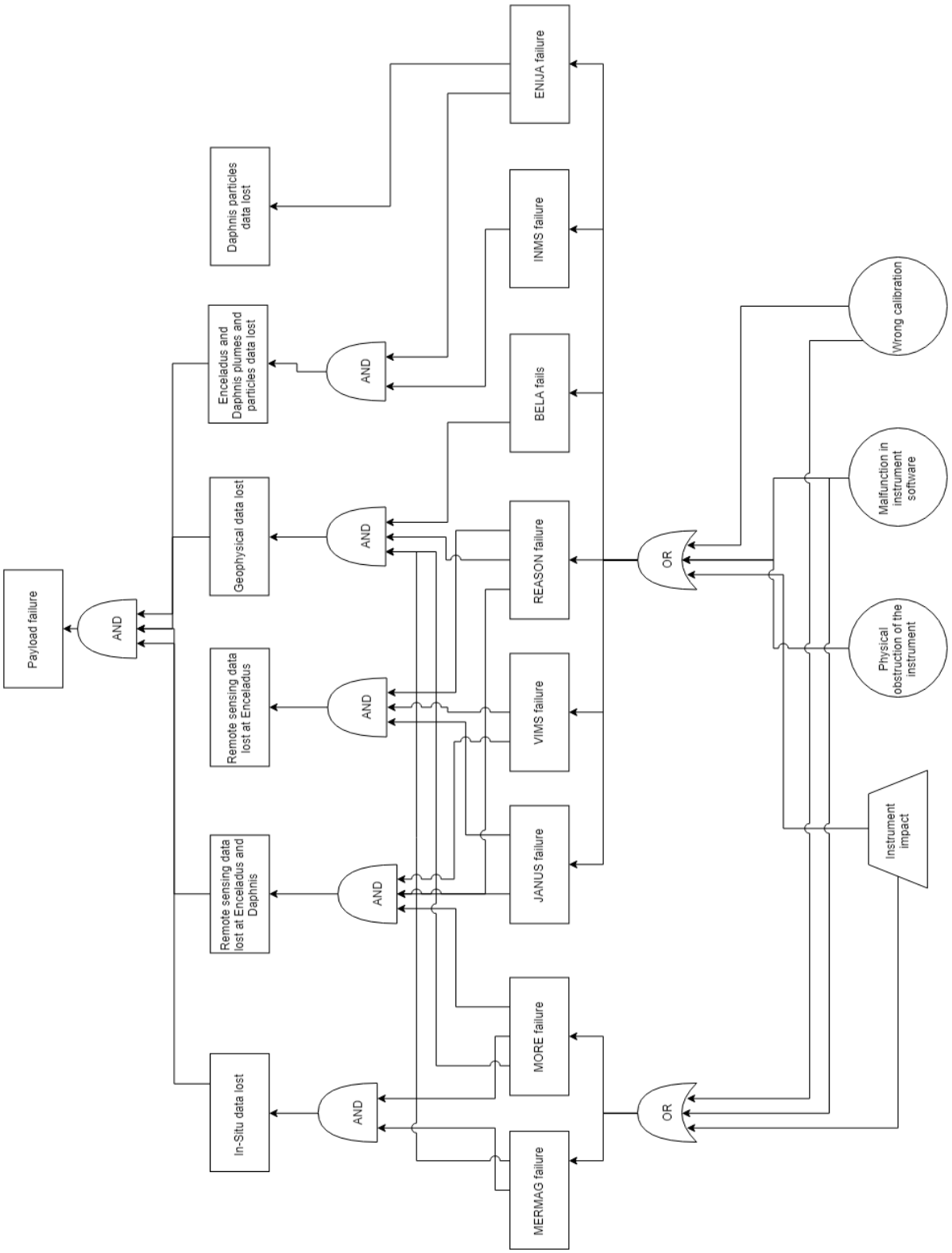

Figure 5.1: Fault tree for payload.

5.7. Risk Analysis

In this section the risks that are likely to occur are discussed on what their impact is and how to mitigate them. These risks are then applied in four different default tree to see which measurements would be lost if one of these risk would occur. Overall the payload will be reliable during the mission with a reliability of 90.1%.

1. **PLR-0.1 Physical obstruction of the instrument**: The instruments need to be able to see the body of interest at all times during measurements. If the instrument is obstructed and can not see the body of interest no data can be generated and will lead to gaps in the produced data or no data at all. Testing all mechanisms on Earth before flight and designing the layout of the spacecraft such that no obstructions occur in front of any instrument will minimise the likelihood of this risk.
2. **PLR-0.2 Instrument impact**: Impact of particles with the satellite while operating is likely to happen during space missions. For EPOSS it is even more likely to happen because it will fly through particles of the plumes at Enceladus. The instruments can be impacted by plume particles or small asteroids while operating and end up being destroyed. Reducing this risk is done by designing the layout so that only the particle characterising instruments are in direct contact with the plumes when the spacecraft flies over them.
3. **PLR-0.3 Malfunction in instrument software**: Malfunctions are quite common in programs and can cause problems like the software that might stop the instrument from working. It also could lead to corrupted data that can not be used for further research. Using two groups of programmers, one for programming and one for debugging, helps to mitigate this risk.
4. **PLR-0.4 Wrong calibration**: Calibration of an instrument is important to let the instrument work properly while it is operating. But the calibration of an instrument can cause corrupted data that can not be used for research. These calibrations have to be done during the flybys around Earth. If something went wrong during these calibrations it can still be resolved before it reaches the end destination and produce the required data.

6 Attitude Determination and Control System

In this chapter, the design of the Attitude Determination and Control System is illustrated. First off, an overview of the configuration is presented in section 6.1, followed by section 6.2 which presents the design requirements of the subsystem. Furthermore, a description of the design approach and the considerations taken during the development is described in section 6.3. A discussion on the verification and validation of the methods and product is given in section 6.4. Lastly, a sensitivity and risk analysis are performed in section 6.5 and section 6.6, respectively.

6.1. Design Overview

Following a preliminary concept analysis and trade-off of the Attitude Determination and Control System (ADCS) in the previous stages of the project [10], the winning concepts are taken into development.
Looking at the attitude determination system, a set of three star trackers and two Internal Measurement Units (IMUs) are selected for this mission due to their excellent accuracy and versatility of operation, which is advantageous due to the variety of environments encountered in the transfer phase (described in subsection 4.3.2). Specifications on the performance of sensors can be consulted in Table 6.8. Sun sensors are also included in the configuration and are operated during the transfer phase.

For attitude control, 3-axis stabilisation is required due to the demanding scientific objectives provided by stakeholders, particularly regarding researching the morphology of Enceladus' surface. Hence, reaction wheels are chosen due to their good performance-to-weight ratio, together with reaction control thrusters used to perform quick manoeuvres and to dump the momentum accumulated by the wheels. Following a more detailed analysis of environmental disturbances and mission requirements as done in section 6.3, momentum wheels are chosen over reaction wheels because they perform better in terms of pointing stability and because they comply with the strict pointing accuracy requirements provided by the payload instruments (ADC-04.02, ADC-05.01 in section 6.2).

Hence, the actuator configuration consists of a set of four wheels in pyramid configuration for full redundancy in case of one wheel failure, commonly due to fatigue. Eight operating thrusters supplemented by eight redundant ones are installed to allow manoeuvring in all directions. An overview of the performance of the sensors and actuators can be consulted in Table 6.8 where quantities are shown per unit component.

Note that the design of the thrusters is done in close collaboration with the propulsion subsystem; the ADCS defines the manoeuvres necessary and performance required of thrusters while the propulsion subsystem, chapter 7, takes care of the specific selection of thrusters and calculation of the propellant mass needed for the mission. For this reason, the thrusters specifications can be found in detail in section 7.3. An overview of the subsystem's characteristics is presented in Table 6.1. A margin of 15% has been applied to the mass budget as imposed by requirement ADC-00.114 in section 6.2.

Table 6.1: Overview of ADCS components, with corresponding mass and power.

Component	Mass [kg]	Nominal Power [W]	Peak Power [W]	Volume [m^3]
Momentum Wheel	8	20	90	0.020
IMU	0.75	12	-	0.00057
Star Tracker	2	5	16	0.056
Sun Sensor	0.22	0	0	0.00036
Total	52.2	77	151.2	0.25

6.2. Requirements Analysis

In this section, the requirements of the ADCS subsystem are presented, together with the verification method, compliance check, and the section in the report where the requirement is met, in Table 6.2. If the requirement is not explicitly mentioned in the report, it is elaborated in this section.

Table 6.2: Compliance matrix for the ADCS requirements.

Code	Requirement	Verification Method	Compliance	Section
ADC-00.100	The ADCS subsystem shall be able to act upon detection of celestial bodies in proximity of collision.	Test	✓	6.3.3
ADC-00.101	The ADCS subsystem shall have a pointing accuracy for the main engine better than 5 deg when performing orbit insertion.	Analysis	✓	6.2
ADC-04.02	The ADCS subsystem shall have a pointing accuracy of at least 50 μ rad when performing global surface observations.	Test and Analysis	✓	6.3.1
ADC-05.01	The ADCS subsystem shall have a pointing accuracy of at least 50 μ rad when performing selected surface observations.	Test and Analysis	✓	6.3.1
ADC-00.04.01	The ADCS subsystem shall ensure a maximum lateral acceleration of 0.12 mrad/s^2 when performing manoeuvres.	Test and Analysis	✓	6.3.1
ADC-00.05.01	The ADCS subsystem shall ensure a maximum angular acceleration of 0.07 mrad/s^2 when performing manoeuvres.	Test and Analysis	✓	6.3.1
ADC-00.102	The ADCS subsystem shall allow a maximum slew rate of 10 mrad/s.	Test and Analysis	✓	6.3.1
ADC-00.103	The ADCS subsystem shall ensure a minimum slew rate of 5 mrad/s.	Test and Analysis	✓	6.3.1
ADC-00.104	The ADCS subsystem shall have a pointing accuracy better than 87 μ rad when communicating to Earth.	Test and Analysis	✓	6.3
ADC-00.105	The ADCS subsystem shall allow for a spacecraft's detumbling rate of maximally 0.12 mrad/s^2.	Test and Analysis	✓	6.3.2
ADC-00.106	The ADCS subsystem shall comply with the requirements given by the thermal subsystem regarding the orientation of the spacecraft.	Analysis	✓	6.2
ADC-00.107	The ADCS subsystem shall occupy a maximum volume of 1 m^3.	Inspection	✓	6.1
ADC-00.108	The ADCS subsystem shall have a maximum mass of 150 kg without including mass thrusters and fuel.	Inspection	✓	6.1
ADC-00.109	The ADCS subsystem shall need a nominal power of maximally 80 w.	Demonstration	✓	6.1
ADC-00.110	The ADCS subsystem shall need a peak power of maximally 100 w.	Demonstration	✓	6.1
ADC-00.111	The ADCS subsystem shall include a in-mission validation process.	Test	✓	6.4
ADC-00.112	A safety margin of 5% shall be applied when using off-the-shelf components.	Analysis	✓	6.1
ADC-00.113	A safety margin of 10% shall be applied when using existing technology with minor modifications.	Analysis	✓	6.1
ADC-00.114	A safety margin of 15% shall be applied when using existing technology with major modifications.	Analysis	✓	6.1
ADC-00.115	A safety margin of 20% shall be applied when using completely new components.	Analysis	✓	6.1
ADC-00.116	The uplink data transferred for ADCS subsystem purposes shall take part of maximally -% of the total.	Demonstration	✓	6.2
ADC-00.117	The downlink data transferred for ADCS subsystem purposes shall take part of maximally 40% of the total.	Demonstration	✓	6.2
ADC-00.118	The ADCS subsystem shall have a reliability of minimum 80%	Analysis	✓	13.5
ADC-00.119	The ADCS subsystem shall have a maximum housekeeping data rate of 0.011 kbits/s.	Demonstration	✓	6.2, 9.2
ADC-00.120	The ADCS subsystem shall have a cost of maximally 70 M €.	Inspection	✓	14.3
ADC-00.121	The longest thruster burn shall be maximally 50 minutes.	Demonstration	✓	6.2, 6.3
ADC-00.122	The total operating time shall be minimally 84 days.	Analysis	✓	6.2, 7.3
ADC-00.123	The number of full stroke actuations shall be at least 6933.	Test	✓	6.2, 7.3

ADC-00.101: This requirement is not mentioned in the design process since it is not driving; it is however met, see ADC-04.02.

ADC-00.106: This requirement is met by the performance of the ADCS in the occasion of the Venus flyby, when the sun shield is pointed towards the Sun. Further details can be found in section 11.3.

ADC-00.117: In collaboration with C&DH as from Figure 9.2, it is shown that this requirement is met since the housekeeping data of ADCS is 35% of the downlink data, as it is illustrated in Figure 9.2.

ADC-00.116: This requirement is left blank because of its ambiguity, since the uplink data strictly depends on the condition of the ADCS during the mission. It might range from percentages as high as necessary when the subsystem has to be maintained (e.g. during safe mode), to low percentages when it is working nominally. This requirement is therefore not considered further.
ADC-00.121: The longest thruster burn occurs during plumes fly through and is equal to 48 min (see subsection 6.3.1). Burn time capability of the thruster MR103 from Aerojet Rocketdyne is up to 3000 s, see more details in the Propulsion subsection 7.3.2.
ADC-00.122 & **ADC-00.123**: This information in provided by the propulsion subsystem, chapter 7.

6.3. Design Approach

The ADCS system is responsible for many situations in the mission timeline from detumbling efforts after launcher deployment to pointing the payload for the intended operation once in-System. The EPOSS mission is characterised by two main operational phases: the orbit phase around Enceladus, which goes from orbit injection to leave; and the transfer and flyby phase, which consists of multiple flybys to bodies of the Solar and Saturnian System necessary to reach Enceladus and to perform the allocated science measurements. Details on the trajectory specification can be found in chapter 4.
In this section, the analysis of the ADCS is done in the two phases mentioned previously. The main drivers for both phases are the environmental disturbances and the payload's specified pointing requirements, which can be found in the requirement analysis section 6.2 and in the explanation as follows. Specifications of the instruments used and of the operational sequence throughout the mission are described in chapter 5.

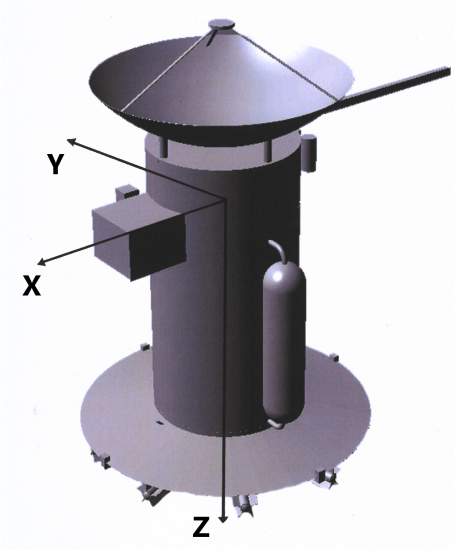

Figure 6.1: Reference system definition for ADCS.

6.3.1. Orbit Phase

EPOSS undergoes an orbital phase around Enceladus, as described in subsection 4.1.2. The main characteristics of this orbit are the altitude range of 50-150 km and the inclination range of 45-90 deg. As previously mentioned, the south pole of Enceladus presents a subsurface ocean with craters from which water plumes erupt. This area is therefore interesting to study but poses challenges for the attitude maintenance. The environmental torques and plume

disturbances are analysed to define the ADCS performance for this phase.

Environmental Disturbances

Amongst the various disturbances present in the space environment, the most notable are the gravity gradient torques by Enceladus and Saturn, magnetic torque caused by Saturn's magnetosphere, and the aerodynamic torque caused by the plumes at the south pole of Enceladus.

The vectorial analysis of the aforementioned torques can be substituted by considering the worst case scenario of torque superposition and taking the latter as design driver for the actuators. In such case, when the spacecraft is opposite to Saturn with respect to Enceladus, the direction of the gravity gradient torques of Saturn and Enceladus and the magnetic torque of Saturn act on the same axis and same direction as shown in Figure 6.2. This simplified situation allows for an efficient design development whilst accounting for the ADCS's performance required throughout orbit.

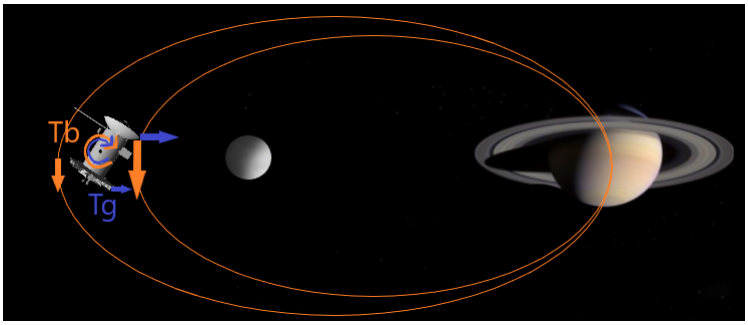

Figure 6.2: Superposition of disturbance torques; Tg = Saturn's and Enceladus' gravity torque; Tb = Saturn's magnetic torque. Not to scale.[105]

The gravity gradient torques depend on the mass distribution of the spacecraft along its axes, in that the more mass that is further away from the centre, the higher torque the spacecraft will undergo around the axes. It can be calculated using Equation 6.1 [121]:

$$T_g = \frac{3\mu}{2R^3}|I_z - I_x|sin(2\theta) \tag{6.1}$$

where μ is body's specific gravitational parameter, R is the distance between the planet's and the spacecraft's centre of gravity. I_z and I_y are the respective moments of inertia of the spacecraft obtained from the CATIA V5 model of EPOSS and θ is the maximum allowed spacecraft rotation from the principal axis. The limit of θ is taken to be 10 deg, this means that the wheels are able to reorient the spacecraft if the disturbance caused a rotation of ≤10 deg, therefore correction manouvers shall be applied before this limit.

Secondly, the magnetosphere of Saturn exerts an influence on surrounding bodies. It is characterised by a stream of plasma which is augmented by the ionisation of Enceladus' plumes [98]. This causes a disturbance parallel to the direction of the field; it can be calculated by [121]:

$$T_m = D(\frac{M}{R^3}\lambda) \tag{6.2}$$

where D is the residual dipole moment of the spacecraft taken to be 10^{-3} Am^2/kg from a NASA case study on classes of spacecraft; EPOSS falls within the class I category which indicates that effort has been put into minimising the internal magnetic field of the spacecraft [20]. Furthermore, λ is a function to adapt the field strength to the latitude of observation which equals one at the equator and two at the poles of Saturn. Given Enceladus' approximately horizontal orbit with respect to. Saturn, λ is taken to be one. Based on the previous discussion and the situation presented in Figure 6.2, the worst case scenario driving the design is equal to:

$$T_d = T_{g_S} + T_{g_E} + T_b \tag{6.3}$$

Note that the aerodynamic torque is not included because it acts during restricted parts of the orbit, as discussed later in this section. A margin of 1.5 has been added to T_d to increase reliability.

Now that the disturbance torques relating to the general orbit conditions have been analysed, a closer look to the south pole of Enceladus is taken. The latter location is characterised by the ejection of plumes from the subsurface ocean through the crust of the moon. Measurements of the plume density have been carried out by the Cassini spacecraft during its multiple flybys. The reference flyby used for the estimation of the aerodynamic torque due to the plumes is the E12, the one that recorded the highest density of the plumes. Some characteristics of the E12 flyby are presented in Table 6.3:

Table 6.3: Characteristics of the E12 flyby [27].

Flyby	Date	Altitude [km]	Latitude [deg]	Velocity [m/s]	Plume Density [kg/m^3]
E12	28-Oct-2015	49	87.5	8.49	45–55 $\cdot 10^{-12}$

EPOSS follows an orbit with altitude and inclination variations as mentioned in subsection 6.3.1. The plumes density is highest at the lowest altitude of 50 km and at the highest inclination of ≈90 deg, which reflects the conditions of the E12 flyby to a close enough degree. Therefore, the plume density registered at the E12 flyby is considered to be a good reference with a factor of 1.5 included to account for plume activity variations. The aerodynamic torque is obtained with Equation 6.4 [121]:

$$T_a = \frac{1}{2}\rho C_d A_r V^2 (cp_a - c_m) \tag{6.4}$$

The quantity $(cp_a - c_m)$ is the z-axis distance between the centre of mass of the spacecraft and the centre of pressure of the spacecraft, acting as the arm of the drag force. A value of 1 m is obtained from a reference value of 1.2 m of the Cassini [7] and a ratio of EPOSS's height (5.8 m, section 12.6, Figure 12.3) to Cassini's height (6.8 m [81]). The validity of this number is supported by the similarity of layout between EPOSS and the Cassini, which results in similar geometrical characteristics. For this same reason, also Cassini's drag coefficient value C_d is taken as reference [66] and used in Equation 6.4.

A summary of the magnitudes of the torques and the data used for calculations can be found in Table 6.4.

Table 6.4: Worst-case disturbance torques and respective data used for calculation during Enceladus' orbit phase.

Characteristic	Value	Characteristic	Value	Characteristic	Value	Characteristic	Value
T_g by Saturn [Nm]	$3.80 \cdot 10^{-6}$	T_g by Enceladus [Nm]	$1.03 \cdot 10^{-7}$	T_m [Nm]	$7.04 \cdot 10^{-13}$	T_a [Nm]	$3.41 \cdot 10^{-2}$
R [km]	$2.38 \cdot 10^{5}$	R [km]	302.1	D [Am^2]	1.63	ρ [kg/m^3]	$8.25 \cdot 10^{-11}$
μ_S [m^3/s^2]	$3.79 \cdot 10^{16}$	μ_E [m^3/s^2]	$7.21 \cdot 10^{9}$	M [N m^2]	$5.78 \cdot 10^{12}$	C_d [-]	2.1
I_z [kgm^2]	3572	I_z [kgm^2]	3572	R [km]	$2.38 \cdot 10^{5}$	A_r [m^2]	16.5
I_x [kgm^2]	6193	I_y [kgm^2]	6193	λ [-]	1	V [m/s]	4885.13
θ [rad]	0.174	θ [rad]	0.174			(c_{p_a}-c_m) [m]	1
$T_{d_{max}}$ [Nm]	$5.86 \cdot 10^{-6}$						

The information displayed in Table 6.4 serve as basis in designing the performance of the actuators, which lead to the physical sizing of the momentum wheels and thrusters, in Table 6.3.1 and section 7.3, respectively.

Station-keeping and Manoeuvring

Momentum wheels are effective for maintaining the spacecraft's stability and for applying torques to manoeuvre; however, they cannot reverse direction while they are spinning, otherwise momentum stability would be lost. For this reason, all manoeuvres are done by the wheels except the ones that would require an inversion of direction, this will happen once after every plumes' fly through as soon described. These manoeuvres are done instead by the thrusters. The thrusters also take care of the momentum dumping and the stabilisation of the spacecraft during plume fly through, given the higher magnitude of the aerodynamic torque.

Given the worst case disturbance torque T_d and the pointing accuracy requirement of 50 μrad, the momentum necessary to correctly operate the payload throughout one orbit is given by Equation 6.5 [121]:

$$H = \frac{T_d P}{4\theta} \tag{6.5}$$

The highest orbital altitude of 150 km, results in a momentum of 553 Nms which the momentum wheels are designed and sized for, together with the torque necessary for the manoeuvres.

Now that the attitude in orbit has been stabilised, the manoeuvres necessary for payload operation is analysed. As it is described in section 13.2, the particle analyser instruments ENIJA and INMS are placed on the opposite side of the spacecraft with respect to the other instruments to prevent damage caused by the impact of plume particles. Therefore, before flying through the plumes, the spacecraft has to turn from nadir pointing to RAM pointing. The pointing modes are defined in Figure 6.3 and Figure 6.4, respectively.

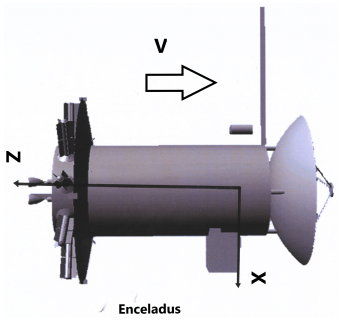

Figure 6.3: NADIR pointing direction.

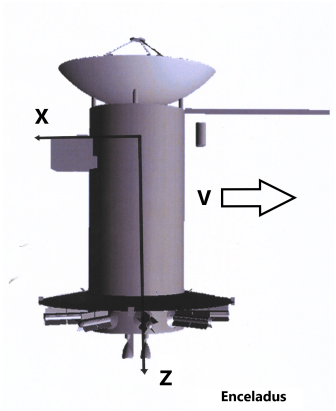

Figure 6.4: RAM pointing direction.

The attitude transformation consists of a -90 deg turn about the y-axis and a 180 deg turn about the z-axis. These manoeuvres shall not be done at the same time as standard due to the limiting peak power provided, however if necessary, this power can be provided by the contingency included in the batteries design, subsection 10.3.2. The torque necessary to perform these manoeuvres, including a 1.5 margin, in the given time is shown in Table 6.5. The maximum torque the wheels can withstand is around 1.1 Nm [65], therefore the time is tuned accordingly. Furthermore, the variation of moment of inertia at BOL and EOL is checked which showed that the performance required by the momentum wheels drops by 40% at EOL.

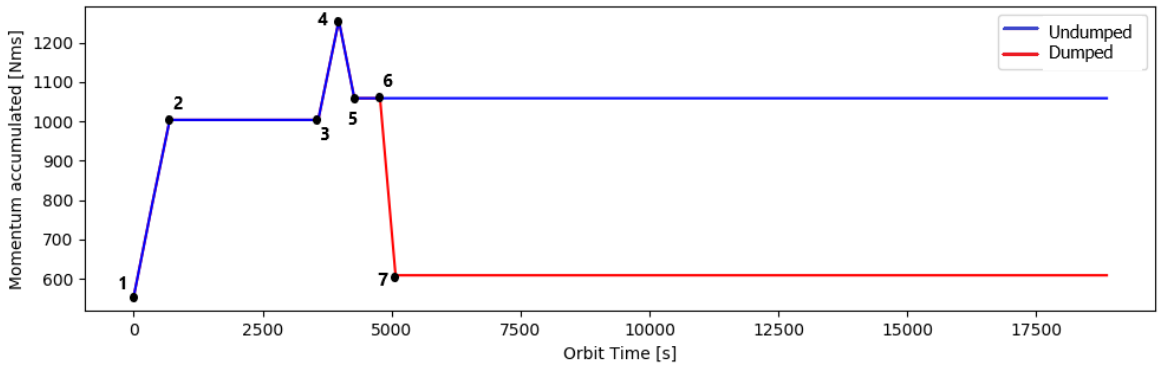

Figure 6.5: Momentum accumulation and dumping each orbit.

Table 6.5: Overview of manoeuvres, with corresponding characteristics.

Manoeuvre	Angle [deg]	Nom time [s]	Nom torque [Nm]	Min time [s]	Max Torque [Nm]
BOL Manoeuvre 1	-90	300	0.64	245	0.97
BOL Manoeuvre 2	180	400	0.42	315	0.67
EOL Manoeuvre 1	-90	300	0.48	245	0.71
EOL Manoeuvre 2	180	400	0.31	315	0.49

The requirement for thruster capability derives from the highest torque necessary for manoeuvres, i.e. 0.97 Nm divided by the arm (≈2 m), and is treated further in section 7.3. During the plume phase, a constant thrust of 0.02 N shall be provided to counteract the aerodynamic torque and maintain spacecraft stability. The thrusters capabilities comply with the long burn time and the low thrust.
When leaving the plume environment, the reverse of the previous transformation must be performed to go back to nadir pointing. The -180 deg can be done by the wheels in both directions, while the 90 deg must be done in the direction opposite the rotation of the wheels. This is why thrusters are used to complete this manoeuvre.
Now that the performance of the actuators has been defined based on the environmental conditions and payload requirements, the momentum accumulation throughout the orbit is analysed. During one orbit, momentum is accumulated by the wheels when performing manoeuvres; if this momentum remains undumped, the wheel will reach its saturation level and the control of the spacecraft will be lost.
The wheel's momentum saturation level is taken to be 2000 Nms, which was obtained from a reference value of 4000 [121] minus a 0.5 factor for safety. The momentum limit is only every three orbits, however the design decision is taken to dump the momentum after each set of four slew manoeuvres (Nadir to RAM, RAM to Nadir, two slews each) to allow for a gradual decrease in propellant mass and thus in general mass. This is beneficial for the accuracy of performance of the wheels since the torque provided is dependent on the moment of inertia of the spacecraft. The variation of momentum, both for the undumped and dumped case is shown in Figure 6.5.
Between Points 1-2, the Nadir to RAM manoeuvre is performed (700 s), 2-3 is plume fly-through time (2882 s), 3-4 is the 180 deg manoeuvre performed with the wheels (400 s), 4-5 is the 90 deg manoeuvre performed by the thrusters in the direction opposite of rotation (245 s), and they also dump momentum while doing so; 5-6 is rest time (500 s) before momentum dumping with thrusters begins at 6 and ends at 7 (300 s). From 7 onward the orbit time expires and a new one follows; average orbit time is 18867 s. Momentum is dumped each orbit. The required performance of the thrusters is presented in Table 6.6.

Table 6.7: Kinematic Capabilities of spacecraft using reaction wheels.

Angular rate	**Min**	**Max**
Angular slew rate [mrad/s]	5	10
Angular acceleration [mrad/s^2]	0.07	0.12

Table 6.6: Thruster performance required for momentum dumping per orbit.

Momentum Accumul. [Nms]	**Momentum to dump [Nm]**	**Thrust required [N]**	**Burn time [s]**
1009	451.6	0.75	300

The design of the thrusters and propellant necessary to comply with this manoeuvring is illustrated thoroughly in section 7.3.

Actuators and Sensors Sizing

Based on the performance of the reaction wheels defined in subsection 6.3.1, the momentum wheels are sized and the outcome is shown in Table 6.8. The mass is estimated by looking at the momentum saturation level and at the maximum rotational speed, from which the moment of inertia of the wheel is found. With this information, the wheel is sized and has dimensions shown in the Table 6.8. A margin of 1.5 has been applied to the required performance of the wheels, in order to increase reliability and safety. Furthermore, the momentum wheels are mounted on each axis with a wheel bearing to ensure that the vibrations due to the rotation are not transmitted to the rest of the spacecraft. This ADCS configuration allows for the angular rates described in Table 6.7.

Following a trade-off of performance and requirements compliance, the sensors were selected from commercially available. Specifically, the ASTRO APS 3 [56] Star Tracker was selected, three of them are mounted on the spacecraft, 120 deg apart to allow attitude determination in any circumstance. The LN-2000S [47] is selected as the IMU for the mission, two mounted on-board one of which redundant. Lastly, the Bradford coarse sun sensor [22] is selected, used mainly during the transfer phase, two operational and one redundant.

Table 6.8: ADCS hardware performance per unit component.

Momentum Wheel		**Star Trackers**	
Mass[kg]	8	Mass [kg]	2
Nominal Power [w]	20	Nominal Power [w]	5
Peak Power [w]	90	Peak Power [w]	16
Nominal Torque [Nm]	0.63-0.66	Pointing Knowledge [μ rad]	< 4.8
Peak Torque [Nm]	1.02	Attitude determination error [μ rad]	8
Momentum Saturation Level [Nms]	2000	Time required for acquisition [s]	8
Max rotational speed [rpm]	4000	**IMU**	
Moment of Inertia [kg m^3]	0.5	Mass [kg]	1.5
Radius [m]	0.35	Volume [dm^3]	0.53
Thickness [m]	0.05	Nominal Power [w]	12

6.3.2. Transfer and In-System Phase

Following deployment, the spacecraft undergoes chaotic rotational motion which requires the action of the actuators to dump (ADC-00.105). Typical tumbling angular rates are 0.1 rad/s [86] per axis and given a maximum angular rate delivered by the wheels of 0.12 mrad/s^2 , the detumbling can be executed in a minimum of 13 minutes which is a reasonable time before

acquiring the first contact with the ground station.
The transfer phase is characterised by flybys at Venus and Earth. The flyby at Venus is an opportunity to collect secondary science data with the MERMAG, JANUS, and VIMS instruments. The magnetic and gravitational disturbance torques are checked and are in acceptable ranges; however, the solar torque of $1.66 \cdot 10^{-4}$ Nm drives the momentum required for the operation of JANUS to an unacceptable extent. Therefore, this instrument will not be used during this flyby. Earth flyby will be used for payload validation, therefore accuracy is not of driving importance for this phase.
At Saturn, the trajectory consists of a moon tour before orbiting Enceladus. During these, the the scientific payload operates at Rhea, Dione, and Thethys. The gravity torques due to Saturn at all locations are lower than the orbital disturbances at Enceladus, ensuring correct operation of payload at all times throughout this phase. Details on the required attitude of the spacecraft throughout the mission have not been achieved at this point, however a generous propellant margin for manoeuvres during transfer and In-System has been allocated as described in section 7.3.
Lastly, the performance of wheels and thrusters is adjusted by a Proportional-Integral-Differential (PID) control system to tune the torques and thrust based on the inputs of the IMUs and accelerometers. This plays part in an efficient as well as more sustainable design.

6.3.3. Guidance and Navigation

The various satellites orbiting the Saturn present a threat to the spacecraft's integrity, particularly due to their abundant number and to the lack of information relating to their masses and dynamics. For this reason, the possibility of a body impacting EPOSS should be avoided (ADC-00.100 in section 6.2) and this is done by the installation of hazard-avoidance cameras. The camera used on board of EPOSS are the same used on the Mars Curiosity rover, Hazcam, built at JPL and performing to state-of-the-art technology standards at minimal weight expenses [70]. Although this camera has been used for different concepts in the past implementation of it on EPOSS will ensure high quality navigation at low design expenses. Relevant data regarding the camera is presented in the Table 6.9:

Specification	**Hazcam**
Field of View (HxV) [deg]	124x124
Depth of Field [m]	0.10 - ∞
Mass [g]	245
Dimensions electronics [mm]	67x69x34
Dimensions head detector [mm]	41x51x15
Power [w]	2.15

Table 6.9: Hazard-avoidance camera specifications [70].

A total of eight cameras are used on EPOSS to allow hazard detection from all directions and they will be operating only at selected areas of the Saturnian system.

6.4. Verification & Validation

The process followed in the design of the ADCS system makes use of verified formulas [65, 121]. The correct application of the method has been verified by studying the response of the formulas to different inputs, and validated by comparing the results to commercially available components and their performances. The list of components collected in [10] has been used for this purpose and showed a positive outcome. Furthermore, a proper validation of the final

design is done during the post-development testing of the momentum wheels in all mission scenarios, as well as the thrusters and sensors. Lastly, the product must have an on-board validation system which ensures the correct operation of the ADCS; this is done by methodically comparing sensor's data and actuators output. The subsystem shall be validated every time it is turned on, and periodically during long operational windows (ADC-00.111).

6.5. Sensitivity Analysis

In this section, the most influential design parameters are varied and their influence on the final outcome of the design is explained. The design of the Attitude Control System strictly depends on the payload and performance requirements; driving factors of the design are the pointing accuracy, environmental disturbance torques, and spacecraft structural properties.

Pointing Accuracy: Decreasing this parameter would result in higher performance required by the momentum wheels. That is, if the parameter is decreased by 20%, the momentum required to ensure stability increases by 25%. Given that the momentum saturation capabilities of the wheel is 2000 Nms and a margin of 450 Nms has to be kept for the momentum accumulated during the manoeuvres, a decrease of 65% in pointing accuracy would drive the design to an unacceptable extent. For a higher momentum, the wheel grows in size and so in mass. This is an extensive margin that will confidently not be reached. Furthermore, if the pointing accuracy decreases below the accuracy of the star sensors, the pointing error will increased to an unacceptable extent. Since the accuracy of 50 μrad is very precise, the team is confident that this value will not decrease further.

Environmental Disturbances: This analysis assumed that the orbital characteristics remain unvaried. There are two main drivers: the worst case disturbance torque in orbit, T_d, and the worst case aerodynamic torque, T_a. The first one depends on recognised and quasi-invariant planetary characteristics; nevertheless, if it grows the momentum necessary to counteract it grows linearly as a result. The limit is again set by the momentum saturation level. The aerodynamic torque depends mostly on the encountered density of the plumes; a change in torque causes a linear change in the thrust required to counteract it. Since the capability of the thruster is way higher than the thrust necessary for plume counteraction, it would take a density increase of 5000% to reach the capability limit of the thruster. In conclusion, the design is safe towards changes in plume density.

Moment of Inertia: A change in moment of inertia influences the performance required by the actuators, both for disturbance counteraction and for manoeuvres. An increase of 20% in moment of inertia causes a linearly proportional change in angular momentum for the wheels, as well as in necessary torque for the manoeuvres. For this reason, it is important to obtain an accurate value for this quantity by using state-of-the-art software such as CATIA V5. Lastly, as mentioned previously, the change of moment of inertia from beginning to end of life is conservative, therefore the only risk/improvement is to optimise the actuators performance based on its change.

6.6. Risk Analysis

In most circumstances, failure of the ADCS results in failure of the entire mission. Listed below are events most likely to occur that present a risk to the mission. Risk associated with the reaction control thrusters is discussed in section 7.6.

1. **ADR-0.1 Momentum wheel failure**: Mechanical and Electrical. This is generally

prevented by allocating enough safety margins. Mechanical failure is avoided by studying the fatigue life of the wheel and accounting for the necessary operational life. Lastly, the presence of a redundant reaction wheel mitigates this risk further.

2. **ADR-0.2 Misalignment of wheel's rotational axis**: Occurrence of misalignment on spin axis, causing unintended rotation on other axes and lost of attitude control. This can be mitigated by extensive pre-launch testing and the implementation of an on-board algorithm that correlates momentum wheel output data and the attitude variations registered by the IMU to ensure compliance between the two.
3. **ADR-0.3 Star tracker failure**: Failure of the star tracker instruments or interface. Mitigation consists in including extra components for redundancy and testing the attitude determination system pre-launch and in-mission.
4. **ADR-0.4 Unexpected disturbances and/or collisions during mission**: Presence of unexpected forces or their underestimation, particularly relating to the plumes' environment and its density. This is mitigated by considering worst-case scenarios and including margin on the propellant necessary for corrective manoeuvres. The risk of collision is mitigated by the inclusion of a hazard-detecting camera on-board

These risks are presented in the Fault Tree Diagram in Figure 6.6, alongside other possible faults. Lastly, the reliability of the system is assessed in section 13.5.

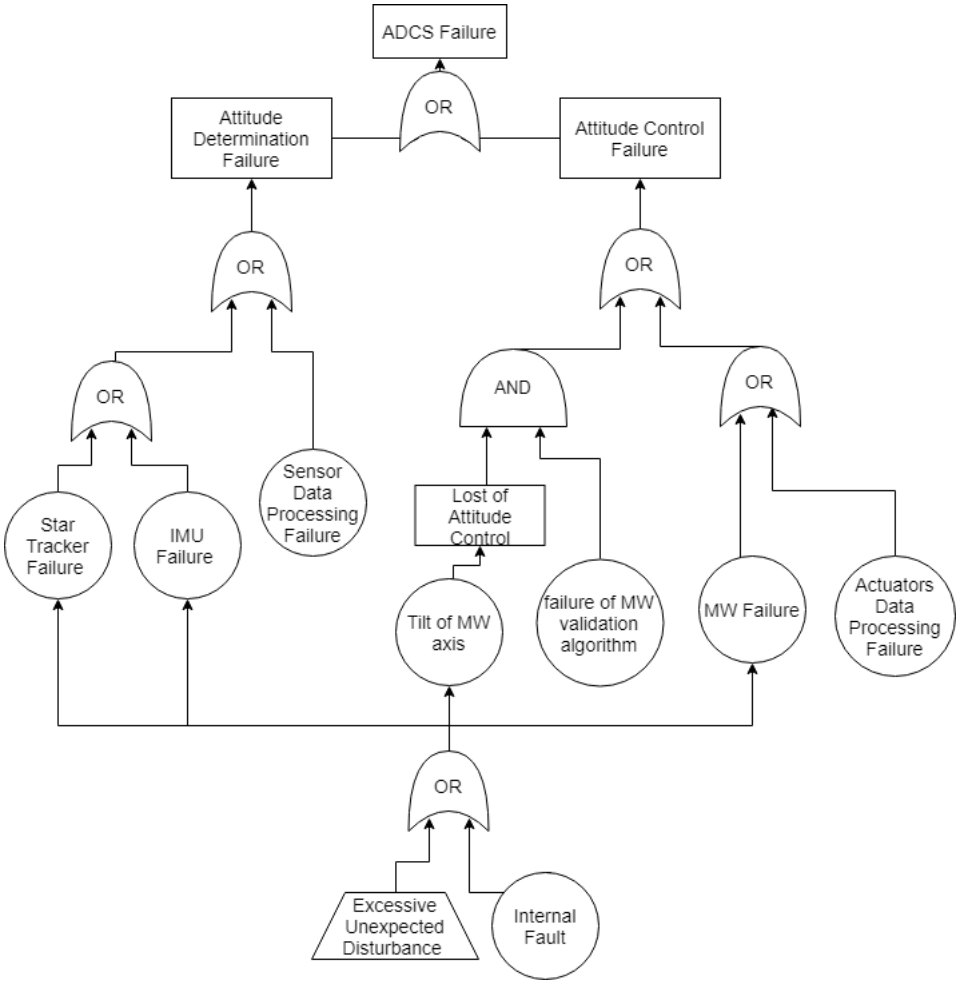

Figure 6.6: Fault tree of the ADCS subsystem.

7 Propulsion

This chapter details the design of the propulsion subsystem. An overview of the current design and its requirement compliance matrix are given in section 7.1 and section 7.2. Following this, section 7.3 describes the approach taken to design the propulsion subsystem to this level. The verification and validation of the design and its method is given in section 7.4. section 7.5 describes the sensitivity analysis conducted for the propulsion system and the subsequent possible design changes required. Section 7.6 summarises the risks and mitigation methods associated with the propulsion system.

7.1. Design Overview

Trade-offs for the propulsion system dealing with criteria such as thrust level, power required, mass, and cost were dealt with previously in [10]. This has led to the selection of a pressure fed, dual mode system relying on bipropellant main engine and monopropellant reaction control system (RCS). This choice was made since the dual mode system enables operation of both thruster and main engine functions while minimising on structural weight and cost due to the sharing of hardware such as tanks and propellant. Furthermore, the choice of type of propulsion, in this case chemical, while having significant flight heritage [16] [15][76] is also influenced by power and trajectory requirements. As mentioned in chapter 10, the necessity of using RTG's as a power source limits nominal power to 351.7 W. This is much lower than the power input required to facilitate electric propulsion. Furthermore, the high thrust capabilities of chemical propulsion over others is also advantageous in terms of transfer time, discussed further in [10].

The propulsion system consists of two main engine, where one is for complete redundancy, and 16 reaction control thrusters, out of which eight are for complete redundancy. Tanks for the fuel (hydrazine), oxidiser (nitrogen tetroxide), and pressurant (helium) along with feed lines and valves comprising the distribution system ultimately make up the propulsion subsystem.

During the high thrust and large ΔV requiring manoeuvres such as the deep space manoeuvres required for the transfer trajectory to Saturn, orbit insertions, and orbital plane changes the system works as bipropellant by use of the main engine. Specific ΔV values for all planned manoeuvres performed by the main engine is found in Table 4.6. Manoeuvres for attitude control, changing of spacecraft orientation, and momentum dumping are performed by the RCS in monopropellant mode. Details of the planned manoeuvres is found in Table 7.3.

In order to deal with the effect of centre of gravity shift due to propellant consumption, the main engines will be equipped with active thrust control such that the engines can be gimballed by cone angle adjustments [95]. An overview of the mass and power budgets of the propulsion system components are given in Table 7.1. The mass budget is given for the entire propulsion system which includes two main engines, 16 RCS thrusters, hydrazine fuel tank, nitrogen tetroxide oxidiser tank, helium pressurant tank, and the distribution system. The peak power budget on the other hand provides values for one engine and one RCS thruster since the total peak power depends on the number of thrusters used simultaneously for various manoeuvres.

Component	Mass [kg]
Main Engines x2	10.4
RCS Thrusters x16	5.3
Oxidiser Tank	44.8
Nitrogen Tetroxide	1405.3
Fuel Tank	119.9
Hydrazine	1732.7
Pressurant Tank	134.5
Helium	15.5
Distribution System	30.9

Components	Peak Power [W]
Main Engine Valves	46
RCS Thruster Valve	8.3
RCS Thruster Valve Heater	1.5
RCS Thruster Catalytic Bed Heater	3.9

Table 7.1: Overview of Propulsion system components, with corresponding mass and power.

7.2. Requirement Analysis

A compliance matrix for the requirements set for the propulsion subsystem is given in Table 7.2.

Table 7.2: Compliance matrix for the propulsion requirements.

Code	Requirement	Verification Method	Compliance	Section
PRP-00.147	The Propulsion subsystem shall provide a minimum ΔV of 3719 m/s for the whole mission duration.	Testing	✓	7.3
PRP-00.148	The Propulsion subsystem shall provide minimally 15% extra ΔV for change of mission possibilities.	Testing	✓	7.3
PRP-00.149	The Propulsion subsystem shall be able to provide a thrust of maximally 445 N.	Testing	✓	7.3
PRP-00.150	The Propulsion subsystem shall provide a minimum ΔV of 231 m/s for end-of-life manoeuvre.	Testing	✓	7.3
PRP-00.151	The Propulsion subsystem shall allow debris-avoiding manoeuvres.	Testing	✓	
PRP-00.152	The Propulsion subsystem shall include a budget for orbit corrections.	Testing	✓	7.3
PRP-00.153	The Propulsion subsystem shall have a maximum volume of 2.96 m^3.	Review of Design	✓	7.3
PRP-00.154	The Propulsion subsystem shall have a maximum mass of 345 kg.	Review of Design	✓	7.3
PRP-00.155	The Propulsion subsystem shall need a nominal power of maximally 0 W.	Testing	✓	7.3
PRP-00.156	The Propulsion subsystem shall need a peak power of maximally 311.5 W.	Test	✓	7.3
PRP-00.157	The Propulsion subsystem shall include an in-mission validation process.	Test	✓	7.4
PRP-00.158	A safety margin of 5% shall be applied when using off-the-shelf components.	Review of Design	✓	7.3
PRP-00.159	A safety margin of 10% shall be applied when using existing technology with minor modifications.	Review of Design	✓	-
PRP-00.160	A safety margin of 15% shall be applied when using existing technology with major modifications.	Review of Design	✓	-
PRP-00.161	A safety margin of 20% shall be applied when using completely new components.	Review of Design	✓	-
PRP-00.162	The Propulsion subsystem shall have a cost of maximum 1.7 M €.	Review of Design	✓	14.3
PRP-00.163	The Propulsion subsystem shall have a minimum reliability of 96.3%.	Review of Design	✓	13.5
PRP-00.164	The Propulsion subsystem shall have a housekeeping data rate of maximally 33 kb/s.	Review of design	✓	9.2
PRP-00.165	Longest engine burn shall be minimally 89 minutes.	Test	✓	7.3
PRP-00.166	Propulsion system shall not have any single points of failure.	Review of Design	✓	7.6
PRP-00.167	Total Operating time shall be minimally 84 days	Test	✓	7.3

Requirements PRP-00.147, PRP-00.148, and PRP-00.150 (Table 7.2) are also discussed in chapter 4. PRP-00.162 and PRP-00.163 (Table 7.2) are detailed further in section 14.3 and subsection 13.5.2.

7.3. Design Approach

The design of the propulsion system takes place in primarily two parts. Initially, the main engine is sized, with information on large ΔV burns for both interplanetary transfer and in-mission manoeuvres so as to satisfy requirements PRP-00.147, PRP-00.148, and PRP-00.150 from Table 7.2. A summary of the ΔV required for each leg of the interplanetary transfer and planned manoeuvres for the in-mission phase is given in Table 4.1 and subsection 4.1.2. This results in a total interplanetary ΔV of 1330 m/s and in-system ΔV of 2366 m/s. The in-mission

ΔV includes a 15% contingency. The required propellant mass to facilitate this total ΔV of 3696 m/s was obtained via Tsiolkovsky's rocket equation, Equation 7.1, resulting in a required main engine propellant mass of 2685.1 kg. This equation uses specific impulse, I_{sp}, Earth's standard gravity, g, ΔV, and the spacecraft dry mass M_{dry} as inputs. The propellant mass calculation was iterative in nature as it started out with using the dry mass estimated in [10], which equalled 1570 kg. Once all other subsystems and the overall structure was sized to a sufficient degree for a mass output, the propulsion sizing was reiterated with the final dry mass of 1229.9 kg, given in section 14.1.

$$M_{prop_{me}} = M_{dry}(e^{\Delta V/I_{sp} \cdot g} - 1) \tag{7.1}$$

A similar propellant requirement analysis is done for the RCS thrusters. Firstly, the functions to be performed by the thrusters are shown in Table 7.3. From the computations mentioned in section 6.3, the time and thrust required for these were obtained. From the maximum torque, divided by the arm (≈2, Table 6.3.1), the required thrust is found. Using Equation 7.2, where F is the thrust, t is the burn time, and v_e is the exhaust velocity, the required propellant mass per orbit is computed. Table 7.3 gives an overview of the time, thrust, and propellant required to perform these manoeuvres per orbit, as computed in Table 6.5, 6.6, and 6.4. The counteraction of torque during a single fly through of the plumes is assumed to be one manoeuvre and hence the total number of manoeuvres for this function equals the number of times the spacecraft flies through the plumes. Apart from these functions, the thrusters have been sized also to perform in-transfer manoeuvres to stabilise the spacecraft and for other anomalous manoeuvres such as for debris avoidance (requirement PRP-00.151 and PRP-00.152, Table 7.2) by accounting for 10% more propellant. Ultimately, this led to a total RCS propellant mass of 335.5 kg.

$$M_{prop_{RCS}} = \frac{F \cdot t}{I_{sp} \cdot g_0} \tag{7.2}$$

Table 7.3: RCS Functions characteristics per manoeuvre.

Function	Minimum Time [s]	Maximum Thrust [N]	Propellant Mass [kg]	Manoeuvres Required
90 deg about Y-axis	245	0.48	0.042	2028
Momentum Dumping	300	0.75	0.071	2877
Plume Torque Counteraction	2882.5	0.017	0.017	2028

7.3.1. Propellant Selection

Hydrazine is selected as fuel and nitrogen tetroxide as oxidiser. The main engine will use this combination as bipropellant whereas the RCS thrusters will use hydrazine as monopropellant with a catalyst for decomposition. The hypergolic nature of this combination makes it an attractive fuel choice as it is storable for a long period of time and it is easily combustible and allows for repeated ignitions. Furthermore, this fuel has shown extensive heritage as it has been used in past missions such as Cassini [16], New Horizons [76], and Galileo [15]. Characteristics of the fuel and oxidiser used in subsequent calculations are given in Table 7.4 [93]. Sustainability of this propellant choice is described in section 16.4.

Table 7.4: Propellant properties.

Propellant	Liquid Density [g/cm^3]	Specific Impulse [s]
Hydrazine (N_2H_4)	1.550	224 (as monopropellant)
Nitrogen Tetroxide (N_2O_4)	1.004	326 (with Hydrazine as bipropellant)

7.3.2. Propulsion System Configuration

The sizing of the main engine required certain parameters such as thrust level, propellant, and specific impulse to be decided on and used as input for tank sizing. Analysis of past missions and off-the-shelf productions found the HiPAT 445 N Dual Mode produced by Aerojet Rocketdyne to be suitable as the main engine. This choice led to an oxidiser to fuel ratio (O/F) of 1.12. With a total propellant mass as 2685.1 kg, the O/F allows for the computation of oxidiser and fuel masses of 1418.5 kg and 1266.6 kg respectively. Adding the hydrazine fuel required for thruster use results in a total hydrazine fuel mass of 1649.8 kg. In order to determine propellant tank volume, an additional margin for ullage and trapped volume of 5% was added to the fuel volume [93]. This results in an oxidiser tank volume of 0.98 m^3 and fuel tank volume of 1.78 m^3. The choice of material for the tanks involved choosing a material that has the most strength for a given mass but also one that is chemically compatible with the chosen propellant. In this case, 2219-Aluminium alloy was decided upon for tank material. Using the tank volume mentioned, the hydrazine fuel tank will be spherical with a radius of 0.7 m and thickness of 4 mm. Similarly, NTO oxidiser tank has a radius of 0.6 m and a thickness of 3.4 mm. The oxidiser tank shape changed from spherical to pill shaped due to iterations considering layout, detailed further in subsection 12.3.1. Tank thicknesses were computed using equations of hoop and longitudinal stress, Equation 7.3 and Equation 7.4. These used yield stresses of the tank material, operating tank pressures, and tank radii as inputs.

$$\sigma_{hoop} = \frac{p \cdot r}{t} \tag{7.3}$$

$$\sigma_{longitudinal} = \frac{p \cdot r}{2t} \tag{7.4}$$

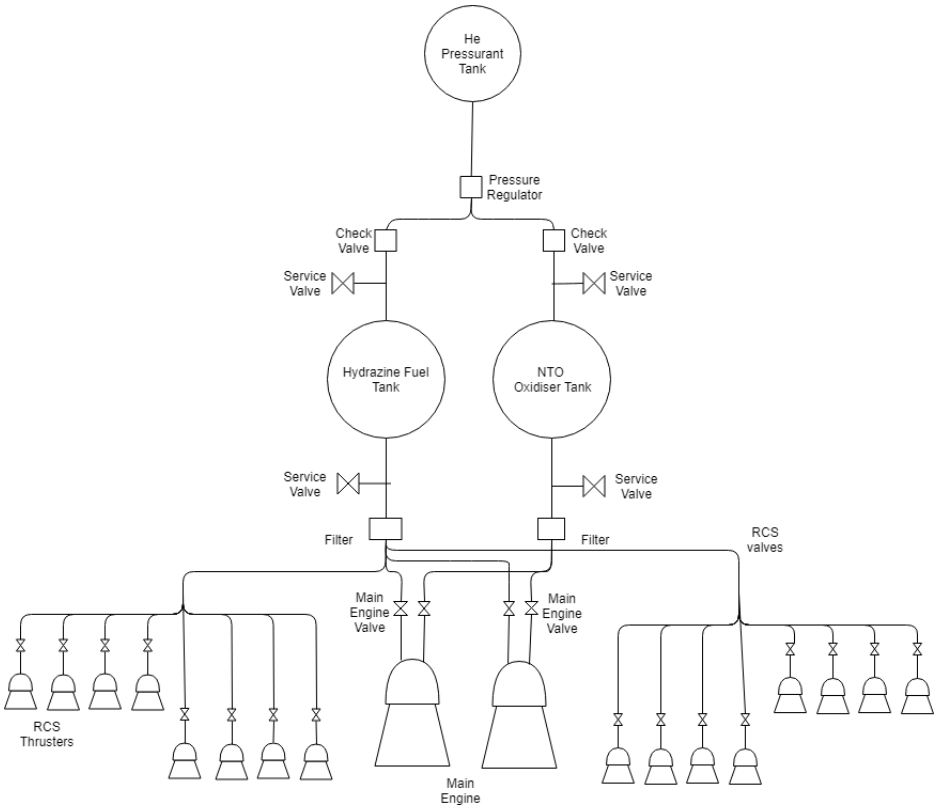

Figure 7.1: Schematic of propulsion system.

In order to size the pressurant tank, fuel and oxidiser tank pressures were computed. Using statistical relations for tank pressure versus tank volume from [93], a fuel and oxidiser tank pressure of 0.86 MPa and 0.93 MPa. Using the average of these along with an operating pressure of 27.6 MPa, obtained from literature study of Cassini[16], a pressurant mass of 15.41 kg was obtained. Determining tank volume of the pressurant included adding a 5% margin, resulting in a pressurant tank volume of 0.32 m^3. The pressurant tank is pill shaped with a total length of 1.22 m and width of 0.65 m. Using stress equations mentioned above, the spherical ends have a thickness of 1.8 mm and the cylindrical part has a thickness of 7 mm. This shape was decided due to the same reasons as mentioned previously for the oxidiser tank.

The distribution system of the propulsion system requires specific material that is compatible with hydrazine. In this case, 2219-Aluminium alloy was chosen. Furthermore, from [93], material of the distribution system was assumed to be 10% of the propulsion dry mass. The thrusters will be fed hydrazine from the fuel tank through a dedicated feed line which splits in order to feed the propellant to each thruster. Two feed lines each from the fuel tank and oxidiser tank feeds each of the main engines as well. A schematic of the propulsion system is shown in Figure 7.1 [61].

It can be seen from Table 7.3 that the required nominal thrust is a maximum of 0.75. In order to facilitate these manoeuvres, off-the-shelf products were deemed acceptable for use. In this case, the MR103 1 N hydrazine monopropellant thrusters from Aerojet Rocketdyne was chosen, which has more than sufficient flight heritage. Analysis of previous missions Cassini [16], New Horizon[76], and Galileo [15] were done to determine the appropriate thruster configuration. 16 thrusters in clusters of four was decided upon to allow for translational and attitude control around all three axes. The configuration can be seen in Figure 7.2 [26].

With regards to spacecraft stability due to propellant usage, it is important to ensure engine alignment with spacecraft centre of gravity during the entire mission duration to maintain spacecraft stability. In order to do so, the variations in centre of gravity due to propellant usage during planned manoeuvres is added is analysed and added to the centre of gravity of the dry spacecraft. This allows for planning of the adjustments of the engine cone angle by the gimbal actuators. A feedback loop is included in which the response thrust of the engine to the adjustments are assessed to see if any torque is produced, in which case further adjustments will be commanded through. The development of this system is included in future recommendations to be done in further design stages. The moment of inertia will also change as propellant is consumed, and this can also be computed in a similar way as mentioned previously. The lower moment of inertia at end of life conditions compared to that at beginning of life implies that the design at this stage is conservative. Spacecraft stability is also impacted by propellant sloshing which can occur during orbital manoeuvres. IMU's present as part of the ADCS sensors will be responsible for measuring changes in spacecraft attitude due to sloshing and feed the information to the propulsion system control system which will in turn command pointing of engines or thrusters as necessarry.

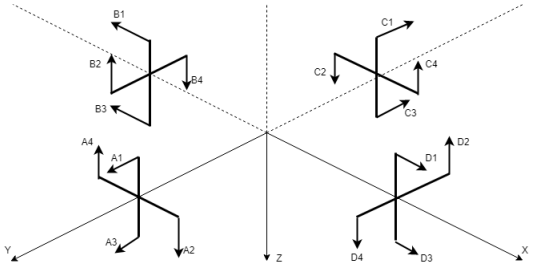

Figure 7.2: RCS thruster configuration.

7.4. Verification & Validation

Unlike the requirement verification methods for other subsystems[43], the method of 'review of design' replaces that of demonstration and the method of inspection is part of analysis[44]. Requirements relating to ΔV, thrust, manoeuvres, and power (PRP-00.147,PRP-00.148,PRP-00.149,PRP-00,150,PRP-00.151,PRP-00.152,PRP-00.155, PRP-00.156, PRP-00.167, Table 7.2) are all verified by means of testing such as firing tests, thruster alignment and electrical tests. Requirements relating to geometry and mass (PRP-00.153, PRP-00.154, Table 7.2) are also verified by means of testing by checking the system dimensions and mass. Those requirements relating to off-the-shelf components, cost, and risk (PRP-00.158, PRP-00.162, PRP-00.163, PRP-00.166, Table 7.2) are verified by means of review of design. Since this mission is distinctive from other outer solar system missions in terms of trajectory and thus ΔV requirements, comparison with propulsion systems of other spacecraft will not serve as valid forms of verification. However, the method of sizing mentioned in section 7.3 is assumed from [93], which is a verified method for this preliminary design phase since it uses established and recognised equations.

7.5. Sensitivity Analysis

A design sensitivity analysis is performed, in which key parameters that drive the design are varied in order to assess the strength of the design to changes. This analysis involves changing values of thrust level, specific impulse, ΔV, and dry mass by a 10% increase or decrease and analysing possible design changes that may become necessary. This margin is chose so as to keep the parameters being varied within their realistic ranges while assessing the impact of their change.

If the maximum thrust output of the main engine were to reduce from 445 N by 10% to 400.5N, there would be an associated increase in burn time by 10% as well. This does not require any significant design changes since the burn times are still within an acceptable range and thus allows the mission to carry on as planned. Similarly, if the RCS thrusters were to experience a 10% reduction in maximum thrust to 0.9 N, they would still be able to perform all manoeuvres mentioned in Table 7.3 since there is a sufficient margin between maximum thrust required for the manoeuvre and maximum thrust producible from the thruster.

Reducing specific impulse by 10% from 326 s to 293 s results in an increase in propellant mass by 17%. Thus, propellant tanks would need to be resized to be larger which could affect overall spacecraft layout and mass. The maximum usable fairing diameter and length are 4.6 m and 11.4 m respectively [107]. The current spacecraft dimensions are 3.8 m in diameter and 5.8 m in length (see section 13.2). This means that the driving dimension is the diameter, which may only increase by 0.8 m until the spacecraft no longer fits. The driving components for the spacecraft diameter are the bus of the spacecraft (1.50 m, see section 12.1), and the

protective skirt (3.6 m, see section 12.1). The sizes of the RTGs (presented in Table 10.3) are set, hence the size of the skirt will only change with the increase in bus size which is affected by propellant mass. However, the increase in propellant mass due to the decrease in specific impulse only results in an increase in propellant tank diameter by 0.05 m, which is clearly not critical in regards to launcher selection.

Increasing ΔV by 10% to 4073.5 m/s causes increase in propellant mass by 15%. Subsequent design changes necessary are similar to those specified previously for specific impulse change.

Finally, increasing dry mass by 10% results in similar 10% increase in propellant mass. Furthermore, burn times see an increase of 3%. Propellant tank only needs an increase by 2% to accommodate this propellant, and hence has no significant impact for the overall design.

7.6. Risk Analysis

The following section highlights the major risks associated with the propulsion subsystem. Failure of the propulsion subsystem would quite obviously be catastrophic to the mission, hence a risk analysis and identification of appropriate mitigation methods is paramount. Figure 7.3 shows the fault tree analysis conducted for the subsystem, with identified risks expanded upon below.

1. **PRR-0.1 Propellant leakage** The probability of propellant leakage is high due to the large amounts of joints in fuel and oxidiser lines, however the severity is low [89]. Thus, allowing for contingency propellant in the propellant budget is a sufficient mitigation method for this risk.
2. **PRR-0.2 Pressurant tank leakage** The risk of pressurant leakage is lower than that of propellant due to the lesser amount of feed lines the pressurant has to travel through. However, should there be a leakage, the system will operate in blow down mode. However, this will cause reduction in engine and thruster performance over time, which will prevent the carrying out of necessary thrusts to carry out the mission. Further mitigation involves constant monitoring of tank pressure and installing of additional valves to control loss of pressure.
3. **PRR-0.3 Catalyst bed heater failure** Failure of the catalyst bed heater results in incomplete decomposition of hydrazine which leads to performance drop of the thruster. The thrusters are equipped with redundant catalyst heater beds to serve as mitigation in case the primary one fails.
4. **PRR-0.4 Catalyst contamination** Similar to the previous risk, contamination of the catalyst reduces the area of decomposition for hydrazine resulting in a performance drop of the thruster. This impact of this risk can be minimised by ensuring stringent cleanliness of all associated components.
5. **PRR-0.5 Valve failure** Inadvertent closing or opening of the valve would result in improper propellant supply to the engines and thrusters. This would be catastrophic to the subsystem. Redundant valves and feed lines to form cross strapped feed system mitigates this risk.
6. **PRR-0.6 Thruster failure** Eight redundant thrusters are included in the design to mitigate for failure of any of the primary thrusters. Furthermore, propulsion system control will allow for thrusters from different batches to be used together as well to ensure continued control about all three axes.
7. **PRR-0.7 Engine failure** Two main engines are included in the design, one of which is for redundancy and serves as mitigation in case the primary one fails. Actuaotrs to gimbal the main engines will then ensure continued alignment with the spacecraft centre

of gravity so as to keep the spacecraft stable.

8. **PRR-0.8 Foreign body impact** Impact of foreign bodies on the subsystem could be catastrophic depending on velocity or debris size. The subsystem structure is designed to withstand a certain level of impact, however due to the unpredictability of this risk, a definite mitigation method is not determined.
9. **PRR-0.9 Pressure regulator failure** Additional isolation valves are incorporated in the design so as to have cross strapping capability if this failure occurs [123].
10. **PRR-0.10 Thermal failure** It is important that the propellants and associated hardware are maintained within their operational temperatures, as specified in Table 11.3, otherwise they will fail. This risk depends on the reliability of the thermal control system.
11. **PRR-0.12 Feed line leakage** Failure of the feed lines could lead to the malfunctioning of the main engines and thrusters due to lack of propellant supply. Leakage of propellants could also cause failure of the rest of the propulsion system as well. This risk can arise due to over-pressurisation of the feed lines causing them to burst or due to structural failure. Mitigation methods include stringent pre-testing as well as introducing redundant feed lines to form a cross-strapped distribution system.

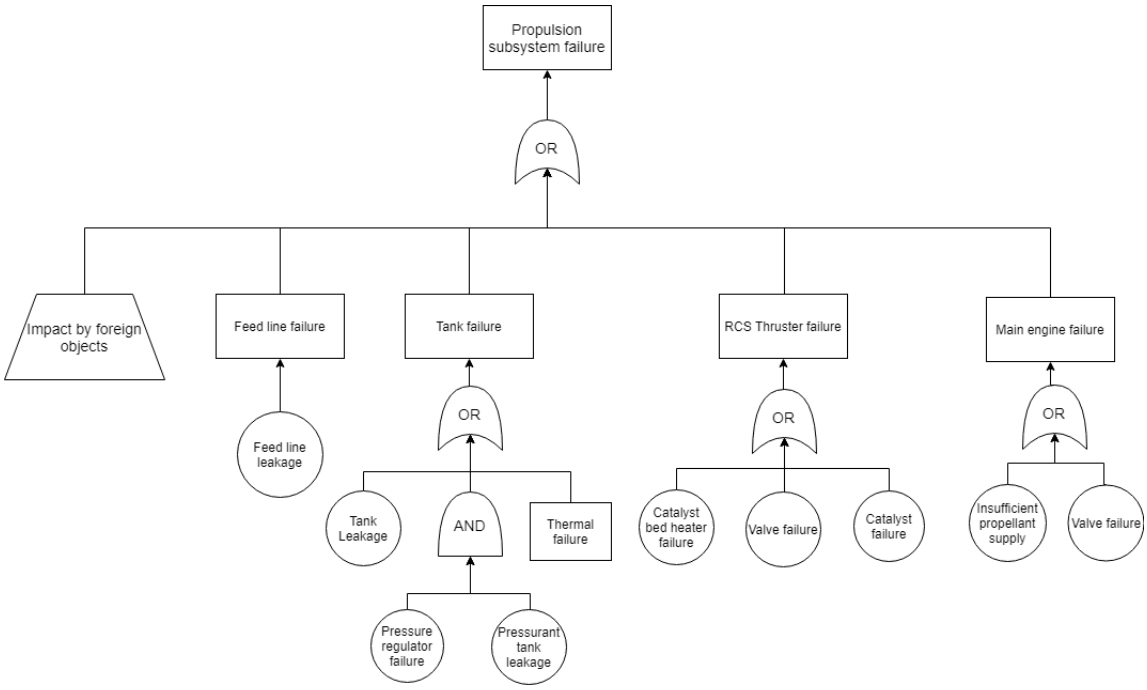

Figure 7.3: Fault tree of the propulsion subsystem.

8 Telemetry, Tracking & Command

In this chapter, the Telemetry, Tracking & Command (TT&C) subsystem design is presented. First, an overview of the design is given in section 8.1. Afterwards, section 8.2 shows the compliance with the requirements and the verification methods to be used. The approach used is described in section 8.3, and this approach is validated in section 8.4. To show the flexibility of the design, a sensitivity analysis is conducted in section 8.5. Finally, risks associated with the subsystem are shown and mitigated in section 8.6.

8.1. Design Overview

This section presents the overview of the link budget of the TT&C subsystem. In Table 8.2, the downlink budgets for both the high gain antenna (HGA) and low gain antennas (LGAs) are given.

Table 8.1: Overview of TT&C components, with corresponding mass and power.

Component	Active P [W]	Sleep/off [W]	Mass [kg]
1 HGA	-	-	60 (scaled from [115])
2 LGAs	-	-	0.8 (scaled from [115])
3 Transmission lines	-	-	10.9 (10% of total)
4 DST 2x (redundancy)	10.2 [115]	0	8 [115]
5 Ka-T 2x (redundancy)	Included in payload (chapter 5)	-	Included in payload (chapter 5)
6 CDU 2x (redundancy)	Powered by DST [115]	-	0.7 [115]
7 TCU 2x (redundancy)	5.2 [115]	0 [115]	7.3 [115]
8 TWTA-X 2x (redundancy)	38.6 (with eff. 70% [63])	9.3 (scaled from [115])	10.8 [115]
9 Waveguide Transfer Switch 4x (redundancy)	- [115]	- [115]	1.5 [115]
10 X-band diplexer (2)	- [115]	- [115]	3.4 [115]
11 Hybrid coupler	- [115]	- [115]	0.1 [115]
12 Ka-band exciter	3.1 [115]	0 [115]	2.4 [115]
13 Ka-band translator	8 [115]	0 [115]	3.5 [115]
14 TWTA-Ka 2x (redundancy)	28.6 (with eff. 70% [63])	6.8 (scaled from [115])	10.8 [115]
15 X-band BPSK (de-)modulator 2x (redundancy)	0.05 [33]	0 [33]	Data unavailable
16 Ka-band BPSK (de-)modulator 2x (redundancy)	0.1 [33]	0 [33]	
17 Turbo encoder 2x (redundancy)	1 [14]	0 [14]	
18 Turbo decoder 2x (redundancy)	1 [14]	0 [14]	
Peak (all functioning)	105.5 (+10% cont.)	17.7 (+10% cont.)	120.3 +20% = 144.3
Total transfer phase (LGAs) (4+7+8+14(sleep)+15x2+17+18)	69.1 (+10% cont.)		
Total orbit phase (HGA) (4+7+8(sleep)+12+13+14+16x2+17+18)	73.3 (+10% cont.)		

Table 8.2: Overview of the downlink budget for closest distance.

		HGA/LGA
Characteristics	Frequency [GHz]	31.8/8.4 [54]
	Antenna diameter [m]	3/0.075
	Maximum pointing error [deg]	0.0085/0.016
	Alpha 1/2 [deg]	0.22/33.33
	Beamwidth [deg]	0.017/0.031 [52]
	Distance [m]	1.272E12 [1,2]/1.84E11 [1]
Transmitter parameters	Antenna efficiency [−]	0.55 [30]
	TWTA power provided [dBm]	43.01/44.31
	Circuit loss [dB]	-0.46 [29]
	Antenna gain [dB]	57.40/13.80
	Coding rate [−]	1/2 (both) [53]
	EIRP [dBm]	99.95/57.65
	Bandwidth efficiency [−]	0.7

		HGA/LGA
Path parameters	DSN G/T [dB]	63.6/61.3 [52]
	Pointing loss [dB]	-1.79E-2/-2.59E-6
	Space loss [dB]	-304.59/-276.23
	Atmospheric attenuation [dB]	-0.2/-0.05 [65]
	Rain attenuation [dB]	0 [65]
Total power summary	Total received power [dBm]	-141.25/-157.33
Carrier performance	Required Eb/N0 [dB]	1.1 [53]
	Link margin [dB]	3 [110]
Telemetry performance	Available E_b/N_0 [dB]	4.57/4.52
	E_b/N_0 margin [dB]	0.47/0.42
	Bandwidth [Hz]	541350/13530
	Capacity [kb/s]	542.64/13.44
	Symbol rate [kb/s]	378.95/9.47
	Data rate [kb/s]	189.47/4.74
	Useful data rate [kb/s]	180.00/4.5

The power used by the subsystem and its mass can be found in Table 8.1. Table 8.2 and 8.3 present the link budgets of the antennas. Three rates are given: two data rates and one symbol rate. The two different data rates represent the total data rate and the useful data rate. The total data rate alone includes the useful data, and other data such as headers and

Table 8.3: Overview of the uplink budget for closest distance.

		HGA/LGA
Characteristics	Frequency [GHz]	34.2/7.4 [54]
	Antenna diameter [m]	34/70 [52]
	Maximum pointing error [deg]	0.0085/0.0315
	Alpha 1/2 [deg]	0.20/37.84
	Beamwidth [deg]	0.017/0.063 [52]
	Distance [m]	1.272E12 [1,2]
Transmitter parameters	Antenna efficiency [−]	0.55 [30]
	Power provided [dBm]	73.01/73.01 [114]
	Circuit loss [dB]	-0.46 [29]
	Antenna gain [dB]	78.5/74.4 [52]
	Coding rate [−]	1/2 (both) [53]
	EIRP [dBm]	151.05/146.95
	Bandwidth efficiency [-]	0.7 [110]

		HGA/LGA
Path parameters	Receiver gain [dB]	58.03/12.69
	Noise temperature [dB]	24.47/24.47 [115]
	Pointing loss [dB]	-2.07E-2/-8.3E-6
	Space loss [dB]	-305.22/-291.92
	Atmospheric attenuation [dB]	-0.2/-0.05 [65]
	Rain attenuation [dB]	0 [65]
Total power summary	Total received power [dBm]	-120.82/-156.79
Carrier performance	Required E_b/N_0 [dB]	1.1 [53]
	Link margin [dB]	3 [110]
Telemetry performance	Available E_b/N_0 [dB]	4.54/4.59
	E_b/N_0 margin [dB]	0.44/0.49
	Bandwidth [Hz]	60150380/15040
	Capacity [kb/s]	59974.16/15.12
	Symbol rate [kb/s]	42105.26/10.53
	Data rate [kb/s]	21052.63/5.26
	Useful data rate [kb/s]	20000.00/5.00

identifiers that indicate what spacecraft sends the signal. This is used in the calculation of E_b/N_0. The useful data rate only includes the scientific or housekeeping data, and is about 95% of the total data rate, according to [111]. Finally, the symbol rate includes extra bits for redundancy due to coding, that do not include any new information. Since the coding rate is 1/2, for every bit, another bit is added for the purpose of encoding the signal.
Furthermore, Table 8.2 and 8.3 show only the link budgets for the minimum distances from Earth to Saturn and Earth to Venus as an example.[1,2] For an overview of the data rates at the minimum and maximum distances, Table 8.4 holds.

Table 8.4: Useful data rates at different distances for the different antennas.[1,2]

Antenna	Maximum distance [m]	Minimum distance [m]	Minimum data rate [bit/s]	Maximum data rate [bit/s]
HGA (downlink)	1.582E12 (at Saturn)	1.272E12 (at Saturn)	120000	180000
LGA (downlink)	1.272E12 (min. at Saturn)/ 1.582E12 (max. at Saturn)	1.840E11 (Earth to Venus)	100/65	4500
HGA (uplink)	1.582E12 (at Saturn)	1.272E12 (at Saturn)	13000000	20000000
LGA (uplink)	1.272E12 (min. at Saturn)/ 1.582E12 (max. at Saturn)	1.840E11 (Earth to Venus)	5000/3500	250000

8.1.1. Spacecraft Systems

The subsystem shall include one HGA (using Ka-band) with a diameter of 3 m, and two omnidirectional LGAs (using X-band) with effective diameters of 0.075 m, their sizes will be elaborated upon in subsection 8.3.2. These LGAs will be used for transmission during the earlier phases of transfer, when the HGA cannot be pointed freely due to its functioning as a sun shield (see section 11.1). When in-situ, the LGAs will only be used to receive commands. The HGA will be used for science data transmission and tracking, especially during the radio experiment. For regular ranging only the DST will be used, whereas both the DST and Ka-T are used during the radio experiment. The HGA can support an average downlink data rate of 150 kbit/s (average of Table 8.4), which is mainly used for science data transmission. The LGAs allow for a downlink data rate of 4.5 kbit/s when at Venus. The maximum data rate necessary for full housekeeping data transmission (based on subsection 9.3.1) occurs when in orbit around Enceladus, and is 29.5 bit/s (from subsection 9.3.1). Housekeeping data shall be sent down along with the scientific data, thus only using a negligible part of the total HGA data rate.

[1]Retrieved from `https://nssdc.gsfc.nasa.gov/planetary/factsheet/saturnfact.html` last opened on June 19, 2019

[2]Retrieved from `https://theskylive.com/3dsolarsystem?obj=11p&h=08&m=12&date=2040-06-13` last opened on June 19, 2019

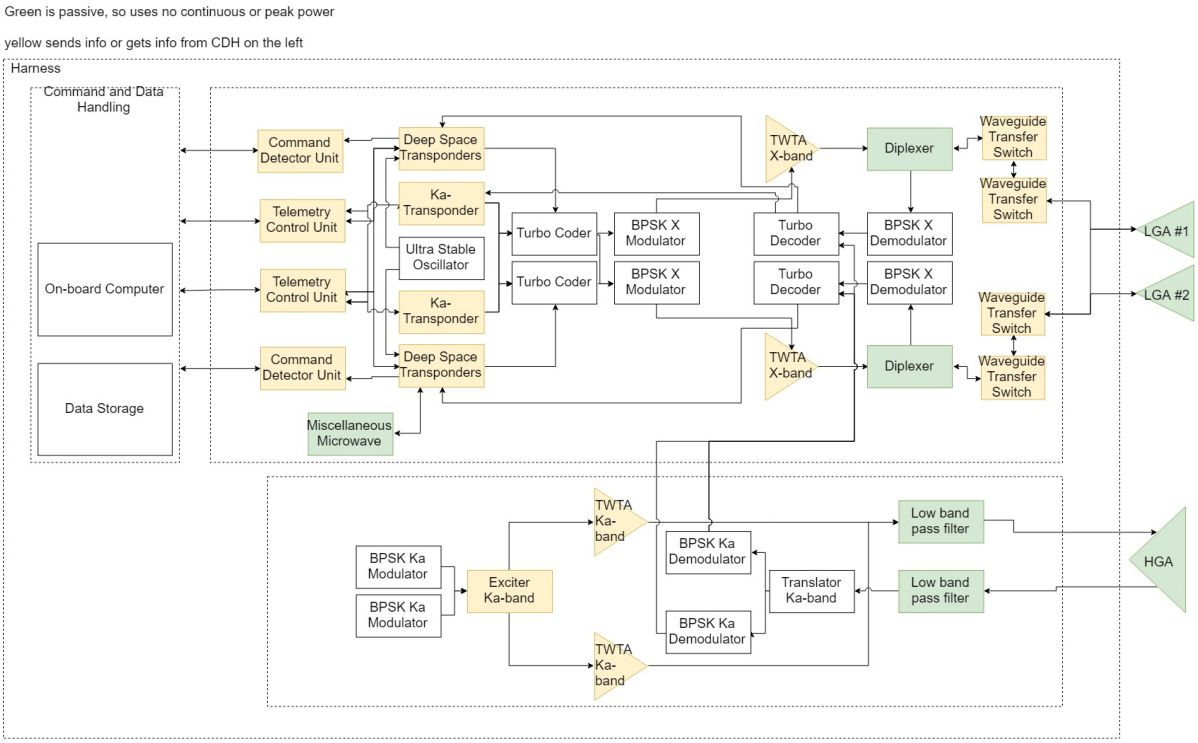

Figure 8.1: Architecture of the TT&C subsystem on the spacecraft.

Aside from the antennas, other systems are present that alter some important qualities of the link budget, such as modulation and coding type, and the transmitter power. The chosen modulation type is binary phase-shift keying (BPSK), and the coding type is turbo coding, which is supported by the Deep Space Network (DSN) [53]. These shall be treated more in-depth in section 8.3. The architecture can be found in Figure 8.1. The components in the architecture will be elaborated upon in section 8.3 and 8.6.

8.1.2. Ground Station

The ground station used for communications is the DSN, located in Madrid, Goldstone, and Canberra. All of these include a 34-m beam waveguide (BWG) antenna, which supports the Ka-band, a 34-m high-efficiency (HEF) antenna, and a 70-m antenna. Since the DSN is located in dry locations, rain attenuation could be assumed to be 0 (see Table 8.2 and Table 8.3). As the HGA uses the Ka-band, only the 34-m BWG antenna can be used for the HGA link. The LGAs use the X-band, thus allowing for the choice of the 70-m antenna for communications. [52]

When at Saturn, the uplink data rate received by the LGAs is 3.5-5 kbit/s, which is more than enough for receiving commands[115], which is useful in case the HGA cannot be pointed. The HGA will receive data on the Ka-band, resulting in a maximum uplink data rate of 13-20 Mbit/s, which is also more than sufficient for receiving commands and tracking.

The main contributions of the uplink data rates are the commands and tracking, which makes use of a ranging signal and the Doppler shift. The ranging method used is Delta Differential One-way (Δ DOR) regenerative pseudo-noise (PN) ranging with weighted-voting balanced Tausworthe, voting ν=4 (T4B) component code, which is supported by the DSN [55]. More about its selection can be found in section 8.3.

Overall, the HGA has Ka-band transmitting and receiving feeds, whereas the LGAs have X-band transmitting and receiving feeds.

8.2. Requirement Analysis

The compliance matrix that shows compliance with all subsystem requirements can be found in Table 8.5.

Table 8.5: Compliance matrix for the TT&C subsystem requirements.

Code	Requirement	Verification Method	Compliance	Section
TTC-00.203	The TT&C subsystem shall have a minimum average downlink data rate of 0.150 $Mbits/s$.	Analysis	✓	8.1 & 8.3.5
TTC-00.204	The TT&C subsystem shall ensure complete transfer of the payload data stored.	Analysis	✓	8.3.1
TTC-00.205.1.1	The TT&C high-gain receiver on-board shall have a minimum gain of 58.0 dB	Test	✓	8.1
TTC-00.205.1.2	The TT&C low-gain receiver on-board shall have a minimum gain of 12.7 dB	Test	✓	8.1
TTC-00.205.2.1	The TT&C high-gain transmitter on-board shall have a minimum gain of 57.4 dB	Test	✓	8.1
TTC-00.205.2.2	The TT&C low-gain transmitter on-board shall have a minimum gain of 13.8 dB	Test	✓	8.1
TTC-00.206	The TT&C Signal to Noise ratio shall be in the range of 0.94 to 1.01.	Analysis	✓	8.1 & 8.2
TTC-00.207	The TT&C subsystem shall transmit with an antenna with diameter of minimum 3 m.	Inspection	✓	8.1
TTC-00.208.1	The TT&C subsystem's HGA shall transmit in the Ka-band.	Demonstration	✓	8.1 & 8.3
TTC-00.208.2	The TT&C subsystem's LGAs shall transmit in the X-band.	Demonstration	✓	8.1 & 8.3
TTC-00.209	The TT&C subsystem shall take into account the Doppler Effect of sending signals.	Analysis	✓	8.2 & 8.3.4
TTC-00.210	The TT&C subsystem shall comply with the communication requirements given by the NASA Deep Space Network.	Analysis	✓	8.2
TTC-00.211	The TT&C shall periodically communicate the status of the system to Earth with a temporal frequency of 4.2 hours.	Analysis	✓	8.3.1
TTC-00.212	The internal part of TT&C shall have a maximum volume of 0.189 m^3.	Inspection	✓	11.1
TTC-00.213	The TT&C subsystem shall have a maximum mass of 145 kg.	Inspection	✓	8.1
TTC-00.214	The TT&C subsystem shall need a nominal power of maximally 73.3 W.	Demonstration	✓	8.1
TTC-00.215	The TT&C subsystem shall need a peak power of maximally 105.5 W.	Demonstration	✓	8.1
TTC-00.216	The TT&C subsystem shall include an in-mission validation process.	Test	✓	8.2
TTC-00.217	A safety margin of 5% shall be applied when using off-the-shelf components.	Analysis	✓	8.1 & 8.2
TTC-00.218	A safety margin of 10% shall be applied when using existing technology with minor modifications.	Analysis	✓	8.1 & 8.2
TTC-00.219	A safety margin of 15% shall be applied when using existing technology with major modifications.	Analysis	✓	8.1 & 8.2
TTC-00.220	A safety margin of 20% shall be applied when using completely new components.	Analysis	✓	8.1 & 8.2
TTC-00.221	The TT&C subsystem shall have a cost of maximum 80M€.	Inspection	✓	14.3
TTC-00.222	The TT&C subsystem shall have a reliability of minimum 92.7%.	Analysis	✓	13.5.2
TTC-00.223	The TT&C subsystem shall have a housekeeping data rate of maximally 197 $kbits/s$.	Demonstration	✓	9.2

Most requirements' compliance can be found in section 8.1 and 8.3, however, some are not explicitly discussed and need some extra clarification.

Requirement TTC-00.206 can be calculated using a formula from [73, p. 17]. It relates to the bandwidth, data rate, and the E_b/N_0. By calculating the actual range, the requirement has been complied to.

Requirement TTC-00.209 is considered during tracking. As tracking relies on Doppler shift to find the position and velocity of the spacecraft (see subsection 8.3.4), this requirement is complied with by default.

Requirement TTC-00.210 compliance flows from the fact that supported architectures from DSN documents are used to size the subsystem [53]. Furthermore, maximum and minimum received powers and data rates that the DSN supports are given in [114], and comply with the values found in this chapter.

Requirement TTC-00.216 is complied with once the system is separated from the launch vehicle. The HGA can be tested when near Earth (as sun shielding is not necessary see subsection 8.3.1), the LGAs can be tested once near Venus. When they work according to plan, they are validated.

Requirements TTC-00.217, TTC-00.218, TTC-00.219, and TTC-00.220 are taken into account during the design of the process (see Table 8.1). The main requirement applicable here is TTC-00.218, as most components in the subsystem are readily available and widely used, but may require small adjustments (such as custom antenna sizes). Hence, a safety margin of 10% is added to the power budget. The masses of some components were hard to find, thus introducing an extra uncertainty in the mass budget. As such, a safety margin of 20% is

added in this part of the budget.

8.3. Design Approach

This section describes the approach that was used to size the TT&C subsystem. The TT&C subsystem influences and is influenced by the payload which determines the necessary data rates (see chapter 5), trajectory which gives communication windows (see chapter 4), C&DH which has a maximum storage size (see chapter 9), thermal control determines when the HGA is no longer necessary for sun shielding (see chapter 11), structures may require some extra mechanisms for the antennas (see chapter 12), and ADCS can provide a certain pointing accuracy (see chapter 6). The approach is structured as follows: first the communication phases are identified in subsection 8.3.1, losses during transmission are found in subsection 8.3.2, modulation and coding methods are chosen in subsection 8.3.3, and the ranging method is chosen in subsection 8.3.4. All this is combined in the link budget in subsection 8.3.5, of which the numerical results can be found in section 8.1.

8.3.1. Communication Phases

The entire mission consists of several phases. There is a transfer phase, and a flyby and orbiting phase once in-situ, as described in chapter 4. For communication, an early transfer phase, which is everything up to the last gravity assist, and a late transfer phase, which is everything from the last gravity assist until end of life, are identified. These two phases have been separated for the purpose of sizing the TT&C subsystem.

Early Transfer As mentioned previously in subsection 8.1.1, the HGA cannot be used during early transfer. However, it is still desirable to contact the spacecraft to receive housekeeping, possibly scientific data (i.e. at Venus), send commands and track the spacecraft. For this purpose, two LGAs will be installed on the spacecraft. Two are necessary as the payloads are on both sides of the spacecraft (see section 13.2), hence when some payloads are used the LGA on one side may not be able to communicate with Earth. This problem is solved by placing two LGAs on either side of the spacecraft. The LGAs are placed on booms such that their coverage is minimally obstructed by other components, such as the HGA and the protective ”skirt” around the power subsystem (see subsection 10.3.1). Since the antenna noise temperature is partially governed by the actual system temperature [29] [110], it is beneficial to place the LGAs in the shadow of the HGA. Using a HGA diameter of 3 m (in compliance with TTC-00.207, (Table 8.5), and the bus has a diameter of 1.74 m (see chapter 12), the total length of the booms is limited to about 0.56 m. As there is still an obstruction at this length caused by the skirt (since the skirt is wider than the HGA, the LGAs are still shielded from the RTGs, see section 12.1) and HGA, the maximum field of view is limited to 168 deg when placing the antennas 70 cm from the top of the HGA. This means that no communication is possible when Earth is directly behind the spacecraft, but this does not occur when at Venus.[1]

Late Transfer Once the spacecraft has passed Earth after the second Earth gravity assist (see subsection 4.1.1), the HGA is no longer necessary for sun shielding (see section 11.1), and can be used for communications. Any data acquired at Venus that could not be sent during the early transfer can be transmitted now. When at Saturn, the LGAs’ receiving capability of 3.5-5 kbit/s is enough for receiving commands in case the HGA cannot be pointed. [115] Furthermore, the HGA will be used for tracking during the radio experiment, and MORE (see section 5.1) makes use of both a deep space transponder (DST) and a Ka-transponder (Ka-T)

for its tracking.[3]
During the Enceladus orbiting phase, per orbit around Saturn a certain amount of time has been allocated to doing measurements, and to science communication. When at an inclination of 45 deg, the time per orbit is 16.92 h; at an inclination of 60 deg, it is 15.29 h; at an inclination of 90 deg, it is 13.45 h (see subsection 5.4.1). The longest time between communication windows is 4.2 h (see requirement TTC-00.211, Table 8.5), which is caused by the eclipse of Enceladus being behind Saturn, and EPOSS being behind Enceladus. From this, the data generated before these windows (see subsection 5.4.1), and the maximum estimated capabilities of the HGA, an initial data rate was estimated, such that the storage necessary could be found (see subsection 9.3.2). In the end the data rate of 150 kbit/s was deemed to be sufficient (see requirement TTC-00.203, Table 8.5), although 140 Earth days are necessary after the mission to transfer all of the remaining scientific data stored. However, as described in chapter 4, the end of life requires a transfer to Tethys, hence this phase can be used to send the remainder of the data (in compliance with TTC-00.204, Table 8.5).

8.3.2. Losses and Gains

In order to determine the link budget for the system, the losses have to be identified. A few losses are considered, and their values can be found in Table 8.2 and 8.3:

- Loss due to finite antenna efficiency.
- Circuit loss, i.e. due to cables.
- Noise temperature (integrated into DSN G/T during downlink).
- Pointing loss, governed by the ground station beamwidth [52] and relations from [29] [30].
- Space loss, governed by the wavelength of the signal squared divided by the distance to Earth squared [29].
- Atmospheric attenuation.
- Rain attenuation, which is 0 for the DSN due to the dry climate.

The noise temperature is only considered on the receiving end of the budget, as it is overpowered by the signal on the transmitting end [110] [115]. The noise temperature is impossible to measure [110], thus the value from Cassini was taken for the spacecraft end of the link budget. There is significant difference between the ground station noise temperature and the spacecraft noise temperature: 31.0 or 20.6 K [52] as opposed to 280 K from Cassini [115]. This is due to the fact that the DSN receivers are cryogenically cooled [52], thus reducing the physical temperature which influences the noise temperature. The systems required for cryogenic cooling are too large and thus not applied in spacecraft, where hardware is often the size of a coffee mug [111].
The gains of antennas are based on their effective diameter, wavelength, and antenna efficiency. As this relationship is quadratic, at some point increasing the size no longer effectively increases the gain. To comply with both the sun shielding, and the relationship mentioned, the HGA diameter is set at 3 m.

8.3.3. Modulation and Coding

A signal has to be modulated to convert the bits of data to a signal that can be sent [110] [30]. Furthermore, the modulation type used determines the minimum E_b/N_0 necessary to reach a certain bit error rate (BER). The BER describes the odds of an error being present in the signal sent. A common BER chosen is 10^{-6}, which means that for a million bits in a signal, one will be corrupted [30]. As this is a common BER, it is also chosen as a maximum BER for

[3]Retrieved from: https://www.cosmos.esa.int/web/bepicolombo/more last opened on June 19, 2019

the EPOSS TT&C. The modulation type also comes with a bandwidth efficiency.
Coding can be used to improve the minimum E_b/N_0 necessary to receive a reliable signal. The downside of this is that it increases the symbol rate, as more bits are sent instead of just the useful data (indicated by the coding rate).
The selection of both the modulation and coding methods depends on what is supported at the ground station. Several architectures are available at the DSN [53]. Both BPSK and quadratic phase-shift keying (QPSK) are modulation options, and are described in [110]. Both BPSK and QPSK have a constant envelope, allowing for more efficient TWTAs to be used, as linearity is not necessary in the amplifier. QPSK requires twice the symbol rate as BPSK, but otherwise behaves similarly to BPSK. An advantage of QPSK is that it has a higher bandwidth efficiency. Since BPSK is extremely well-known and widely used in interplanetary missions, simpler, requires a lower symbol rate than QPSK, and bandwidth is not a limiting factor; BPSK is chosen. In combination with BPSK, methods such as Reed-Solomon, convolutional, concatenated coding and turbo coding can be chosen. As EPOSS' TT&C subsystem has quite demanding requirements, with the HGA requiring an average data rate of up to 150 kbit/s to comply with TTC-00.203, the method that reduces the necessary E_b/N_0 the most is chosen. In this case, it is turbo coding with a coding rate of 1/2, which reduces the E_b/N_0 to 1.1 dB [53].

8.3.4. Tracking

Tracking requires a combination of ranging data and Doppler shift. The DST processes the ranging signal, and transmits it back. When the HGA can be used for ranging, both the DST and Ka-T can be used, where the latter is especially essential during the radio experiment (MORE, see chapter 5). The DSN supports sequential, non-coherent, and (non-)regenerative PN ranging. They are described in [55]. For the radio experiment (MORE, see chapter 5) a more accurate ranging method is preferred. Overall, PN ranging outperforms the other methods. Furthermore, an advantage of the regenerative version versus the non-regenerative version is that the former has less noise in the signal after processing on the spacecraft. However, this does cause some jitter, which may cause some errors in the ranging. This can be compensated for by selecting the T4B component code, instead of weighted-voting balanced Tausworthe, voting ν=2 (T2B). Although T2B uses less power and is faster, T4B is more accurate and recommended for deep space missions. [55]
This setup results in an error due to thermal noise of 0.2-0.3 m. Furthermore, an acquisition tolerance of 99% is advised. This means that range acquisitions that have a probability higher than 99% of being good will be passed as valid. All other acquisitions will be rejected. Finally, ΔDOR ranging will be chosen over two-way and three-way ranging, as it outperforms the other methods [2]. It is advised to use the same bands for uplink and downlink for ranging. As such, ranging with the HGA will solely be done on the Ka-band, and ranging with the LGAs will only make use of the X-band. [55]

8.3.5. Link Budget

Combining the previous sections, the link budget was found. The minimum E_b/N_0 is 1.1 dB due to the BPSK turbo coding combination, to which a margin of 3 dB will be added as this is advised by ESA [110]. The E_b/N_0 is calculated using Equation 8.1 from [29]:

$$\frac{E_b}{N_0} = EIRP + L_p - R - k \tag{8.1}$$

Where Effective Isotropic Radiated Power (EIRP) is the sum of the power provided, circuit loss, and antenna gain. Furthermore, L_p is the sum of all path losses and gains in dB, R is the data rate in dB, and K is the Boltzmann constant in dB. The achievable data rate results in a

E_b/N_0 higher than the desired value of 4.1 dB. The symbol rate results form the coding rate, the bandwidth from the bandwidth efficiency (0.7 for BPSK [110]), and the capacity from the bandwidth and signal-to-noise ratio (SNR). The results can be found in Table 8.2 and 8.3.
Finally, the power provided is not equal to the power input, as the travelling-wave tube amplifiers (TWTAs) used to amplify the signal have an efficiency of 70% [63].

8.4. Verification & Validation

The method used in section 8.3, and thus the results presented in section 8.1, must be validated. As [115] presents the entire link budget of the Cassini spacecraft, some characteristics can be filled into the method used here to show that they yield similar results. For this purpose, Cassini's HGA downlink budget from 2004 was used. The antenna gain, transmitter power, pointing loss, and ground station gain and noise temperature were directly filled into the budget, as these are specific to the system. The same value was taken for the circuit loss (-0.46 dB) as this was taken from an estimation from [29], hence the same uncertainty should be implemented in the validation. Other losses were calculated using Cassini's HGA downlink frequency, and the largest distance from Earth to Saturn as presented in Table 8.4. Lastly, the data rate resulting from Cassini's link budget in dB was deducted from the resulting total received power. This resulted in an available E_b/N_0 of 2.23 dB. Since the resulting available E_b/N_0 in the actual link budget is 1.94 dB, the method has an error of 0.29 dB. The link budgets have an extra margin of about 0.4 dB (see Table 8.2 and 8.3), so this error does not significantly affect the resulting data rates. As such, the method has been validated.

8.5. Sensitivity Analysis

During the design phase, some parameters influenced the design more than others as they were considered as more critical. Space loss has a significant impact on the link budget, being around 300 dB for all cases presented in Table 8.4. Both the worst and best cases are considered in the design, and the data rates are sufficient for both. To illustrate, the minimum distance to Saturn may be off by 100000 km, but this may change the space loss by only 0.0007 dB, hence it is negligible. The calculated space loss is thus deemed to be reliable.
Furthermore, there may be unexpected losses that were not considered in this analysis. For example, small losses in the order of -0.1 dB due to suppression may occur [115]. Suppression loss is caused by imperfections in the filtering process, which separates the ranging signal from the telemetry data. These losses are quite small, however, and will mainly influence the extra margin of about 0.4 dB (see Table 8.2 and 8.3), thus still leaving the advised margin of 3 dB. Overall, the LGAs are more sensitive to unexpected extra losses, as their supported data rates at Saturn are relatively low. A small change may impact this significantly. When the actual gain of the antennas is not high enough, the link budget may go below the advised margin of 3 dB. However, a lower margin than 3 dB, although not preferred, is not disastrous [111]. Furthermore, a contingency of 10% is present in the power budget (see Table 8.1), hence more power could be used when the signal is not strong enough.
Finally, the main uncertainty in the uplink budget is the noise temperature. As this is nearly impossible to measure and estimate [110], values from the Cassini spacecraft are taken in this calculation [115]. First of all, the uplink data rate currently is more than sufficient, as the uplink rate during Cassini's mission was about 500 bit/s [115]. This means that a reduction of about 3000 bit/s is still allowable for the LGAs. This translates to a reduction in 8.45 dB of received power. When this is attributed to the noise temperature, it means that the actual noise temperature is 1960 K, 1680 K higher than Cassini's value. As this increase is incredibly high, it is deemed unrealistic. Hence, the uplink budget is flexible enough.
Taking everything mentioned here into consideration, it can be concluded that the design is

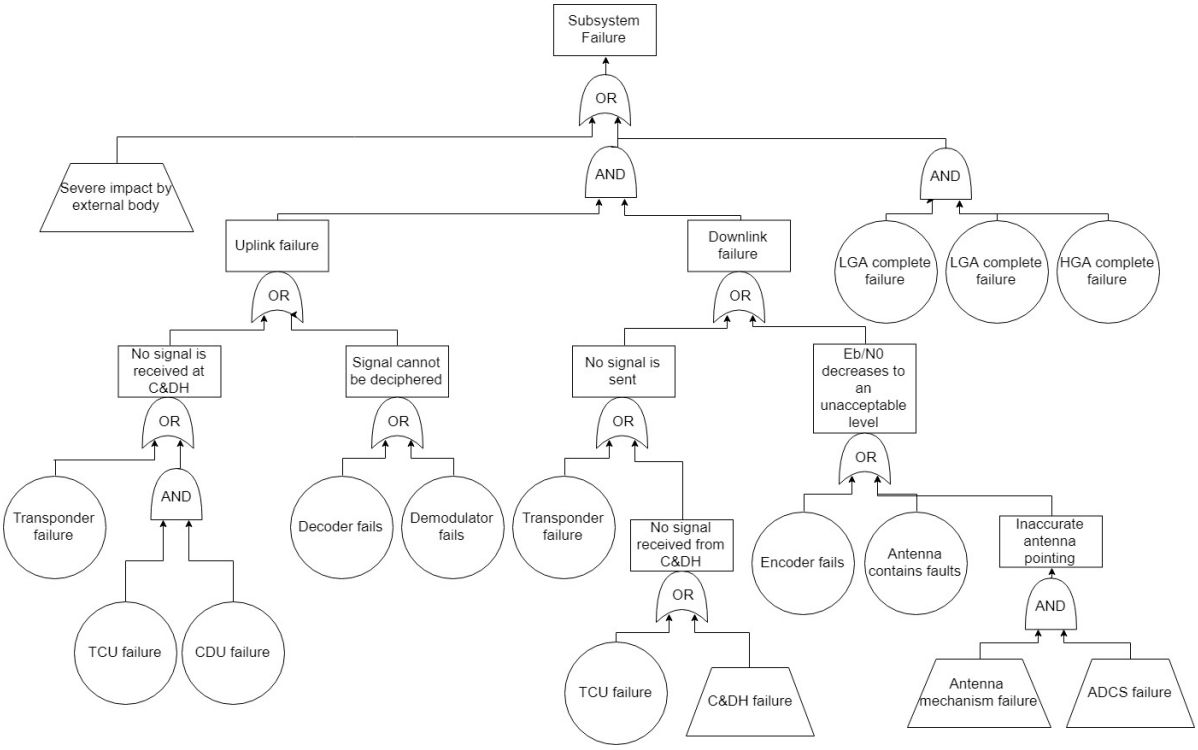

Figure 8.2: Fault tree of the TT&C subsystem.

reliable and flexible enough, given the knowledge available at this stage of the design process.

8.6. Risk Analysis

In this section, selected failure modes and their mitigation are elucidated. The fault tree can be found in Figure 8.2. The intermediate failure modes (square blocks) caused by internal failures will be highlighted, hence failures caused by trapezoidal boxes are not mitigated here.

1. **TTR-0.1 No signal is received at C&DH:** There are two different causes for no signal being received at the C&DH subsystem: transponder failure, and a combination of telemetry control unit (TCU) and command detection unit (CDU) failure. The risk can be decreased by installing two of each on the spacecraft. As such, redundancy of these components is added. This can be seen in Figure 8.1.
2. **TTR-0.2 Signal cannot be deciphered:** The signal will not be able to be deciphered when either the decoder or demodulator fails. As such, two of all have been implemented into the architecture, as shown in Figure 8.1.
3. **TTR-0.3 No signal is sent:** No signal is sent when the transponder fails, or when no signal is received from C&DH. Both transponder failure and TCU failure have already been mitigated previously, by installing two of each on the spacecraft.
4. **TTR-0.4 E_b/N_0 decreases to an unacceptable level:** When the E_b/N_0 decreases too far below the 3 dB margin, the signal received is no longer reliable. First of all, should everything work correctly, the signal sent is safe due to the 3 dB link margin [110], which can be found in subsection 8.3.5. Furthermore, an extra margin of higher 0.4 dB is present per communication mode. Thus, unexpected increases in E_b/N_0 do not automatically result in unreliable signals. Additionally, internal sources of this error are encoder failure and faults in the antennas. Extensive checking of the antennas before installing them on the spacecraft, and encoder redundancy can mitigate this.

9 Command & Data Handling

This chapter covers the design of the C&DH subsystem. A general overview of the subsystem with a mass, power and volume table can be found in section 9.1. The full C&DH design is described in detail in section 9.3 with the verification and validation methods of the approach in section 9.4. Finally, the risk relative to faults in the subsystem are discussed in section 9.6.

9.1. Design Overview

In Table 9.1, an overview of the command and data handling (C&DH) sizing can be seen. This subsystem is mainly made of three components namely the on-board computer (OBC), the storage unit and the harness which includes cables and wires necessary to connect the pieces of hardware with each other. All components have been sized including a 10% margin as indicated by requirement CDH-00.195 (Table 9.2) as minor modifications, such as implementing the scalable memory and perhaps software modifications, may be included in the design. The harness has been sized based on relationships reported in [124]. Regarding the cost, the C&DH has been estimated to cost 5.8 M € as from section 14.3, so a maximum of 6 M€ has been accounted for in CDH-00.198, in order to account for uncertainties which may arise in the future. This is rough estimate from literature, as the confidentiality around the hardware pieces made cost estimation troubling [121].

Table 9.1: Overview of C&DH components, with corresponding mass, powers and volume.

Component	Mass [kg]	Nominal Power [W]	Stand-by Power [W]	Volume [m^3]
On-Board Computer	5.5	15.8	11	0.078
Solid State Recorder (SSR)	9	16.5	5.5	0.15
Harness	21.6	-	-	-
Total	36.1	32.3	16.50	0.23

9.2. Requirement Analysis

The EPOSS mission is subjected to specific requirements, made in order to fulfil all objectives the designing team has set. In Table 9.2, the compliance containing the requirements relative to this subsystem is laid out. The majority of the requirement's compliance can be found in text as indicated in Table 9.2, however some of them may be clarified below.
Requirements CDH-00.201 implies that the C&DH shall have a processing power of 16 W maximally. This value is found from the chosen OBC nominal power with a 10% margin to comply with CDH-00.195, as minor modifications to the software will be applied. Requirement CDH-00.188 states that the C&DH shall comply with the payload data size up to maximally 150565.5 Mbits. This value has been found by considering the maximum amount of data to be generated in one phase before it can be downlinked as from subsection 5.4.1. This occurs at the fifth phase when BELA and REASON are collecting data over Enceladus.

9.3. Design Approach

In terms of hardware, the C&DH subsystem can be divided in two main components, the on-board computer (OBC) and the storage unit. In the following sections, the methods used to determine the specifics of each components will be given.

Table 9.2: Compliance matrix for C&DH subsystem requirements.

Code	Requirement	Verification Method	Compliance	Section
CDH-00.183	The C&DH subsystem shall have a data storage of minimally 0.23 TB.	Demonstration	✓	9.3.2
CDH-00.184	The C&DH subsystem shall exhaust all data stored during by the end of the TT&C contact window.	Analysis	✓	9.3.2
CDH-00.185	The the data in the C&DH subsystem shall have a maximum life of 5880 hr before transmission to Earth.	Analysis	✓	9.3.2
CDH-00.186	The C&DH subsystem shall prioritise outgoing data over incoming information in case of space insufficiency.	Analysis	✓	9.3.2
CDH-00.187	The C&DH subsystem shall comply with payload data rate requirements up to maximum 0.15 Mbits/s.	Demonstration	✓	9.3.2
CDH-00.188	The C&DH subsystem shall comply with payload data size requirements up to maximum 150650.5 Mbits.	Demonstration	✓	9.2
CDH-00.189	The C&DH subsystem shall have a maximum mass of 40 kg.	Inspection	✓	9.1
CDH-00.190	The C&DH subsystem shall need a nominal power of maximally 33 W.	Demonstration	✓	9.1
CDH-00.191	The C&DH subsystem shall have a maximum volume of maximally 0.23 m^3.	Inspection	✓	9.1
CDH-00.192	The C&DH subsystem shall need a peak power of maximally 49 W.	Demonstration	✓	9.1
CDH-00.193	The C&DH subsystem shall include an in-mission validation process.	Test	✓	9.4
CDH-00.194	A safety margin of 5% shall be applied when using off-the-shelf components.	Analysis	✓	9.1
CDH-00.195	A safety margin of 10% shall be applied when using existing technology with minor modifications.	Analysis	✓	9.1
CDH-00.196	A safety margin of 15% shall be applied when using existing technology with major modifications.	Analysis	✓	9.1
CDH-00.197	A safety margin of 20% shall be applied when using completely new components.	Analysis	✓	9.1
CDH-00.198	The C&DH subsystem shall have a cost of maximum 6 M €.	Inspection	✓	9.1
CDH-00.199	The C&DH subsystem shall have a risk of maximum 91.1 %.	Analysis	✓	9.6
CDH-00.200	The C&DH subsystem shall have a data rate of minimally 2.9 $\cdot 10^{-5}$ Mbits/s.	Analysis	✓	9.3.1
CDH-00.201	The C&DH subsystem shall have a processing power of maximally 16 W.	Demonstration	✓	9.2
CDH-00.202	The C&DH subsystem shall be protected from maximum radiation levels of 25 microT from Saturn.	Inspection	✓	9.6

9.3.1. On-Board Computer

The on-board computer can be considered to be the brain of the spacecraft, in charge of dividing tasks and processing data. The OBC has to take into account the functions required by each subsystem and how subsystems relate and affect each other. To have a clear overview of the necessary communication which will occur during the spacecraft's operational period, an interface diagram, as from Figure 9.1 has been created. This has been designed by closely working with the subsystem's chiefs so to have a overview of the brain of the system. The functions to be performed can be divided in ones related to housekeeping, and ones related to the payload on board of EPOSS. In Table 9.3, an estimation for the bits size, throughput, execution frequency and single lines of code (SLOC) for a general-purpose processor are given [121]. An analysis of the functions to be performed by each subsystem has been conducted resulting in the percentages of housekeeping data shown in Figure 9.2. It is worth mentioning that for the thermal and propulsion subsystems, the percentage of the housekeeping only reflects on one redundant set of components. Considering the thermal subsystem uses multiple thermal sensors, the amount of data may increase once the number of sensors is further defined. With these percentages, an estimation can be made on how many instructions per second (IPS) and how much memory the OBC needs for housekeeping. As it can be seen from Table 9.3, the processor on the OBC needs to be able to handle around 230 KIPS. The OBC should also have enough memory to store the code and data required to perform the required functions. For example, in order for the star trackers to determine the attitude of the spacecraft, they have to compare the surroundings they observe with star maps, which are stored as data in the OBC. With performing this comparison, specific lines of code will be required which are also stored in the OBC. From Table 9.3, the code is estimated to be about 1166 kbits while the data is 1155 kbits. As housekeeping data is to be sent down along with the scientific data as from subsection 8.1.1, the housekeeping data rate is found by estimating the total

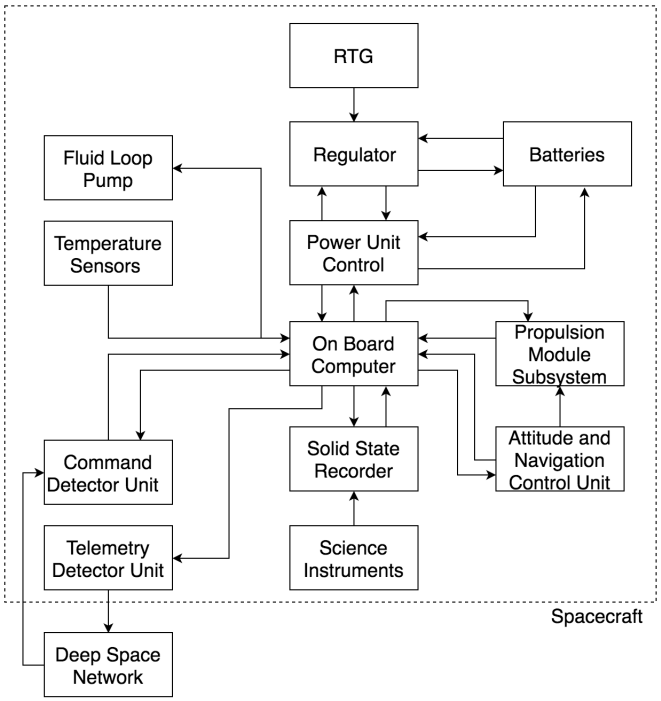

Figure 9.1: Interface diagram.

amount of data which can be downlinked in the smallest communication window together with the scientific data. This results in a data rate of 29.5 bits/s as from subsection 8.1.1.
The EPOSS will implement the Airbus OSCAR on-board computer based on the LEON3 processor.[1] This OBC has high reliability due to its failure tolerant architecture based on a fully redundant configuration, 15 years of compliance with GEO and a single event upset tolerance. The OBC will easily compute the necessary 300 KIPS of housekeeping as it is designed to process 26 MIPS. The code for processing the housekeeping functions will be stored in the OSCAR electrically erasable programmable read-only memory (EEPROM) while the data housekeeping data will be held in the extensive Random Access Memory (RAM) provided by the OSCAR. As it was not possible to estimate the IPS and the data size for the payload, due to the difficulties encountered in finding specific documentation and the specificity of the mission. The high margin of IPS and storage that result from choosing the OSCAR will compensate for these unknowns in the payload. As at this stage only the housekeeping was estimated, the choice of a computer with 26 MIPS leaves 25.7 MIPS available for the payload. With this level of contingency, the team is confident the payload will be within this margin. General communication services with the avionics, payload equipment, and external storage units is done through an on-board communication bus based on the MIL STD 1553 bus, a standard connection widely used in space applications.

9.3.2. Storage Unit

In order to size the storage unit on board of the EPOSS, other subsystems need have to be taken into account. This has been done by first making a data handling diagram, as from Figure 9.3, so to make the data and commands distribution is organised and flows in and out of the SSR and the OBC. By determining the amount of scientific data collected by the instruments, as from subsection 5.4.1, and the amount of data which can be downlinked dur-

[1] Retrieved from https://spaceequipment.airbusdefenceandspace.com/avionics/platform-on-board-computers/oscar/ last opened on July 2, 2019

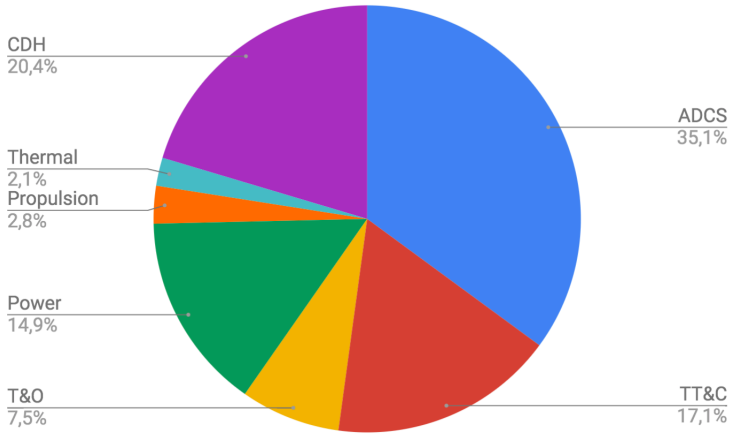

Figure 9.2: Housekeeping data divided in subsystem's related functions.

ing the appropriate communication windows, the excess data to be stored in the Solid State Recorder can be determined. The maximum excess data to be stored at any time has been approximated to be 0.23 TB as mentioned in subsection 5.4.1, and by using the indicated contingency as from [65], the amount of data storage necessary can be sized at 0.5 TB.
The chosen SSR is the Airbus NEMO 1200, a non-volatile extendable memory on-board compact and scalable flash-based solid state recorder with a 0.5 TB user capacity and a fully redundant unit, made of two identical and independent slices of memory controlled and monitored by a MIL STD 1553 Bus.[2] This results in easy integration of OBC and memory, as both use the same communication bus.
In subsection 8.1.1, the data rate required to downlink the payload data has been determined to be 0.15 Mbits/s. With this data rate, starting with the first day of phase 1, there are 106 days until the first day dedicated solely to sending excess data and 139 days to send all this excess data which is accumulated in one storage unit of NEMO. This comes down to 245 d, or 5880 h which is the maximum amount of time which any data is stored in the SSR. The OBC will be programmed so to continue sending down excess data over collecting new one in case of space insufficiency, although the NEMO by having two storage units, includes enough storage to account for double the amount of maximum excess data to be stored, as mentioned above.

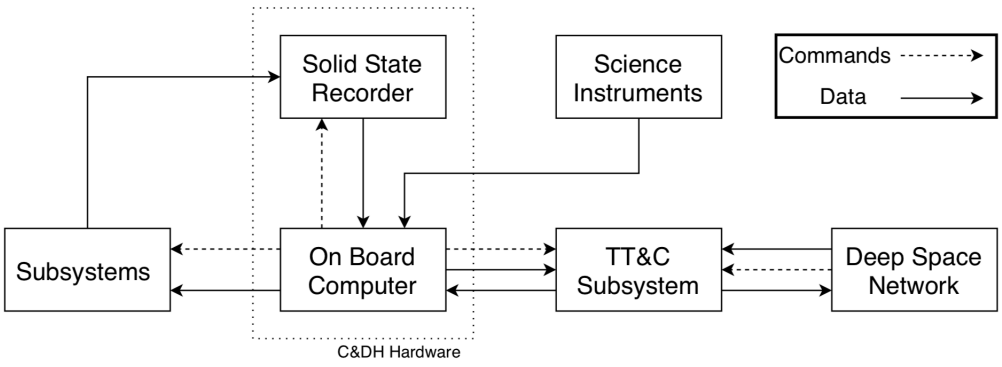

Figure 9.3: Data handling diagram.

[2]Retrieved from https://spaceequipment.airbusdefenceandspace.com/payload-products/payload-data-handling-with-memory/nemo/ last opened July 2, 2019

Table 9.3: Values characterising general on-board computer performance retrieved from [65]. The values are taken for a 'general use mission'. Considering the uncertainties this invokes, appropriate margins of contingency have been taken.

	Size [kbits]				
Functions	**Code**	**Data**	**Throughput [KIPS]**	**Execution Frequency [Hz]**	**SLOC**
Communication					
Command Processing	16	66	7	10	1000
Telemetry	16	41	3	10	3500
Attitude Sensor Processing					
Star Trackers	33	246	2	0.01	2000
IMU	20	150	5	0.01	1500
Sun Sensors	2	0.4	1	1	500
ADC					
Kinematic Integration	33	3	15	10	2000
Error Determination	33	2	12	10	800
Precession Control	54	25	30	10	3500
Thruster Control	10	7	1.2	2	1200
Reaction Wheel Control	16	5	5	2	1200
Ephemeris Propagation	33	5	2	1	2000
Complex Ephemeris	57	41	4	0.5	4000
Orbit Propagation	213	66	20	1	8500
Autonomy					
Complex Autonomy	246	164	29	10	5000
Fault Detection					
Monitors	66	16	15	5	4000
Fault Correction	33	164	5	5	5000
Others					
Power Management	20	8	5	1	1200
Thermal Control	13	25	3	0.1	800
Software					
Executive	57	33	60	-	2000
Run Time Kernel	131	66	0	-	1000
I/O Divide Handlers	33	11	0.2	-	1000
Built in Test Diagnostics	11	7	0.5	-	500
Math Utilities	20	3	0	-	100
Total	1166	1155	224.9	-	50800

9.4. Verification & Validation

All the requirements will be verified, although validation may be fully proven only once the spacecraft is launched and operative, as it not always possible to replicate the operational conditions which the EPOSS will be subjected to. For requirements which are physically measurable, such as CDH-00.189 and CDH-00.191, inspection is used. Requirements involving power, data volume and/or storage can be verified by initialising the hardware and demonstrating that the requirements are met by observing e.g the power usage. Requirement CDH-00.193 can be verified by testing that the validation procedure in the software works accordingly to what it is intended to do. Finally, all requirements verified by analysis will undergo tests by using models which show similar behaviour to real spacecraft system in order to verify the correct functioning and compliance with the requirements.
The hardware composing the C&DH can be considered to be validated as it comes directly off the shelf and it has been successfully implemented in operational spacecraft since 2012.[3]

9.5. Sensitivity Analysis

For the design of the OBC, some values were found from literature, such as the ones reported in Table 9.3. If these were to be different, possible changes in the OBC would have to be taken into account. If the IPS were to increase the current choice for the OBC would still be feasible, as there is more than 100% margin in the amount of IPS required and the ones available in the current OBC. If the amount of code and data would increase the storage in the EEPROM and RAM may not be enough to store them. In that case a different OBC might be considered, or storing the code in the OSCAR exchange memory. This however, shall not be a pending problem, as many types of OBC with characteristics which comply to the ones needed by the EPOSS are available.[4]
Regarding the sizing of the storage unit, the biggest impact is unarguably done by the payload data to be stored. If the payload data were to increase over the capacity of the current SSR, different approaches can be made in terms of C&DH design. Firstly, the payload can be designed so that its software makes the executive decision to filter some of the data and discard the unnecessary one [51]. This automatically decreases the data volume, which may result in the feasibility of the NEMO as is. Another possibility is to compress the data to be stored, which may result in a complex software but a smaller data volume. In the case of the data volume not being small enough, with the measures discussed before already implemented, the NEMO offers the option to increase its storage, being a fully scalable SSR.[2]
Therefore, with the considerations on OBC and SSR design, the current C&DH design can be considered flexible enough to account for unknowns which have not been investigated so far.

9.6. Risk Analysis

The command and data handling is often prone to failures due to its many small and delicate components [124]. Within C&DH, failures can be caused by both the software and the hardware. By using relationships illustrated in [124], the C&DH subsystem has been approximated to be 91.1% reliable over 16 years period: this is mostly due to the highly reliable hardware selected. However, risks have to be taken into account so to make sure the system is designed with uncertainties such faults in mind. In this section, the fault tree diagram with the consequences regarding the most likely to occur risks is presented in Figure 9.4, as well as a

[3]Retrieved from https://spaceequipment.airbusdefenceandspace.com/avionics/platform-on-board-computers/oscar/ last opened on July 2, 2019
[4]Retreived from https://www.esa.int/Our_Activities/Space_Engineering_Technology/Onboard_Computer_and_Data_Handling/Onboard_Computer_and_Data_Handling2 last opened on July 2, 2019

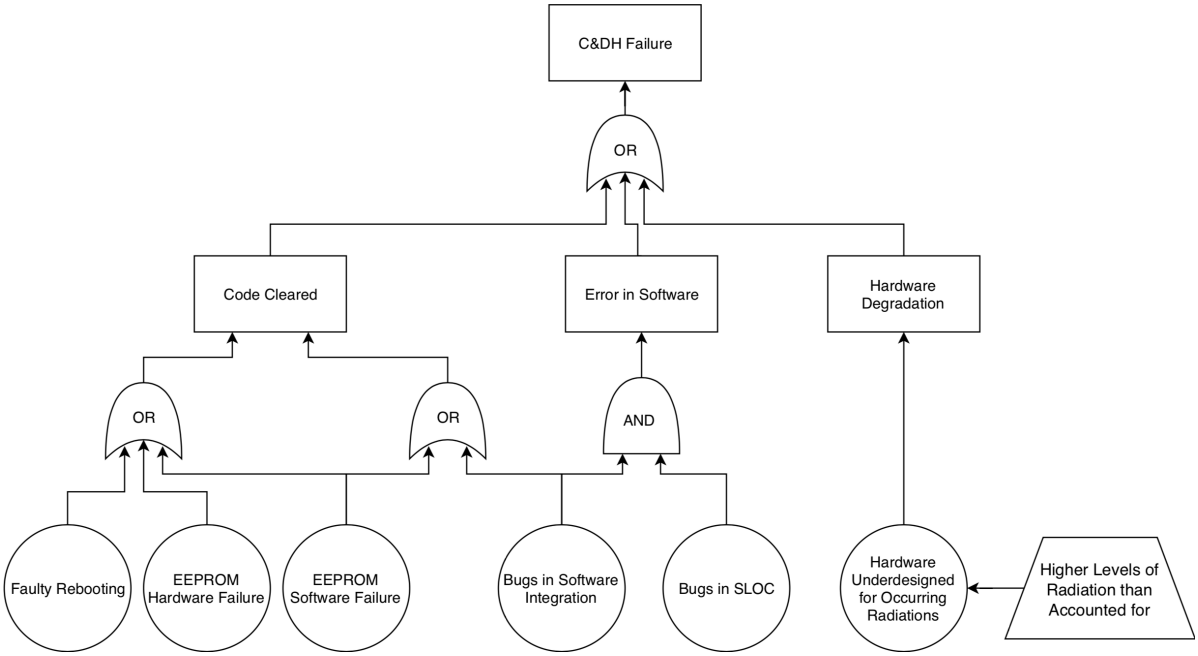

Figure 9.4: Fault tree diagram of the C&DH subsystem.

mitigation of the risks most likely to occur.

1. **CDR-0.1 Code cleared:** in the OBC, the code used to initiate processes and commands within both the C&DH and other subsystems, is saved in the EEPROM. In the event of EEPROM failure due to either rebooting, harware issues and/or software malfunction, the system will loose all ability to perform the functions for which it is designed for. For redundancy, the same code is copied in the RAM, which can be used to copy the code back to the EEPROM in case of failure. In the case of simultaneous failure of both EEPROM and RAM, the OSCAR offers an external 512 MBytes of exchange memory in which all codes will be stored so to mitigate the worst case scenario mentioned above.
2. **CDR-0.2 Error in software program:** errors in the programming of the software will occur as the software is estimated to have 50800 SLOC. Software errors are hard to mitigate for, therefore the best strategy is to implement verification and validation procedures to spot bugs and prevent failures. A system to allow for in-flight updates will also be implemented, but its design is considered to be outside the scope of this report.
3. **CDR-0.3 Degradation due to radiation:** due to the harsh environment to which EPOSS is subjected to, radiation has to be taken into account when designing hardware components. The radiation to which the spacecraft will be subjected during its life does not have certain value, due to the unknowns that the Saturnian System hold. Therefore, the C&DH components will be overdesigned so not to be damaged by radiation. Both the OSCAR and the NEMO are compliant with environment subjected to radiation thanks to the casing made of aluminised Teflon described subsection 11.3.2 and to their design specification provided by the manufacturer.[5,6]

[5]Retrieved from `https://spaceequipment.airbusdefenceandspace.com/avionics/platform-on-board-computers/oscar/` last opened on July 2, 2019
[6]Retrieved from `https://spaceequipment.airbusdefenceandspace.com/payload-products/payload-data-handling-with-memory/nemo/` last openend on July 2, 2019

10 Power

The power subsystem provides the necessary power to all spacecraft components throughout the entire mission duration. This chapter provides an overview of the design solutions used for the EPOSS mission. An overview of the subsystem is given in section 10.1, including an electrical block diagram. The requirement analysis is covered in section 10.2 followed by the design approach to satisfy the subsystem requirements, which is covered in section 10.3. Section 10.4 treats the analysis, verification and validation of the requirements. Finally, the sensitivity analysis, and the risk considerations and fault tree and are covered in section 10.5, and section 10.6 and Figure 10.3 respectively.

10.1. Design Overview

As presented in the spacecraft budget in Table 2.1, the power subsystem has to provide a total of 351.7 W nominal power to the different subsystems. Next to this, the maximum peak power that has to be provided is 467.7 W. The power cable losses and battery charging power are already included in these budgets through a process of iterations. A safety margin of 10% and a power control unit (PCU) loss of 10% are used for required nominal power the subsystem has to provide, being 422.0 W. A safety margin of 10%, a PCU loss of 10% and uncertainty of 50% are imposed to the capacity of the energy storage. These margins will be further discussed in section 10.3. The main power source provides the necessary power to satisfy the nominal power, while a secondary power source will store part of this energy which is released during peak power moments to satisfy the peak power requirement. It is an iterative process to find an optimal ratio of how much power is provided by the primary and secondary power source. During this process, there is an explicit focus on the cost because of the high estimate of the power subsystem cost in [10], being 611.7 M €.

It was found that a set of nine Americium-based Radioisotope thermoelectric generators are capable to provide an end of life power of 438.6 W, while two Lithium-ion rechargeable batteries are used to supply the additional power during peak moments. section 10.3 explains in more detail how the power subsystem is designed. An overview of the total power subsystem cost and mass is presented in Table 10.1. The volume of 0.71 m^3 includes the volume of the RTGs, battery boxes, PCU and a rough estimate for the power cable volume.

Table 10.1: Overview of the power subsystem, with corresponding mass, cost and volume.

	Total mass [kg]	**Total cost [M €]**	**Volume [m^3]**
Power subsystem	289.6	573.5	0.71

10.2. Requirement Analysis

This section presents the requirements the power subsystem has to fulfil and how these requirements will be verified.

Table 10.2: Compliance matrix for the power subsystem requirements.

Code	Requirement	Verification Method	Compliance	Section
PWR-00.224	The power subsystem shall provide a power of minimally 351.7 W during nominal payload operations.	Demonstration	✓	10.3.1
PWR-00.225 468.1	The power subsystem shall provide a peak power of minimally W for minimally 400 seconds.	Demonstration	✓	10.3.2
PWR-00.226	The power subsystem shall provide minimally 200 W for launch operations.	Demonstration	✓	10.3.1
PWR-00.227	The power subsystem shall provide a power of minimally 233 W during deployment and de-tumbling operations.	Analysis	✓	10.3.2
PWR-00.228	The power subsystem shall provide a power of minimally 233 W during safe-mode.	Demonstration	✓	10.3.1
PWR-00.229	The power subsystem shall provide a power of minimally 200 W during transfer operations.	Analysis	✓	10.3.1
PWR-00.230	The power subsystem shall allow for end-of-mission manoeuvre.	Analysis	✓	10.3.1
PWR-00.231	The power subsystem shall provide minimally 50 W at any conditions.	Analysis	✓	10.3.1
PWR-00.232	The power subsystem shall have a maximum volume of 4.5 m^3.	Inspection	✓	10.1
PWR-00.233	The power subsystem shall have a maximum mass of 350 kg.	Inspection	✓	10.1
PWR-00.234	The power subsystem shall include an in-mission validation process.	Test	✓	10.1
PWR-00.235	A safety margin of 5% shall be applied when using off-the-shelf components.	Analysis	✓	10.3.1/10.3.2
PWR-00.236	A safety margin of 10% shall be applied when using existing technology with minor modifications.	Analysis	✓	10.3.1/10.3.2
PWR-00.237	A safety margin of 15% shall be applied when using existing technology with major modifications.	Analysis	✓	10.3.1/10.3.2
PWR-00.238	A safety margin of 20% shall be applied when using completely new components.	Analysis	✓	10.3.1/10.3.2
PWR-00.239	The power subsystem shall have a cost of maximum 800 M €.	Inspection	✓	10.1
PWR-00.240	The power subsystem shall have a minimum reliability of 90%.	Analysis	✓	
PWR-00.241	The power subsystem shall have a data rate of maximally 200 kbit/s.	Demonstration	✓	9.2
PWR-00.242	The power subsystem shall be able to sustain Earth reentry without dispersing radioactive material in the atmosphere.	Analysis	✓	10.3.1
PWR-00.243	The power subsystem shall be able to provide minimally 1.546 kWh of electrical energy.	Demonstration	✓	10.3.2
PWR-00.244	The power subsystem radiation level shall be significantly low to allow the payload instruments to fulfil their requirements.	Analysis	-	10.3.1

Following from the total power subsystem budget in Table 10.1, the total mass, cost and volume are 289.6 kg, 573.5 M euros and 0.71 m^3. All three of these values fall within the limits of requirements PWR-00.233, PWR-00.239 and PWR-00.232 respectively. The safety margins stated in requirements PWR-00.235, PWR-00.236, PWR-00.237 and PWR-00.238 are respected as 10% margins are used to size the RTGs and batteries. This is described in subsection 10.3.1 and subsection 10.3.3. section 10.6 indicates that the power subsystem reliability is 92%, which falls within the acceptable range of requirement PWR-00.240. From statistical data is found that the power system generates about 4.42 bits/s of housekeeping data, which satisfies requirement PWR-00.241.

The current power subsystem design poses no limits on the requirement that the vehicle is to have an end of life manoeuvre, stipulated by requirement PWR-00.230.

Because of the limited amount of literature available on Americium-241 radiation shielding, more information has to be obtained from experts in order to fully satisfy requirement PWR-00.244. The payload instruments are absolutely shielded from the alpha radiation emitted by the Americium-241 decay by the skirt, as described in subsection 10.3.1. A more thorough analysis has to performed to quantify the gamma intensity emitted by the Neptunium decay product and Americium itself. This consideration is included in section 16.3. The alpha radiation energy from the Americium and Neptunium makes up for nearly 100% of the total energy emitted, as they mainly an alpha-emitters. The gamma emission is considered to be soft [87] [88].

10.3. Design Approach

The power subsystem is divided in three different sections: the power control and distribution, main power source and power storage.

10.3.1. Main Power Source

RTGs provide the EPOSS vehicle with the necessary power to operate nominally. These devices convert the heat generated by the natural decay of heavy elements to electrical power by using thermocouples. In contrast to nuclear reactors, no nuclear fission processes are present, hence there is no possibility of a melt-down or sudden temperature changes. The fact that RTGs use merely thermocouples and no moving parts makes them a reliable, predictable and less complex power source.[1]

RTGs on missions in the past usually used Plutonium-238 as energy source. Because the availability of Plutonium in the world is decreasing significantly, an alternative nuclear energy source is to be used. ESA does not even have the Plutonium stock available for a 100 W RTG. [31] The USA is still in the process of restarting their Plutonium production. Russia currently has Plutonium-238 available, however they are not selling theirs. For this reason, ESA has been working on an Americium-241 based RTG design[31]. Tests have been conducted with an RTG capable to deliver up to 50 W in 2016 by the National Nuclear Laboratory to power ESA's future deep space missions[6]. Because this Americium based RTG design has a TRL level of 6 (2016), the EPOSS mission will make use of this RTG design with as little deviations as possible to minimise any development delay risks.

Using Americium-241 based RTGs instead of conventionally used Plutonium-238 has several consequences for the design of the power subsystem and the spacecraft itself.

- Plutonium-238 has roughly four times the power density of Americium-241, which causes the RTGs on board EPOSS to be heavier in order to provide the same amount of power compared to Plutonium-238 RTGs. [31]
- Americium-241 has a half-life of 432.4 years, while Plutonium-238 has a half-life of 87.7 years. This means that a Plutonium based RTG will reduce in performance 4.7 times faster. On a timescale of 16 years, the power loss of Americium-241 and Plutonium-238 is 2.6% and 11.9% respectively. Hence the additional Americium mass that is needed to cover the power decrease over time is less than for Plutonium. [31]
- The current production cost of Americium-241 and Plutonium-238 are roughly 1.4 M €/kg and 1.7 M €/kg respectively. Americium seems to be more cost effective, however there is about four times the amount of Americium-241 needed to generate the same amount of power. Hence Americium-based RTGs are more costly. [49]
- Americium-241 is available in larger quantities than Plutonium-238 because Americium-241 has been accumulated over the years as a waste product in nuclear power plants. It still has to be filtered from the other waste products to guarantee a high Americium-241 concentration. [4] [31]
- Similarly to Plutonium-238, Americium-241 emits mainly α radiation. However the decay product, Neptunium-237 emits γ radiation as well. While alpha radiation is easy to shield, gamma radiation is not. Due to the long half-life time of Americium, only about 2.5% of the Americium will have been turned into Neptunium-237 after 16 years, limiting the gamma radiation. It is quoted to have a radiation level of 8.48 mSv/hr/MBq at one metre distance [3]. To limit the interference of the RTG radiation with the payload instruments

[1] Retrieved from `https://www.cosmos.esa.int/web/ulysses/rtg,UlyssesRTGs-ESA` last opened on June 23, 2019

and electronics, a radiation skirt is placed above the RTGs. Because alpha radiation can already be blocked by even a piece of paper, no heavy lead protection is necessary. To reduce the gamma radiation levels, the RTGs will be placed further away from the payload and electronics.

RTGs inherently convert only a minority of the heat produced by the nuclear fuel source to useful electricity. An expected value of 20 thermal watts (W_t) for each produced electrical watt (W_e) is used to calculate the thermal impact of the RTGs on the spacecraft.[6] Part of this heat is used for thermal control of the spacecraft, as covered in chapter 11. The excess heat is radiated into space through radiator fins on the RTG itself.

As discussed in section 10.6, the risk of a launch failure exists. Because the dispersion of radioactive material in the atmosphere could have catastrophic consequences, the fuel inside the RTG should be able to withstand atmospheric reentry, impact and years of corrosion, satisfying requirement PWR-00.242. This is done by using three different measures:

- The Americium will be used in a ceramic form, namely Americium-dioxide AmO_2, instead of a pure metallic form. This significantly reduces the Americium from dissolving in other substances, such as air or water.
- The Americium fuel capsule will have a graphite cover to prevent the capsule from breaking due to impact or due to the heating and forces of atmospheric reentry.
- An iridium layer around the fuel capsule will prevent it from corroding in almost any environment, because it is one of the most corrosion resistant materials currently known.

All three of these measures have proven to work for RTGs in the past. For example: the Nimbus-I spacecraft had a launch failure with an RTG on board. The fuel capsules were found back intact at sea after months after which the Plutonium fuel was reused in an RTG on board of one of the other Nimbus spacecraft. [40]

From the risk analysis performed in section 10.6, the protection of people from radiation is found to be of great importance. In order to protect the personnel working close to the RTGs as close as possible, the RTGs are equipped with several attachment points. These will be used to handle the RTGs remotely, limiting the received radiation by the personnel. Because there will be hardly any Neptunium before the mission launch, the more harmful gamma radiation will be of a very low intensity as well.

In order to satisfy the nominal EOL power demand of 351.7 W, a total of nine 50 W RTGs is necessary to satisfy requirement PWR-00.224. Because the RTGs can produce electricity continuously without a significant risk off degradation, they provide a power of minimally 438.6 W at all times during a 16 year time period. Hence the power subsystem satisfies requirements PWR-00.226, PWR-00.227, PWR-00.228, PWR-00.229 and PWR-00.231. To reduce the risk of development delays, it was decided upon not to deviate significantly from this prototype design. The specifications of the RTGs on board the EPOSS vehicle are presented in Table 10.3. The total cost of 572.8 M € for the RTGs is found from the cost analysis performed in section 14.3 and divided by nine to give an indication on the estimated cost of each RTG.

Figure 10.1: Illustrative plot of power provided versus time, indicating the power distribution between RTG and batteries (merely illustrative, not to scale).

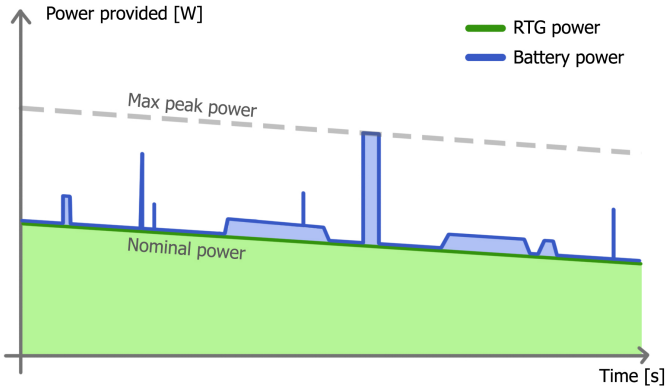

Table 10.3: RTG specifications.

Parameter	Single RTG	Nine RTGs
Mass [kg]	22.7	204.5
Power BOL [W_e]	50.0	450.0
Power EOL [W_e]	48.7	438.6
Cost [M €]	64.6	572.8
Dimensions [m]	0.84 x 0.31 x 0.31	NA
Americium mass BOL [kg]	7.1	64.0
Thermal power BOL [W_t]	1000	9000

10.3.2. Power Storage

The spacecraft has moments where the peak power is significantly larger than the nominal power, usually for a relatively short duration. Sizing the main power source for the peak power of 467.7 W would be unnecessarily expensive. Instead, a rechargeable power storage system is used in the form of a Lithium-ion battery. The stored energy will be released during peak power moments and recharged by the main power supply. If there would be no batteries used, there would have to be thirteen RTGs instead of nine, leading to a significant reduction in cost and resources.

Lithium-ion batteries have a high power density, specific power and long lifetime compared to Nickel based batteries. Battery performance is heavily influenced by the operating conditions, such as temperature. For this reason, a contingency of 60% is set for the battery capacity. This value is comprised of a 10% safety factor and 50% for under performance from not-optimal temperatures and 15% for manufacturing imperfections. The battery core temperature is kept between +10 °C and +35 °C by the thermal control subsystem (see chapter 11). Because the battery has to go through more than 5000 cycles, a depth of discharge (DOD) of 30% is taken to extend the battery's lifetime. Additionally a performance reduction of 30% is used to account for the degradation (η) over the mission duration. Next a 10% increase is needed to account for the power loss of the PCU (L_{PCU}). Finally, the total energy that the battery contains is calculated using the relation in Equation 10.1. [67] [13]

$$E_{total} = \frac{(1 + L_{PCU}) \cdot (1 + contingency) \cdot \sum P_{peak} \cdot t_{peak}}{DOD \cdot (1 - \eta)} \tag{10.1}$$

The total energy the battery has to provide during a discharge depends on the mission phase as different instruments and subsystems have varying peak power values and times. The Enceladus orbiting phase was identified as the most critical time period for the battery. This is mainly because most of the instruments are active when orbiting Enceladus. Table 10.4 shows the worst case peak and nominal power, peak time, and accumulated energy for each subsystem during one orbit. This leads to a useful energy storage of about 1564.1 kWs or 0.43 kWh that has to be readily available each orbit by the battery.

Table 10.4: Power distribution and energy accumulation per subsystem.

Subsystem	Nominal power [W]	Peak power [W]	Peak time [s]	Energy storage [kWs]
CD&H	32.3	32.3	NA	0
TT&C	73.3	73.3	NA	0
Payload	105.3	134.5	24,120	1,514.2
Thermal	4.2	4.2	NA	0
Structures	13.0	18.0	10	0.05
Propulsion	0.0	41.2	210	0.86
ADCS	77.0	151.2	550	40.8
Power	46.6	13.0	NA	0
Total	351.7	467.7	NA	1,564.1

Including the DOD, contingency and degradation, the total capacity of the battery is 2638 Wh or 120 Ah assuming a voltage of 22 V. This satisfies requirements PWR-00.225 and PWR-00.243, mentioned in Table 10.2. From the risk analysis treated in section 10.6, it follows that having two separated batteries is preferred in case to account for failure. Hence the total required battery capacity is split equally over two separate batteries. A energy density of 180 Wh/kg is used to size the batteries, leading to a total mass of 14.7 kg (7.3 kg per battery). Using a specific energy of 500 kWh/m^3, the total battery volume is 5.3 litres (2.6 litres per battery). An overview of the characteristics of the batteries can be found in Table 10.5.

In between the peak power moments, the batteries should be recharged. To shortest duration that the batteries should be charged fully is the orbital period around Enceladus minus the sum of all peak times, leading to a duration of just under 22.0 hours. Hence a minimum charging power of 33.6 W should be delivered by the main power source to the batteries. The discharge power can be adjusted to the needs, although a lower value is preferred. This way the subsystem is able to satisfy requirements SSR-00.08 and SSR-00.09 discussed in Table 2.3

Table 10.5: Battery specifications.

Parameter	Single battery	Combined batteries
Energy storage [Wh]	1319.0	2637.9
Mass [kg]	7.3	14.7
Charging power [W]	16.8	33.6
Internal volume [m^3]	0.0026	0.0053
Cost estimate [M €]	0.38	0.75

10.3.3. Power Distribution

The power distribution makes sure the generated power is regulated and delivered correctly to the different subsystems. The power produced by the RTGs is converted and combined possibly with the battery power before being distributed to each subsystem. As the name implies, the voltage regulators ensure that each subsystem receives a correct voltage. Cable losses and power losses in the power control unit are set to be 2.5% and 10% of the total peak power respectively, being 63.9 W combined. An overview of the power subsystem can

Figure 10.2: Power block diagram.

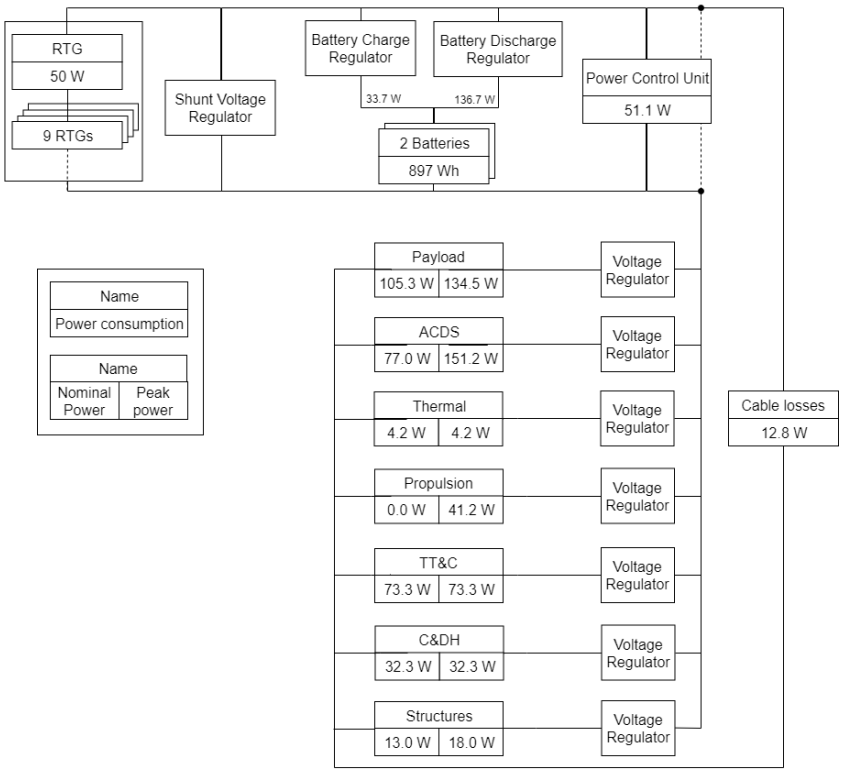

be seen in Figure 10.2 in the form of an electrical block diagram. The mass and power estimates of the power distribution were found using SMAD [65] and are presented in Table 10.6. SMAD can be used as the power control and distribution system contains the same elements for most spacecraft.

The PCU will communicate with the spacecraft main computer by continuously sending housekeeping date. This allows for a validation process of the power subsystem during the mission, satisfying requirement PWR-00.234.

Table 10.6: Overview of power control components, with corresponding mass and power.

Parameter	**Mass [kg]**	**Power loss [W]**
Power Cables	49.0	12.78
Power Control Unit	10.8	51.1
Regulators & Converters	10.8	0.0
Total	70.6	63.9

10.4. Verification & Validation

The compliance matrix found in Table 10.2 includes the verification methods that will be used to prove that the design satisfies the requirements. All power requirements will be verified by demonstrating that the necessary power level can be achieved with the design.
Verification of the design process used in this report is performed by comparing outcome to reference missions or subsystems. The following discrepancies or similarities are most noteworthy:

- RTGs have been a very popular choice for deep space missions to the outer solar system,

similarly to EPOSS. [72] Although Americium-based RTGs are new, the concept of using nuclear decay in RTGs stays the same as for previous RTGs.
- The nominal and peak power levels of the EPOSS vehicle are within the same order of those of similar missions such as Cassini (663 W peak power EOM). The choice to allocate some of the nominal power to the batteries instead of the RTGs explains why the nominal power is lower than average. [77]
- Although nine is a lot more than previous missions such as Cassini, it should be noted that the Americium based RTGs on board EPOSS are based on the prototype tested by the NNL. [6]
- Older missions to the outer solar system did not always use batteries as they could rely on the stable power output of the RTGs only. The EPOSS vehicle does use batteries to reduce its total cost.
- The cost and mass of the EPOSS RTGs is considerably more compared to other RTGs. This is mainly because of the fact that Am-241 has about a four times lower power density compared to Pu-238, resulting in a higher mass and cost, as discussed in subsection 10.3.1. [120] [31]

10.5. Sensitivity Analysis

In order to verify whether the designed power subsystem is flexible enough to have a similar design with a change in requirements, a sensitivity analysis is performed. The input parameters of the subsystem that are altered are: required nominal power, required peak power, mission lifetime, battery cycles and battery temperature.

- Increasing the required nominal power has no effect on power subsystem design up to an increase of 11.5% or 46.6 W of the nominal power. The reason for this is that the current design has nine RTGs while in theory only 8.18 are necessary. Rounding the number up gives the design a contingency margin of 11.5%. The battery sizing is only slightly influenced by the nominal power increase.
- Increasing the required peak power mainly influences the battery size and mass, as more capacity is needed to store the power deficit between nominal and peak power. The battery size can be increased by using more of anode, cathode and catalyst material. Because the battery still has to be recharged in the same time, a higher recharge power has to be provided by the RTGs. In order to keep the number of RTGs the same, the battery capacity, and hence the peak power, should not increase with more than 14.9%.
- If the lifetime is increased, both the battery and RTG performance decreases. Because Americium-241 has a half-life of about 432 year, the reduction in power over a couple additional years will not be very pronounce. A lifetime extension of one year would result in an RTG power reduction of 0.16% or 0.7 W, which can be considered negligible. Because the battery degradation is harder to predict, it has a contingency of 70% as explained in section 10.3. If it would be decided upon to increase the lifetime when spacecraft is already in space, the DOD can be reduced to extend the battery lifetime.
- If the number of cycles the battery is supposed to perform would increase during the mission, the depth of discharge could be decreased to extend the battery performance for longer, similarly to the extension of lifetime. The 70% contingency on the battery sizing also allows for a longer battery life if necessary.
- In case the core temperature of the battery falls outside of the optimal range (+10 °C to +35 °C), the performance decreases. The 70% contingency on the battery sizing accounts for an under performance of the battery.

10.6. Risk Analysis

The power subsystem is prone to risks, similarly to other subsystems. The risk is considered for the RTGs, the batteries and finally the power control system. Looking at the failure rates of past spacecraft, it can be found that the power subsystem has a reliability of 84.4% over a time span of 16 years. [124] However this value is not entirely representative because most spacecraft use solar arrays, which have a lower reliability compared to RTGs, which have a success rate of 100%[46]. Reasoning that the main power generation and battery storage have an equal contribution to the failure rate, a rough estimate of the EPOSS power subsystem reliability can be made, assuming an RTG reliability of 1.0. This value is found to be 92%, which is considered to be acceptable. Batteries are considered as a risk because they can leak, vent electrolyte and even have rapid exothermic reactions leading to a burst or fire. A breakdown of the risks within the power subsystem can be found in Figure 10.3.

Because RTGs have no moving parts and are relatively simple in design, they are not prone to failure. RTGs have only failed because of launch failures[36]. Two times in the history of spaceflight, an RTG did disintegrate upon reentry after a launch failure. Both events happened before 1970 and safety requirements on RTGs have increased greatly ever since (see the first quote below). The improved safety regulations on the RTG fuel cells have proven to be successful. For example the nuclear fuel cells on board of the Nimbus-I spacecraft were safely recovered from the ocean after a launch failure and reused successfully on the Nimbus-III spacecraft[40].The RTGs on board of the EPOSS vehicle have to satisfy the same safety requirements to guarantee a sustainable and safe design. A continuous communication and collaboration with stakeholder parties such as the INSRP (Interagency Nuclear Safety Review Panel) is critical in order to launch from a US launch site with a US launcher (See the second quote below)[46]. When an RTG disintegrates in the atmosphere, the released radioactive material can get carried along with the wind, dispersing it over a wide area. Inhaling these particles greatly increases the probability of developing cancer.

> ”Although three missions were aborted by launch vehicle or spacecraft failures, all of the RTGs that flew met or exceeded design expectations, and demonstrated the principles of safe and reliable operation, long life, high reliability, and versatility of operating in hostile environments.”
>
> - G.R. Schmidt and T.J. Sutliff from NASA Glenn Research Center and L.A. Dudzinski from NASA Headquarters (2011) [36]

> ”The launch approval process in U.S. typically takes three years. Separate from the INSRP’s independent analyses, every launch sites in U.S. develops a specific contingency plan to manage hazards associated with a post-crash event.”
>
> - Dr. F. Allahdadi and Dr. S. Bakhtiyarov from the Space Safety Division, US Air Force Safety Center/SES interviewed by Andrea Gini for the Space Safety Magazine (21/10/2011) [46]

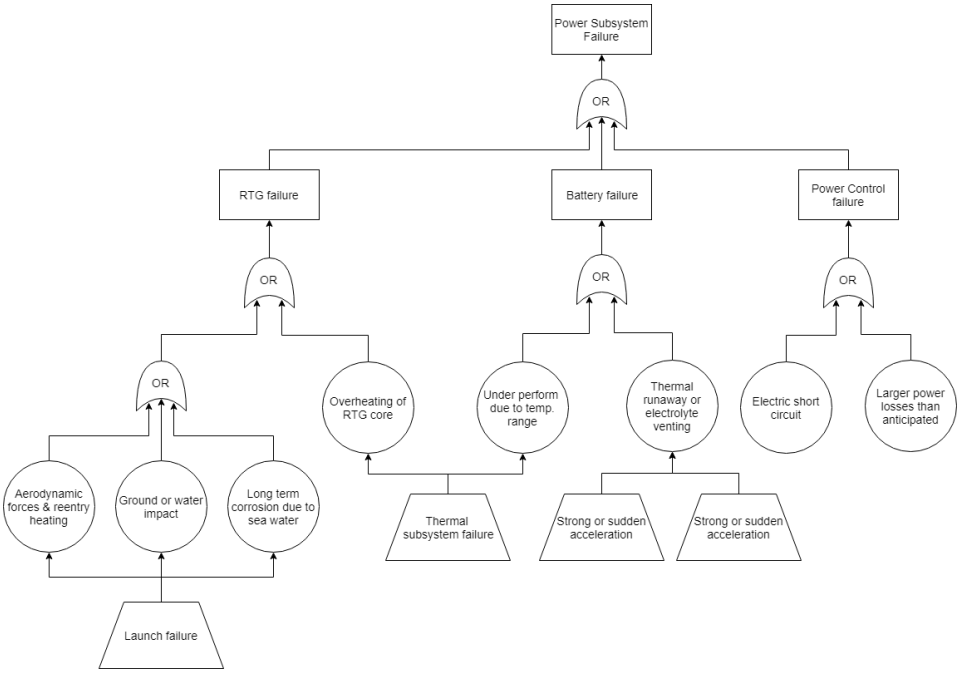

Figure 10.3: Fault tree of the power subsystem.

For risks with the highest severity or probability within the power subsystem, the used mitigation measures are discussed below.

- **POR-0.2.1 RTG breaking up on Earth** The RTGs are able to withstand a launch failure without releasing any radioactive material in the atmosphere or environment. By encapsulating the fuel cells with a graphite and iridium cover, they can sustain reentry heating, impact and years of corrosion. This is discussed more elaborately in subsection 10.3.1.
- **POR-0.2.2 RTG overheating** Overheating of the RTG core due to a thermal subsystem failure could result in a pressure build-up, leading to a rupture. A pressure relief disc is installed to avoid this scenario.
- **POR-0.3 Battery thermal runaway** The vehicle will use two smaller batteries instead of one large to prevent a single point of failure. By having them placed apart, the probability of a thermal runaway is reduced. If one battery fails, the other can still give the required peak power. Both batteries will have their separate battery box with a pressure release to contain any leaks or fires and to gradually relief any pressure build-up.
- **POR-0.4 Power Control Failure** The power control system can fail due to shorts or broken power cables. By installing fuses on regular places resolves this risk.
- Americium based RTGs have no flight heritage so far, which could be the reason for a development delay. However RTGs are not as complex in design compared to other systems, because for example that there are no moving parts involved. Using Americium-241 is not fundamentally different from using Plutonium-238 as fuel source because they basically act as 'hot stones'. The fact that EPOSS uses RTGs are strongly based on the recently tested models by the NNL reduces the development delay risk even more.

11 Thermal Control

The thermal control of the satellite will be explained in this chapter. Satellite components are typically designed for, or based on, conditions on Earth. They operate nominally in a temperature range based on this design. Therefore, this temperature range has to be controlled for proper operation of these subsystems. First, a design overview is given in section 11.1, then the requirement compliance is shown in section 11.2, after which a design approach follows in section 11.3. Furthermore, verification & validation, sensitivity and risk analysis are discussed in respectively section 11.4, section 11.5 and section 11.6.

11.1. Design Overview

As was concluded in the previous report, the thermal control has been split up into external and internal heat control [10]. The difference between them is that internal heat transfer methods deal with controlling the temperature inside the bus, whereas the external one shall make sure that exactly the right amount of heat is dissipated or absorbed [65, p. 411]. For both, multiple systems were selected in order to keep the satellite functioning in a preferred environment.

For the external heat control, a sun shield, louvres, radiators, Multi-Layer Insulation (MLI) and coating are used. All of these systems will be explained in subsection 11.3.2. Louvres are dynamic systems, whereas all others work in a static manner. Dynamic in this case is defined as the system is movable, and thus does not use any power per se. The reason why multiple systems will be used on the satellite is that using simply one or two of them will not be capable of controlling the heat sufficiently. Therefore, multiple systems have to work together in order to be able to work properly. Next to that, the internal heat control is satisfied by the heat generated from the RTGs and transferred by heat pipes. The sizing of all these systems is done by determining the total heat going in and out of the satellite at different locations, and sizing for the worst-case scenarios. This can be seen in section 11.3. The mass and power estimations for these systems can be found in Table 11.1 (THM-00.134 to THM-00.136, Table 11.2). Note that the sun shield and RTG's mass is covered in other subsystems (chapter 8 and 10).

Table 11.1: Overview of thermal control subsystem components, with corresponding mass and power.

	Mass [kg]	**Power [W]**
External heat transfer		
Sun shield	-	0
Louvres	5.9	0
Radiators	4.8	0
MLI	10.7	0
Coating	-	0
Internal heat transfer		
RTGs	-	0
Heat pipes	15.7	4.2
Total	37.1	4.2

A schematic overview of the thermal control system can be found in Figure 11.1. Here, the

gold represents the MLI blankets, black are structural components, Purple are the heat pipes systems and the red squares are the CFRP insulations. The method used is derived from [85].

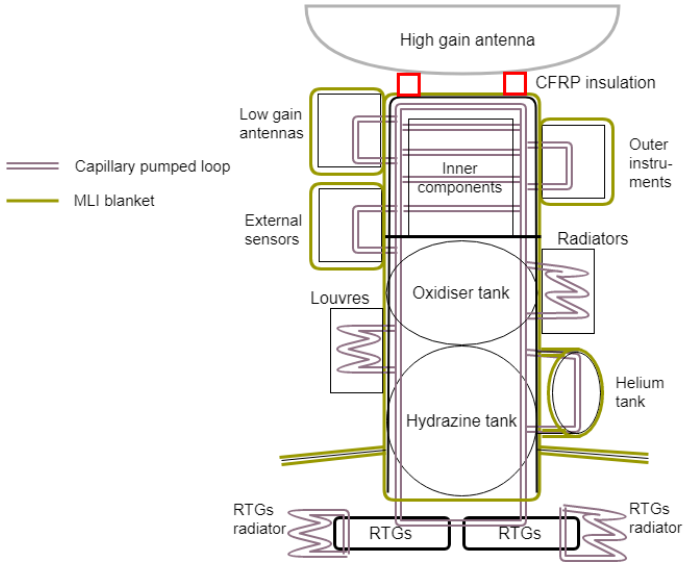

Figure 11.1: Schematic overview of the thermal control system.

11.2. Requirement Analysis

In Table 11.2, one can find the compliance matrix for the thermal control subsystem.

Table 11.2: Compliance matrix for the thermal control requirements.

Code	Requirement	Verification Method	Com-pliance	Section
THM-13.01	The spacecraft shall withstand launch temperatures inside the fairing between 273 K and 373 K [107, p. 34].	Test	✓	11.3.1
THM-00.124	The spacecraft shall withstand temperatures encountered during the transfer to the Saturnian System up to a maximum solar irradiance of 2600 W/m^2.	Analysis	✓	11.3.1
THM-00.125	The spacecraft shall withstand temperatures in the Saturnian System with a minimum solar irradiance of 10 W/m^2.	Analysis	✓	11.3.1
THM-00.126	The thermal subsystem shall account for solar irradiance at all points of the mission.	Analysis	✓	11.3.1
THM-00.127	The thermal subsystem shall account for albedo irradiance at all points of the mission.	Analysis	✓	11.3.1
THM-00.128	The thermal subsystem shall account for the albedo of the planets encountered in the trajectory to the Saturnian System.	Analysis	✓	11.3.1
THM-00.129	The thermal subsystem shall account for the albedo of moons in the Saturnian System.	Analysis	✓	11.3.1
THM-00.130	The thermal subsystem shall account for the internal heating of the components.	Analysis	✓	11.3.2
THM-00.131	The thermal subsystem shall keep the spacecraft within the set temperature ranges in Kelvin throughout the mission.	Analysis	✓	11.3.1
THM-00.131.01	The thermal subsystem shall keep the inner core of the spacecraft within the temperature range 283 K to 308 K throughout the mission.	Analysis	✓	11.3.1
THM-00.132	The thermal subsystem shall fail at the conclusion of the end-of-mission manoeuvre.	Analysis	✓	-
THM-00.133	The thermal subsystem shall have a maximum area of 8 m^2. (subsection 12.3.1)	Inspection	✓	11.3.2
THM-00.134	The thermal subsystem shall have a maximum mass of 75 kg.	Inspection	✓	11.1
THM-00.135	The thermal subsystem shall need a nominal power of maximally 10 W.	Demonstration	✓	11.1
THM-00.136	The thermal subsystem shall need a peak power of maximally 20 W.	Demonstration	✓	11.1
THM-00.137	The thermal subsystem shall include an in-mission validation process.	Test	✓	2.2
THM-00.138	A safety margin of 5% shall be applied when using off-the-shelf components.	Analysis	✓	-
THM-00.139	A safety margin of 10% shall be applied when using existing technology with minor modifications.	Analysis	✓	11.3.2
THM-00.140	A safety margin of 15% shall be applied when using existing technology with major modifications.	Analysis	✓	11.3.2
THM-00.141	A safety margin of 20% shall be applied when using completely new components.	Analysis	✓	11.3.2
THM-00.142	The thermal subsystem shall account for the requirements imposed by other subsystems.	Analysis	✓	11.3.2
THM-00.143	The thermal subsystem shall account for the heat produced in the operation of other subsystems up to 313 K.	Test	✓	11.3.2
THM-00.144	The thermal subsystem shall have a reliability of 97.5%.	Analysis	✓	13.5.2
THM-00.145	The thermal subsystem shall have a data rate of maximally 0.063 kbits/s.	Demonstration	✓	9.2
THM-00.146	The thermal subsystem shall have a cost of maximum 25 M €.	Inspection	✓	14.3

Requirement THM-00.132 (Table 11.2) made sure the thermal control would stop working whenever the end-of-mission manoeuvre would put the spacecraft in an orbit. However, as the end-of-life strategy is to crash onto Tethys, the thermal control subsystem will stop functioning afterwards.

11.3. Design Approach

In order to size the thermal subsystem, the required conditions for the satellite are determined, as well as the environmental conditions throughout the whole mission. This is done in subsection 11.3.1. After that, both the external and internal heat control systems are sized in respectively subsection 11.3.2 and subsection 11.3.3.

11.3.1. Environmental Considerations

All of the parts within the satellite have a temperature range in which they operate properly and a broader temperature range in which they will survive. The most critical parts will be placed within the cylinder, in order not to have much fluctuations in the temperature. The inner part of the cylinder can be split into three sections, being the internal components, and two tanks. For each of these sections, the temperature is considered homogeneous. For all the systems that are placed inside this cylindrical part, the temperature ranges have been listed in Table 11.3. These values are taken from [65, p. 410] and [39, p. 364].

Table 11.3: Temperature ranges for specific systems.

Temperature Range	Lower limit [K]	Higher limit [K]
Electronics	273	313
Batteries	283	313
Propellant	280	308
On-board Computer	263	323
Microprocessors	268	313
Thrusters	280	338
Sensors	253	323
TT&C mechanisms	253	333

From this table, it can be concluded that the temperature range will be set to 283 K to 308 K, or 10 °C to 35 °C. These values are derived primarily from the batteries and propellant constraints. Consequentially, the temperature within the cylinder is homogeneous. Therefore, the constant distribution of heat and the small variations in temperature over the cylinder reduce the complexity of the heat pipe system. Thus, requirement THM-00.131.01 (see Table 11.2) is complied with.

Next to that, throughout the mission, the worst-case hottest thermal environments will be encountered during a gravity-assist by Venus, according to [85]. The worst-case coldest thermal environment is experienced at the Saturnian system. The received thermal radiation at these locations can be calculated. This value consists of solar radiation coming directly from the sun, the albedo radiation, which is the radiation from the sun reflected by the planet, and lastly the planetary radiation, which comes from the planet itself. For the aforementioned two cases and for the earth flybys, the total heat has been calculated and can be found in Table 11.4. Note that for the Saturnian system, both Saturn, Enceladus and Daphnis are taken into account (requirements THM-00.124 up to THM-00.129, Table 11.2). However during the whole mission, there will be times at which the total received radiation is only coming from the sun, or even close to zero when the satellite is in eclipse behind Saturn. Hence the last value is the worst-case cold scenario. These values have been calculated according to the methods

in [124], together with planetary parameters[1] [2], radii given in subsection 4.3.3 and subsection 4.3.6 and satellite dimensions given in subsection 12.3.1. With this, the requirements THM-00.124 up to THM-00.129 (Table 11.2) are complied with.

Table 11.4: Received radiation for three different cases.

Radiation Parameter	**Venus**	**Earth**	**Enceladus**	**SOI**
Solar radiation [W]	5331.3	2152.0	40.9	40.2
Albedo radiation [W]	1036.3	670.4	34.1	0
Body radiation [W]	619.1	1429.4	12.3	0
Total received thermal radiation [W]	6986.6	4251.8	87.2	40.2

Next to that, as the satellite will be in eclipse for some time, thermal inertia considerations have been determined in order to find out if they have to be taken into account. this can be calculated according to the following equation [124, p. 92].

$$\Delta T = \frac{\dot{Q}\Delta t}{mC} \tag{11.1}$$

Here ΔT is the change in temperature in K, $\dot{Q}$ is the heat flow rate in W/s, Δ t represents the time difference in s, m is the mass in kg and lastly C is the heat capacity, which is 920 J/kgK for the aluminium cylinder.[3] However, calculating the temperature difference shows that the decrease in temperature is in the order of millikelvin and thus thermal inertia is not taken into further consideration.

Finally, the last consideration is the temperature during launch. According to [107], the maximum temperature in the fairing is 373 K. The outer temperature of the RTGs is lower than this maximum value as well because of their insulation. When looking at the temperatures of the outside of the satellite induced during the worst case hot scenario at Venus which can be seen in subsection 11.3.2, the maximum launch temperature is lower and thus will not be critical (THM-13.01, Table 11.2).

11.3.2. External Heat Control

In this subsection, the systems taking care of external heat control are sized. The values for the dimensions are taken from the structural sizing. The absorptivity α and emissivity ϵ values for the different components can be found in Table 11.5.

[1] Retrieved from `https://nssdc.gsfc.nasa.gov/planetary/factsheet/saturnfact.html` last opened on June 17, 2019

[2] Retrieved from `https://nssdc.gsfc.nasa.gov/planetary/factsheet/venusfact.html` last opened on June 17, 2019

[3] Retrieved from `https://www.engineersedge.com/materials/specific_heat_capacity_of_metals_13259.htm` last opened on June 18, 2019

Table 11.5: Absorptivity and emissivity values for different thermal systems.

Characteristic	**Absorptivity**	**Emittance**	**Source**
HGA aluminium sun shield	0.248	0.031	[65]
Radiator	0.08	0.66	[65]
Louvres opened	0.71	0.88	[45]
Louvres closed	0.115	0.88	[45]
MLI coated and backed Kapton	0.54	0.81	[45]
MLI aluminised Mylar	0.13	0.04	[45]
Black coating	0.975	0.874	[65]
White coating	0.248	0.924	[65]

Sun Shield The sun shield is something that will shield (part of) the satellite from solar radiance at Venus flyby. As the solar radiance is the highest radiation source, the high gain antenna will be pointed to the Sun. Due to this, it is assumed that the albedo and planetary radiation will heat up one side of the satellite. However, calculations with [124, eq. 54] and Equation 11.1 on the heat transfer through the aluminium cylinder showed that the time needed to transfer heat from the sun-lit side to the shadow side is in the order of a couple of minutes.

Thus it is assumed that the total radiation received is equal over the whole cylindrical structure. In order to reflect most radiation, the antenna is coated with Z93 white paint ([65, p. 436]). The antenna heats up to a temperature of 333 K. Typical operational temperatures for an antenna are inbetween 173 and 373 K, hence this falls within the feasible range [65, p. 428]. Because of this, the antenna will radiate heat from the backside of the antenna to the upper side of the satellite. Most parts of the cylinder are wrapped with MLI, which will receive the rest of the heat. This will be further discussed below. In order to further decrease the amount of heat received on the cylinder, the four supports of the antenna pointing mechanism will be made of insulating material, for which Carbon Fiber Reinforced Plastics (CFRP) will be used (Figure 13.5). The thermal conductivity of CFRP is very low, i.e. around 0.5-0.6 W/m · K, according to [57] and thus it is assumed heat will only be radiated to the cylinder. As the sun shield is the secondary function of the antenna, its mass is taken into account in the TT&C subsystem.

Louvres

Louvres are mechanisms which have different irradiation for both sides of the surfaces. The effective α/ϵ increases to over six times when the louvres are opened, as can be seen in Table 11.3. These systems are used in order to dissipate the extra heat received at Venus relative to the Saturnian system, i.e. the difference in total heat between the second and fifth column of Table 11.4. The mechanism works on a bimetallic spring-based system, where each of the blades will move independently when their temperature increases. [45, p. 331] This decreases the risk as there is not one single point of failure. The louvres are sized according to Equation 11.2 [45, p. 335], where Δ Q is the difference in received heat in W, T is the temperature in K, A the area in m^2 and σ the Stefan-Boltzmann constant as defined in the Nomenclature.

$$\epsilon = \frac{\Delta Q}{A\sigma T^4} \tag{11.2}$$

After calculating the temperature of the skin, the total area of the louvres needed is determined to be 1.13 m^2 with a 15% margin, placed on the outside of the cylinder. Vane louvres from Starsys will be the type of louvres assembled to the satellite. This type is flight-qualified

and has been implemented on similar missions like Cassini [45, p. 333]. With this type, the mass is determined to be 5.9 kg.

Radiators

The radiators are used to maintain internal heat control, by dissipating the excess heat from the RTGs. In most of the cases the temperature inside the satellite is within its limits and thus the radiators will dissipate most of the heat that goes in the satellite. Only during moments when the temperature should be increased, the radiators will dissipate less heat by controlling the heat flow in the heat pipes. By using Equation 11.2 again, the radiators are sized. This time Q represents the total heat that will have to be dissipated and is the sum of the heat input by the RTGs (600 W) and the internal heat generated (60 W) minus the heat that is emitted by the inside of the cylinder (306 W). The internal heat generated is based on a efficiency factor of 0.85, hence 15% of the peak power is converted to heat. The radiator temperature is assumed to be the same as the inside temperature of the spacecraft and with the emissivity for radiators from Table 11.5, the radiator surface is determined to be 1.58 m^2, placed on the outside of the cylinder as well. This gives a total mass of 4.8 kg, according to [45, p. 214].

Multi-Layer Insulation

Most of the spacecraft's effective area will be covered with insulation blankets in order to decrease the heat flowing in and out as much as possible. This is made sure by using multi-layer blankets on both the outside and inside of the cylinder. The absorptivity and emissivity are very different for both sides, as can be seen in Table 11.5. For the outer one coated and backed Kapton will be used, and aluminised Mylar for the inner layer as it is the most common material used. The reason Kapton is used for the outer one is that Beta Cloth is relatively heavy and only used when electrostatic requirements are driving. Mylar is incompatible with UV exposure and Teflon is known to lose its mechanical strength. [45, p. 170] The sides, top and bottom of the cylindrical structure will be wrapped in MLI, as well as both sides of the skirt shielding the RTGs. Cutouts are made on locations where the radiators and louvres are placed. The instruments that are place on the outside all have their own MLI blanket as well. Furthermore, they have a heat pipe running along it as well, however the thermal control of these instruments is different from the internal core, as the temperature ranges are different.

The thickness of the outer layer is 0.127 mm, and for the inner one the thickness is 0.013 mm, as this is the most optimal thickness looking at the α and ϵ values, as well as the densities. By taking the effective area from the structural subsystem and the densities from [45, p. 172 & 173], the total weight for the MLI is 10.7 kg. Here, a margin of 15% is used. As was calculated for the sun shield, the radiation on the top of the cylinder is 2602 W. By adding the radiation of the sides of 1655 W, a total radiation of 4204 W Due to this, the outside of the satellite heats up to 538 K and the heat that will go into the satellite is 170 W. In fact, as the MLI layers are connected to each other and the structure on as little locations possible, there will also be some heat transferred via conduction, however this is assumed to be equal to zero. This is because of the relatively low area on where these layers touch. Hence the conduction heat is negligible compared to radiation.
The heat generated during firing of the main engine is assumed to be in the direction away of the spacecraft. The heat radiation coming from the hot propulsion system will be shielded away with reflecting disks which are placed on top of the nozzles, following the way Cassini tackled this problem.[4] An MLI layer on the bottom of the hydrazine tank will take care of the

[4]Retrieved from `https://solarsystem.nasa.gov/missions/cassini/engine/` last opened on June 19, 2019

heat that will radiate to the spacecraft from the engine.

Coating
Systems such as the instruments and antennas cannot be insulated with MLI as their structure or function does not allow it. For example, the radar and antenna's will not be able to send signals through the metallic blanket. Next to that, the particle instruments have to be possible to receive particles which would not be able if there was an MLI blanket blocking it. Hence, the second option in order to have passive thermal control is to coat these areas with a special coating. Paints or second surface mirrors can be used for instruments or antennas respectively. It is assumed that the mass of these coatings is already added in the total mass of the specific instrument or antenna on which these coatings are applied, hence no additional mass is added from a thermal point of view.

11.3.3. Internal Heat Control
As described in subsection 10.3.1, for every electrical Watt that is produced, 20 thermal Watts are coming with it. However, only 1.33 thermal Watts will be used to distribute heat throughout the spacecraft. As said in subsection 10.3.1, the RTGs are stable on its own and specifically sized for this ratio of thermal to electrical Watts. This comes down to a total of 600 W, which will be distributed by a system of heat pipes. This value is taken in order to have enough redundancy to keep the spacecraft within its temperature limits and to increase the temperature inside within a reasonable time if needed, i.e. increasing the temperature 5 K of all the instruments within the cylinder within 45 minutes, according to Equation 11.1 for example during or right after a safe mode.
The heat pipe system is a closed two-phase liquid-flow cycle with an evaporator and condenser [45, p. 489]. The system that distributes this heat is called a Capillary Pumped Loop hybrid system (CPL). This system is not only based on the capillary function of the fluid, but can change the flow velocity via a regulated pump [45, p. 496]. A system of heating pipes will run trough the spacecraft on which units will mounted, after which it will run through the radiators in order to dissipate heat. These heat pipes will run along all instruments, the tanks and other components in the cylinder. As the peak thermal power this pump could deliver is 140 W, in order to pump the fluid around, a total of five pumps from the Nederlandse Aerospace Center (NLR) [82] are needed. By adding two redundant pumps, a total of seven pumps will be placed. This is due to the fact that the cylinder in the satellite is relatively long, and by distributing these pumps throughout the system, it will have sufficient power, together with its capillary capability. By changing the power of these pumps, the flow velocity and thus the heat output can be regulated. This comes down to a total electrical power of 4.2 W and a mass for the pumps of 0.7 kg. The total mass of the heat pipes is scaled from [45, p. 214] and found to be 15.0 kg. This adds up to a total of 15.7 kg. The mass of the RTGs is already taken into account in the power subsystem.
As for the heating system, no extra heaters will be placed on the spacecraft, as the RTGs are very reliable and predictable, together with the fact that multiple of them will be installed, thus having enough redundancy, as will be explained in section 11.5.

11.4. Verification & Validation
As can be seen from the compliance matrix in Table 11.2, different methods will be used for verification. The sizing will be based on analysis, by calculating the incoming and outgoing radiation, as was done in section 11.3. After that, tests will take place where the environment is changed and the internal and external temperatures are measured. The numerical analysis that is done before and after these tests can then be verified by making a thermal simulation.

In the case for this mission, the model is verified by filling in different parameters. The first set of parameters are for verification, i.e. filling in zero or a significantly higher value than the current parameters. Comparing this to general mathematical answers, the model was verified. Next to that, the second set of parameters to be filled in are radii of orbits and planets and dimensions of other satellites. Examples are Cassini-Huygens or even earth orbiting satellites. These parameters result in correct equivalences, concluding the model is correct. The equations used are compared to the ones from [124] and [39], which all use either the same equations or have a maximum deviation of 16.8%.

11.5. Sensitivity Analysis

The parameters that influence the design of the thermal control subsystem can change due to a lot of factors. By changing the driving parameters, the thermal control systems will have different dimensions and weights, however the fundamental combination of control systems will not change. The driving parameters for the design are the received radiation, the required temperature range and the satellite dimensions. Looking at external heat transfer, if the received radiation changes, the louvres and radiator sizes will change. Next to that, the current area of the louvres and radiators take approximately 14% of the total area available, so increasing the area needed will not cause any problems. Furthermore, as was discussed in subsection 10.3.1, the thermal Watts generated per electrical Watt, is a ratio of about 20:1, hence with the current ratio of 1.33:1, the internal heat received from the RTGs can be increased significantly. Continuing on this, if the required temperature range, satellite dimensions, received radiation or internal heat production change, the received heat from the RTGs can easily be both decreased and increased. Thus, a lot of freedom is available in sizing the heat input from the RTGs.

11.6. Risk Analysis

As can be seen in Figure 11.2, one event or combinations of events can fail the thermal control subsystem. Three thermal system failures need some more explanation on how to mitigate them, which can be found below.

1. **THR-0.1 MLI Failure:** The original intention of MLI was thermal insulation, however the sheets have improved in such a way that they can act as shielding protection against micro meteoroids, atomic oxygen, electron charge accumulation, and rocket-engine plume impingement [45, p. 161]. The probability is high for this risk as these events definitely happen during the mission. However, due to this, the thermal systems can be designed for requirements STR-00.168 and STR-00.170 (Table 12.2), hence the MLI blankets will contain a layer which shields the rest of the MLI and the spacecraft from these degradation factors. Next to that, the amount of space plasma in the Saturnian system is relatively high, so the MLI is required to control electrical charge and discharge, as this can damage electrical components within the spacecraft when a sudden discharge takes place. [45, p. 158]. As the MLI consists of multiple layers, failure of an layer does not immediately result in a subsystem failure, hence redundancy is present.
2. **THR-0.2 Louvre Failure:** The sun shield and louvres are of great importance in hot environments, as the spacecraft will heat up to too high temperatures and instruments will not survive. Hence the severity of such a failure is of the highest order. However, the condition for such a failure is that it happens during a flyby around Venus or Earth, as the received heat is relatively high around there. This reduces the probability by a lot. Besides that, louvres and radiators operate in the same manner and thus their function

can be interchanged if needed.
Next to that, as was said in subsection 11.3.2, the panels of the louvres can operate independently and thus only part of the louvre fails if a part of the mechanism stops working. The way this is accounted for is by adding a safety margin of 15% for both the louvres and radiators.

3. **THR-0.3 Heat pipes Failure:** Whenever the heat pipes get jammed up, no more heat can be distributed, having a high severity. However, as this CPL system is a fully closed system, no material can enter or leave this system, hence the probability of a failure is very low. The only way this can fail is by changes in the flowing liquid. When looking at the second risk, pump failure, mitigation takes place due to a redundant number of pumps. When one of the pumps fail, the others continue to work, and even in the rare case that all of the pumps stop working, the heat is still transported due to capillary action. Lastly, the third risk is generating too much heat internally. There will only be a thermal control subsystem failure however as either one of those last two risks happen combined with a radiator failure.
   As the temperature range for the instruments in the cylinder is relatively small, having another cycle dedicated for these parts would result in a more precise temperature control. The same can be done for other group of instruments or components, in order to not have one loop in series, but rather multiple loops running in parallel.

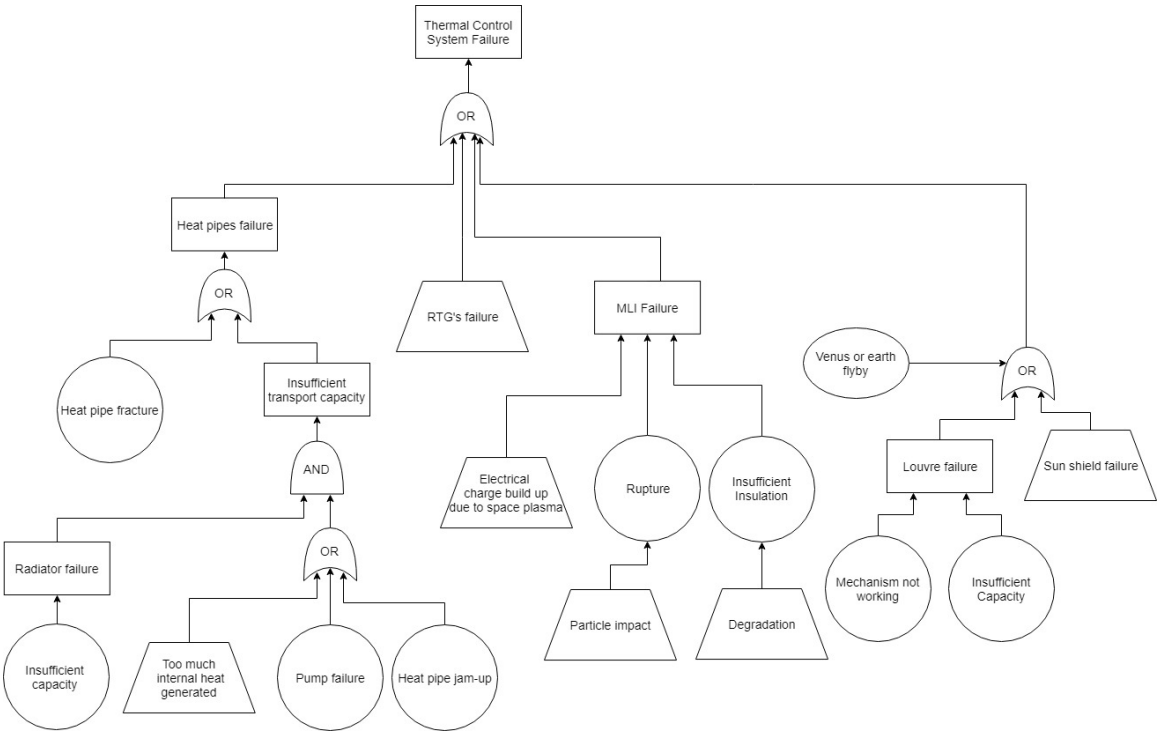

Figure 11.2: Fault tree of the thermal control subsystem.

12 Structures

The structure of the satellite has to mechanically support and integrate the subsystems. It has to be sized such that it does not fail when subject to launch loads. First, the design overview can be seen in section 12.1. The requirement analysis is given in section 12.2. Afterwards, the design approach is described in section 12.3, followed by verification and validation in section 12.4. The sensitivity analysis and risk analysis are given in section 12.5 and section 12.6 respectively.

12.1. Design Overview

The semi-monocoque structure of the satellite is designed to be a cylindrical structure strengthened with stiffeners and stringers. Attached to this cylinder is a skirt, shielding the rest of the satellite from the radiation coming from the RTGs, and within the cylinder a mounting disk supports the internal instruments. The mounting for the propulsion system and the supports for the HGA are also considered part of the structural subsystem. The latter is made of CFRP and the rest of the structure is made of the aluminium alloy 7075-T6. This material has been chosen as its material properties suit the structural requirements (see Table 12.2) for this mission as well as the ease of manufacturing [1].
Three mechanisms are present on the satellite: the deployment mechanisms for the radar and magnetometer boom, and the antenna pointing device. All parameters for the structure can be found in Table 12.1 (Requirements STR-00.173 to STR-00.175, Table 12.2). The masses of the structure are determined by multiplying the volume of specific part with the density of the aluminium alloy of 2795.7 kg/m^3, from [1, p. 3-371]. The technical drawing of the structure with the payload can be seen in Figure 12.3

Table 12.1: Overview of the structural components, with its corresponding mass and power.

Component	Mass [kg]	Power [W]	Remark
Cylinder	121.6	-	Bottom is supported with stringers.
Skirt	36.7	-	-
HGA support	0.5	-	Conductive insulating CFRP.
Mounting disk	11.0	-	Bottom is supported with stiffeners.
Propulsion system mounting	3.9	-	-
Radar deployment mechanism	-	-	Mass is included in the total radar mass. Power is included in the peak radar power.
Magnetometer boom deployment	3.4	5	One-time use only and the power provided is the peak power.
Antenna pointing device	10.5	13	Dual-axis.
Total	187.6	13	Nominal power

12.2. Requirement Analysis

The compliance matrix for the structural subsystem can be seen in Table 12.2.

Table 12.2: Compliance matrix for the structural subsystem requirements.

Code	Requirement	Verification Method	Compliance	Section
STR-13.05	The spacecraft's structure shall be able to withstand a maximum longitudinal acceleration of 6g from the launch [107, p. 16].	Test	✓	12.3.2
STR-13.06	The spacecraft's structure shall be able to withstand a maximum lateral acceleration of 2g from the launch [107, p. 16].	Test	✓	12.3.2
STR-13.07	The spacecraft shall have a minimum natural frequency in Hz [107, p. 19].	Test	✓	12.3.2
STR-13.07.01	The spacecraft shall have a minimum natural frequency above 35 Hz in longitudinal direction [107, p. 18].	Test	✓	12.3.2
STR-13.07.02	The spacecraft shall have a minimum natural frequency above 5 Hz in lateral direction [107, p. 19].	Test	✓	12.3.2
STR-00.168	The structure shall be able to withstand micro meteoroids with a debris velocity up to 18 km/s.	Test	✓	12.6
STR-00.169	The structure shall be able to withstand limit loads deriving from spacecraft's propulsion system.	Test	✓	12.3.2
STR-00.169.01	The structure shall be able to withstand a torque due to slew of maximally 5 Nm.	Test	✓	12.3.2
STR-00.169.02	The structure shall be able to withstand a maximum bending moment of maximally 500 Nm.	Test	✓	12.3.2
STR-00.170	The structure shall ensure the support and protection of all the elements of the spacecraft.	Test	✓	12.3.3
STR-00.171	Fatigue over lifetime shall not compromise mission quality.	Analysis	✓	12.3.1
STR-00.172	The mechanisms in the structure shall not obstruct any payload view during observation phase.	Demonstration	✓	12.3.3
STR-00.173	The structure shall have a maximum mass of 300 kg.	Inspection	✓	12.1
STR-00.174	The structure shall need a nominal power of 13 W.	Demonstration	✓	12.1
STR-00.175	The structure shall need a peak power of maximally 20 W.	Demonstration	✓	12.1
STR-00.176	A safety margin of 5% shall be applied when using off-the-shelf components.	Analysis	✓	12.3.4
STR-00.177	A safety margin of 10% shall be applied when using existing technology with minor modifications.	Analysis	✓	12.3.1
STR-00.178	A safety margin of 15% shall be applied when using existing technology with major modifications.	Analysis	✓	12.3.1
STR-00.179	A safety margin of 20% shall be applied when using completely new components.	Analysis	✓	12.3.1
STR-00.180	The structure shall account for the size and placement requirements imposed by other subsystems.	Analysis	✓	12.1
STR-00.181	The structure shall have a cost of maximum 225 M €.	Inspection	✓	14.3
STR-00.182	The structure shall have a reliability of minimum 97.5%.	Analysis	✓	Table 13.4

12.3. Design Approach

In order to size the structure of the satellite, first the primary structure has to be sized, as can be seen in subsection 12.3.1. After this, a load case evaluation follows in subsection 12.3.2, followed by the instrument placing in subsection 12.3.3 and the mechanisms in subsection 12.3.4.

12.3.1. Primary Structure

The primary structure of the satellite consists of a cylinder, on which every part is mounted. For vibrational reasons, a larger cylinder diameter is preferred (Equation 12.1a & Equation 12.1b), however when looking at pure tensile and compressive forces, the exact opposite is wanted (Equation 12.2a & Equation 12.2b). For its sizing, several propulsion tank configurations were traded-off. The optimal solution was found by using the largest diameter tank (hydrazine tank) as leading for the structure design. The placement of these structures can be found in Figure 13.5

To avoid buckling, the middle tank is compressed to form two oval shapes attached to each other, in order to have the sides still touching the cylinder. Considering that increasing length of the cylinder would increase forces too much, the smallest tank is placed outside. The tank is pill shaped in order to stay in the shadow of the sun shield in this configuration.

Above these tanks, a space with a length of 1.07 m is reserved for the internal components. This value is based on adding the volumes of all internal components and adding extra space due to the shape of these instruments and wiring. This length has then been validated by placing boxes of groups of instruments in CATIA software and checking if this would fit. These instruments are placed on a mounting disk, which is strengthened by two crossing stiffeners below it. The top of the cylinder is closed with a second disk, which carries the antenna. This disk is strengthened as well.

Above the cylinder, the HGA support holds the HGA. This antenna has a length of 0.65 m, as scaled from the Cassini spacecraft.

Below the tanks, the cylinder continues for 0.3 m. On the lower side of the cylinder, nine

RTGs are placed with equal spacing. As these RTGs are mounted on the cylinder, the effective area of the cylinder carrying the load is decreased by 54%. This decrease causes stress concentrations around the mountings and in order to cope with this, nine stringers are placed vertically between every RTG on the inside of the cylinder.

A skirt is placed above the RTGs with a slight angle facing down. The function of this skirt is to shield the rest of the spacecraft from the RTGs. This skirt is placed such that both the horizontal part of the radar instrument and the magnetometer are protected from radiation.

Below the cylinder, no disk is placed as this would not carry any loads if the lower tank would not be mounted on this disk. Furthermore, this improves the accessibility for the engines to reach the propulsion feeding system. However, an MLI blanket will be placed to shield the lower side of the tank from external influences.

Summarising this, the dimensions of these parts can be found in Table 12.3 and a visualisation of this can be found in Figure 13.5. Note that the thicknesses are from the structural subsystem, i.e. the tank thickness is different and can be found in subsection 7.3.2. Parts without a value do not have a physical dimension in the specific case. The value of 1.84 mm is determined in subsection 12.3.2, whereas the 2 mm thickness is determined in section 12.4. The total area available on the primary cylinder and the skirt for the placement of systems is determined to be 24 m^2, to be used for thermal control, instruments and other external systems.

Table 12.3: Primary structure dimensions.

Part	**Length [m]**	**Diameter [m]**	**Skin thickness [mm]**
HGA	0.65	3.0	-
HGA support (3x)	0.05	0.09	Honeycomb
Cylinder	3.97	1.50	1.84
Instruments spacing	1.07	1.50	1.84
Mounting disk	-	1.50	2.0
Upper tank	1.10	1.50	1.84
Lower tank	1.50	1.50	1.84
RTG section	0.30	1.50	1.84
Skirt	-	3.60	2.0
Structural length	4.67	-	-

12.3.2. Loads Analysis

The four different loads that are looked at are the vibrations in both lateral and longitudinal direction, and compression and tensile forces, which all happen during launch. For these four cases, the minimum required thickness of the cylinder can be determined, from which the highest value will be the leading thickness. Starting with the vibrations, the satellite is assumed to be a uniform beam. The most mass can be found on the bottom of the cylinder, where the two largest tanks can be found, hence the assumption of taking a uniform beam is the most applicable one. The equations for these vibrations can be found in Equation 12.1a and Equation 12.1b for the lateral and longitudinal direction respectively [124, p. 80].

$$f_{lat} = 0.560\sqrt{\frac{EI}{mL^3}} \qquad (12.1a)$$

$$f_{long} = 0.250\sqrt{\frac{AE}{mL}} \qquad (12.1b)$$

Here f_{lat} and f_{long} are the lateral frequency and longitudinal frequency in Hz, E is the Young's modulus which is 71.02 GPa [1, p. 3-371], I is the area moment of inertia of the cylinder in

m^4, A represents the area in m^2, the mass M is given in kg and lastly the length L is given in m. The maximum applied loads are experienced during launch, which can be found in Table 12.2, where g_x is 6g and g_y is 2g in longitudinal and lateral direction respectively [107]. For the calculations, the dimensions of the cylinder are used, together with the minimum required vibrations, as stipulated in Table 12.2 as well. A safety factor of 1.25 is applied on these load calculations, as can be found in [65, p. 439]. Following from this, the minimum required thickness can be found in Table 12.4.
Furthermore, the equations for both critical buckling and tensile forces can be found in Equation 12.2a and Equation 12.2b respectively [124, p. 81-82].

$$\sigma_{cr} = E\left(9\left(\frac{t}{R}\right)^{1.6} + 0.16\left(\frac{t}{L}\right)^{1.3}\right) \quad (12.2a)$$

$$\sigma_{tot} = \frac{g_y m L R}{I} + \frac{g_x m}{A} \quad (12.2b)$$

Here σ_{cr} and σ_{tot} are the critical buckling stress and total stress in MPa respectively, and m represents the weight in kg here. The thickness t and R are both expressed in m. Taking the same safety factor here, the minimum required thickness are determined and given in Table 12.4.

Table 12.4: Minimum required thickness per load case.

	Minimum required thickness [mm]
Lateral vibrations	0.20
Longitudinal vibration	1.84
Compression	0.58
Tensile	1.04

Table 12.5: Final values with the minimum thickness.

	Final load case
Lateral vibrations	19.28 [Hz]
Longitudinal vibration	43.75 [Hz]
Compression	165.4 [MPa]
Tensile	45.2 [MPa]

From Table 12.4 it can be concluded that the thickness of the longitudinal frequency is leading. By using this thickness again, the maximum stresses are calculated and can be found in Table 12.5. Important to note is that for calculations on these values, a thickness of 1.90 mm is used, as this is the highest minimum required thickness. When comparing this with the ultimate tensile strength (538 MPa), tensile yield strength (476 MPa) and compressive yield strength (490 MPa) of the 7075-T6 aluminium alloy, the maximum stresses during launch are below these values [1, p. 3-371]. The range of vibrations is discussed in section 12.5. With this requirements STR-13.05 to STR-13.07.02 (Table 12.2) are complied with.

Other considerations that are taken into account are torsion and bending moment. When looking at the force the thrusters at the end of the skirt produce, which is 2.2 N and yields a total torque between 3 and 4 Nm, it is safe to assume this is negligible. Bending due to thrusters can be assumed negligible in the same manner (STR-00.169, Table 12.2).

The last considerations are the maximum and random vibrations. According to [107, p. 26], random vibrations start increasing from 100 Hz on. Next to that the maximum longitudinal and lateral vibrations are 75 Hz and 85 Hz respectively. The actual natural frequencies from Table 12.5 are below these three values and thus no extra sizing has to be done.

After translating this idea into CATIA and consequently importing this into ANSYS software, finite element analysis (FEA) has been performed on the model. From this analysis, it can be found extra stiffness measures are to be taken, as can be found in section 12.4. These

measures are translated back into the CATIA model by means of an iterative process.

12.3.3. Instruments Placing

As was already discussed in subsection 12.3.1, the placing of the three tanks was leading in the design, as two of those are placed inside the cylinder. The other components that are placed inside the cylinder are listed below.

- two IMUs
- four momentum wheels
- radioscience instrument
- TT&C internal architecture
- on-board computer
- storage unit
- two batteries
- power management instrument

Inner components need a stable temperature, shielding from radiation and impacts, or they need to be placed as close as possible to the principal axis. The other components are placed outside of the cylinder. Except for the radio science, are payload is placed on the outer upper part. The reasons for this location are to be both the furthest away from the RTGs to have as low radiation as possible, and the closest to the internal components to have the cables as short as possible. Both the LGAs are on opposite sides of the highest part of the cylinder, for increased field of view. Lastly, the thrusters are placed on the skirt in order to have the moment as high as possible. A visualisation of this can be found in Figure 13.5. With this, requirements STR-00.170, STR-00.172 ans STR-00.180 are complied with (Table 12.2).

12.3.4. Mechanisms

There are a number of mechanisms that are included in the structural design of EPOSS. These are mostly mechanisms that allow for a deployment. A deployment is needed for several subsystems in order to be fitted in the launch fairing. The first mechanism is a launch vehicle adaptor, which is a 1575 mm diameter bolted launcher specific interface from [107]. Secondly, the radar deployment mechanism is an axial deployment device which is integrated in the instrument itself. That is also the reason why there is not a specific mass and power budget for the mechanism, as it is included in the instrument which can be seen in Table 5.1 [21]. Note an in-depth analysis of the risks introduced by trajectory for the radar, this being a delicate instrument, is recommended for further work. Possible consequences of orbit insertion or inclination changes on deployed radar are out of the scope of this report. Thirdly, the magnetometer boom deployment consists of a hinged articulated boom deployment mechanism, with a mass of 3.4 kg and is developed by RUAG [94]. Peak power is 5 W and the nominal power for this mechanism is 0 W as it is only used once and then set in place. Finally, the antenna pointing mechanism is selected based on the maximum pointing error displayed in Table 8.2. With a mass of 10.5 kg and a nominal power of 13 W, an accuracy of 0.005 degrees can be achieved, which is better than the 0.0085 degrees maximum pointing error [124, p. 84].

12.4. Verification & Validation

After this preliminary sizing, the structure is verified by using FEA. It is done with the use of a static structural problem to verify if the load carrying structure does not exceed a compression stress of 165.4 MPa experienced during launch, as well as to iterate on the overall design. The load case taken in the FEA is the case during launch, where the accelerations are a magnitude of 6g in axial and 2g in lateral direction [107].

The result is that the plates between the antenna and the tank have to be reinforced due to the high deflections it has to endure. That is also logical due to the low stiffness in the plane of the acceleration. Also, reinforcements have been added at the ring of the RTG attach-

ment which was identified as the critical point in the overall stress distribution. The stiffeners resulted in an addition to the mass of 4.26 kg, while the reduction in stress was a factor 3. This strong reduction can also be explained by the method of meshing,[1] because the visualisation also shows that the stress concentration is at a very local spot.

The final iteration (with reinforcements) can be seen in Figure 12.1. It can be seen that the nominal stress in the cylinder is around 30.8 MPa, whereas the stress raises to a value of 46.8 MPa and 58.2 MPa in the lower and higher part of the cylinder, respectively. This is as expected from the values seen in Table 12.5. The maximum stress of 177.2 MPa in the legend is considered to be due to the meshing of the FEA. The optimisation of the mesh is assumed to be out of the scope and therefore these values can be neglected. That statement is supported by the fact that in the picture, the maximum stress indicator indicates a small spot. This also holds for the lower bound value, where it can be seen that the indicated nominal stress values do not coincide with the legend.

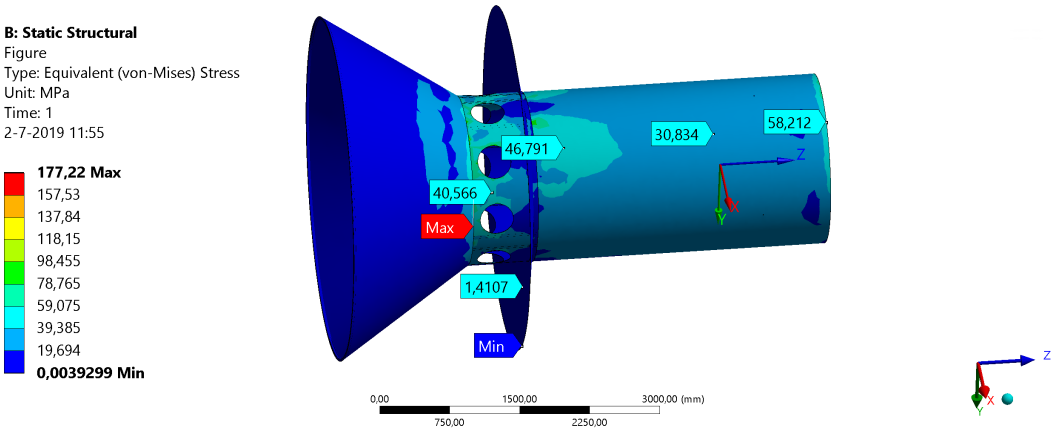

Figure 12.1: Visualisation of the Finite Element Analysis.

12.5. Sensitivity Analysis

In the structural design there are a couple of design factors that affect the design in a considerable way. These factors are discussed in this section. Firstly, if the launcher were to change due to a weight or volume increase there would be a number of considerations to the structure. The launch vehicle adaptor is different, so the structure has to modify in a way that it can connect to the adaptor. Also, the acceleration loads and vibrations due to natural frequency change which changes the structure considerably since this is the main design load case which can be seen in section 12.1.
Secondly, if the axial or natural frequency changes it should be taken into account that it shall not exceed the natural frequency range provided by the launcher characteristics. The axial natural frequency is 43.8 Hz while the allowed value is between 35 and 75 Hz [107]. The lateral frequency has a value of 19.3 Hz while the allowed value is between 5 and 85 Hz [107]. This allows for a maximum change of 25% in natural frequency of the spacecraft such that it still fulfils this requirement. Thirdly, the change in tank size is a considerable design factor due to its size. If this changes the diameter of the spacecraft changes. This results in a change in vibrations and stresses and thus an evaluation should be done.
Finally, if the spacecraft mass increases by 10%, the thickness of the primary load carrying

[1]Retrieved from `https://www.comsol.nl/multiphysics/mesh-refinement` last opened on June 18, 2019

cylinder needs to increase by 0.18 mm or 21.9 % due to the extra loads it is exposed to. This results in a change in structural mass of 9.6 kg. Concluding this, a change in launcher will not cause any difficulties as only minor modifications have to be done. However, changing the tank size will initiate a snowball effect in increasing the cylinder and thus decreasing the thickness and thus mass. This will result in a lower dry mass and thus less propellant. This will cause a number of iterations before the mass and cylindrical dimensions are finalised.

12.6. Risk Analysis

From Figure 12.2 it can be seen that four major failures can lead to structural failure. All of these risks are single-point failures as they will directly lead to failure of the subsystem. Hence, thorough safety measures are taken into account in order to mitigate these risks.

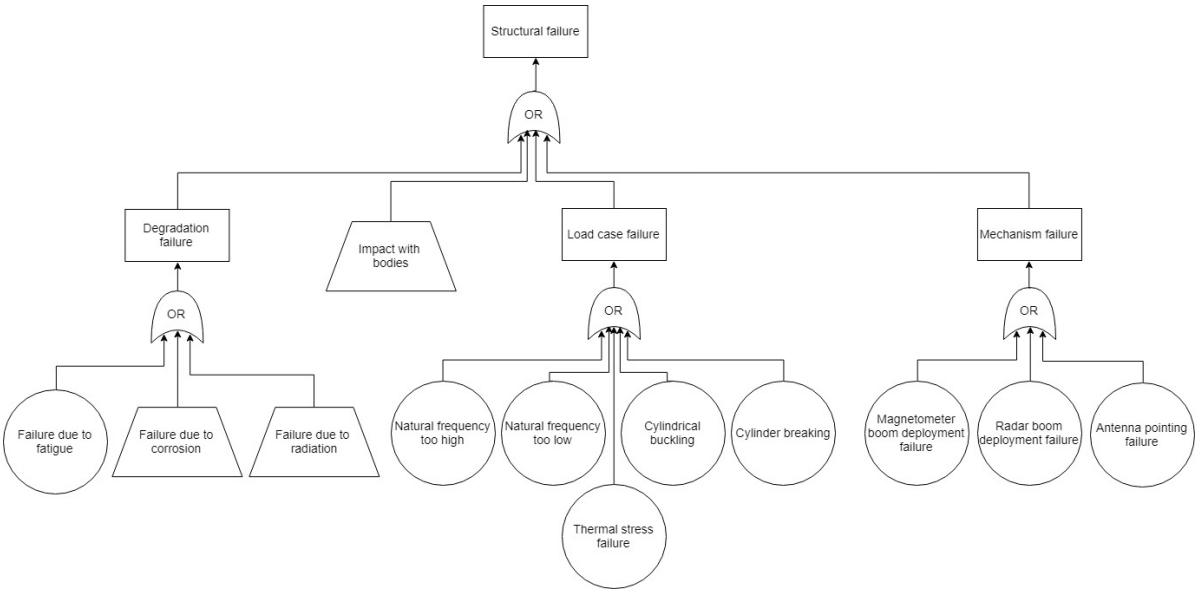

Figure 12.2: Fault three of the structural subsystem.

1. **STR-0.1 Mechanism failure:** The three mechanisms in the spacecraft only operate once, however, failure probability should be reduced since the consequences are critical. Therefore, highly reliable mechanisms are used, as the magnetometer boom deployment has a technology readiness level of six and will have an expected TRL of nine in 2021 [94]. Furthermore, in case the antenna pointing mechanism fails, the ADCS subsystem can take over by controlling the attitude, therefore a redundancy is added.
2. **STR-0.2 Load case failure:** As the primary structure of the satellite carries all of the instruments, redundant safety margins are applied. According to [65, Table 11-48], a safety factor to design for is 1.25 times the ultimate strength. This value is taken as the spacecraft structure can be tested thoroughly hence this safety factor is on the low side in the safety factor range.
3. **STR-0.3 Degradation failure:** As the mission lifetime is over 16 years, degradation of the structure will happen in terms of corrosion and radiation. Hence, as the probability is as high as possible, designing should be based on lowering the severity. This is done by MLI shield, as explained in section 11.6.
4. **STR-0.4 Impact with bodies:** A Whipple shield is attached to the outside of the satellite which shields against particle impact, as was already discussed in section 11.6. This stuffed shield is made of Nextel and Kevlar and can withstand micro meteroids having the size of dust grains impacting up to 18 km/s.[32]

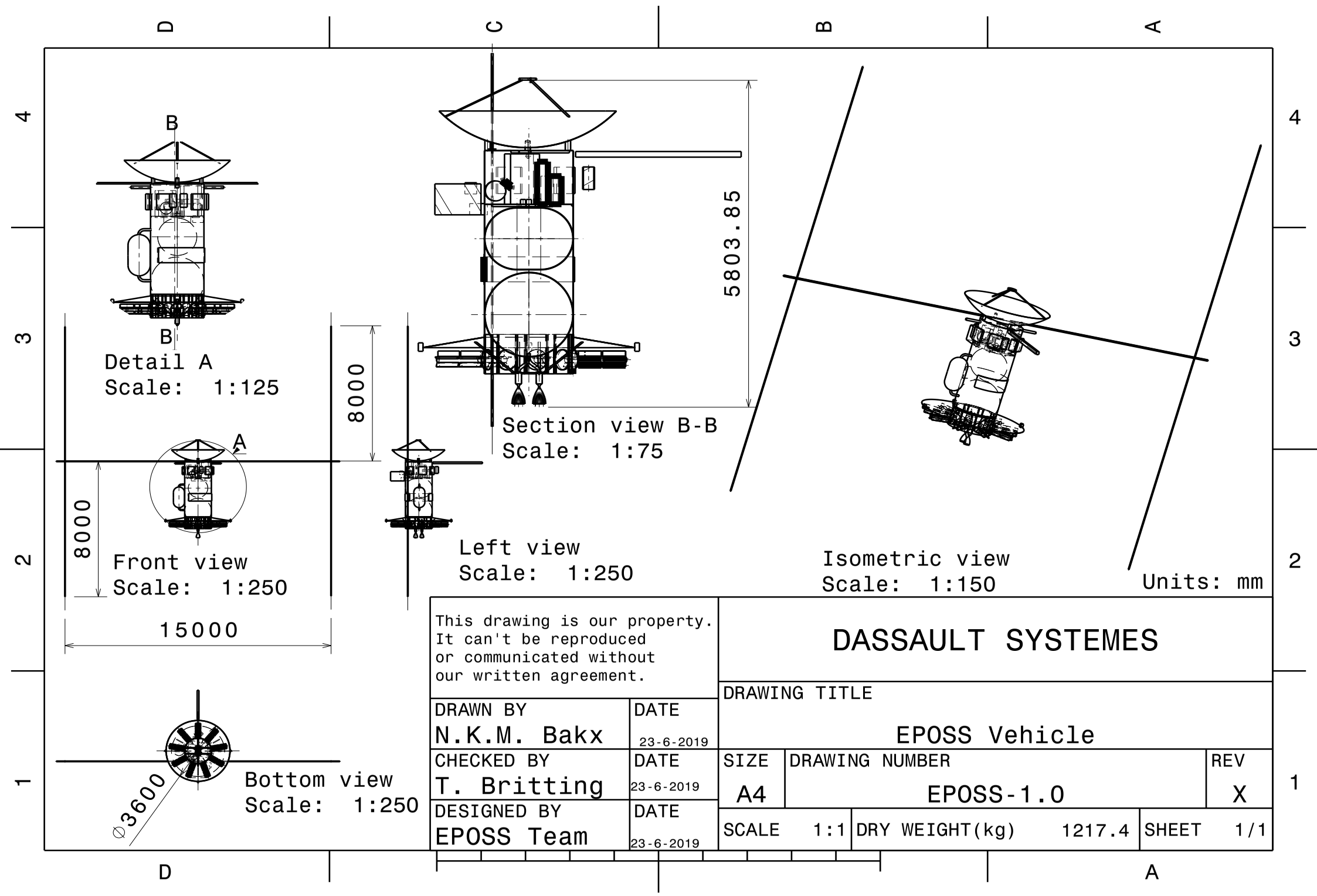

Figure 12.3: Technical drawing of EPOSS.

13 Final Design

In this chapter, the final design is presented. First, the integration tools used to come to a coherent design between subsystems are presented in section 13.1. Next, the final spacecraft layout can be found in section 13.2. This final design should be verified before launch, and the interface verification methods are described in section 13.3. As all factors influence the final design, the general sensitivity analysis in section 13.4 explains how the design changes when general characteristics change. Finally, the risks related to the mission, and the reliability of the subsystems are discussed in section 13.5.

13.1. Integration Tools

All subsystems have been designed in the previous chapters. In order to identify how all these subsystems work together, this section presents two N2-charts. The first chart, presented in subsection 13.1.1, shows how the design of all subsystems depend on each other. The second chart, presented in subsection 13.1.2, shows the physical integration of all subsystems.

13.1.1. Design Integration

In order to gain an overview of what team needs to know about what values, an N2-chart was created. It can be found in Figure 13.1, and clearly shows how all subsystems depend on each other. The design process started with preliminary values yielded from [10], which were updated once subsystems found new values. Inputs needed for the subsystem design can be found horizontally, whereas outputs from a subsystem can be found vertically.

13.1.2. Hardware Integration

The hardware integration shows how different physical subsystems present on the spacecraft interact with each other and the ground station. The N2-chart can be found in Figure 13.2. It can be seen that all subsystems interact with the OBC, as this component handles all data flows on the spacecraft (see chapter 9). The OBC also handles all commands, and tells other systems what to do and when, and includes the payload data storage segment. It should be noted that the sensors are passive, and thus do not require commands. Furthermore, it sends commands to the power regulator, which in turn regulates the power from the batteries and RTGs and sends it to the required systems. Finally, only one subsystem interacts with the ground station, which is the TT&C subsystem. However, all data from and to TT&C again flow through the OBC before storage or retrieval from the storage.

Physical interfaces within the spacecraft are provided by the structure subsystem, which ensures mounting and protection of all other components (chapter 12). Other physical interfaces include the power distribution interface and the command and data interface. Interfaces between the spacecraft and the launcher include the launcher adaptor and spacecraft deployment mechanisms. Verification and validation of interfaces is discussed in section 13.3.

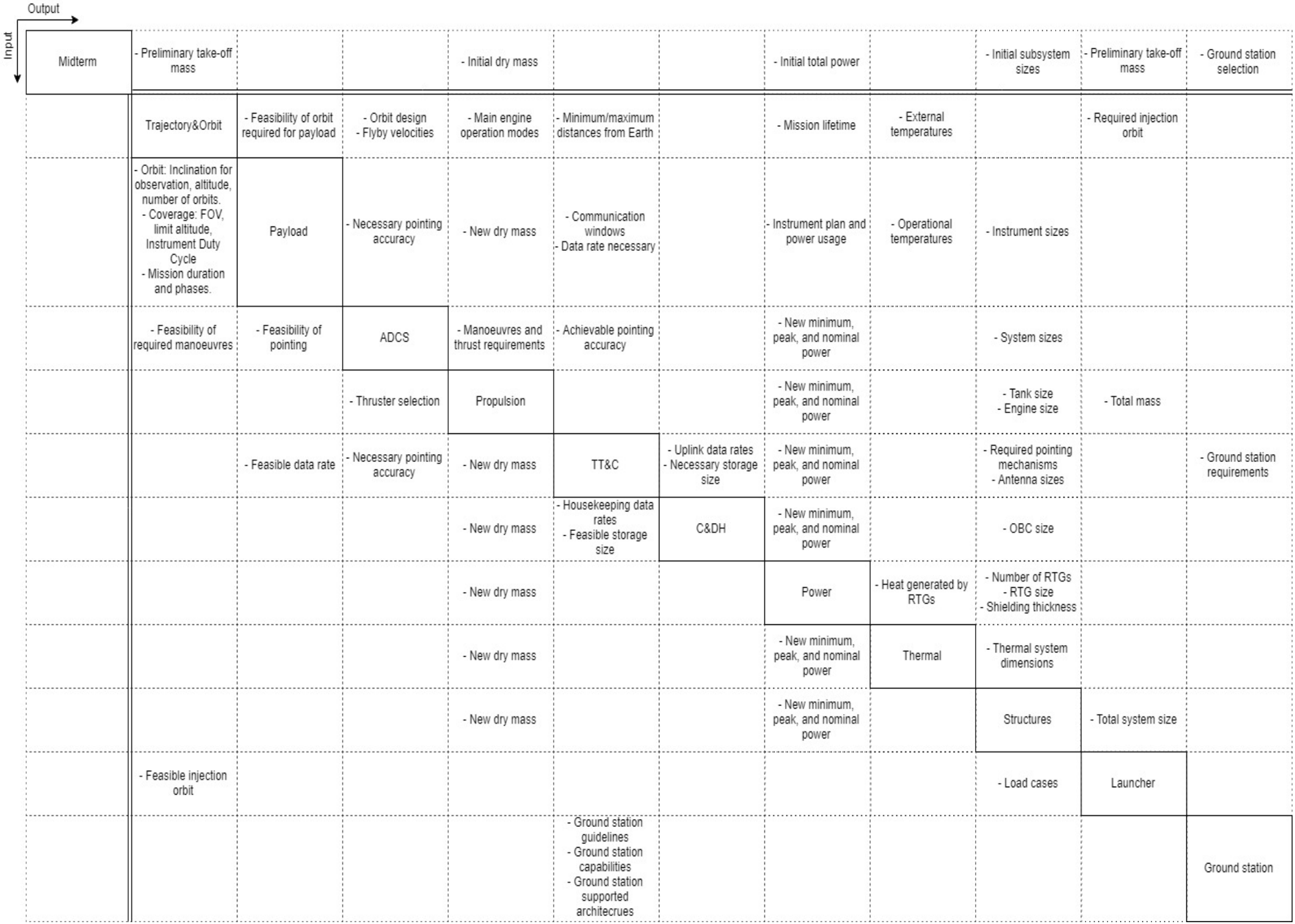

Figure 13.1: N2-chart for design integration.

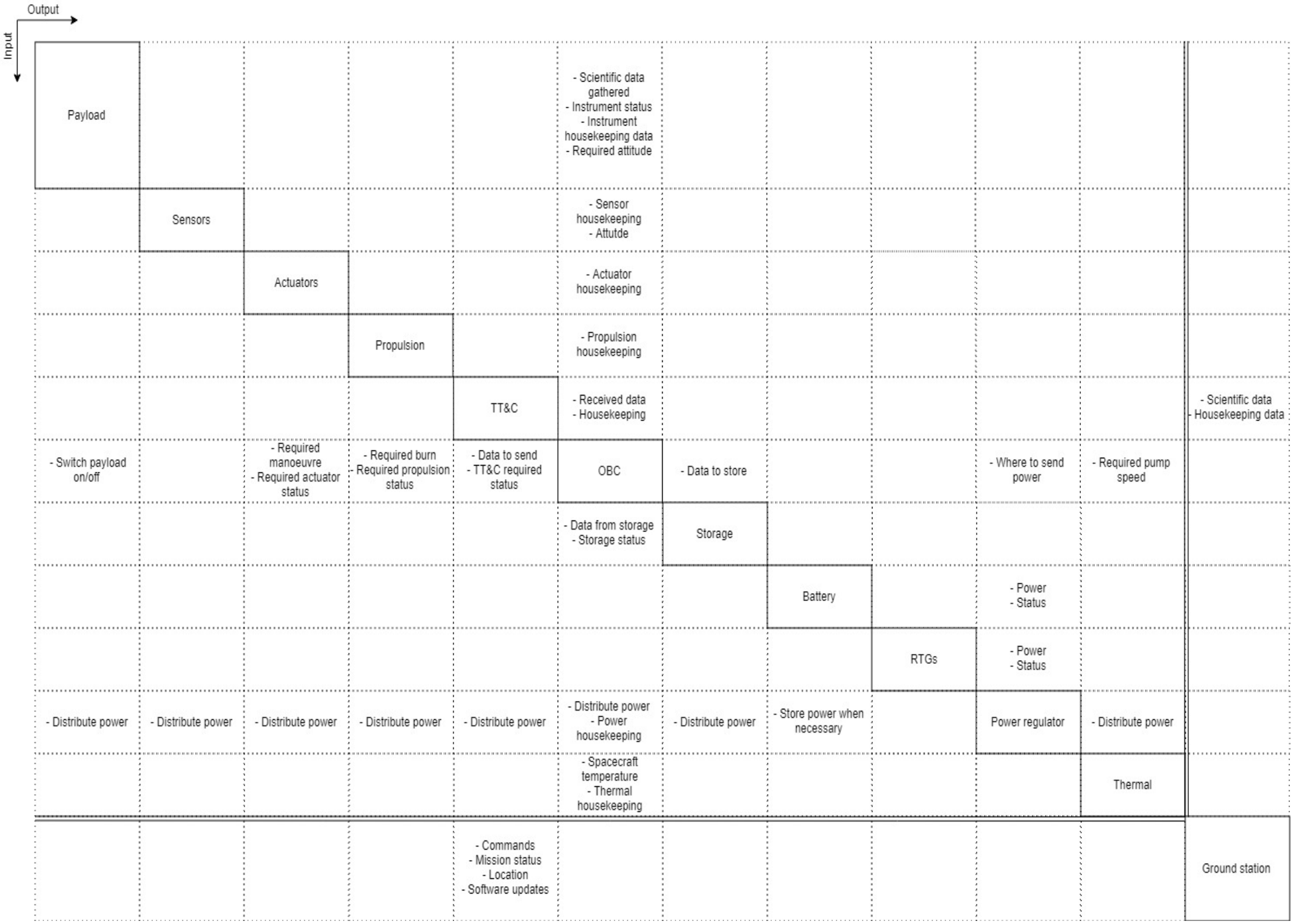

Figure 13.2: N2-chart for hardware integration.

13.2. Spacecraft Layout

The vehicle can be divided in a sections as it is shown in Figure 13.4 and Figure 13.5. The bottom section houses the RTGs, radiation skirt, ADCS thrusters and the propulsion subsystem (excluding the propellant tanks). The middle section includes the fuel, oxidiser and pressurant tank and radiators. The top section of the vehicle contains the payload instruments, electronics, TT&C subsystem, reaction wheels and batteries. The main structure of the vehicle is represented in all sections. The reasoning for the location of the components is given below.

- As indicated in section 10.6, the RTGs should preferably be located as far as possible and shielded from the payload instruments and electronics. This is why all of the nine RTGs are placed on the bottom around the main cylinder, above which the shielding skirt is placed.
- The electrical devices on board are sensitive to temperature differences, radiation and impacts. Therefore, most of them are placed inside the main cylindrical structure in the top section of the vehicle, where a regulated environment protects them. They are mounded on a circular disc, which is then attached to the main cylinder.
- To limit any cable losses, the TT&C instruments are closely located to the high- and low-gain antennas. The high-gain antenna is placed on the top of the cylinder where it fulfils its secondary role of sun-shield. The low-gain antennas are placed on opposite sides of the main cylinder to maximise their coverage.
- To minimise the shift in centre of gravity throughout the mission, the oxidiser and fuel tanks are placed in the cylindrical structure to allow for symmetry in the x and y axis. This also prevents them from experiencing higher temperature differences and add stiffness to the structure. Because the spherical fuel tank fits all around the cylindrical tank, a duct for the oxidiser fuel line and electronic cabling is installed.
- Because of the lower mass and volume of the pressurant tank, it is placed along and outside of the cylinder. In order to stay within the shadow of the larger antenna, it has an elongated pill-shape.
- The optical instruments are all located on one side of the spacecraft, which allows them to work simultaneously. To minimise the risk of the instrument's lenses being damaged by particles, they are placed on the opposite side of the mass spectrometer on the vehicle.
- The magnetometers are located on a deployable boom to minimise the influence of the induced magnetic field by the electronics.
- The radar instrument has a 'H' shape, which is situated parallel to the principal axis of the vehicle and perpendicular to the optical instrument's viewing direction. This allows for measurements to be taken while the optical instruments are operational as well.
- The louvres are installed close to the electronics and payload to guarantee a more constant temperature, even during the Venus flyby.

The spacecraft should fit inside the launch vehicle fairing. Because the spacecraft in its operational shape would not fit, some systems are deployable. The the magnetometer boom and radar instrument are folded closer to the spacecraft because of their large dimensions. The outer dimensions of the spacecraft during launch are 8.50 m by 3.74 m by 3.74 m, which fits inside the launch vehicle dimensions of 11.4 m by 4.6 m by 4.6 m [107]. The vehicle's deployed dimensions of 16.0 m by 16.0 m by 5.46 m. A technical drawing of the spacecraft including the outer dimensions can be seen in Figure 13.1. An image of the spacecraft in the launch vehicle can be seen in Figure 13.3. Two renders of the spacecraft can be seen in Figure 13.4 and Figure 13.5

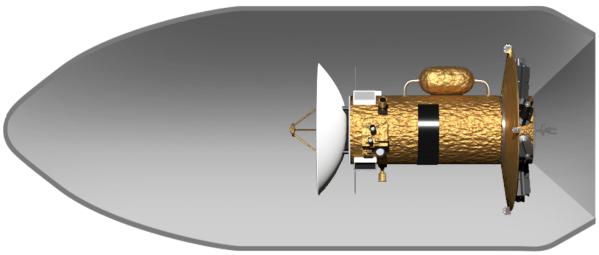

Figure 13.3: EPOSS in the Falcon Heavy launch vehicle fairing.

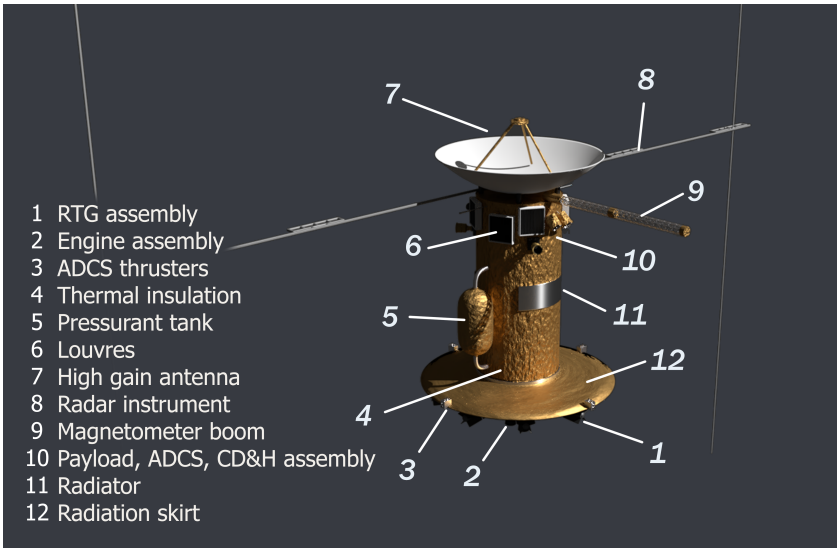

Figure 13.4: External view of the EPOSS vehicle.

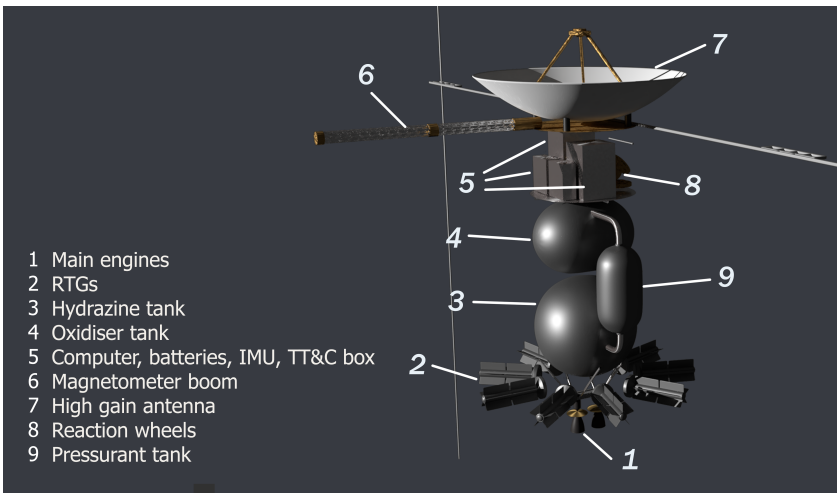

Figure 13.5: Internal view of the EPOSS vehicle

Table 13.1: Verification of Mass Budget.

Subsystem	bottom-up mass fraction	top-down mass fraction	Absolute Error	Percentage Error [%]
Payload	0.112	0.154	0.0418	27.2
Thermal	0.030	0.064	0.0338	52.9
Power	0.235	0.214	0.0213	-9.9
ADCS	0.0425	0.060	0.0175	29.2
Propulsion	0.281	0.134	0.147	-110.1
Structures	0.153	0.254	0.101	39.7
TT&C	0.117	0.0738	0.0433	-58.6
C&DH	0.029	0.0438	0.0148	33.7
Propellant	2.510	1.1	1.410	-128.2
Wet Mass	3.510	2.096	1.414	-67.4

13.3. Verification & Validation

As opposed to the subsystem verification and validation, this section aims to discuss theoretical verification methods for integration interfaces, not actual verification that has been applied to their design method in this report, although the mass fractions are compared to the reference fractions from [65] as well. A few integration interfaces discussed here are: the physical interface (structures, see chapter 12), the power interface (power regulator, see subsection 10.3.3), the data interface (OBC, see chapter 9), and the external interface that connects the spacecraft to the launcher (launch adaptor and deployment mechanisms, see subsection 12.3.4).

The physical interface includes the structures and mechanisms of the spacecraft. These can be verified through extensive testing under different load cases, such as the vibrational loads during launch and the shock loads during separation from the launcher; and the mechanism functioning can be demonstrated. Zero-g testing shall be done according to the guidelines stipulated by NASA in [79].

The power interfacing is governed by the power regulator, which distributes the power amongst the subsystems. Its verification will be achieved by extensive testing, including and comparable to thermal tests. Furthermore, demonstrating that it can handle the power distribution further verifies the component. Testing with the fuelled RTGs will be done as well, although additional safety measures should be taken.

The data interface (OBC) is an off-the-shelf component (see section 9.3), and hence should have been tested by Airbus. However, tests will still be conducted to show that it meets the specifications described by Airbus and thus EPOSS' requirements.

Finally, there is an external interface that connects the spacecraft to the launcher and deploys it. As this is done by the launcher, SpaceX should verify this system before launch. It should be ensured that the spacecraft can be deployed in the correct orbit with the correct velocity such that it can commence its transfer to Venus.

By comparing the bottom-up masses found in this report to the fractions from [65], the data in Table 13.1 is found. It can be seen that especially propulsion and propellant are significantly higher than the reference fractions. This is caused by EPOSS going into orbit with Enceladus, thus requiring more propellant, and increasing the tank and propulsion system size. Furthermore, both thermal and TT&C fractions are more than 50% larger, caused by the extreme conditions of the Saturnian system and large distance from Earth.

13.4. Sensitivity Analysis

The sensitivity analysis shows the flexibility of the design, and how the design would change when a parameter changes. Specific analyses for subsystems have already been done in chapters 4, 5, 6, 7, 8, 9, 10, 11, and 12. Hence, this section shall only consider changes to

the overall design, and how this would affect the mission design. Changes that may affect the launcher (see subsection 13.4.1) will be considered, and how changes to subsystems affect other subsystems (see subsection 13.4.2). The effects of changes on subsystems can also be found in Figure 13.1.

13.4.1. Effects on Launcher Selection

Things that affect launcher selection are the mass, volume, and budget. Currently, the reusable Falcon Heavy is the launcher of choice, as presented in subsection 15.1.2. The maximum mass it can launch while still providing the correct hyperbolic excess velocity is 4840 kg.[1] With the current spacecraft wet mass of about 4300 kg, an increase of 540 kg is needed to require a different launcher. When this mass is exceeded the fully expendable Falcon Heavy is the next option, with a payload capability of 11840 kg.[1] This would also increase the cost, from 80M € to 133M €. In the budget, presented in chapter 14, an increase in 70M € is still within the budget. Hence, it is possible to upgrade the launch mass. However, an increase in mass also increases the overall cost for the spacecraft. A 40% contingency is present in the cost estimation, hence this increase in cost can be supported. A downside of using the fully expendable launcher is that it is not as sustainable, as described in section 16.4.
Diameter changes are mainly related to the fuel tank size, and is discussed in section 7.5.

13.4.2. Subsystem Changes

Furthermore, overall increases in mass, power, and volume generally result in a snowball effect. For example, an increase in power requires more RTGs, which results in a higher cost and mass, which results in more fuel, which results in more cost and mass, etc. Safety margins have been included to ensure that an increase in either of those values does not automatically result in a complete redesign of the system.

13.5. Risk and Reliability

This section presents the risk and reliability of the system. First, the risks are shown and mitigated in subsection 13.5.1. Then, the reliability of the subsystems and the system as a whole can be found in subsection 13.5.2.

13.5.1. Risk

In chapters 5, 4, 6, 7, 8, 9, 10, 11, and 12, the risks pertinent to the respective subsystems are presented and discussed. In this section, the technical risk register is presented in Table 13.3 and the probability and severity of these risks is assessed according to the convention presented in Table 13.2, note that these risks do not include mitigation. This analysis outputs two main risk management tools: the technical risk map (Figure 13.7) and the mission's fault tree diagram showing how subsystem failures influence each other (Figure 13.6). In Figure 13.7, the unmitigated risks are presented. As it can be observed, most risks occupy the orange area of the map, meaning that even without mitigation they are not catastrophic, but still dangerous, for the mission. Furthermore, mitigation will decrease them towards the green area of the map. Similarly, for the red risk factors, they will decrease towards the yellow/green area. The mitigation of the subsystem risk is discussed in the previously mentioned chapters, the mitigation of the launcher and integration risks is hereby mentioned:

1. **LAR-0.1 Deployment mechanism failure**: Mechanical or electrical failure of the deployment mechanism. This can be avoided by testing the mechanism until enough confidence is reached.

[1] Retrieved from `https://elvperf.ksc.nasa.gov/Pages/Query.aspx` last opened on June 19, 2019

2. **LAR-0.2 Booster failure**: Failure of the booster of the launcher. Responsibility of the launcher provider.
3. **LAR-0.3 Fairing failure**: Failure of the fairing. The mitigation is done in collaboration with the launcher provider.
4. **INR-0.1 Launcher adaptor failure**: Mechanical Failure of the interface between the spacecraft and the launcher. This event would cause irreversible damage to primary and secondary spacecraft's components. Mitigation consists in testing the adaptor prior to launch until enough confidence is gained on its performance.
5. **INR-0.2 Power regulator failure**: Failure of power regulator, this would cause the incorrect operation or electrical failure of most spacecraft components. This can be mitigated by including a back-up regulator and by increasing the the operational voltage range of the instruments.
6. **INR-0.3 Impact of bodies with any of the subsystems parts**: Impact of asteroids on the journey to the Saturnian system or at the system itself. This risk is mitigated by the inclusion of a hazard-avoidance cameras in the navigation system.
7. **INR-0.4 Short circuit of electrical interface**: Overflow of a current in a circuit. It is prevented by the installation of fuses which stop the current when it reaches a threshold value.

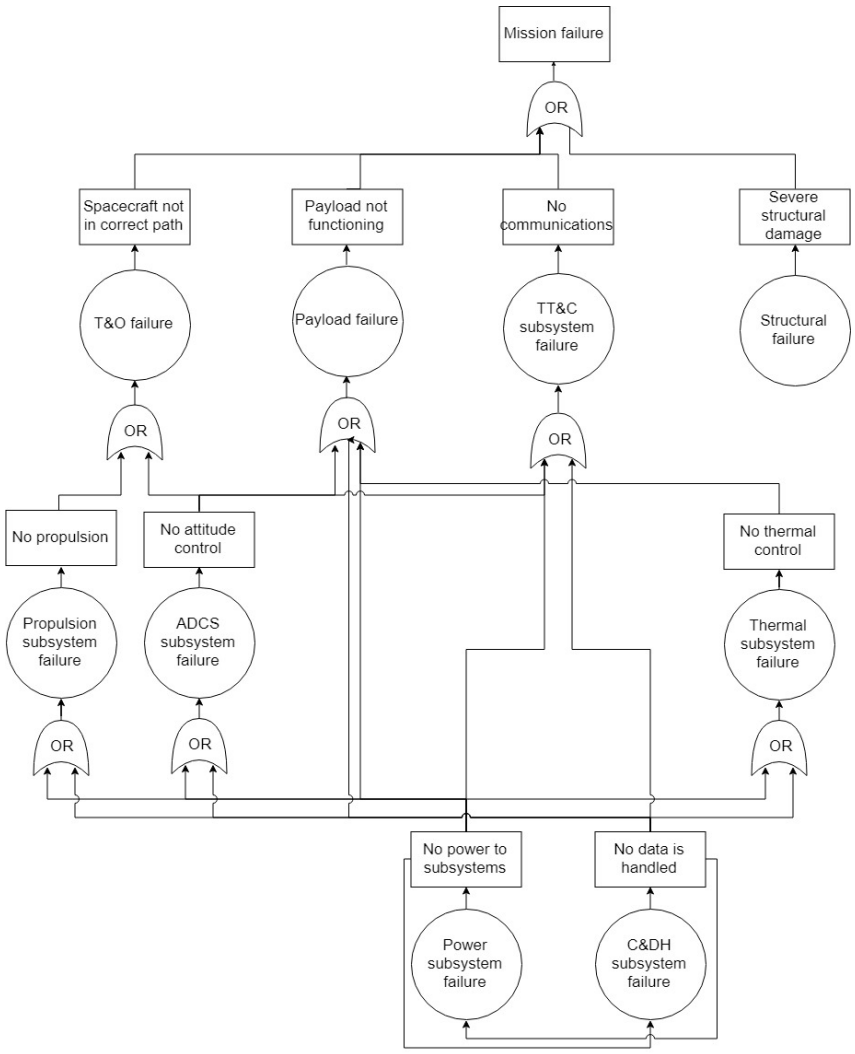

Figure 13.6: Fault tree of the mission.

Table 13.2: Score descriptions and risk classification system.

	Probability (P)	ID	Classification
1	Rare - Possible but minimal chance of occurring	PLR	Payload Risk
2	Unlikely - Marginal chance of occurring	TRR	Trajectory Risk
3	Possible - Average likelihood of occurring	ADR	Attitude Determination and Control System Risk
4	Likely - Expected to occur during the nominal life-time at least once	PRR	Propulsion Risk
5	Certain - Frequent or continuous exposure to the risk	TTR	Telemetry and Telecommunication Risk
	Severity (S)	CDR	Command and Data Handling Risk
1	Negligible - Minimal impact	PWR	Power Risk
2	Marginal - Short term or temporal impact	THR	Thermal Risk
3	Significant - Reversible impact	STR	Structures Risk
4	Critical - Leads to mission failure or violation of laws	LAR	Launcher Risk
5	Catastrophic - Leads to irreversible and permanent damage	INR	Integration

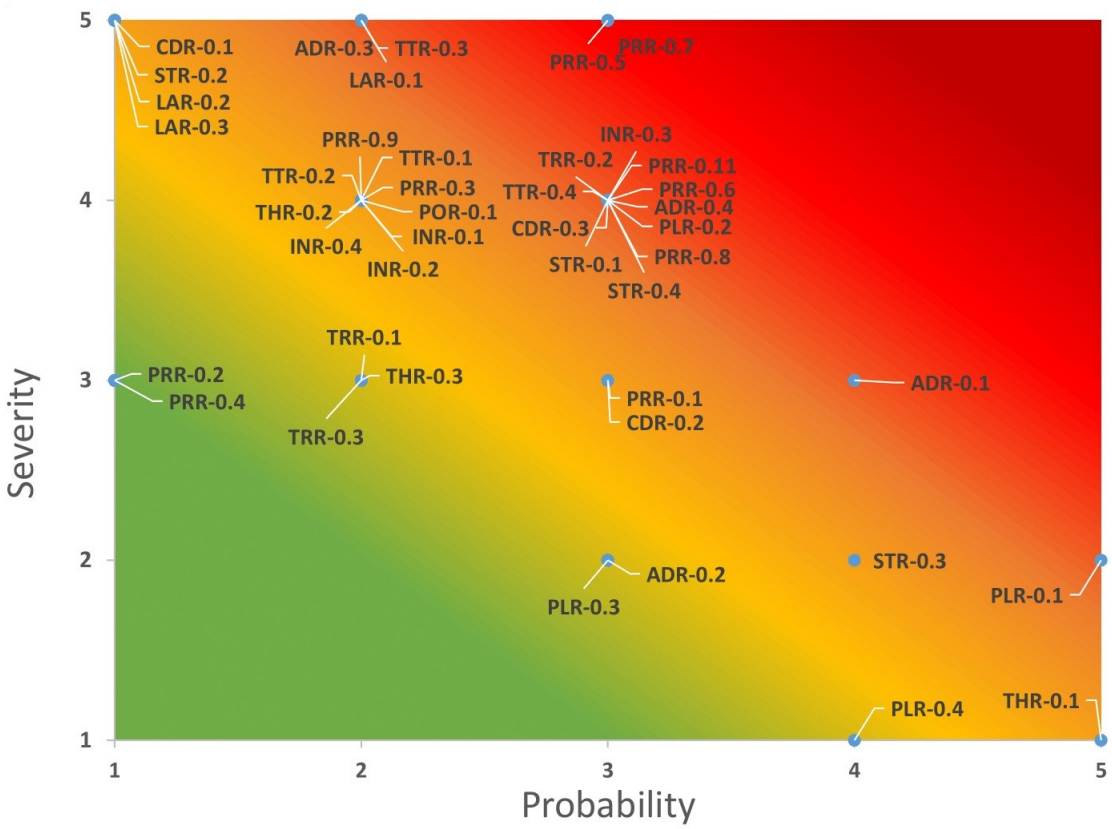

Figure 13.7: Technical risk map.

13.5.2. Reliability

The overall reliability requirement (MIS-10, see section 2.4) dictates that the reliability of the system shall be greater than 90%. The subsystem reliabilities can be found in Table 13.4. The reliabilities are calculated using relationships from [124], which are based on statistics

Table 13.3: EPOSS risk register.

ID	Risk Description	S	P	Risk
PLR-0.1	Physical obstruction of the instrument	2	5	10
PLR-0.2	Impact of bodies on instruments	4	3	12
PLR-0.3	Malfunction of instrument software	2	3	6
PLR-0.4	Wrong Calibration	1	4	4
TRR-0.1	Polar orbit transition & maintenance failure	3	2	6
TRR-0.2	Impact with body	4	3	12
TRR-0.3	Unexpected necessary manoeuvres	3	2	6
ADR-0.1	Momentum wheel failure	3	4	12
ADR-0.2	Misalignment of wheel's rotational axis	2	3	6
ADR-0.3	Star tracker failure	5	2	10
ADR-0.4	Unexpected disturbances and/or collisions during mission	4	3	12
PRR-0.1	Propellant tank leakage	3	3	9
PRR-0.2	Pressurant tank leakage	3	1	3
PRR-0.3	Catalyst bed heater failure	4	2	8
PRR-0.4	Catalyst contamination	3	1	3
PRR-0.5	Valve failure	5	3	15
PRR-0.6	Thruster failure	4	3	12
PRR-0.7	Engine failure	5	3	15
PRR-0.8	Impact with body	4	3	12
PRR-0.9	Pressure regulator failure	4	2	8
PRR-0.11	Feed line leakage	4	3	12
TTR-0.1	No signal is received at C&DH	4	2	8
TTR-0.2	Signals cannot be deciphered	4	2	8
TTR-0.3	No signal is sent	5	2	10
TTR-0.4	Eb/No decreases to an unacceptable level	4	3	12
CDR-0.1	Code cleared	5	1	5
CDR-0.2	Error in software program	3	3	9
CDR-0.3	Degradation due to radiation	4	3	12
POR-0.2	RTG Failure	4	1	4
POR-0.3	Battery Failure	4	3	12
POR-0.4	Power Control Failure	4	3	12
THR-0.1	MLI, rupture and small particle impact	1	5	5
THR-0.2	Louvre failure	4	2	8
THR-0.3	Heat pipe failure	3	2	6
STR-0.1	Mechanism failure	4	3	12
STR-0.2	Load case failure	5	1	5
STR-0.3	Degradation failure	2	4	8
STR-0.4	Impact with body	4	3	12
LAR-0.1	Deployment mechanism failure	5	2	10
LAR-0.2	Booster Failure	5	1	5
LAR-0.3	Fairing Failure	5	1	5
INR-0.1	Launcher adaptor failure	4	2	8
INR-0.2	Power regulator failure	4	2	8
INR-0.3	Impact of bodies with any of the subsystems parts	4	3	12
INR-0.4	Short circuit of electrical interface	4	2	8

Table 13.4: Reliability of subsystems.

Subsystem	**Reliability**
ADCS	90.1%
Propulsion	96.3%
Power	92.0%
C&DH	91.1%
TT&C	92.7%
T&O	96.3%
Thermal	97.5%
Structures	97.5%

from other spacecraft failure causes. Two exceptions are the ADCS and power subsystems. Power resulted in a lower reliability than the one shown in Table 13.4, however, these are based on spacecraft with solar panels. RTGs have a very high (near 100%) reliability, as mentioned in section 10.6, where the main reliability is related to the batteries. Finally, the ADCS subsystem contains many redundancies, increasing its reliability to over 90%, instead of the 85.7% which resulted from the statistical relations.
By multiplying the reliabilities of all subsystems, a final reliability of 61.7% can be found. However, this is based on the industry itself. Overall, according to [124], the industry has been 61.7% reliable when extrapolating this to a mission duration of 16 years. As such, it does not directly reflect the reliability of EPOSS. According to [124], with sufficient investment in testing, the reliability can be significantly increased. Furthermore, the success of a significant number of other space missions to the outer solar system with similar or longer mission durations such as Cassini-Huygens,[1] Ulysses,[2] Pioneer 10 & 11,[3] and Voyager 1 & 2,[4] further reinforces the increase in reliability. Requirement MIS-10 (see section 2.4) states that the mission's reliability, aside from launch failure, shall exceed 90%. Due to the reasons stated above, this requirement is checked with reservation.

[1]Retrieved from `https://solarsystem.nasa.gov/missions/cassini/overview/` last opened on June 24, 2019
[2]Retrieved from `https://www.esa.int/Our_Activities/Space_Science/Ulysses_overview` last opened on June 24, 2019
[3]Retrieved from `https://www.nasa.gov/centers/ames/missions/archive/pioneer.html` last opened on June 24, 2019
[4]Retrieved from `https://voyager.jpl.nasa.gov/` last opened on June 24, 2019

14 Spacecraft Budgets

This chapter explains why each budget is needed and how they originated. Three budgets are elaborated on in the following sections. In section 14.1 the mass budget is explained. The power budget is explained in section 14.2, followed by the cost budget in section 14.3.

14.1. Mass Budget

The mass of the EPOSS satellite with contingencies of each subsystem is given in Table 14.1. To comply with the requirements every subsystem has used a 5% contingency if they used off-the-shelf components, to 20% when the components are still to be developed. Only the structure has used a different contingency of 25% based on [65, p.439] which is explained in section 12.4. The total dry mass is 1229.9 kg and total launch mass is 4288.2 kg. The total launch mass includes the contingencies and so it can be assumed that if all uncertainties add up during the design process, the mass will still be within the limit of 4840 kg. A contingency value of 10% has been applied to the total (original) mass, in compliance with SRR-00.11 in Table 2.3.

Table 14.1: Mass budget.

Subsystem	**Mass [kg]**	**Contingency [%]**	**Mass w. Contingency [kg]**
Payload	124.7	10	137.2
Propulsion	329.4	5	345.8
Power	263.3	10	289.6
ADCS	45.4	15	52.2
C&DH	32.8	10	36.1
Thermal	32.3	15	37.1
TT&C	120.3	20	144.3
Structures	150.1	25	187.6
Propellant	2780.2	10	3058.3
Total dry mass w. contingency	1229.9		
Total mass	4288.2		

14.2. Power Budget

The power is important for sizing the batteries and RTGs used in the satellite. In Table 14.2 all subsystems are given with their respective nominal and peak powers. The power budget is determined from all the different subsystems and operating times of the instruments explained in section 5.4. The power subsystem is designed following from the worst case scenario when the satellite has the highest power consumption, this is during the orbiting phase around Enceladus when most measurements will be performed. The difference between power nominal and peak power is due to the batteries charging during the nominal stage and discharging during peak.

14.3. Cost Budget

The cost of the EPOSS mission is has to comply with requirement MIS-14: The full mission cost without payload cost shall be less than 1.5 B € in FY2019. The budget includes all the costs presented in Table 14.3 except for the payload cost 270 M €, which is based on the payload

cost of the JUICE mission and will be paid for by the stakeholders.[1] The launch vehicle cost is mentioned in subsection 15.1.2, being 79.9 M €, since the falcon heavy from SpaceX will be used.
The cost of the power subsystem is 573.5 M € and is quite high compared to previous space mission. Americium-241 is used instead of Plutonium because the latter is no longer available, but four times as much is needed compared to Plutonium to produce the same amount of power. The cost estimate is based on a cost analysis for the Cassini Plutonium-238 RTGs for which the cost of Plutonium is replaced by the cost of the Americium. [120] Each of Cassini's 300 W RTGs costed about 113.5 M €. For the other elements of the EPOSS mission a cost estimation tool made by B. Zandbergen[2] based on [65] is used and all outcomes of the cost estimations can be found in Table 14.3. The method used in the estimation tool is based on the cost of earlier produced spacecraft for each of their subsystems and the related mass. This results in the cost of the spacecraft bus, program level, and production, which are based on the mass of the subsystems. The total dry mass cost only includes the spacecraft bus cost, whereas the total cost includes the operations and spacecraft bus costs. The cost estimation for the ground segment and the software cost are based on the number of lines of code and the data needed to run the program as explained in subsection 9.3.1. In Table 14.3 it can be seen that propulsion will only cost 1.7 M € according to the estimation tool which is to low for a mission going to Saturn. Therefore A 40% margin is added to the total cost because of this low propulsion cost and that this is only a preliminary cost estimation, and it should be taken into account that the cost will likely increase [124]. With this margin a total cost of 1.431 B € is estimated and requirement MIS-14 is met found in Table 2.2.

Table 14.2: Power budget.

Subsystem	Nominal power [W]	Peak power [W]
CD&H	32.3	32.3
TT&C	73.3	73.3
Payload	105.3	134.5
Thermal	4.2	4.2
Structures	13.0	18.0
Propulsion	0.0	41.2
ADCS	77.0	151.2
Power	46.6	13.0
Total	**351.7**	**467.7**

Table 14.3: Cost budget

Element	Cost [M € in FY2019]
Payload	270
Operations	
flight software	13.3
Ground software	6.6
Ground system	60.1
Launch vehicle	79.9
Production	160.9
Program level	54.9
Spacecraft bus	
Power	573.5
Thermal	4.8
ADCS	17.5
TT&C	29.2
C&DH	5.4
Propulsion	1.7
Structures	14.8
Total dry mass cost	**646.9**
Total cost	**1022.6**
Total cost with 40% margin	**1431.6**

[1] Retrieved from https://www.bbc.com/news/science-environment-17917102 last opened on June 18, 2019

[2] Retrieved from https://webcache.googleusercontent.com/search?q=cache:OBv7oyd7yE4J:lr.home.tudelft.nl/fileadmin/Faculteit/LR/Organisatie/Afdelingen_en_Leerstoelen/Afdeling_SpE/Space_Systems_Eng./Space_Links/doc/Space_mission_cost_v1.02.xls+&cd=1&hl=nl&ct=clnk&gl=nl last opened on June 15, 2019

15 Operations and Logistics

This chapter outlines the operational timeline and logistical planning of the EPOSS mission. Spanning over four general phases, the operational timeline in section 15.1 covers the mission from design of the spacecraft to end-of-life activities. Following this, section 15.2 elaborates on the detailed design and development phases to be conducted after the DSE period. Manufacturing, integration, and assembly of the spacecraft is covered in subsection 15.2.2

15.1. Mission Operations

subsection 15.1.1 discusses pre-launch activities leading to subsection 15.1.2 which details launcher selection. subsection 15.1.3 describes operational activities during the actual mission followed by subsection 15.1.4 which explains end-of-life options.

15.1.1. Pre-launch

Sufficient planning in the early phases of the mission is crucial for mission success. This planning includes design of the spacecraft, mission phases, along with acquisition of personnel and required facilities for subsequent mission phases. Initially, a baseline is defined which determined the requirements governing the design of the spacecraft. This started off with a general set of requirements pertaining to required science measurements which then flowed down to subsystem specific requirements. For example, strict pointing accuracy requirement for the altimeter BELA required ADCS actuator design to be able to facilitate this accuracy. Following this, various concepts that can carry out the mission is developed, which in case of EPOSS included a single spacecraft, double spacecraft and swarm spacecraft concepts. The concepts varied in the way each of them carry out the science objectives. A design trade-off ensued, leading to the selection of the final concept that would enter the detailed design phase. The production phase is planned to begin well before the detailed design phase ends as engineering and qualification models can be begun to be built. Once the detailed design is finished to a sufficient degree, the development phase results in the building of test models to verify the model against various mission environments and loads the spacecraft is expected to encounter. These tests pertaining to this spacecraft are explained further in chapter 16. Once the test models and ultimately the design are verified and passes the critical design review, manufacturing of the flight model of the spacecraft may begin. This is the version that will be launched and will be tested further for electric, software, and navigation functioning for full integration before being transported to the launch site.[1] [10]

15.1.2. Launch

The design of a launcher is out of scope for this mission and instead will rely on selection of launchers available during the required launch period. A launcher capable of injecting the spacecraft into the interplanetary orbit with a V_∞=3.49 km/s is required. With a wet mass of 4288.2 kg, the partially reusable Falcon Heavy from SpaceX is selected since it has a payload capacity of 4840 kg while still providing the correct hyperbolic excess velocity, which still allows the launcher to be reusable.[2] The spacecraft will be launched within a launch window of 140 minutes starting at 08:50 am on 19th of April, 2028 [84, table 7.2][75]. The initial

[1] Retrieved from https://www.esa.int/Our_Activities/Space_Science/Building_and_testing_spacecraft last opened on June 19, 2019

[2] Retrieved from https://elvperf.ksc.nasa.gov/Pages/Query.aspx last opened on June 19, 2019

decison was the Vulcan launcher,[3] however this option is discarded due to the risks associated with its TRL and since it might not be available by 2028. The reusability of the launcher is particularly attractive from a mission sustainability point of view, and will be discussed further in section 16.4. A back-up launch option is identified to be the fully expendable Falcon Heavy launcher which has a payload capacity of 11840 kg,[2] in case a larger safety margin for allowable payload mass becomes necessary for the launcher. The spacecraft will be launched from the Vandenberg Air Force Base launch complex on 19-04-2028 and with a transfer time of 9.8 years, will reach the Saturnian system on 13-02-2038, requirements relating to the launch segment are given in Table 15.1 which also specifies verification methods for each requirement.

Table 15.1: Compliance matrix for the launcher requirements.

Code	Requirement	Verification Method	Com-pliance	Section
LSR-15	The spacecraft shall be available for launch by 2030.	Analysis	✓	subsection 15.1.2
LSR-13	The mission shall use existing ground segment infrastructure.	Inspection	✓	subsection 15.1.2
LSR-13.01	The launch shall not compromise the future use of launch site.	Analysis	✓	subsection 15.1.2
LSR-13.02	The system shall fit in the payload of the launch vehicle with a max volume of 160 m^3.	Demonstration	✓	subsection 15.1.2
LSR-13.03	All system connections to the launcher shall be separable.	Test	✓	subsection 15.1.2
LSR-13.04	The system shall be transported to selected ground segment infrastructure without damage.	Analysis	✓	subsection 15.1.2
LSR-00.03	The launch system shall have a cost of maximum 90 M €.	Inspection	✓	subsection 15.1.2
LSR-00.04	The launch system shall comply with all political constraints.	Inspection	✓	subsection 15.1.2
LSR-00.04.01	The launch system shall not obstruct any political relationships within the country of launch.	Inspection	✓	subsection 15.1.2
LSR-00.04.02	The launch system shall adhere to all (inter)national laws concerning launch.	Inspection	✓	subsection 15.1.2
LSR-00.04.03	The launcher shall have a reliability of minimum 95%.	Analysis	✓	subsection 15.1.2

15.1.3. Operations

The operations phase covers everything from injection into the interplanetary transfer object to end of mission once science objectives have been met. Initially, an orbit checkout will be done in which all subsystems, payload, and interfaces will perform in-system validation. Any anomalies detected during this time will be transmitted via the LGAs, and updates to fix these anomalies can be received in the same manner.

Interplanetary Transfer

Transmission and reception of data, such as that for housekeeping, during the early transfer phase from Earth to Venus is performed by the LGA due to the use of the HGA as a heat shield during this time (see section 11.1). An analysis of secondary requirements has resulted in the identification of science observations that can be made at Venus during the gravity assist (see subsection 5.4.3). This includes the usage of MERMAG and VIMS payload for solar wind and flux rope characterisation and for the examination of cloud processes and composition distribution of Venus. Once the spacecraft has passed Earth after the second Earth gravity assist, the HGA can be used for communications. Data recorded during the Venus flyby that was not transmitted by the LGA can then be done by the HGA. The NASA Deep Space Network (DSN) will serve as the ground station for all communications throughout the mission since this is the only ground station capable of receiving signals from such a distance, and Estrack

[3]Retrieved from `https://www.ulalaunch.com/rockets/vulcan-centaur` last opened on June 24, 2019

does not support Ka-band transmission.[4,5] The DSN will provide global coverage however time slots will have to be decided on so as not to interfere with other missions using the ground station.
The use of gravity assists during the interplanetary transfer greatly reduces the required ΔV on the spacecraft, however a large deep space manoeuvre of 541.23 m/s is required to set the spacecraft on route from Earth to Saturn (see Table 4.1). Furthermore, the Saturn orbit insertion is also imposing on the propulsion system as it requires a ΔV=560.97 m/s followed by a periapse raising manoeuvre requiring a Δv=335 m/s (see Table 4.2). These manoeuvres will be done by the main engines, however ensuring spacecraft stability will be provided by the throttle-able main engines with supplementary assistant from the RCS if needed.

In-system

As detailed in chapter 4, the in-mission trajectory sees the EPOSS spacecraft perform Titan flybys following the Saturn orbit insertion, leading to Enceladus flybys in order to meet science requirements pertaining to global imaging and subsurface characterisation of Enceladus with JANUS, VIMS, REASON, and BELA payloads active. The trajectory then leads to four Daphnis flybys in order to perform science measurements involving imaging of leading and trailing edges, surface and bulk composition and morphology as well as to characterise the interaction of particles between Saturn's rings and Daphnis. Active payloads are JANUS, VIMS, REASON, BELA, and ENIJA. A moon tour of Rhea, Dione, and Tethys is performed before the final leg of the science mission which involves the orbiting of Enceladus. Once the spacecraft has entered into orbit around Enceladus, eight phases during which specific measurements are taken are identified. This involves changing orbital inclination from 45 deg to 60 deg followed by 90 deg where plume particle characterisation is done primarily during the 90 deg polar phase whereas 60 deg inclination orbit only allow for measurement of 15% of the plumes. The specific payload usage periods can be seen in chapter 5. All science data will be transmitted by the HGA, however tracking and receiving of commands during measurement phase can be done via the LGA due to its positioning on the same side as the payload. Power saving mode is also possible by using the LGAs to transmit any non-scientific data.

15.1.4. End-of-life

In order to meet requirements MIS-11, MIS-12, and MIS-00.01 a clear end-of-life strategy that complies with COSPAR's Planetary Protection Policy and then EPOSS Sustainability Policy so as to minimise debris and contamination was developed. As of now, the best end-of-life strategy requiring a ΔV=231 m/s involves ejection out of Enceladus orbit followed by a Tethys impact. However, if there is sufficient propellant, corresponding to a ΔV=384 m/s, available after the main mission has reached completion, an extension of the end-of-life strategy to include a back track of the moon tour to perform secondary science measurements before an eventual Tethys impact can be performed. A detailed analysis of all end-of-life possibilities that did and did not make the cut can be seen in subsection 4.1.2.

15.2. Logistics

The logistics of carrying out the EPOSS mission is detailed in this section.

[4]Retrieved from https://www.esa.int/Our_Activities/Operations/ESA_and_DLR_in_joint_study_to_support_deep_space_missions last opened on June 19, 2019
[5]Retrieved from https://www.esa.int/Our_Activities/Operations/Estrack/Cebreros_-_DSA_2/(print) last opened on July 1, 2019

15.2.1. Post DSE Planning

Between the end of the DSE period and the launch of EPOSS, there are 106 months available for development, testing and production. This time is spread amongst the different phases according to how much time is needed for each process. The different phases of the post-DSE program are discussed below.

The detailed design phase follows from the current level of design described in this report. During this phase, the subsystems are sized in more detail which includes sizing of specific components and assemblies. Computer Aided Design (CAD) models and technical drawings result as output of this phase. Furthermore, procedures for implementation, integration, verification and validation, and operations and coding of software are also done [80]. This phase is scheduled for 21 months.

The technical details from the detailed phase lead to the production of prototypes of the components of subsystems which are subjected to specific testing. Off-the-shelf components would need to be verified for appliance to requirements apart from the testing performed by the manufacturer. Components built in-house would need to go through tests specific to each subsystem. The phase is allocated 23 months for completion. A further look on the tests performed can be found in subsection 15.2.2.

Once all components are tested and passes their qualifications, the assembly prototype can be made which also undergoes rigour testing and if necessary, further iterations. This phase is scheduled for 38 months.

Once all components, assemblies, and integrated system passes all tests and checks, the flight model, which is the version that will be launched, can be produced. This final product also has to pass quality and compliance checks before being certified as ready for launch. This phase is allocated a time of 36 months for activities such as acquisition of materials and tools, production, and testing. This long period is necessary in particular for the power subsystem as RTGs require around three years for qualification.

The final phase in the development of EPOSS is the launch preparation. This phase includes preparation of launch, operations, and ground system infrastructure and personnel and finally transport to launch site and integration with launch vehicle. From [80], training for initial system operators and maintainers and on contingency planning is carried out in this phase. Apart from this, validation of telemetry and ground data processing, and flight readiness checks on system and support elements are also performed. 17 months are designated for this phase. Ultimately, the mission is set to launch by April 2028. A visual representation of this planning is seen in Figure 15.2, which shows the post DSE project Gantt chart.

15.2.2. Development, Manufacturing, and Testing

This section details the development, manufacturing, and testing required to produce a launch worthy spacecraft. The design and development logic is conceptualised in Figure 15.1.

Development

A number of components are purchased off the shelf. These require rigorous testing but no development and manufacturing by the EPOSS team. Any mission specific components are manufactured by first producing prototypes, subjecting these to component specific testing, and subsequently iterating the design where necessary as part of the development process. Hereafter, the components will be assembled in an EPOSS prototype, subsequently subjected to further testing including vibration, acoustic, shock, and thermal vacuum tests. The integrated prototype's components are iterated when the assembled prototype does not meet the integration tests, as a means of further development and increasing reliability. Components meeting the requirements are manufactured for further assembly. The major models built for

testing include, the Structural and Thermal Model (STM), Engineering Model (EM), and Qualification Model (QM).[1] Assembly and testing of these models takes 38 months and is described in subsection 15.2.1 and included in the post DSE Gantt chart (see Figure 15.2). Special care should be taken as each of these models include RTGs in their design, the process of handling these RTGs is described hereafter. The major tests to which individual components and later, the models will be subject to include the following:

- **Vibration** These tests are intended to replicate the loads incurred on the spacecraft during launch. Vibration tests involve 'shaking' the satellite to different levels up to conditions 25% more intense than at actual lift-off.[4] This may be a destructive test when unsuccessful, and is undergone by the STM.
- **Acoustic** Acoustic tests comprise the spacecraft being placed in a reverberant chamber and subjected to noise levels similar to those experienced during launch. Again, the STM undergoes this testing.[4]
- **Shock** This test involves initiating the devices that cause shock during flight, preferably in sequence in the appropriate environment condition. The system that separates the spacecraft from the launch vehicle is one example. This test is also undergone by the STM. [60]
- **Thermal Vacuum** This testing involves placing the models in a vacuum chamber with a sun simulator in order to reproduce the space environment the spacecraft will have to endure. The qualification and engineering models are subject to these tests. The QM is intended for verification of the system to a good margin while the EM is intended to demonstrate the systems capacity to cope with launch loads, that subsystems work well together and to confirm the spacecraft is compatible with ground systems.[4]

Assembly

Post development and manufacturing, the components are assembled into sub-assemblies. These sub-assemblies should be assembled concurrently to save time and cost for this phase of the project as a means to comply with lean manufacturing. Special care should be taken when assembling the radioisotope thermal generators as they pose a significant health hazard to people working with these RTGs. Furthermore, similar constraints exist for working with the selected propellants mentioned in section 16.3. As a result this process should be continuously monitored and systems mitigating the risks imposed by working with such materials should be available. When assembling the various structural elements special care has to be taken to avoid any defects in the components or assembly of said components which may lead to critical failure. Additionally, payload should be handled with care in compliance with their functional requirements, see Table 5.4-5.6.

Final Testing

Finally, all sub-assemblies are joined together into the flight model. This flight model will then be subject to the non-destructive tests mentioned previously. Following this round of testing, the flight model will be subject to qualification and acceptance checks which includes electric system checks, telemetry validation, ground system data checks, software validation, and navigation and pointing checks. In the event that the checks are satisfied and the integrated system successfully meets all requirements the launch operations are initiated, including transport to launch site and integration of EPOSS with the launcher prior to launch of EPOSS.[4]

[1]Retrieved from `https://www.esa.int/Our_Activities/Space_Science/Building_and_testing_spacecraft`last opened June 19, 2019

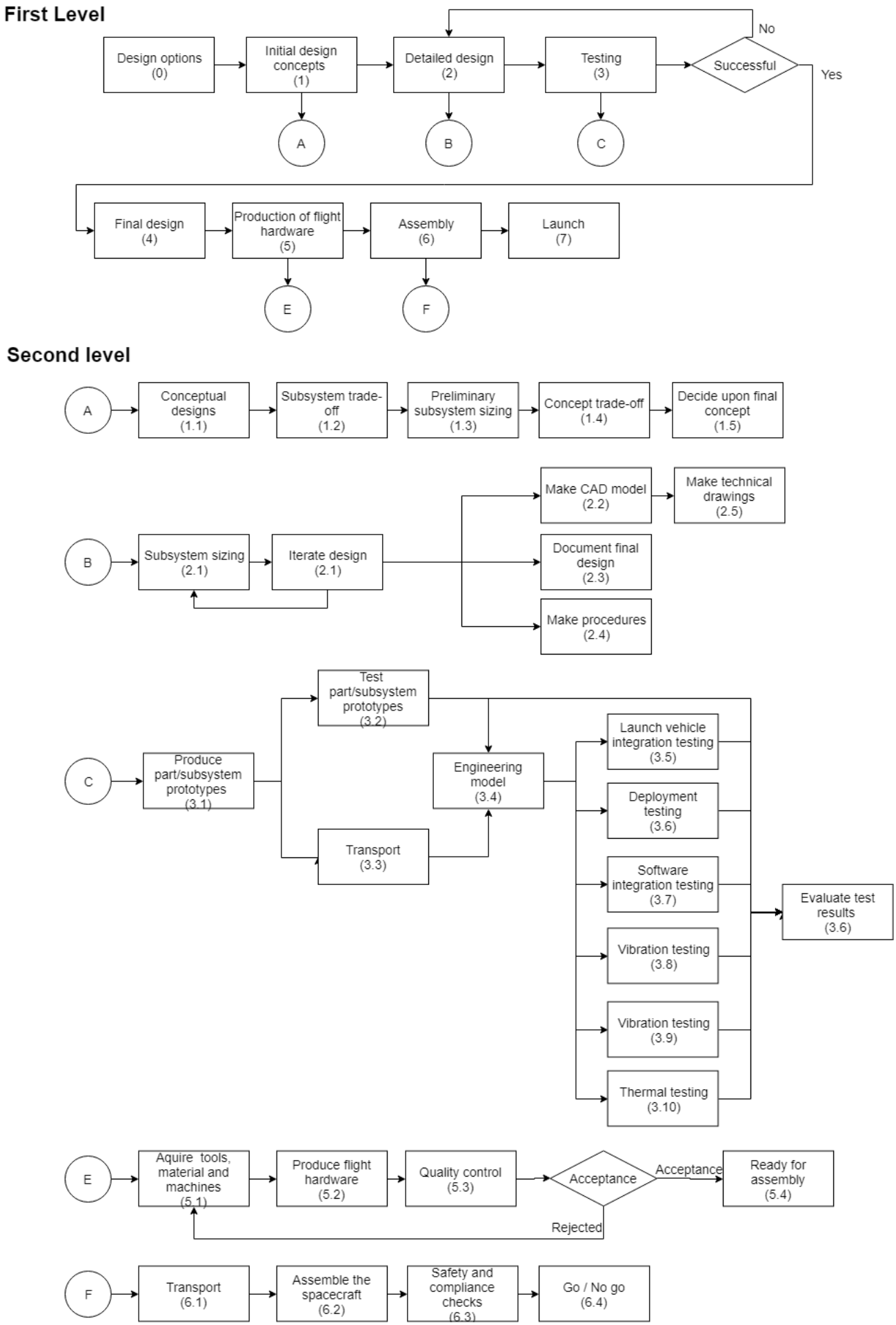

Figure 15.1: Design and Development logic for EPOSS.

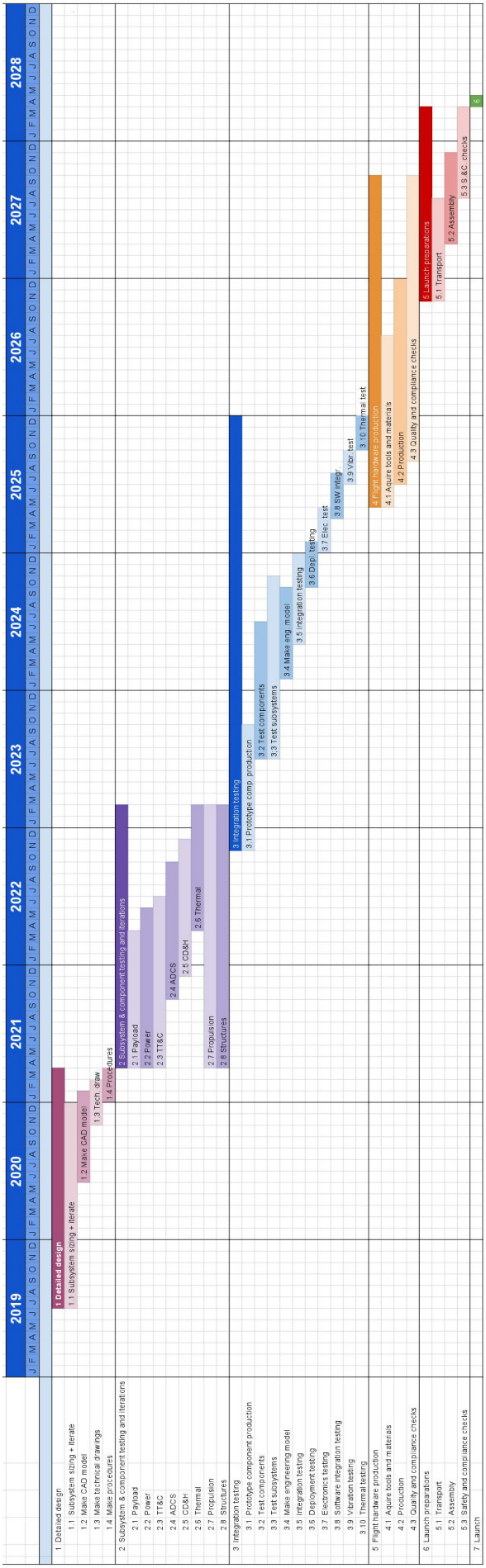

Figure 15.2: Post DSE Gantt Chart.

16 Mission Considerations

This chapter provides a clear insight about the availability, maintainability, and safety of the mission in section 16.1, section 16.2 and section 16.3 respectively. Lastly, the sustainability will be elaborated upon in section 16.4.

16.1. Availability

The availability of the mission is a combination of two aspects: will the spacecraft be available before the launch date with all the required resources, and will it be able to perform all measurements and send them back to Earth to meet the requirements.
In subsection 15.2.2 it is proven that the full design, manufacturing process, and testing will be done before the launch date in 2038. The main resources that are needed before launch are the launcher, the transport, the RTGs, and testing and assembly facilities. The availability of the launcher and RTGs are mentioned in subsection 15.1.2 and 10.3.1 respectively. The satellites subsystems will be assembled and tested by ESA's facilities and transport will be provided to transport the sub-assemblies to the launch site in the United States.
The availability to perform the measurements is inter-related with the reliability of the mission's lifetime. It is shown in subsection 13.5.2 that the satellite will still be working after 16 years with a reliability of 90%. This means that the satellite can perform the measurements with the same reliability and will succeed to obtain all data needed. Lastly, subsection 8.3.1 discusses the time needed to send all the gathered data to Earth in the mission's lifetime. And it is shown that it can all be sent back with the same reliability as previously mentioned.

16.2. Maintainability

The EPOSS satellite cannot be physically maintained because it is operating in the Saturnian system. Even in this case there are still parts of the mission that can be maintained, namely:

- Ground Station: The ground station can be maintained during the EPOSS mission. There are several aspects that can be maintained or updated if needed. One important one is the communication performance, this needs updates throughout the mission to keep the same uplink data rate if the performance of the satellite drops due to degradation. Others besides this one, that may be updated, are the algorithms and the antenna's pointing accuracy.[1]
- Onboard software: The satellite contains a software to operate everything on board. This software might need updates to enhance capability and to work around failures of hardware. The best way to perform such an update is as follows: after extensive testing on the ground either a patch or a completely new copy of the software is uploaded to the spacecraft. The upload is carefully verified. Then the patch is applied or the vehicle reboots to the new software. There is always a safeguard in place, where for example the previous software is kept on board, which is automatically rebooted in case of a fatal software error in the new patch or copy of the software.[2]

[1] Retrieved from https://spacenews.com/op-ed-the-future-of-space-ground-solutions/ last opened on June 20, 2019
[2] Retrieved from https://space.stackexchange.com/questions/24359/are-software-updates-to-satellites-or-in-general-space-craft-commonplace-during Last opened on June 20, 2019

The satellite's onboard software also includes a safe mode, which is an operating mode to maintain the satellite's safety and keep it functional. This mode is entered automatically when the software detects malfunctions in one of the subsystems. These malfunctions include operating conditions which have a sudden drastic change or a lack of received commands which come from hardware failures or mis-programming the satellite. Hence, the software might need an update. The satellite can enter safe mode at all time except during the polar orbits and while passing through the rings of Saturn, since there is a high chance of crashing.[3]

16.3. Safety

The safety of the mission includes two aspects. The safety of the people during manufacturing, testing, and integration; as well as keeping the instruments and the spacecraft safe during operations. In the following sections: section 4.6, 5.7, 6.6, 7.6, 8.6, 9.6, 10.6, 11.6, 12.6. The main risks and the corresponding mitigations can be found for every subsystem throughout the report.

According to NASA measures have to be taken to avoid critical risks that could occur related to the workforce. Measures that can be applied to provide a safe work space are: investigating and examining the workplace for potential dangers and hazards, researching and developing techniques to anticipate and control potentially dangerous situations, and training and educating the workforce about job-related risks. Besides these measures a medical clinic is provided 24/7 to assure a top level of health of the workforce.[4]

Two examples of safety hazards during the EPOSS mission are concerning the propellant and the power. Hydrazine is used as propellant and its risk during assembly should be taken into account. To avoid the workforce being exposed to the hydrazine, protective clothing is provided and the air is ventilated to keep the amount of hydrazine in the air under the acceptable level. [104]

The power subsystem makes use of americium-241 RTGs and also measures need to be taken to avoid accidents. The workforce working within the vicinity of the fuelled RTGs must wear appropriate personal protective equipment to reduce the direct exposure to the alpha radiation. Limiting the exposure time of personnel will reduce the radiation doses as well. The RTGs are provided with attachment points for remote handling to reduce the exposed time of personnel. All the mitigations mentioned above and throughout the report have shown that the EPOSS mission will be safe for the workforce during assembly and safe for the satellite during its operational lifetime. [46]

16.4. Sustainability

Being a major concern for the EPOSS mission, sustainability has been addressed throughout design. This chapter presents the current state of the mission's sustainability and an overview of how it is being assessed. Firstly, subsection 16.4.1 gives an update on the ESPPP, created prior to this design phase. Secondly, subsection 16.4.2 describes how the current design complies with the policy, and addresses the main points of concern. Lastly, subsection 16.4.3 provides concluding remarks regarding mission sustainability.

16.4.1. EPOSS Sustainability an Planetary Protection Policy

With the intent to adhere to the sustainability goals and standardise the application of methods, a set of measures were created and documented. These are a set of hard requirements and

[3] Retrieved from https://web.archive.org/web/20090709171549/http://cassini-huygens.jpl.nasa.gov/cassini/english/ops/anomsafe.shtml last opened June 21, 2019

[4] Retrieved from https://www.nasa.gov/centers/wstf/about_us/safety_and_mission_assurance/industrial_hygiene_and_occupational_health.html last opened June 20, 2019

considerations regarding trade-offs, encapsulated in a policy as described below.

Policy Statement

Considering the environmental risks introduced by EPOSS, and agreeing with the relevance of ensuring resources are not compromised, ESPPP intends to ensure a sustainable project development, and aims to draw attention to sustainability at all distinct design stages. Furthermore, tools are provided to allow for continuous application of the methods.

The policy is thus pertinent to all decisions and trade-offs, and divided into two main fields, defined as follows:

- With regards to Earth's state and resources: the impact of the mission on the environment must be reduced, with a special attention to use of resources.
- With regards to planetary protection: the mission must not compromise future investigation of the bodies, nor be detrimental to potential space exploration missions.

Additionally, the policy deals with social and budget sustainability concerns. Lastly, it intends to provide all stakeholders and affected parties with a reference document regarding sustainability.

The policy is to be applied by all members of AE3200 Design Synthesis Exercise (DSE) Group 6 at all stages of technical product development. [9]

At this point in time, the third version of the ESPPP is in force, as given in [9].

16.4.2. Policy Compliance

Through sustainable project management, policy compliance has been scrutinised ensuring EPOSS does not hinder future missions. As described in the previous design progress report [10], the selected concept for the mission scored the highest for sustainability. Not only that, but this factor was also appraised in every subsystem trade-off in a bottom-up approach. For example, sustainability had a weight of four (in a scale up to five), for trajectory and orbit trade-off.

At this stage in design, certain parameters have a major impact on the mission's sustainability. An in-depth analysis of said parameters and their compliance with the ESPPP is described below.

Power

The choice of RTGs for the mission can be considered problematic with regards to sustainability, for they introduce environmental and health risks both before launch and upon collision with Earth.

Evidently, launched RTGs will comply with international requirements on safety (subsection 10.3.1). Extensive international treaties discuss the consequences of RTG failure, and associated responsibilities for involved countries [18] [118]. This implies social sustainability concerns of nuclear power sources in space has already been discussed in depth and agreed upon.

Furthermore, it is important to note that, should RTGs undergo reentry and impact Earth, radioactive material dispersal hazard will not exceed limits stipulated by international accords [17]. In other words, RTGs are designed to survive reentry and impact. On top of that, extensive testing and use in past missions reduces the risk of nuclear fuel release significantly [40]. Not only that, but the risk of reentry happening during the flyby is low. Cassini had

a one in a million chance of impact [78]; considering the technological advancements made since its launch, EPOSS reentry risk is expected to be below this value, meeting MIS-00.02 (Table 2.2). Furthermore, the reliability of the Falcon Heavy ensures low risk of impact at launch. Therefore, use of RTGs is not critical for the mission's sustainability.
As discussed in subsection 10.3.1, plutonium resources are scarce. Americium-241, produced from stored separated plutonium, is chosen [6].
This power subsystem selection thus complies with the ESPPP and does not compromise use of resources.

Propulsion

The use of hydrazine might seem in first instance detrimental for environmental sustainability and a violation of the ESPPP considering other options are available. As explained in [10], while it is true that green alternatives are currently being developed, these are still in early stages. In other words, the extensive use of hydrazine in the past yields a deep understanding of the associated risks; safety and contingency measures have been developed and tested to reduce said risks. This is not the case for alternatives such as the AF-M315E, being developed by the U.S Air Force Base Laboratory and not yet used in flight, which ultimately introduces a bigger hazard for the mission, and therefore its sustainability.[5]
That is, choosing hydrazine does not violate the ESPPP since it currently ranks higher in sustainability than feasible greener alternatives.

Launch

Launch site and launcher selection raises numerous concerns regarding sustainability, and is thus assessed in detail with regards to said subject. For EPOSS, launch with the Falcon Heavy from Vandenberg Air Force Base (VAFB) has been selected. Note that this is different from the previously discussed Vulcan and Cape Canaveral selection, the change being caused by a change in design mass.
Selecting the Falcon Heavy has numerous advantages when compared to other launchers. Firstly, using an existing launcher reduces cost associated with design of a new one contributing to the budget. Secondly, the Falcon Heavy is reusable, meaning less resources are consumed, complying with the concerns of the ESPPP. Thirdly, the price of a reusable Falcon Heavy falls within budget, and is cheaper than alternatives that would be selected if the spacecraft mass were to be higher. Under consideration of the fact that meeting the National Environmental Policy Act (NEPA) falls within the ESPPP objectives, it is important to note that the former has already been implemented and approved for the selected launcher and launch site. As a matter of fact,

> After reviewing and analysing available data and information on existing conditions and potential impacts, the Federal Administration of Aviation (FAA) has determined issuance of launch and reentry licenses to SpaceX for Falcon 9 and Falcon Heavy commercial launch operations at VAFB would not significantly affect the quality of the human environment within the meaning of NEPA. [37]

Booster landing has equally been approved and found to have no significant impact on the environment [37] [38].

[5] Retrieved from `https://www.nasa.gov/mission_pages/tdm/green/overview.html` last opened June 20, 2019

Secondary Science

Despite a detailed analysis of secondary science being out of the scope of this report, possible side scientific studies have been introduced (subsection 5.4.3). Secondary science offers an opportunity to expand the missions market, increase profit and be overall more economically sustainable (section 3.3).

End of Life

Sustainability concerns were driving for system disposal strategy. Contemplating the necessity of keeping inadvertent contamination of Enceladus under a probability of 10^{-4} (considered in trajectory, subsection 4.1.2, last paragraph), as set out by the COSPAR Planetary Protection Policy for category III and IV missions to Enceladus, colliding with its surface was discarded (MIS-12, Table 2.2) [62]. System disposal on the body would have implied significant increase in risk of introducing organisms and possibly compromise future missions. By doing so, it would also cause a bad impression on the scientific community. Furthermore, costs involving reduction of bioburden would increase, affecting budget sustainability.
Therefore, in spite of exiting Enceladus orbit being costly in terms of ΔV, going to Tethys was selected subsection 4.1.2. This body, unlike Enceladus, falls under category II, since there is only a remote chance of contamination compromising future science [62]. This implies less stringent requirements on cleanliness and documentation, and provides more opportunities for secondary science, being positive for sustainability.

16.4.3. Sustainability Overview

Sustainability has been regarded and assessed in depth at all points in design. A coherent application of this discipline has been possible through the consistent use of the ESPPP. As explained in this chapter, the current mission design complies with the policy, and the points of major concern such as use of RTGs and hydrazine have not resulted to be critical for the mission's sustainability. EPOSS does thus not compromise future missions, and is at this point in design economically, socially and environmentally sustainable.

17 Conclusion & Recommendations

This report covers the development of the interplanetary mission EPOSS: Exploration of Plumes and Oceans of the Saturnian System. EPOSS aims to characterise the geophysical properties of moons such as Enceladus and Daphnis in order to answer the scientific community's open questions when it comes to the possibility of extra-terrestrial life. By studying the plumes on the south pole of Enceladus, the team hopes to investigate the possibility of life in the moon's sub-crustal ocean while the interaction of Daphnis with the rings may delineate the workings of different bodies in the Solar System.
First, a conclusion is given below in section 17.1, after which multiple recommendations are followed in section 17.2.

17.1. Conclusion

The EPOSS mission will be carried out by a spacecraft to be launched by the Falcon Heavy with eight scientific instruments on, chosen to fulfil the scientific requirements set by the team. Launch is scheduled on the 19^{th} of April 2028 at the Vandenberg Air Force Base. With an interplanetary ΔV of 1330 m/s, the spacecraft will perform a Venus and two Earth flybys in order to reach Saturn, where it will intersect with Saturn's orbit between the F and G rings. The Venus flyby offers the unique possibility to characterise the planet and to perform secondary science for interested stakeholders. The payloads MERMAG and VIMS, which perform solar wind and flux rope characterisation, and examine cloud processes and composition distributions of Venus will be used during this flyby. The spacecraft will spend 9.8 years in transit until arrival in the Saturn orbit in February 2038.

Once in the Saturnian system, using an in-system ΔV of 2366 m/s, the spacecraft will undergo four Enceladus flybys, in which the instruments will be used to perform plume and particle characterisation; and geophysical, remote sensing, and in-situ analysis of the moon. Four Daphnis flybys will perform similar science measurements while the moon tour to reach the necessary destinations will give the opportunity to expand the current knowledge of other moons of the Saturnian System. MERMAG and MORE can be used for Saturn's magnetic and gravity field. JANUS will be used to image the moons, whereas VIMS will characterise the surface composition. As last BELA and REASON will be used for the morphology and core characterisation and ENIJA and INMS will analyse the particles around and in between the moons. Using a ΔV of 231 m/s, end of mission will occur by flying the spacecraft into the moon Tethys in February 2044, unless the mission can be extended further if there is propellant remaining. Secondary payload can be implemented in the design by external stakeholders for secondary research because a spare of 230 kg still can be used without exceeding the maximum mass the launcher can launch.

The design of the spacecraft was undertaken in parts initially, with the trajectory and payload required to carry out the science objectives detailed first. Once this was done to a sufficient degree, seven other subsystems were sized almost concurrently. The current design allows for the carrying out of all primary science requirements in 457 Enceladean days of orbit around Enceladus, four Enceladus flybys and four Daphnis flybys. ADCS allows for three-axis stabilisation with the use of, accounting for system's redundancy, three Star Trackers, three Sun Sensors, two IMU's, four momentum wheels, and 16 RCS thrusters. A dual

mode bipropellant main engine and monopropellant RCS system comprises the propulsion system. TT&C functions are carried out by use of one HGA using the Ka-band and two LGAs using the X-band with BPSK modulation and turbo coding. The C&DH system comprises of an Airbus OSCAR On-Board Computer, a NEMO Solid State Recorder along with associated cables and wiring. EPOSS relies on nine Americium based RTGs as its primary power source, supplemented by two Lithium-ion batteries. Thermal control consists of louvres, radiators, MLI, and coating as its external thermal control; while internal thermal control is carried out by the RTGs and the Capillary Pumped Loop. Finally, the main structure of the spacecraft is an Al 7075-T6, semi-monocoque strengthened cylindrical structure. It has a skirt for shielding from RTGs radiation with stiffeners and stringers for support. Mechanisms for radar deployment, magnetometer boom deployment, and antenna pointing are also included in the design.

The mission will cost 1.43 B € including all operations and accounting for 1229.9 kg of dry mass and a total of 4288.2 kg wet mass to be launched. EPOSS uses 351.7 W of nominal power drawn from nine innovative Americium RTGs and two Lithium-Ion batteries for secondary power. During the design of the spacecraft, an extensive risk analysis has been performed in order to ensure the reliability of the system and to mitigate the failures which would result from system faults. Risks that would lead to a mission failure include no signal transmission (TTR-0.3) which is mitigated by including redundancies in the design. Apart from this, propulsion system failures such as valve failure (PRR-0.5) and engine failure (PRR-0.7) are also mitigated by including redundancies in the design. By considering methods and procedures to verify and validate the design, which include verification of design methods for each subsystem as well as testing methods for manufactured parts, the team feels confident that the mission can be performed to fulfil the requirements set in the beginning of the design phase.

As the space industry moves towards a more sustainable future, the EPOSS team made sure to incorporate sustainability into every step of the design so far. Thus, the EPOSS sustainability policy, ESPPP, was developed which implements sustainability requirements on various mission phases such as launch and end-of-life. Apart from this, design choices such as the use of RTGs for a power source and hydrazine as primary fuel, however unsustainable they may seem at first glance, prove to be the only design choices available due to lack of suitable alternatives. In such cases, the EPOSS team have still managed to be innovative in terms of sustainability by using RTGs from recycled nuclear waste, for example. Apart from this, the compact spacecraft design also allows for the fully reusable Falcon Heavy launcher which will result in the reduction of enormous amounts of waste usually associated with spacecraft launches.

17.2. Recommendations

Considering the fact this design is a preliminary one, not all aspects of the design of a full mission to Saturn could be detailed. Therefore, in the following section a list of aspects which should be taken into account in further stages of the design will be presented.

General Recommendations

- Considering the uncertainties which have been not accounted for, the team suggests to conduct further research to decrease the number of unknowns and increase reliability.
- As the interaction of different space agencies is required for this mission to succeed, it is recommended to investigate in the possible political issues involved with international collaborations and which benefits can be drawn for this.

- Considering the amount of time and the complexity of the project, a further improvement is to implement more models to validate the results drawn in these ten weeks.

Trajectory & Orbit Recommendations

- It is advised to perform a better study on the gravity interaction of the bodies in the Saturnian System to have a more detailed estimate of its effect during Saturn orbit insertion.
- Studying Enceladus' orbit insertion at higher inclinations (i.e. larger than 45 deg as it was not investigated further enough in this stage.
- Orbit maintenance for high inclinations at Enceladus should as well be investigated further, together with the latter recommendation.
- In this study, the deep space manoeuvres for interplanetary transfer where retrieved using external tools. In detailed design, it is advised to develop a tool in-house specifically for the EPOSS mission to get more specific results and to validate it by using externally developed models.
- In further studies, it is advised to study the possibility to perform flybys around other bodies of interest perhaps to perform secondary science.
- An alternative end-of-life mission scenario should be investigated in order to open possibilities to extend the mission for scientific purposes.
- Study the possibility of reducing in-system ΔV requirements through optimisation of in-system orbit design related to flyby design, moon-tour design, and the orbit phase design.

Payload Recommendations

- As the instruments on board of EPOSS are designed for different interplanetary missions, an in-depth analysis of the different modifications which they may undergo to be adapted to the mission should be performed.
- Distribution on when science is performed and its effects on downlinking the data should be elaborated upon.
- The secondary science across the duration of the mission should be further defined, as at this stage the team mainly focused on primary science in order to meet the mission's requirements.

ADCS Recommendations

- Due to time constrains and the difficulties of approximating disturbances during interplanetary transfer and in orbit, it is suggested to define the exact manoeuvring of the spacecraft during these times; primarily needed, to estimate better the manoeuvres necessary and propellant needed.
- For the same reasoning as above, a better definition of the manoeuvres required to meet the pointing for the communication windows shall be further defined.
- A more extensive definition of manoeuvres necessary for object avoidance shall be made.
- A more detailed analysis of a detumbling situation shall be made, as it has not been extensively investigated at this stage.
- The attitude acquisition times and modes shall be defined more accurately, as they have not been defined in this study.
- A better estimation of the moment of inertia changes and centre of mass shifts throughout the mission should be done in order to better approximate the required manoeuvres.

This can be done by modelling a full and empty spacecraft in all different payload and antenna configurations.
- Lastly, further efforts shall be done in the modelling of the centre of pressure of the spacecraft, which combined with the centre of mass location, will lead to a more accurate aerodynamic torque estimation and an optimised ADCS design.

Propulsion Recommendations

- More detailed analysis on the thermal effects on other subsystems as a result of heat from the propulsion shall be done, as it only has been considered on a preliminary level so far.
- A more detailed design of the propulsion's feed lines shall be done, as it has not been investigated in this document.
- Develop main engine gimbal actuator control system in response to centre of gravity changes.

TT&C Recommendations

- Different types of losses shall be looked into in order to make a more complete estimation of the system's performance.
- Hardware shall be looked into more specifically, as only the general characteristics have been defined at this stage.
- Look more into tracking methods and their implications on the system.
- Further investigation of the coupling with payload.

C&DH Recommendations

- The complete software shall be generated in further stages of the design, as in this report only the functions that C&DH has to perform and not the way they are performed are investigated.
- A more in-depth analysis of the sizing of the processor shall be done, including the payload processing needs and its software integration with the rest of the design.
- A more in depth analysis of the electric and electronic components shall be done, as the team had not enough technical knowledge on the subject to perform accurate estimations.
- A more defined picture of the data handling mechanisms and the workings of the OBC shall be done.
- More information regarding the hardware shall be acquired before a choice is to be finalised.

Power Recommendations

- As only limited literature was found on the necessary shielding from Americium and Neptunium, further analysis on alpha and gamma radiation shielding shall be performed.
- RTGs are an innovative solution. Considering the lack of testing time, more in depth tests of this power sources shall be performed.
- The effects of radiation on hydrazine and the necessity of a shield on the propellant tank shall be investigated in further design phases.
- The National Nuclear Laboratory (NNL) shall be contacted about their current development planning and to discuss a possible collaboration with the EPOSS team on the RTG design.

- Because of the long duration of RTG safety procedures, it is necessary to contact the INSRP to discuss the launch approval process and to initiate a detailed safety analysis report.
- Solar arrays will be further analysed as back option for the power subsystem.

Thermal Recommendations

- Considering the duration of the mission and the different environments the EPOSS is subjected to, a dynamic analysis over the entire time span shall be done, as the thermal subsystem is currently designed on a worst case scenario basis.
- A more complete heat model shall be made, as at this stage only a uniform heat distribution has been accounted for.

Structural Recommendations

- In order to design a more realistic structure, an in-depth load case analysis shall be performed in further design stages.
- The natural frequency of the model shall be accurately delineated in order to generate a complete vibrational study of the structure.
- Identify and assess risks introduced by trajectory on deployed radar structure.

Operations and Logistics

- Include a Gantt chart for the mission itself, showing phases and their duration.

Bibliography

[1] *Metallic Materials and Elements for Aerospace Vehicle Structures*, second ed. No. MIL-HDBK-5J in 1. Jan. 2003.

[2] DELTA-DOR — Technical Characteristics and Performance. Tech. rep., The Consultative Committee for Space Data Systems, May 2013.

[3] Nuclear Reactors and Radioisotopes for Space. `http://www.world-nuclear.org/`, May 2019.

[4] UK Generates Usable Electricity from Americium. `https://www.world-nuclear-news.org/`, May 2019.

[5] Agrawal, P., et al. An Assessment of Aerocapture and Application to Future Missions, Feb. 2016.

[6] Ambrosi, R., et al. Development and Testing of Americium-241 Radioisotope Thermoelectric Generator: Concept Designs and Breadboard System. *Nuclear and Emerging Technologies for Space* (2012).

[7] Andrade, L. J., and Burk, T. Titan Density Reconstruction Using Radiometric and Cassini Attitude Control Flight Data. Tech. rep., Jet Propulsion Laboratory, Caltech.

[8] Antreasian, P. G., et al. Cassini Orbit Determination Performance During the First Eight Orbits of the Saturn Satellite Tour.

[9] Argenziano, F., et al. Baseline Report, May 2019. Design Synthesis Exercise Report.

[10] Argenziano, F., et al. Midterm Report, Jun. 2019. Design Synthesis Exercise Report.

[11] Argenziano, F., et al. Project Plan, Apr. 2019. Design Synthesis Exercise Report.

[12] Atkins, P., and Jones, L. Chemistry. Molecules, Matter and Change. *W.H. Freeman* (1997).

[13] Balcer, S., et al. International Space Station Lithium-Ion Batteries, 2016. NASA Glenn Research Center, Aerojet Rocketdyne.

[14] Banakar, R. M. A Low Power Design Methodology for Turbo Encoder and Decoder.

[15] Barber, T. Final Galileo Propulsion System In-Flight Characterization. Tech. rep., Jet Propulsion Laboratory.

[16] Barber, T., and Cowley, R. Initial Cassini Propulsion System In-Flight Characterization. Tech. rep., Jet Propulsion Laboratory.

[17] Bennett, G. Overview of the U.S. Flight Safety Process for Space Nuclear Power. *Nuclear Safety 22* (Aug. 1981).

[18] Bennett, G. Proposed Principles on the Use of Nuclear Power Sources in Space. Tech. rep., Office of Special Applications U.S. Department of Energy, 1998.

[19] Billings, L. Excitement builds for the possibility of life on Enceladus. *Scientific American* (2016).

[20] Blackburn, E. P., et al. Spacecraft Magnetic Torques. *NASA Case File Copy* (Mar. 1969).

[21] Blankenship, D. F. Radar for Europa Assessment and Sounding: Ocean to Near-surface (REASON). UTIG JPL Presentation.

[22] Bradford. Bradford coarse sun sensor. http://bradford-space.com. Datasheet.

[23] Brown, R. H., et al. The Cassini Visual and Infrared Mapping Spectrometer (VIMS) Investigation.

[24] Buffington, B. Trajectory Design for the Europa Clipper Mission Concept.

[25] Buffington, B., et al. Evolution of Trajectory Design Requirements on NASA's Planned Europa Clipper Mission.

[26] Burk, T. Cassini Orbit Trim Maneuvers at Saturn - Overview of Attitude Control Flight Operations. *AIAA Guidance, Navigation, and Control Conference* (Aug. 2011).
[27] Burk, T., and Lorenz, R. Enceladus Plume Density from Cassini Spacecraft Attitude Control Data. *Icarus 300* (Jan. 2018).
[28] Campagnola, S., et al. A Fast Tour Design Method Using Non-Tangent V-Infinity Leveraging Transfer.
[29] Cervone, A. AE2111-II Lecture 09: Spacecraft Telecommunications.
[30] Cervone, A. AE2111-II Lecture 10: Spacecraft Telecommunications.
[31] Chahal, D. M. S. European Space Nuclear Power Programme: UK Activities presentation, Feb. 2012. UK Space Agency.
[32] Christiansen, E. L., et al. Enhanced Meteoroid and Orbital Debris Shielding. *Elsevier Science Ltd. 17* (1995).
[33] Cook, B., Dennis, M., Kayalar, S., Lux, J., and Mysoor, N. Development of the Advanced Deep Space Transponder. Tech. rep., Jet Propulsion Laboratory, Feb. 2004.
[34] Della Corte, V., et al. The JANUS Camera Onboard JUICE Mission for Jupiter System Optical Imaging. *Space Telescopes and Instrumentation 9143* (2014).
[35] Dirkx, D. Returning to Saturn - Characterising the Icy Moons and Rings - Project Guide. Design Synthesis Exercise, Mar. 2019.
[36] Dudzinski, L. e. a. Radioisotope Power: A Key Technology for Deep Space Exploration, 2011. NASA.
[37] FAA. Finding of No Significant Impact and Record of Decision for Issuing Launch and Reentry Licenses to Space Exploration Technologies Corp. for Falcon 9 and Falcon Heavy Commercial Launch Operations at Vandenberg Air Force Base, California. Tech. rep., 2013.
[38] FAA. Adoption of the Environmental Assessment and Finding of No Significant Impact for Boost-back and Landing of Falcon Heavy Boosters at Landing Zone-1, Cape Canaveral Air Force Station, Florida. Tech. rep., 2017.
[39] Fortescue, P., and Stark, J. *Spacecraft Systems Engineering*, second ed. John Wiley and sons, Chichester, England, 1995.
[40] Furlong, R., et al. *U.S. Space Missions Using Radioisotope Power Systems*. American Nuclear Society, Apr. 1999.
[41] Genova, A., et al. Mercury Radio Science Experiment of the Mission BepiColombo. *Mem. S.A.It. Suppl 20* (2012).
[42] Giesen, J. Hohmann Transfer Orbit Applet, Oct. 2015.
[43] Gill, E. AE3211-I Lecture 6: Verification and Validation for the Attitude and Orbit Control System. TU Delft, Feb. 2019.
[44] Gill, E. AE3211-I Lecture 7: Verification and Validation for the Propulsion System. TU Delft, Feb. 2019.
[45] Gilmore, D. G. *Spacecraft Thermal Control Handbook*, second ed., vol. Volume I: Fundamental Technologies. The Aerospace Press, El Segundo, California, 2002.
[46] Gini, A. Safety of Nuclear Powered Missions. Interview of Dr. F. Allahdadi and Dr.S.Bakhtiyarov, Oct. 2011. Space safety magazine.
[47] Grumman, N. LN200S Inertial Measurement unit. www.northropgrumman.com, 2013. Datasheet.
[48] Gunderson, K., et al. A Laser Altimeter Performance Model and Its Application to BELA. *IEEE Transactions on Geoscience and Remote Sensing 44* (Oct. 2006).
[49] Hore-Lacy, I. Can americium replace plutonium in space missions? `http://www.world-nuclear-news.org/`, Jul. 2014.
[50] Ikeda, S., et al. Systematic Analysis of Venus Earth Gravity Assist (VEGA) Sequence and

its Application to Mission Design. Tech. rep., Kyushu University, Jun. 2013.
[51] J., B., et al. JUICE: JUpiter ICy Moons Explorer: Exploring the Emergence of Habitable Worlds Around Gas Giants (Red Book). Tech. rep., ESA, Sep. 2014.
[52] Jet Propulsion Laboratory. Low-Noise Systems in the Deep Space Network. Tech. rep., NASA, Feb. 2008.
[53] Jet Propulsion Laboratory. Telemetry Data Decoding. Tech. rep., NASA, 2013.
[54] Jet Propulsion Laboratory. Frequency and Channel Assignments. Tech. rep., NASA, 2014.
[55] Jet Propulsion Laboratory. Pseudo-Noise and Regenerative Ranging. Tech. rep., NASA, 2015.
[56] jonaoptronik. ASTRO APS Sun Sensor. www.jena-optronik.de. Datasheet.
[57] Joven, R., et al. Thermal Properties of Carbon Fiber-Epoxy Composites with Different Fabric Weaves.
[58] Kallenbach, R., et al. Space-qualified Laser System for the BepiColombo Laser Altimeter. *Applied Optics 52* (2013).
[59] Kemble, S. Interplanetary Mission Analysis and Design. Springer, 2006.
[60] Kern, L., and Scharton, T. D. NASA Handbook for Spacecraft Structural Dynamics Testing. Tech. rep., Jet Propulsion Laboratory.
[61] Kevin R. Gagne, M. R. M., and Hitt, D. L. A Dual Mode Propulsion System for Small Satellite Applications. Tech. rep., University of Vermont, Burlington, USA, 2018.
[62] Kminek, G., Conley, C., Hipkin, V., and Yano, H. COSPAR's Planetary Protection Policy. Tech. rep., ESA, NASA, CSA, and JAXA, 2017.
[63] Komm, D. S., et al. Advances in Space TWT Efficiencies. *IEEE Tansactions on Electron Devices 48* (Jan. 2001).
[64] Landau, D., et al. Mission Design for the Titan Saturn System Mission Concept.
[65] Larson, W. J., and Wertz, J. R. *Space Mission Analysis and Design*. Kluwer Academic Publishers, Microcosm, 1998.
[66] Liechty, D. S. Cassini-Huygens Aerodynamics with Comparison to Flight . Tech. rep., NASA.
[67] Loyselle, P., et al. Guidelines on Lithium-Ion Battery Use in Space Applications. Glenn Research Center, Cleveland, Ohio, 2009. NASA Engineering & Safety Center.
[68] Lunine, J. I. Ocean Worlds Exploration. *Acta Astronautica 131* (2017).
[69] M., D., et al. JUICE: JUpiter ICy Moons Explorer: Exploring the Emergence of Habitable Worlds Around Gas Giants (Yellow Book). Tech. rep., ESA, Dec. 2011.
[70] Maki, J., et al. The Mars Science Laboratory Engineering Cameras.
[71] McKay, C. P., et al. The Possible Origin and Persistence of Life on Enceladus and Detection of Biomarkers in the Plume. *ASTROBIOLOGY* (2008).
[72] Miller, D., et al. Spacecraft Power Systems Presentation, 2003. MIT Aeronautics Lecture Notes 13.
[73] MIT OpenCourseWare. Principles of Digital Communication II.
[74] Mitri, G., et al. Explorer of Enceladus and Titan (E2T): Investigating Ocean Worlds' Evolution and Habitability in the Solar System. *Planetary Space and Science* (Jun. 2018).
[75] NASA. Cassini launch. Tech. rep., NASA.
[76] NASA. New horizons. Tech. rep., NASA.
[77] NASA. *Cassini Spacecraft Mission, Explore the Planet Saturn: Environmental Impact Statement*. Northwestern University, 1995.
[78] NASA. *Cassini Spacecraft Mission, Explore the Planet Saturn: Environmental Impact Statement*. Northwestern University, 1995.
[79] NASA. Spacecraft Deployed Appendage Test Guidelines, Oct. 1995.

[80] NASA. *Systems Engineering Handbook*, second ed. Washington DC, Dec. 2007.
[81] NASA. Cassini Launch, Press Kit. Tech. rep., Oct. 2017.
[82] NLR. Advanced Satellite Thermal Control - Pumped Cooling Systems. f412-01.
[83] Noomen, R. AE2104: Flight and Orbital mechanics Lecture 11, 12: Interplanetary Flight. TU Delft Open Course Software, Oct. 2012.
[84] Palma, D. Preliminary Trajectory Design of a Mission to Enceladus, Dec. 2016.
[85] Peyrou-Lauga, R. and Darel, A. JUICE Thermal Architecture and Performance. *47th International Conference on Environmental Systems*, ICES-2017-1 (2017).
[86] Pignède, A. Detumbling of the NTNU Test Satellite. Tech. rep., Norwegian Institute of Science and Technology, NTNU Trondheim, Dec. 2014.
[87] Pubchem, N. C. f. B. I. Americium. U.S. National Library of Medicine, Jun. 2019.
[88] Pubchem, N. C. f. B. I. Neptunium. U.S. National Library of Medicine, Jun. 2019.
[89] Ray, P. Independant Review of the Failure Modes of F-1 Engine and Propellants System. Tech. rep., University of Alabama, 2002.
[90] Razzaghi, A. I., et al. Enceladus Flagship Mission Concept Study, Aug. 2007.
[91] Reh, K., et al. Titan Saturn System Mission: A Joint Endeavour by ESA and NASA. *ESA Team* (2009).
[92] Restano, M., et al. Effects of the passage of Comet C/2013 A1 (SidingSpring) observed by the Shallow Radar (SHARAD)on Mars Reconnaissance Orbiter. *Geophysical research letters* (Jun. 2015).
[93] Ronald W. Humble, Gary N. Henry, W. J. L. *Space Propulsion Analysis and Design*, second edition ed. Kluwer and Microcosm Publishers, 1995.
[94] RUAG. Datasheet - Articulated Booms Deployable Mechanism. RUAG, Jan. 2019.
[95] Rudolph, D. Design and Development of the Cassini Main Engine Assembly Gimbal Mechanism. Tech. rep.
[96] Russel, P. R., et al. Resonance Hopping Transfers Between Moon Science Orbits. *Georgia Tech Special Problems Report* (Apr. 2009).
[97] Russel, R. P., and Lara, M. On the Design of an Enceladus Science Orbit.
[98] Rymer, A. M., et al. Electron sources in Saturn's magnetosphere. *JOURNAL OF GEO-PHYSICAL RESEARCH* (Feb 2007).
[99] Sarani, S. Enceladus Plume Density Modeling and Reconstruction for Cassini Attitude Control System.
[100] Sava, P., and Asphaug, E. 3D Radar Wavefield Tomography of Comet Interiors. *Advances in Space Research 61* (Oct. 2017).
[101] Schenk, P., et al. *Enceladus and the Icy Moons of Saturn*. The University of Arizona Press in collaboration with Lunar and Planetary Institute, Houston, 2018.
[102] Schroeder, D. M., et al. Assessing the Potential for Passive Radio Sounding of Europa and Ganymede with RIME and REASON. *Planetary and Space Science 134* (Oct. 2016).
[103] Schulz, R., et al. BepiColombo: Payload and Mission Updates. *Advances in Space Research 38* (2006).
[104] Simpson, D. K. Safety and Handling of Hydrazine. Tech. rep., Olin Research Center.
[105] Sotin, C. Saturn's moons Enceladus and Titan. Presentation Slides, Jet Propulsion Laboratory, Nov. 2017.
[106] Sotin, C., et al. JET: a Journey to Enceladus and Titan. *AGU Fall Meeting Abstracts -1* (Nov. 2010).
[107] SpaceX. Falcon User's Guide. Tech. rep., Space Exploration Technologies Corp., Jan. 2019.
[108] Spencer, J. Planetary Science Decadal Survey Enceladus Orbiter.
[109] Spencer, J., and Niebur, C. Planetary Science Decadal Survey Enceladus Orbiter.

[110] Speretta, S. Satellite Communication Systems.
[111] Speretta, S. Personal Communication, Jun. 2019.
[112] Steinbrugge, G., et al. Assessing the Potential for Measuring Europa's Tidal Love Number h2 Using Radar Sounder and Topographic Imager Data. *Earth and Planetary Science Letters 482* (2018).
[113] Sturm, E. J. Ensuring Cassini's End-of-Mission Propellant Margins.
[114] Taylor, J. The Deep Space Network: A Functional Description. Tech. rep., NASA.
[115] Taylor, J., Sakamoto, L., and Wong, C.-J. Cassini Orbiter/Huygens Probe Telecommunications. Tech. rep., California Institute of Technology, Jan. 2002. DESCANSO Design and Performance Summary Series Article 3.
[116] Thomas, N., et al. The BepiColombo Laser Altimeter (BELA): Concept and Baseline Design. *Planetary and Space Science 55* (2007).
[117] Tsou, P., et al. LIFE: Life Investigation For Enceladus. A Sample Return Mission Concept in Search for Evidence of Life. *Astrobiology* (2012).
[118] U.N. Principles Relevant to the Use of Nuclear Power Sources In Outer Space . Tech. rep., 1992.
[119] Vetter, J. R. Fifty years of orbit determiantion: Development of modern astrodynamic methods. *Johns Hopkins APL Technical Digest 27* (2007).
[120] Werner, J., et al. Cost Comparison in 2015 Dollars for Radioisotope Power Systems — Cassini and Mars Science Laboratory, 2016. Idaho National Laboratory.
[121] Wertz, J. R., Everett, D. F., and Puschell, J. J. *Space Mission Engineering: The New SMAD*. Microcosm Press, 2011.
[122] Wiesel, W. E. *Spaceflight Dynamics*, second ed. Irwin/McGraw-Hill, Boston, 1997.
[123] Wiley, S., D. K. Design and Development of the Messenger Propulsion System. Tech. rep., Aerojet-General Corporation, 2003.
[124] Zandbergen, B. *Aerospace Design & Systems Engineering Elements I Part: Spacecraft (Bus) Design and Sizing*. Delft University of Technology, Delft, Nov. 2015.